576381

Analysis Report documenting Solubility and Complexation of Iron, Lead, Magnesium, Neodymium, and Boron in the WIPP-Relevant Brines under TPs 06-03, 08-02, 12-02, 14-03, 14-05, 16-02, 19-01, and 20-01

Revision 0

Jay Jang, Priya Hora, Leslie Kirkes, Chammi Miller, and Luzheng Zhang

Organization 08882

Sandia National Laboratories

Carlsbad, New Mexico, U.S.A.

Effective Date: November 23, 2021

WIPP:4.4.2.2.1:TD:QA-C:RELERT:576379

17 APPROVALS

Authored by:	Jay Jang Print Name	 Signature	11/18/2021 Date
Authored by:	Priya Hora Print Name	 Signature	11/18/2021 Date
Authored by:	Leslie Kirkes Print Name	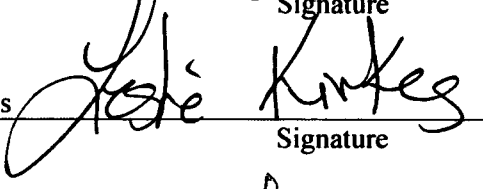 Signature	11/22/21 Date
Authored by:	Chammi Miller Print Name	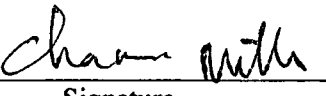 Signature	11/18/2021 Date
Authored by:	Luzheng Zhang Print Name	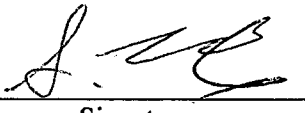 Signature	11/18/2021 Date
Reviewed by:	Pat Brady Print Name Technical Reviewer	Signature on file Signature	9/27/2021 Date
Reviewed by:	Shelly R. Nielsen Print Name Quality Assurance Reviewer	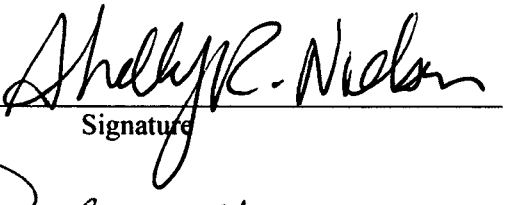 Signature	11-19-2021 Date
Approved by:	Paul Shoemaker Print Name Senior Manager	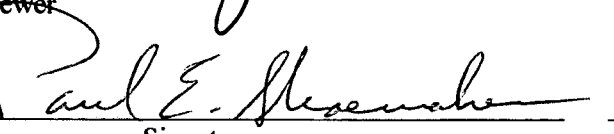 Signature	11/23/2021 Date

18

I. INTRODUCTION

I.1. Scope of this Report

This report analyzes experimental data from Test Plans TP 08-02, TP 12-02, and TP 20-01 to add new log K values and Pitzer interaction parameters for Fe, Pb, Mg, Nd and B reactions to the WIPP geochemical thermodynamic database, data0.fm1.

I.2. Organization

After a few introductory sections (including this section), this report is organized by element - Fe, Pb, Mg, Nd and B - in the format shown in Table I.2-1.

Section IX. CONCLUSIONS starting in page 133 summarizes the reactions, their log Ks, and Pitzer interaction parameters adopted from literature and derived in this report. They are the recommended new additions to the current SNL WIPP geochemical brine model.

Table I.2-1. Organization of Sections.

IV. Iron (Fe)
...
IV.n. An experimental system identified by composition: FeOxalate.2H_2O(s) - NaCl - H_2O
IV.n.1. Chemical System
IV.n.2. Goals and Hypotheses
IV.n.3. Reactor Preparation
IV.n.4. Data - Aqueous
IV.n.5. Data - Solids
IV.n.6. Observations
IV.n.7. Model Parameterization: Pitzer Approach
IV.n.8. Summary
IV.(n+1). Other system
...

I.3. Analytical Instruments and Operation

Solubility-limiting solids and salts were weighed using calibration-checked chemical balances. Class A volumetric glassware was used. pHr is a reading from the display of pH meter when the meter and electrode are calibrated using commercial pH buffers of low ionic strength. Dissolved Fe, Pb, Mg, Nd, Na, and B were measured by ICP-AES or ICP-MS. Dissolved chloride ions and organic anions were measured by IC. Concentrations of some organic anions were measured using a coulometer. Instruments were operated under their corresponding Activity Specific Procedures (SPs), which were current to the dates of operation.

I.4. Properties of WIPP-Relevant Brines

Table I.4-1 lists calculated chemical properties of NaCl - $MgCl_2$ solutions used in the considered experiments. Polynomial regressions of density and M:m (Molarity-to-molality conversion factor) as functions of salt concentration can be developed from tabulated values, and later used to calculate density and M:m for individual experiments.

Table I.4-1. Calculated properties of model WIPP-Relevant Experimental Brines at 25 °C using EQ3/6, Version 8.0a. I is Ionic strength; A is a correction factor to convert pHr to pcH; $\{H_2O\}$ is the activity of water; and M:m is a Molarity-to-molality conversion factor (Jang, 2020a).

NaCl, m	NaCl, M	$MgCl_2$, m	$MgCl_2$, M	I, m	I, M	A	$\{H_2O\}$	Density, g/mL	M:m, L/kg	EQ3/6 input file[1]
0.01	0.0100	0	0	0.01	0.0100	-0.04	0.9997	1.001	0.999	nacl_01.3i
0.1	0.100	0	0	0.1	0.0999	-0.10	0.9967	1.005	1.001	nacl_02.3i
0.5	0.495	0	0	0.5	0.4952	-0.09	0.9835	1.020	1.010	nacl_03.3i
1	0.980	0	0	1	0.9803	-0.03	0.9669	1.038	1.020	nacl_04.3i
2	1.92	0	0	2	1.9210	0.14	0.9316	1.073	1.041	nacl_05.3i
3	2.82	0	0	3	2.8246	0.33	0.8932	1.107	1.062	nacl_06.3i
4	3.69	0	0	4	3.6931	0.53	0.8515	1.139	1.083	nacl_07.3i
5	4.53	0	0	5	4.5286	0.74	0.8068	1.170	1.104	nacl_08.3i
6	5.33	0	0	6	5.3324	0.96	0.7594	1.200	1.125	nacl_09.3i
0	0	0.01	0.0100	0.03	0.0300	-0.07	0.9995	1.002	0.999	mgcl2_01.3i
0	0	0.1	0.0998	0.3	0.2993	-0.11	0.9954	1.007	1.0025	mgcl2_02.3i
0	0	1	0.968	3	2.9033	0.23	0.9418	1.060	1.0333	mgcl2_03.3i
0	0	1.5	1.43	4.5	4.2841	0.49	0.8995	1.088	1.0504	mgcl2_04.3i
0	0	2	1.87	6	5.6206	0.77	0.8481	1.115	1.0675	mgcl2_05.3i
0	0	2.5	2.30	7.5	6.9144	1.06	0.7886	1.141	1.0847	mgcl2_06.3i
0	0	3	2.72	9	8.1685	1.36	0.7227	1.167	1.1018	mgcl2_07.3i
4	3.69	0.01	0.01	4.03	3.7194	0.54	0.8506	1.140	1.0835	namgc_01.3i
4	3.68	0.1	0.09	4.3	3.9573	0.58	0.8426	1.144	1.0866	namgc_02.3i
4	3.58	1	0.89	7	6.2645	1.07	0.7499	1.189	1.1174	namgc_03.3i
4*	3.53	1.5	1.32	8.5	7.4923	1.36	0.6903	1.213	1.1345	namgc_04.3i
4*	3.47	2	1.74	10	8.6836	1.65	0.6268	1.237	1.1516	namgc_05.3i
4*	3.42	2.5	2.14	11.5	9.8400	1.95	0.5613	1.259	1.1687	namgc_06.3i
4*	3.37	3	2.53	13	10.962	2.25	0.4955	1.281	1.1859	namgc_07.3i

[1] These files can be found at /cvs/CVSLIB/WIPP_EXTERNAL/ap190.

NaCl, m	NaCl, M	$MgCl_2$, m	$MgCl_2$, M	I, m	I, M	A	$\{H_2O\}$	Density, g/mL	M:m, L/kg	EQ3/6 input file[1]
5	4.53	0.01	0.01	5.03	4.5541	0.75	0.8059	1.171	1.1045	namgc_08.3i
5	4.51	0.1	0.09	5.3	4.7851	0.80	0.7970	1.175	1.1076	namgc_09.3i
5*	4.39	1	0.88	8	7.0274	1.30	0.6977	1.219	1.1384	namgc_10.3i
5*	4.33	1.5	1.30	9.5	8.2215	1.58	0.6364	1.242	1.1555	namgc_11.3i
5*	4.26	2	1.71	11	9.3809	1.88	0.5726	1.264	1.1726	namgc_12.3i
5*	4.20	2.5	2.10	12.5	10.506	2.17	0.5081	1.286	1.1898	namgc_13.3i
5*	4.14	3	2.49	14	11.600	2.47	0.4444	1.307	1.2069	namgc_14.3i
6	5.33	0.01	0.01	6.03	5.3576	0.97	0.7584	1.201	1.1255	namgc_15.3i
6*	5.32	0.1	0.09	6.3	5.5821	1.02	0.7488	1.205	1.1286	namgc_16.3i
6*	5.18	1	0.86	9	7.7626	1.52	0.6449	1.247	1.1594	namgc_17.3i
6*	5.10	1.5	1.27	10.5	8.9248	1.81	0.5829	1.269	1.1765	namgc_18.3i
6*	5.03	2	1.68	12	10.053	2.10	0.5197	1.291	1.1937	namgc_19.3i
6*	4.96	2.5	2.06	13.5	11.150	2.40	0.4570	1.312	1.2108	namgc_20.3i
6*	4.89	3	2.44	15	12.216	2.70	0.3961	1.333	1.2279	namgc_21.3i
*Indicates that solution is supersaturated with halite.										

II. TRANSCRIPTION, TRACEABILITY, AND UNIT CONVERSION OF EXPERIMENTAL DATA

Experimental data used for model validation and parameterization were compiled in the Excel file "VOL_CRC_GEOC-21-11_Mgmt.xlsx" where unit conversion, statistical data processing, and data plotting were done.

Associated files are archived at /cvs/CVSLIB/WIPP_EXTERNAL/ap190.

The source of the experimental data for the Subsection IV.1 is Kim et al. (2017).

The experimental data for Sections IV (Iron, with one exception above, i.e., Subsection IV.1), V (Lead), and VI (Magnesium) were transcribed from Scientific Notebooks and Binders into the Excel file. Locations of individual measurements in the Scientific Notebooks are listed in the Excel file.

The experimental data for Sections VII (Neodymium) and VIII (Boron) were selected with statistical scrutiny from a Milestone Report (Kirkes and Hora, 2020), and were copied into the Excel file. Links to Scientific Notebooks and Binders are listed in the Milestone Report.

III. BASIS GEOCHEMICAL BRINE THERMODYNAMIC MODEL

III.1. DATA0.FM1

Data0.fm1 (Xiong, 2011) is an electronic text file containing the 25 °C thermodynamic quantities, i.e., log Ks of reactions and relevant Pitzer Interaction Parameters (PIPs). The thermodynamic quantities therein represent the geochemical brine thermodynamic model of SNL WIPP Geochemistry. They are organized in computer-friendly fashion in the text file to be used as the thermodynamic database for EQ3/6, Version 8.0a (Wolery and Jarek, 2003).

Table III.1-1 and Table III.1-2 are the reproduction of data0.fm1 in element-by-element fashion, so that readers can easily look up for the thermodynamic quantities of interest in the following Sections IV to VIII. Table III.1-1 lists the reactions and their log Ks. Table III.1-2 lists the PIPs relevant to reactions listed in Table III.1-1.

In data0.fm1, references are missing for multiple log Ks, and analog approach taken for multiple reactions are not explicitly noted. While completing the Table III.1-1, the missing references were restored, and the log Ks were verified. Analog approaches were explicitly noted. Multiple instances were found where log Ks were calculated using information obtained from multiple references other than noted in data0.fm1: the required references were traced and restored. Table III.1-2 was completed in similar way.

The new log Ks and PIPs reported in Sections IV to VIII, which are summarized in Section IX. CONCLUSIONS, were derived and/or validated with respect to the log Ks and PIPs selected from Table III.1-1 and Table III.1-2. Therefore, the new log Ks and PIPs should be used in conjunction with relevant thermodynamic quantities selected from Table III.1-1 and Table III.1-2. Otherwise, users of the new thermodynamic quantities of this report could create model inconsistency issues.

Table III.1-1. Reactions and log Ks retrieved from our basis model, i.e., data0.fm1. Selected reactions and log Ks will be consistently used for the thermodynamic model validation and parameterization. Log Ks are truncated to the second digit below the decimal point. The values were not rounded-up to keep the traceability to values listed in data0.fm1. This Table continues through multiple pages until readers find "End of Table III.1-1".

Reactions	LogK	Source
Aqueous reactions		
-Protonation		
$H^+ + OH^- = H_2O$	13.99	Harvie et al. (1984)
$CO_3^{-2} + H^+ = HCO_3^-$	10.33	Harvie et al. (1984)
$CO_2(aq) + H_2O = H^+ + HCO_3^-$	-6.33	Harvie et al. (1984)
$HSO_4^- = SO_4^{-2} + H^+$	-1.97	Harvie et al. (1984), Shock and Helgeson (1988)
$B(OH)_3(aq) + H_2O = B(OH)_4^- + H^+$	-9.23	Felmy and Weare (1986)
$B_3O_3(OH)_4^- + 5H_2O = 3B(OH)_4^- + 2H^+$	-20.18	Felmy and Weare (1986)
$B_4O_5(OH)_4^{-2} + 7H_2O = 4B(OH)_4^- + 2H^+$	-20.82	Felmy and Weare (1986)
$H_3PO_4(aq) = 2H^+ + HPO_4^{-2}$	-9.35	Rai et al. (1992) + Novak (1995)
$H_2PO_4^- = H^+ + HPO_4^{-2}$	-7.20	Rai et al. (1992) + Novak (1995)
$PO_4^{-3} + H^+ = HPO_4^{-2}$	12.34	Novak (1995)
$H_4EDTA(aq) = 4H^+ + EDTA^{-4}$ [2]	-23.03	Choppin et al. (2001)
$H_3EDTA^- = 3H^+ + EDTA^{-4}$	-20.53	Choppin et al. (2001)

[2] $EDTA^{4-}$: $C_{10}H_{12}O_8N_2^{-4}$

Reactions	LogK	Source
$H_2EDTA^{-2} = 2H^+ + EDTA^{-4}$	-17.45	Choppin et al. (2001)
$HEDTA^{-3} = H^+ + EDTA^{-4}$	-10.57	Choppin et al. (2001)
$H_3Citrate(aq) = 3H^+ + Citrate^{-3}$ [3]	-14.50	Choppin et al. (2001)
$H_2Citrate^- = 2H^+ + Citrate^{-3}$	-11.26	Choppin et al. (2001)
$HCitrate^{-2} = H^+ + Citrate^{-3}$	-6.42	Choppin et al. (2001)
$H_2Oxalate(aq) = 2H^+ + Oxalate^{-2}$ [4]	-5.65	Choppin et al. (2001)
$HOxalate^- = H^+ + Oxalate^{-2}$	-4.25	Choppin et al. (2001)
$HAcetate(aq) = H^+ + Acetate^-$ [5]	-4.75	Choppin et al. (2001)
$HLactate(aq) = H^+ + Lactate^-$ [6]	-3.82	Choppin et al. (2001)
Mg		
-Hydroxide		
$MgOH^+ + H^+ = Mg^{+2} + H_2O$	11.80	Harvie et al. (1984)
-Carbonate		
$MgCO_3(aq) + H^+ = Mg^{+2} + HCO_3^-$	7.41	Harvie et al. (1984)
-Sulfate		
None		
-Borate		
$MgB(OH)_4^+ = Mg^{+2} + B(OH)_4^-$	-1.39	Felmy and Weare (1986) + Harvie et al. (1984)
-Organic		
$MgEDTA^{-2} = Mg^{+2} + EDTA^{-4}$	-10.12	Giambalvo (2002, Org.)+Choppin et al. (2001)+Harvie et al. (1984)
$MgCitrate^- = Mg^{+2} + Citrate^{-3}$	-5.29	Giambalvo (2002, Org.)+Choppin et al. (2001)+Harvie et al. (1984)
$MgOxalate(aq) = Mg^{+2} + Oxalate^{-2}$	-3.79	Giambalvo (2002, Org.)+Choppin et al. (2001)+Harvie et al. (1984)
$MgAcetate^+ = Mg^{+2} + Acetate^-$	-1.11	Giambalvo (2002, Org.)+Choppin et al. (2001)+Harvie et al. (1984)
Ca		
-Hydroxide		
None		
-Carbonate		
$CaCO_3(aq) + H^+ = Ca^{+2} + HCO_3^-$	7.18	Harvie et al. (1984)
-Sulfate		
None		
-Borate		
$CaB(OH)_4^+ = Ca^{+2} + B(OH)_4^-$	-1.65	Felmy and Weare (1986) + Harvie et al. (1986)
-Organic		
$CaEDTA^{-2} = Ca^{+2} + EDTA^{-4}$	-10.12	Analogue to MgEDTA in Giambalvo (2002, Org.)
$CaCitrate^- = Ca^{+2} + Citrate^{-3}$	-5.29	Analogue to MgEDTA in Giambalvo (2002, Org.)
$CaOxalate(aq) = Ca^{+2} + Oxalate^{-2}$	-3.79	Analogue to MgEDTA in Giambalvo (2002, Org.)
$CaAcetate^+ = Ca^{+2} + Acetate^-$	-1.11	Analogue to MgEDTA in Giambalvo (2002, Org.)

[3] $Citrate^{3-}$: $C_6H_5O_7^{-3}$
[4] $Oxalate^{2-}$: $C_2O_4^{-2}$
[5] $Acetate^-$: CH_3COO^-
[6] $Lactate^-$: $C_3H_5O_3^-$

Reactions	LogK	Source
Am(III): Analog to Nd(III)		
-Hydroxide		
$AmOH^{+2} + H^+ = Am^{+3} + H_2O$	7.55	Fanghanel and Kim (1998) < Fanghanel et al. (1994), p.86
$Cm^{+3} + OH^- = CmOH^{+2}$	6.44±0.09	Fanghanel and Kim (1998) < Fanghanel et al. (1994), p.86
$H_2O = H^+ + OH^-$	-13.9955	Fanghanel et al. (1994), p.83 < Wagman et al. (1982)
$Am(OH)_2^+ + 2H^+ = Am^{+3} + 2H_2O$	15.69	Fanghanel and Kim (1998) < Fanghanel et al. (1994), p.86
$Cm^{+3} + 2OH^- = Cm(OH)_2^+$	12.3±0.2	Fanghanel and Kim (1998) < Fanghanel et al. (1994), p.86
$H_2O = H^+ + OH^-$	-13.9955	Fanghanel et al. (1994), p.83 < Wagman et al. (1982)
$Am(OH)_3(aq) + 3H^+ = Am^{+3} + 3H_2O$	25.69	Giambalvo (2002, An(III)) + Harvie et al. (1984). No discussion in Konnecke et al. (1997)
-Chloride		
$AmCl^{+2} = Am^{+3} + Cl^-$	-0.24	Fanghanel and Kim (1998); Konnecke et al. (1997)
	-0.23 [7]	Giambalvo (2002, An(III)) + Harvie et al. (1984)
$AmCl_2^+ = Am^{+3} + 2Cl^-$	0.74	Fanghanel and Kim (1998); Konnecke et al. (1997); Giambalvo (2002, An(III)) + Harvie et al. (1984)
-Carbonate		
$AmCO_3^+ + H^+ = Am^{+3} + HCO_3^-$	2.23	Fanghanel and Kim (1998); Fanghanel et al. (1999); Log K analyzed to mu/RT in Giambalvo (2002b) + Harvie et al. (1984)
$Am(CO_3)_2^- + 2H^+ = Am^{+3} + 2HCO_3^-$	7.67	Fanghanel and Kim (1998), Fanghanel et al. (1999); Log K analyzed to mu/RT in Giambalvo (2002, An(III)) + Harvie et al. (1984)
$Am(CO_3)_3^{-3} + 3H^+ = Am^{+3} + 3HCO_3^-$	15.81	Fanghanel and Kim (1998), Fanghanel et al. (1999); Log K analyzed to mu/RT in Giambalvo (2002, An(III)) + Harvie et al. (1984)
$Am(CO_3)_4^{-5} + 4H^+ = Am^{+3} + 4HCO_3^-$	28.35	Fanghanel and Kim (1998), Fanghanel et al. (1999); Log K analyzed to mu/RT in Giambalvo (2002, An(III)) + Harvie et al. (1984)
-Sulfate		
$AmSO_4^+ = Am^{+3} + SO_4^{-2}$	-3.24	Giambalvo (2002, An(III)) + Harvie et al. (1984) < Fanghanel and Kim (1998)
$Am(SO_4)_2^- = Am^{+3} + 2SO_4^{-2}$	-3.70	Giambalvo (2002, An(III)) + Harvie et al. (1984) < Fanghanel and Kim (1998)
-Organic		
$AmEDTA^- = Am^{+3} + EDTA^{-4}$	-18.97	Giambalvo (2002, Org.) < Choppin et al. (2001)
$AmCitrate(aq) = Am^{+3} + Citrate^{-3}$	-8.79	Giambalvo (2002, Org.) < Choppin et al. (2001)

[7] Selected in data0.fm1

Reactions	LogK	Source
$AmOxalate^{+} = Am^{+3} + Oxalate^{-2}$	-6.15	Giambalvo (2002, Org.) < Choppin et al. (2001)
$AmAcetate^{+2} = Am^{+3} + Acetate^{-}$	-2.74	Giambalvo (2002, Org.) < Choppin et al. (2001)
$AmLactate^{+2} = Am^{+3} + Lactate^{-}$	-3.70	Giambalvo (2002, Org.) < Choppin et al. (2001)
Th(IV)		
-Hydroxide		
$Th(OH)_4(aq) + 4H^{+} = Th^{+4} + 4H_2O$	17.50 [8]	Nowak (2005) < Neck et al. (2002) + Harvie et al. (1984)
	19.28	Giambalvo (2002, An(IV)), p.6 < Ryan and Rai (1987) + Harvie et al. (1984)
-Hydroxide-Carbonate		
$Th(OH)_3(CO_3)^{-} + 4H^{+} = Th^{+4} + HCO_3^{-} + 3H_2O$	14.04	Giambalvo (2002, An(IV)) < Novak (1996) < Felmy et al. (1997) + Harvie et al. (1984)
-Carbonate		
$Th(CO_3)_5^{-6} + 5H^{+} = Th^{+4} + 5HCO_3^{-}$	24.58	Giambalvo (2002, An(IV)) < Novak (1996) < Felmy et al. (1997) + Harvie et al. (1984)
-Sulfate		
$Th(SO_4)_2(aq) = Th^{+4} + 2SO_4^{-2}$	-11.59	Giambalvo (2002, An(IV)) < Felmy and Rai (1992)
$Th(SO_4)_3^{-2} = Th^{+4} + 3SO_4^{-2}$	-12.42	Giambalvo (2002, An(IV)) < Felmy and Rai (1992)
-Organic		
$ThEDTA(aq) = Th^{+4} + EDTA^{-4}$	-23.55	Giambalvo (2002, Org) + Giambalvo (2002, An(IV)) + Choppin et al. (2001)
$ThCitrate^{+} = Th^{+4} + Citrate^{-}$	-15.23	Giambalvo (2002, Org) + Giambalvo (2002, An(IV)) + Choppin et al. (2001)
$ThOxalate^{+2} = Th^{+4} + Oxalate^{-2}$	-11.38	Giambalvo (2002, Org) + Giambalvo (2002, An(IV)) + Choppin et al. (2001)
$ThAcetate^{+3} = Th^{+4} + Acetate^{-}$	-7.36	Giambalvo (2002, Org) + Giambalvo (2002, An(IV)) + Choppin et al. (2001)
$Th(Acetate)_2^{+2} = Th^{+4} + 2Acetate^{-}$	-11.23	Giambalvo (2002, Org) + Moore et al. (1999)
$ThLactate^{+3} = Th^{+4} + Lactate^{-}$	-6.82	Giambalvo (2002, Org) + Giambalvo (2002, An(IV)) + Choppin et al. (2001)
$Th(Lactate)_2^{+2} = Th^{+4} + 2Lactate^{-}$	-11.19	Giambalvo (2002, Org < Moore et al. (1999) + Choppin et al. (2001)
Np(V)		
-Hydroxide		
$NpO_2OH(aq) + H^{+} = NpO_2^{+} + H_2O$	11.30	Giambalvo (2002, An(V)) < Fanghanel et al. (1995) + Harvie et al. (1984)
$NpO_2(OH)_2^{-} + 2H^{+} = NpO_2^{+} + 2H_2O$	23.53	Giambalvo (2002, An(V)) < Fanghanel et al. (1995) + Harvie et al. (1984)

[8] Selected in data0.fm1

Reactions	LogK	Source
-Carbonate		
$NpO_2CO_3^- + H^+ = NpO_2^+ + HCO_3^-$	5.32	Giambalvo (2002, An(V)) < Fanghanel et al. (1995) + Harvie et al. (1984)
$NpO_2(CO_3)_2^{-3} + 2H^+ = NpO_2^+ + 2HCO_3^-$	14.23	Giambalvo (2002, An(V)) < Fanghanel et al. (1995) + Harvie et al. (1984)
$NpO_2(CO_3)_3^{-5} + 3H^+ = NpO_2^+ + 3HCO_3^-$	25.68	Giambalvo (2002, An(V)) < Fanghanel et al. (1995) + Harvie et al. (1984)
-Sulfate		
None		
-Borate		
None		
-Organic		
$NpO_2EDTA^{-3} = NpO_2^+ + EDTA^{-4}$	-8.53	Giambalvo (2002, Org) < Choppin et al. (2001)
$NpO_2HEDTA^{-2} = NpO_2^+ + H^+ + EDTA^{-4}$	-15.54	Giambalvo (2002, Org) < Choppin et al. (2001)
$NpO_2H_2EDTA^- = NpO_2^+ + 2H^+ + EDTA^{-4}$	-20.86	Giambalvo (2002, Org) < Choppin et al. (2001)
$NpO_2Citrate^{-2} = NpO_2^+ + Citrate^-$	-3.49	Giambalvo (2002, Org) < Choppin et al. (2001)
$NpO_2Oxalate^- = NpO_2^+ + Oxalate^{-2}$	-4.24	Giambalvo (2002, Org) < Choppin et al. (2001)
$NpO_2Acetate(aq) = NpO_2^+ + Acetate^-$	-4.17	Giambalvo (2002, Org) < Choppin et al. (2001)
	-1.37 [9]	Giambalvo (2003, FMT) < Choppin et al. (2001)
$NpO_2Lactate(aq) = NpO_2^+ + Lactate^-$	-1.96	Giambalvo (2002, Org) < Choppin et al. (2001)
Dissolution		
Non-metall(oid)ic		
$H_2Oxalate.2H_2O(s) = 2H^+ + Oxalate^{-2} + 2H_2O$	-5.66	Giambalvo (2002, Oxalate, Org) + Harvie et al. (1984)
Na		
NaCl(s) (Halite) = Na+ + Cl-	1.57	Harvie et al. (1984)
$NaHCO_3(s)$ (Nahcolite) $= Na^+ + HCO_3^-$	-0.40	Harvie et al. (1984)
$Na_2CO_3.10H_2O(s) + H^+ = 2Na^+ + HCO_3^- + 10H_2O$	9.51	Harvie et al. (1984)
$Na_6CO_3(SO_4)_2(s)$ (Burkeite) $+ H^+ = 6Na^+ + HCO_3^- + 2SO_4^{-2}$	9.56	Harvie et al. (1984)
$Na_2CO_3.7H_2O(s) + H^+ = 2Na^+ + HCO_3^- + 7H_2O$	9.87	Harvie et al. (1984)
$Na_2CO_3.H_2O(s)$ (Thermonatrite) $+ H^+ = 2Na^+ + HCO_3^- + H_2O$	10.82	Harvie et al. (1984)
$Na_3H(CO_3)_2.2H_2O(s)$ (Trona) $+ H^+ = 3Na^+ + 2HCO_3^- + 2H_2O$	9.29	Harvie et al. (1984)
$Na_2SO_4(s)$ (Thenardite) $= 2Na^+ + SO_4^{-2}$	-0.28	Harvie et al. (1984)
$Na_2SO_4.10H_2O(s)$ (Mirabilite) $= 2Na^+ + SO_4^{-2} + 10H_2O$	-1.22	Harvie et al. (1984)
$Na_3H(SO_4)_2(s) = 3Na^+ + H^+ + 2SO_4^{-2}$	-0.81	Harvie et al. (1984)
$NaHOxalate.H_2O(s) = Na^+ + H^+ + Oxalate^{-2} + H_2O$	-6.06	Giambalvo (2002, Oxalate, Org) + Harvie et al. (1984)
$Na_2Oxalate(s) = 2Na^+ + Oxalate^{-2}$	-2.40	Giambalvo (2002, Oxalate, Org) + Harvie et al. (1984)

[9] Selected in data0.fm1 due to inconsistency of the normalized chemical potential of Choppin et al. (2001) noted in Figure 1 of Giambalvo (2003, FMT).

Reactions	LogK	Source
Mg		
$MgCl_2.6H_2O(s)$ (Bischofite) = $Mg^{+2} + 2Cl^- + 6H_2O$	4.45	Harvie et al. (1984)
$KMgCl_3.6H_2O(s)$ (Carnallite) = $K^+ + Mg^{+2} + 3Cl^- + 6H_2O$	4.33	Harvie et al. (1984)
$Mg_2CaCl_6.12H_2O(s)$ (Tachyhydrite) = $2Mg^{+2} + Ca^{+2} + 6Cl^- + 12H_2O$	17.38	Harvie et al. (1984)
$Mg(OH)_2(s)$ (Brucite) $+2H^+ = Mg^{+2} + 2H_2O$	17.10	Harvie et al. (1984); c.f., Altmaier et al. (2003), 17.1 ± 0.2 [10]
$Mg_2Cl(OH)_3.4H_2O(s)$ (Mg-Phase-3, Korsnunovskite) $+3H^+ = 2Mg^{+2} + Cl^- + 7H_2O$	26.02 [11]	Harvie et al. (1984); c.f., Altmaier et al. (2003), 26.0 ± 0.2 [12]
	26.03 [13]	Harvie et al. (1984)
$Mg_3Cl(OH)_5.4H_2O(s)$ (Mg-Phase-5) + $5H^+ = 3Mg^{+2} + Cl^- + 9H_2O$	42.96(±0.32)[14]	Xiong et al. (2010), p.4610, PACE
	42.92	Xiong et al. (2010), p.4610, PACE + Harvie et al. (1984)
	43.21(±0.33)	Xiong et al. (2010), p.4605, SIT
	-46.59	Xiong et al. (2010), p.4605, SIT + Harvie et al. (1984)
$MgCO_3.3H_2O(s)$ (Nesquehonite) + $H^+ = Mg^{+2} + HCO_3^- + 3H_2O$	5.17	Harvie et al. (1984)
$MgCO_3(s)$ (Magnesite) + $H^+ = Mg^{+2} + HCO_3^-$	2.50	Harvie et al. (1984)
$CaMg(CO_3)_2(s)$ (Dolomite) + $2H^+ = Ca^{+2} + Mg^{+2} + 2HCO_3^-$	3.59	Harvie et al. (1984)
$Mg_5(CO_3)_4(OH)_2.4H_2O(s)$ (Hydromagnesite5424) + $6H^+ = 5Mg^{+2} + 4HCO_3^- + 6H_2O$	32.25 [15]	Xiong (2005) < Robie and Hemingway (1973) + Harvie et al. (1984)
	31.49	Robie and Hemingway (1973) + Harvie et al. (1984)
$Mg_4(CO_3)_3(OH)_2.3H_2O(s)$ (Hydromagnesite4323) + $5H^+ = 4Mg^{+2} + 3HCO_3^- + 5H_2O$	28.81 [16]	Xiong (2005) < Langmuir (1965) + Harvie et al. (1984)
	28.53	Langmuir (1965) + Harvie et al. (1984)
$Na_2Mg(SO_4)_2.4H_2O(s)$ (Bloedite) = $2Na^+ + Mg^{+2} + 2SO_4^{-2} + 4H_2O$	-2.34	Harvie et al. (1984)
$MgSO_4.7H_2O(s)$ (Epsomite) = $Mg^{+2} + SO_4^{-2} + 7H_2O$	-1.88	Harvie et al. (1984)
$MgSO_4.6H_2O(s)$ (Hexahydrite) = $Mg^{+2} + SO_4^{-2} + 6H_2O$	-1.63	Harvie et al. (1984)
$KMgClSO_4.3H_2O(s)$ (Kainite) = $K^+ + Mg^{+2} + Cl^- + SO_4^{-2} + 3H_2O$	-0.19	Harvie et al. (1984)
$MgSO_4.H_2O(s)$ (Kieserite) = $Mg^{+2} + SO_4^{-2} + H_2O$	-0.12	Harvie et al. (1984)
$K_2Mg(SO_4)_2.6H_2O(s)$ (Picromerite/Schoenite) = $2K^+ + Mg^{+2} + 2SO_4^{-2} + 6H_2O$	-4.32	Harvie et al. (1984)
$K_2Mg(SO_4)_2.4H_2O(s)$ (Leonite) = $2K^+ + Mg^{+2} + 2SO_4^{-2} + 4H_2O$	-3.97	Harvie et al. (1984)
$K_2MgCa_2(SO_4)_4.2H_2O(s)$ (Polyhalite) = $2K^+ + Mg^{+2} + 2Ca^{+2} + 4SO_4^{-2} + 2H_2O$	-13.74	Harvie et al. (1984)
Ca		
$CaCl_2.4H_2O(s) = Ca^{+2} + 2Cl^- + 4H_2O$	5.71	Harvie et al. (1984)
$Ca(OH)_2(s)$ (Portlandite)+ $2H^+ = Ca^{+2} + 2H_2O$	22.80	Harvie et al. (1984)
$Ca_4Cl_2(OH)_6.13H_2O(s)$ (CaOxychloride_A) + $6H^+ = 4Ca^{+2} + 2Cl^- + 19H_2O$	68.73	Harvie et al. (1984)

[10] Altmaier et al. (2003) verified Harvie et al. (1984) by performing their own experiments different from the experiments performed in references cited in Harvie et al. (1984).
[11] Selected in data0.fm1
[12] Altmaier et al. (2003) verified Harvie et al. (1984) by performing their own experiments different from the experiments performed in references cited in Harvie et al. (1984).
[13] JJ's verification using Harvie et al. (1984)
[14] Selected in data0.fm1
[15] Selected in data0.fm1
[16] Selected in data0.fm1

Reactions	LogK	Source
$Ca_2Cl_2(OH)_2.H_2O(s)$ (CaOxychloride_B) + $2H^+ = 2Ca^{+2} + 2Cl^- + 3H_2O$	26.53	Harvie et al. (1984)
$CaCO_3(s)$ (Calcite) + $H^+ = Ca^{+2} + HCO_3^-$	1.93	Harvie et al. (1984)
$CaCO_3(s)$ (Aragonite) + $H^+ = Ca^{+2} + HCO_3^-$	2.11	Harvie et al. (1984)
$Na_2Ca(CO_3)_2.2H_2O(s)$ (Pirssonite) + $2H^+ = 2Na^+ + Ca^{+2} + 2HCO_3^- + 2H_2O$	11.43	Harvie et al. (1984)
$CaNa_2(CO_3)_2.5H_2O(s)$ (Gaylussite) + $2H^+ = Ca^{+2} + 2Na^+ + 2HCO_3^- + 5H_2O$	11.25	Harvie et al. (1984)
$CaSO_4(s)$ (Anhydrite) = $Ca^{+2} + SO_4^{-2}$	-4.36	Harvie et al. (1984)
$Na_2Ca(SO_4)_2(s)$ (Glauberite) = $2Na^+ + Ca^{+2} + 2SO_4^{-2}$	-5.24	Harvie et al. (1984)
$Na_4Ca(SO_4)_3.2H_2O(s)$ (Labile_Salt) = $4Na^+ + Ca^{+2} + 3SO_4^{-2} + 2H_2O$	-5.67	Harvie et al. (1984)
$CaSO_4.2H_2O(s)$ (Gypsum) = $Ca^{+2} + SO_4^{-2} + 2H_2O$	-4.58	Harvie et al. (1984)
$K_2Ca(SO_4)_2.H_2O(s)$ (Syngenite) = $2K^+ + Ca^{+2} + 2SO_4^{-2} + H_2O$	-7.44	Harvie et al. (1984)
$CaOxalate.H_2O(s)$ (Whewellite) = $Ca^{+2} + Oxalate^{-2} + H_2O$	-8.75	Xiong (2004), p.4 + Harvie et al. (1984)
K		
$KCl(s)$ (Sylvite) = $K^+ + Cl^-$	0.89	Harvie et al. (1984)
$K_2CO_3.3/2H_2O(s) + H^+ = 2K^+ + HCO_3^- + 1.5H_2O$	13.37	Harvie et al. (1984)
$KHCO_3(s)$ (Kalicinite) = $K^+ + HCO_3^-$	0.28	Harvie et al. (1984)
$K_8H_4(CO_3)_6.3H_2O(s) + 2H^+ = 8K^+ + 6HCO_3^- + 3H_2O$	27.68	Harvie et al. (1984)
$KNaCO_3.6H_2O(s) + H^+ = K^+ + Na^+ + HCO_3^- + 6H_2O$	10.22	Harvie et al. (1984)
$K_2NaH(CO_3)_2.2H_2O(s)$ (K_Trona) + $H^+ = 2K^+ + Na^+ + 2HCO_3^- + 2H_2O$	11.57	Harvie et al. (1984)
$K_3H(SO_4)_2(s) = 3K^+ + H^+ + 2SO_4^{-2}$	-3.54	Harvie et al. (1984)
$K_2SO_4(s)$ (Arcanite) = $2K^+ + SO_4^{-2}$	-1.77	Harvie et al. (1984)
$KHSO_4(s)$ (Mercallite) = $K^+ + H^+ + SO_4^{-2}$	-1.40	Harvie et al. (1984)
$K_8H_6(SO_4)_7(s) = 8K^+ + 6H^+ + 7SO_4^{-2}$	-10.80	Harvie et al. (1984)
$NaK_3(SO_4)_2(s)$ (Aphthitalite/Glaserite) = $Na^+ + 3K^+ + 2SO_4^{-2}$	-3.80	Harvie et al. (1984)
B		
$Na_2B_4O_7.10H_2O(s)$ (Borax) = $2Na^+ + 4B(OH)_4^- + 2H^+ + H_2O$	-24.49	Felmy and Weare (1986) + Harvie et al. (1984)
$B(OH)_3(s) + H_2O = H^+ + B(OH)_4^-$	-9.26	Felmy and Weare (1986) + Harvie et al. (1984)
$KB_5O_8.4H_2O(s)$ (K-Pentaborate(30C)) + $8H_2O = K^+ + 5B(OH)_4^- + 4H^+$	-41.52	Felmy and Weare (1986) + Harvie et al. (1984)
$K_2B_4O_7.4H_2O(s)$ (K-Tetraborate(30C)) + $5H_2O = 2K^+ + 4B(OH)_4^- + 2H^+$	-23.04 [17]	Felmy and Weare (1986) + Harvie et al. (1984)
	-23.05	Felmy and Weare (1986) + Harvie et al. (1984)
$NaBO_2.4H_2O(s)$ (Na_Metaborate) = $Na^+ + B(OH)_4^- + 2H_2O$	0.32	Felmy and Weare (1986) + Harvie et al. (1984)
$NaB_5O_8.5H_2O(s)$ (Na_Pentaborate) + $7H_2O = Na^+ + 5B(OH)_4^- + 4H^+$	-40.29 [18]	Felmy and Weare (1986) + Harvie et al. (1984)
	-40.30	Felmy and Weare (1986) + Harvie et al. (1984)
$NaBO_2.NaCl.2H_2O(s)$ (Teepleite(20C)) = $2Na^+ + B(OH)_4^- + Cl^-$	1.60	Felmy and Weare (1986) + Harvie et al. (1984)
Am(III): Analog Nd(III)		
$Am(OH)_3(s) + 3H^+ = Am^{+3} + 3H_2O$	14.49	Giambalvo (2002, An(III)) + Harvie et al. (1984)

[17] Selected in data0.fm1

[18] Selected in data0.fm1

Reactions	LogK	Source
$AmOHCO_3(s) + 2H^+ = Am^{+3} + H_2O + HCO_3^-$	1.63	Giambalvo (2002, An(III)) + Harvie et al. (1984)
$NaAm(CO_3)_2.6H_2O(s) + 2H^+ = Na^+ + Am^{+3} + 2HCO_3^- + 6H_2O$	-0.71	Giambalvo (2002, An(III)) + Harvie et al. (1984)
$AmPO_4(s) + H^+ = Am^{+3} + HPO_4^{-2}$	-12.45	Giambalvo (2002, An(III)) + Novak (1995) < Rai et al. (1992a,b), Rai et al. (1995a)[19]
Th(IV)		
$ThO_2(s, am) + 4H^+ = Th^{+4} + 2H_2O$	10.48	Giambalvo (2002, An(IV)) < Felmy et al. (1991) + Harvie et al. (1984)
$Th(SO_4)_2.9H_2O(s) = Th^{+4} + 2SO_4^{-2} + 9H_2O$	-12.99	Giambalvo (2002, An(IV)) < Felmy and Rai (1992) + Harvie et al. (1984)
$Th(SO_4)_2.8H_2O(s) = Th^{+4} + 2SO_4^{-2} + 8H_2O$	-12.89	Giambalvo (2002, An(IV)) < Felmy and Rai (1992) + Harvie et al. (1984)
$Th(SO_4)_2.Na_2SO_4.6H_2O(s)$ (16C) $= Th^{+4} + 2Na^+ + 3SO_4^{-2} + 6H_2O$	-17.64	Giambalvo (2002, An(IV)) < Felmy and Rai (1992) + Harvie et al. (1984)
$Th(SO_4)_2.K_2SO_4.4H_2O(s)$ (16C) $= Th^{+4} + 2K^+ + 3SO_4^{-2} + 4H_2O$	-18.07	Giambalvo (2002, An(IV)) < Felmy and Rai (1992) + Harvie et al. (1984)
$Th(SO_4)_2.2K_2SO_4.2H_2O(s)$ (16C) $= Th^{+4} + 4K^+ + 4SO_4^{-2} + 2H_2O$	-21.23	Giambalvo (2002, An(IV)) < Felmy and Rai (1992) + Harvie et al. (1984)
$2[Th(SO_4)_2.7/2K_2SO_4(s)]$ (16C) $= 2Th^{+4} + 14K^+ + 11SO_4^{-2}$	-49.31 [20]	Giambalvo (2002, An(IV)) < Felmy and Rai (1992) + Harvie et al. (1984)
	-49.32	Giambalvo (2002, An(IV)) < Felmy and Rai (1992) + Harvie et al. (1984)
Np(V)		
$NpO_2OH(s, aged) + H^+ = NpO_2^+ + H_2O$	4.51	Giambalvo (2002, An(V)), p.4 < log K in Neck et al. (1995) + Harvie et al. (1984)
$NpO_2OH(s, am) + H^+ = NpO_2^+ + H_2O$	5.21	Giambalvo (2002, An(V)), p.4 < log K in Neck et al. (1995) + Harvie et al. (1984)
$2[NaNpO_2CO_3.7/2H_2O(s)] + 2H^+ = 2Na^+ + 2NpO_2^+ + 2HCO_3^- + 7H_2O$	-1.50	Giambalvo (2002, An(V)), p.4 < log K in Neck et al. (1995) + Harvie et al. (1984)
$Na_3NpO_2(CO_3)_2(s) + 2H^+ = 3Na^+ + NpO_2^+ + 2HCO_3^-$	6.49	Giambalvo (2002, An(V)), p.4 < log K in Neck et al. (1995) + Harvie et al. (1984)
$KNpO_2CO_3(s) + H^+ = K^+ + NpO_2^+ + HCO_3^-$	-3.26	Giambalvo (2002, An(V)), p.4 < Novak et al. (1997) + Harvie et al. (1984)
$K_3NpO_2(CO_3)_2(s) + 2H^+ = 3K^+ + NpO_2^+ + 2HCO_3^-$	4.74	Giambalvo (2002, An(V)), p.4 < Novak et al. (1997) + Harvie et al. (1984)
Gas		
$CH_4(g) + 2O_2(g) = H^+ + H_2O + HCO_3^-$	135.49	data0.ymp.R5[21]
$CO_2(g) + H_2O = H^+ + HCO_3^-$	-7.81	data0.ymp.R5
$H_2(g) + 0.5O_2(g) = H_2O$	41.55	data0.ymp.R5
$H_2O(g) = H_2O$	1.49	data0.ymp.R5

******End of Table III.1-1******

[19] For Rai et al. (1995a), manuscript dated 1994 is cited in Novak (1995)

[20] Selected in data0.fm1

[21] Locator for data0.ymp.R5 is DTN: SN0612T0502404.014. Data0.ymp.R5 is the output of Wolery and Jove-Colon (2007).

Table III.1-2. Pitzer interaction parameters (PIPs) retrieved from data0.fm1. Selected PIPs will be consistently used for the thermodynamic model validation and parameterization: This Table continues through multiple pages until readers find "End of Table III.1-2".

i	*j*	α_1/α_2[A, 22]	$\beta^{(0)}$	$\beta^{(1)}$	$\beta^{(2)}$	C^{φ}	Source
Na^+	Cl^-	2.0/12.0	0.0765	0.2664	0.0	0.00127	Harvie et al. (1984)
Na^+	OH^-	2.0/12.0	0.0864	0.253	0.0	0.0044	Harvie et al. (1984)
Na^+	HCO_3^-	2.0/12.0	0.0277	0.0411	0.0	0.0	Harvie et al. (1984)
Na^+	CO_3^{-2}	2.0/12.0	0.0399	1.389	0.0	0.0044	Harvie et al. (1984)
Na^+	HSO_4^-	2.0/12.0	0.0454	0.398	0.0	0.0	Harvie et al. (1984)
Na^+	SO_4^{-2}	2.0/12.0	0.01958	1.113	0.0	0.00497	Harvie et al. (1984)
Na^+	$H_2PO_4^-$	2.0/12.0	-0.0533	0.0396	0.0	0.00795	Pitzer (1991)
Na^+	HPO_4^{-2}	2.0/12.0	-0.0583	1.466	0.0	0.0294	Pitzer (1991) (Error corrected)
Na^+	PO_4^{-3}	2.0/12.0	0.1781	3.851	0.0	-0.05154	Pitzer (1991)
Na^+	ClO_4^-	2.0/12.0	0.0554	0.2755	0.0	-0.00118	Pitzer (1991)
Na^+	Acetate-, [23]	2.0/12.0	0.1426	0.22	0.0	-0.00629	Choppin et al. (2001)
Na^+	$H_2Citrate^-$	2.0/12.0	-0.1296	0.29	0.0	0.013	Choppin et al. (2001)
Na^+	$HCitrate^{-2}$	2.0/12.0	-0.0989	1.74	0.0	0.027	Choppin et al. (2001)
Na^+	$Citrate^{-3}$, [24]	2.0/12.0	0.0887	5.22	0.0	0.047	Choppin et al. (2001)
Na^+	H_3EDTA^-	2.0/12.0	-0.2345	0.29	0.0	0.059	Choppin et al. (2001)
Na^+	H_2EDTA^{-2}	2.0/12.0	-0.1262	1.74	0.0	0.054	Choppin et al. (2001)
Na^+	$HEDTA^{-3}$	2.0/12.0	0.5458	5.22	0.0	-0.048	Choppin et al. (2001)
Na^+	$EDTA^{-4}$, [25]	2.0/12.0	1.016	11.6	0.0	0.001	Choppin et al. (2001)
Na^+	$Lactate^-$	2.0/12.0	-0.0563	0.29	0.0	0.047	Choppin et al. (2001)
Na^+	HOxalate	2.0/12.0	-0.2448	0.29	0.0	0.068	Choppin et al. (2001)
Na^+	$Oxalate^{-2}$, [26]	2.0/12.0	-0.2176	1.74	0.0	0.122	Choppin et al. (2001)
Na^+	$MgCitrate^-$	2.0/12.0	0.1742	0.29	0.0	-0.06923	Giambalvo (2002, Org)
Na^+	$CaCitrate^-$	2.0/12.0	0.1742	0.29	0.0	-0.06923	Analogue to Mg in Giambalvo (2002, Org)
Na^+	$MgEDTA^{-2}$	2.0/12.0	0.2134	1.74	0.0	0.00869	Giambalvo (2002, Org)
Na^+	$CaEDTA^{-2}$	2.0/12.0	0.2134	1 74	0.0	0 00869	Analogue to Mg in Giambalvo (2002, Org)
Na^+	$B(OH)_4^-$	2.0/12.0	-0.0427	0.089	0.0	0 0114	Felmy and Weare (1986)
Na^+	$B_3O_3(OH)_4^-$	2.0/12.0	-0.056	-0.91	0.0	0.0	Felmy and Weare (1986)
Na^+	$B_4O_5(OH)_4^{-2}$	2.0/12.0	-0.11	-0.4	0 0	0.0	Felmy and Weare (1986)
Na^+	$Am(CO_3)_2^-$	2.0/12.0	-0.24	0.224	0.0	0.0284	Fanghanel et al. (1999)
Na^+	$Am(CO_3)_3^{-3}$	2.0/12.0	0 125	4 73	0.0	0 0007	Fanghanel et al. (1999)
Na	$Am(CO_3)_4^{-5}$	2.0/12.0	2.022	19.22	0.0	-0.305	Fanghanel and Kim (1998), Fanghanel et al. (1995)
Na^+	$Am(SO_4)_2^-$	2.0/12.0	-0.354	0 4	0.0	0.051	Fanghanel and Kim (1998)
Na [27]	AmEDTA	2.0/12.0	-0.2239	0.29	0.0	0 002	Choppin et al. (2001), typo in original
Na^+	$Th(CO_3)_5^{-6}$	2.0/12.0	1.31	30	0 0	0 0	Felmy and Rai (1992)
Na^+	$Th(SO_4)_3^{-2}$	2.0/12.0	0 12	0.0	0.0	0 0	Felmy and Rai (1992)
Na^+	$NpO_2CO_3^-$	2.0/12.0	0.1	0.34	0.0	0.0	Fanghanel et al. (1995)
Na^+	$NpO_2(CO_3)_2^{-3}$	2.0/12.0	0.48	4.4	0.0	0.0	Fanghanel et al. (1995)

[22] α_1 and α_2 are pre-set constants used in the Pitzer activity coefficient equation. α_1 and α_2 apply for only cation-anion binary pair. α_2 is not applied when $\beta^{(2)}$ is zero or not used. Unit for α_1 and α_2 is $kg^{1/2} \cdot mol^{-1/2}$.

[23] Acetate-: $C_2H_3O_2^-$

[24] $Citrate^{3-}$: $C_6H_5O_7^{3-}$

[25] $EDTA^{4-}$: $C_{10}H_{12}O_8N_2^{4-}$

[26] $Oxalate^{2-}$: $C_2O_4^{2-}$

[27] Cl^- is mistakenly listed in the place of Na^+ in Choppin et al. (2001), p.97

Na^+	$NpO_2(CO_3)_3^{-5}$	2.0/12.0	1.8	22.7	0.0	0.0	Fanghanel et al. (1995)
$Na^{+,28}$	$NpO_2Citrate^{-2}$	2.0/12.0	-0.4226	1.75	0.0	0.142	Choppin et al. (2001), typo in original
$Na^{+,29}$	$NpO_2EDTA^{-3,30}$	2.0/12.0	0.683	5.911	0.0	0.0	Choppin et al. (2001), listed correctly in Pokrovsky et al. (1998)
Na^+	NpO_2HEDTA^{-2}	2.0/12.0	0.4733	-1.504	0.0	0.0	Pokrovsky et al. (1998)
Na^+	$NpO_2H_2EDTA^-$	2.0/12.0	-0.8285	0.2575	0.0	0.256	Pokrovsky et al. (1998)
$Na^{+\ 31}$	$NpO_2Oxalate^-$	2.0/12.0	-0.5418	0.29	0.0	0.095	Choppin et al. (2001), correctly listed in Borkowski et al. (2001)
K^+	Cl^-	2.0/12.0	0.04835	0.2122	0.0	-0.00084	Harvie et al. (1984)
K^+	OH^-	2.0/12.0	0.1298	0.32	0.0	0.0041	Harvie et al. (1984)
K^+	HCO_3^-	2.0/12.0	0.0296	-0.013	0.0	-0.008	Harvie et al. (1984)
K^+	CO_3^{-2}	2.0/12.0	0.1488	1.43	0.0	-0.0015	Harvie et al. (1984)
K^+	SO_4^{-2}	2.0/12.0	0.04995	0.7793	0.0	0.0	Harvie et al. (1984)
K^+	HSO_4	2.0/12.0	-0.0003	0.1735	0.0	0.0	Harvie et al. (1984)
K^+	H_2PO_4	2.0/12.0	-0.0678	-0.1042	0.0	0.0	Pitzer (1991)
K^+	HPO_4^{-2}	2.0/12.0	0.0248	1.274	0.0	0.0164	Pitzer (1991)
K^+	PO_4^{-3}	2.0/12.0	0.3729	3.972	0.0	-0.0868	Pitzer (1991)
K^+	$Acetate^-$	2.0/12.0	0.1587	0.3251	0.0	-0.0066	Source unknown
K^+	$H_2Citrate^-$	2.0/12.0	-0.1296	0.29	0.0	0.013	Analog to Na in Choppin et al. (2001)
K^+	$HCitrate^{-2}$	2.0/12.0	-0.0989	1.74	0.0	0.027	Analog to Na in Choppin et al. (2001)
K^+	$Citrate^{-3}$	2.0/12.0	0.0887	5.22	0.0	0.047	Analog to Na in Choppin et al. (2001)
K^+	H_3EDTA^-	2.0/12.0	-0.2345	0.29	0.0	0.059	Analog to Na in Choppin et al. (2001)
K^+	H_2EDTA^{-2}	2.0/12.0	-0.1262	1.74	0.0	0.054	Analog to Na in Choppin et al. (2001)
K^+	$HEDTA^{-3}$	2.0/12.0	0.5458	5.22	0.0	-0.048	Analog to Na in Choppin et al. (2001)
K^+	$EDTA^{-4}$	2.0/12.0	1.016	11.6	0.0	0.001	Analog to Na in Choppin et al. (2001)
K^+	$Lactate^-$	2.0/12.0	-0.0563	0.29	0.0	0.047	Analog to Na in Choppin et al. (2001)
K^+	$HOxalate^-$	2.0/12.0	-0.2448	0.29	0.0	0.068	Analog to Na in Choppin et al. (2001)
K^+	$Oxalate^{-2}$	2.0/12.0	-0.2176	1.74	0.0	0.122	Analog to Na in Choppin et al. (2001)
K^+	$MgCitrate^-$	2.0/12.0	0.1742	0.29	0.0	-0.06923	Analog to Na^+/$MgCitrate^-$ in Giambalvo (2002, Org)
K^+	$MgEDTA^{-2}$	2.0/12.0	0.2134	1.74	0.0	0.00869	Analog to Na^+/$MgEDTA^{-2}$ in Giambalvo (2002, Org)
K^+	$CaCitrate^-$	2.0/12.0	0.1742	0.29	0.0	-0.06923	Analog to Na^+/$MgCitrate^-$ in Giambalvo (2002, Org)
K^+	$CaEDTA^{-2}$	2.0/12.0	0.2134	1.74	0.0	0.00869	Analog to Na^+/$MgEDTA^{-2}$ in Giambalvo (2002, Org)
K^+	$B(OH)_4^-$	2.0/12.0	0.035	0.14	0.0	0.0	Felmy and Weare (1986)
K^+	$B_3O_3(OH)_4^-$	2.0/12.0	-0.13	0.0	0.0	0.0	Felmy and Weare (1986)

[28] Cl^- is mistakenly listed in the place of Na^+ in Choppin et al. (2001), p.97
[29] Cl^- is mistakenly listed in the place of Na^+ in Choppin et al. (2001), p.97
[30] Typo in Choppin et al. (2001), p.97
[31] Cl^- is mistakenly listed in the place of Na^+ in Choppin et al. (2001), p.97

K^+	$B_4O_5(OH)_4^{-2}$	2.0/12.0	-0.022	0.0	0.0	0.0	Felmy and Weare (1986)
K^+	$Am(CO_3)_2^-$	2.0/12.0	-0.24	0.224	0.0	0.0284	Fanghanel and Kim (1998)
K^+	$Am(CO_3)_3^{-3}$	2.0/12.0	0.125	4.73	0.0	0.0007	Fanghanel and Kim (1998)
K^+	$Am(CO_3)_4^{-5}$	2.0/12.0	2.022	19.22	0.0	-0.305	Analog to Na in Fanghanel and Kim (1998)
K^+	$Am(SO_4)_2^-$	2.0/12.0	-0.354	0.4	0.0	0.051	Analog to Na in Fanghanel and Kim (1998)
K^+	$AmEDTA^-$	2.0/12.0	-0.2239	0.29	0.0	0.002	Analog to Na in Choppin et al. (2001)
K^+	$Th(CO_3)_5^{-6}$	2.0/12.0	1.31	30	0.0	0.0	Felmy et al. (1997)
K^+	$Th(SO_4)_3^{-2}$	2.0/12.0	0.9	0.0	0.0	0.0	Felmy and Rai (1992)
K^+	NpO_2CO_3	2.0/12.0	0.1	0.34	0.0	0.0	Novak et al. (1997)
K^+	$NpO_2(CO_3)_2^{-3}$	2.0/12.0	0.48	4.4	0.0	0.0	Novak et al. (1997)
K^+	$NpO_2(CO_3)_3^{-5}$	2.0/12.0	2.34	22.7	-96	-0.22	Novak et al. (1997)
K^+	$NpO_2Citrate^{-2}$	2.0/12.0	-0.4226	1.75	0.0	0.142	Analog to Na in Choppin et al. (2001)
K^+	$NpO_2H_2EDTA^-$	2.0/12.0	-0.8285	0.2575	0.0	0.256	Pokrovsky et al. (1998)
K^+	NpO_2HEDTA^{-2}	2.0/12.0	0.4733	-1.504	0.0	0.0	Analog to Na^+/NpO_2EDTA^{-2} in Pokrovsky et al. (1998)
K^+	NpO_2EDTA^{-3}	2.0/12.0	0.683	5.911	0.0	0.0	Analog to Na in Choppin et al. (2001)
$K^{+,\ 32}$	$NpO_2Oxalate^-$	2.0/12.0	-0.5418	0.29	0.0	0.095	Analog to Na in Choppin et al. (2001)
Ca^{+2}	Cl^-	2.0/12.0	0.3159	1.614	0.0	-0.00034	Harvie et al. (1984)
Ca^{+2}	OH^-	2.0/12.0	-0.1747	-0.2303	-5.72	0.0	Harvie et al. (1984)
Ca^{+2}	HCO_3	2.0/12.0	0.4	2.977	0.0	0.0	Harvie et al. (1984)
Ca^{+2}	SO_4^{-2}	1.4/12.0	0.2	3.1973	-54.24	0.0	Harvie et al. (1984)
Ca^{+2}	HSO_4	2.0/12.0	0.2145	2.53	0.0	0.0	Harvie et al. (1984)
Ca^{+2}	ClO_4	2.0/12.0	0.4511	1.756	0.0	-0.005	Pitzer (1991)
Ca^{+2}	$NpO_2CO_3^-$	2.0/12.0	0.1	0.34	0.0	0.0	Analog to Na^+ in Fanghanel et al. (1995)
Ca^{+2}	$NpO_2(CO_3)_2^{-3}$	1.4/50.0	0.48	4.4	0.0	0.0	Analog to Na^+ in Fanghanel et al. (1995)
Ca^{+2}	$NpO_2(CO_3)_3^{-5}$	1.4/50.0	2.07	22.7	-48	-0.11	$\beta^{(0)}$, $\beta^{(2)}$, and C^ϕ are averages of those of $Na^+/NpO_2(CO_3)_3^{-5}$ (Fanghanel et al, 1995) and $K^+/NpO_2(CO_3)_3^{-5}$ (Novak et al., 1997)
$CaB(OH)_4^+$	Cl^-	2.0/12.0	0.12	0.0	0.0	0.0	Felmy and Weare (1986)
$CaAcetate^+$	Cl^-	2.0/12.0	-0.0833	0.29	0.0	0.0987	Analog to $MgAcetate^+/Cl^-$ in Giambalvo (2002, Org)
Mg^{+2}	Cl^-	2.0/12.0	0.35235	1.6815	0.0	0.00519	Harvie et al. (1984)
Mg^{+2}	HCO_3	2.0/12.0	0.329	0.6072	0.0	0.0	Harvie et al. (1984)
Mg^{+2}	SO_4^{-2}	1.4/12.0	0.221	3.343	-37.23	0.025	Harvie et al. (1984)
Mg^{+2}	HSO_4	2.0/12.0	0.4746	1.729	0.0	0.0	Harvie et al. (1984)
Mg^{+2}	ClO_4	2.0/12.0	0.4961	2.008	0.0	0.009578	Harvie et al. (1984)
Mg^{+2}	$NpO_2CO_3^-$	2.0/12.0	0.1	0.34	0.0	0.0	Analog to Na^+ in Fanghanel et al. (1995)
Mg^{+2}	$NpO_2(CO_3)_2^{-3}$	1.4/50.0	0.48	4.4	0.0	0.0	Analog to Na^+ in Fanghanel et al. (1995)
Mg^{+2}	$NpO_2(CO_3)_3^{-5}$	1.4/50.0	2.07	22.7	-48	-0.11	$\beta^{(0)}$, $\beta^{(2)}$, and C^ϕ are averages of those of $Na^+/NpO_2(CO_3)_3^{-5}$ (Fanghanel et al, 1995) and

[32] Cl^- is mistakenly listed in the place of Na^+ in Choppin et al. (2001), p.97

							$K^+/NpO_2(CO_3)_3^{-5}$ (Novak, 1997)
$MgOH^+$	Cl^-	2.0/12.0	-0.1	1.658	0.0	0.0	Harvie et al. (1984)
$MgB(OH)_4^+$	Cl^-	2.0/12.0	0.16	0.0	0.0	0.0	Felmy and Weare (1986)
$MgAcetete^+$	Cl^-	2.0/12.0	-0.0833	0.29	0.0	0.0987	Giambalvo (2002, Org)
H^+	Cl^-	2.0/12.0	0.1775	0.2945	0.0	0.0008	Harvie et al. (1984)
H^+	SO_4^{-2}	2.0/12.0	0.0298	0.0	0.0	0.0438	Harvie et al. (1984)
H^+	HSO_4	2.0/12.0	0.2065	0.5556	0.0	0.0	Harvie et al. (1984)
H^+	ClO_4	2.0/12.0	0.1747	0.2931	0.0	0.00819	Pitzer (1991)
H^+	$Th(SO_4)_3^{-2}$	2.0/12.0	0.84	0.0	0.0	0.0	Felmy and Rai (1992)
Am^{+3}	Cl^-	2.0/12.0	0.5856	5.6	0.0	-0.0166	Fanghanel and Kim (1998), Konnecke et al. (1997)
$AmCl^{+2}$	Cl^-	2.0/12.0	0.593	3.15	0.0	-0.006	Fanghanel and Kim (1998), Konnecke et al. (1997) in analogy to Cm
$AmCl_2^+$	Cl^-	2.0/12.0	0.516	1.75	0.0	0.01	Fanghanel and Kim (1998), Konnecke et al. (1997) in analogy to Cm
$AmOH^{+2}$	Cl^-	2.0/12.0	-0.055	1.6	0.0	0.05	Fanghanel and Kim (1998), Konnecke et al. (1997) in analogy to Cm
$Am(OH)_2^+$	Cl^-	2.0/12.0	-0.616	-0.45	0.0	0.05	Fanghanel and Kim (1998), Konnecke et al. (1997) in analogy to Cm
Am^{+3}	SO_4^{-2}	1.4/50.0	1.792	15.04	0.0	0.6	Fanghanel and Kim (1998)
Am^{+3}	ClO_4	2.0/12.0	0.8	5.35	0.0	-0.0048	Felmy et al. (1990)
Am^{+3}	H_2PO_4	2.0/12.0	0.0	0.0	-92.9	0.0	Rai et al. (1995a)
$AmCO_3^+$	Cl^-	2.0/12.0	-0.072	0.403	0.0	0.0388	Fanghanel and Kim (1998), Fanghanel et al. (1999) in analogy to Cm
$AmSO_4^+$	Cl^-	2.0/12.0	-0.091	-0.39	0.0	0.048	Fanghanel and Kim (1998) in analogy to Cm
$AmAcetate^{+2}$	Cl^-	2.0/12.0	0.3088	1.74	0.0	-0.132	Giambalvo (2002, Org)
$AmLactate^{+2}$	Cl^-	2.0/12.0	0.8397	1.74	0.0	-0.332	Giambalvo (2002, Org) < Choppin et al. (2001)[33]
$AmOxalate^+$	Cl^-	2.0/12.0	-0.9374	0.29	0.0	0.248	Giambalvo (2002, Org) < Choppin et al. (2001) + Borkowski et al. 2001
Th^{+4}	Cl^-	2.0/12.0	1.092	13.7	-160	-0.112	Roy et al. (1992)
Th^{+4}	SO_4^{-2}	1.4/50.0	1.56	0.0	0.0	0.0	Felmy and Rai (1992)
Th^{+4}	HSO_4	2.0/12.0	1.44	0.0	0.0	0.0	Felmy and Rai (1992)
Th^{+4}	ClO_4^-	2.0/12.0	1.19	27.3	0.0	-0.057	Novak (1996, Preliminary ...)
$ThAcetate^{+3}$	Cl^-	2.0/12.0	1.061	5.22	0.0	0.109	Giambalvo (2002, Org) < Choppin et al. (2001)
$Th(Acetate)_2^{+2}$	Cl^-	2.0/12.0	0.4671	1.74	0.0	0.143	Giambalvo (2002, Org) < Moore et al. 1999
$ThCitrate^+$	Cl^-	2.0/12.0	-0.7467	0.29	0.0	0.319	Giambalvo (2002, Org) < Choppin et al. (2001)
$ThLactate^{+3}$	Cl^-	2.0/12.0	0.6677	5.22	0.0	0.341	Giambalvo (2002, Org) < Choppin et al. (2001) < Moore et al. (1999)

[33] Need to be corrected in data0.fm1

$Th(Lactate)_2^{+2}$	Cl^-	2.0/12.0	0.5058	1.74	0.0	0.225	Giambalvo (2002, Org) < Moore et al. 1999
$ThOxalate^{+2}$	Cl^-	2.0/12.0	-0.343	1.74	0.0	0.5	Choppin et al. (2001), Borkowski et al. (2001)
NpO_2^+	Cl^-	2.0/12.0	0.1415	0.281	0.0	0.0	Neck et al. (1995)
NpO_2^+	ClO_4	2.0/12.0	0.257	0.18	0.0	0.0081	Neck et al. (1995)

i	*j*	$\theta_{cc'}$ or $\theta_{aa'}$	Source
Na^+	K^+	-0.012	Harvie et al. (1984)
Na^+	Ca^{+2}	0.07	Harvie et al. (1984)
Na^+	Mg^{+2}	0.07	Harvie et al. (1984)
Na^+	H^+	0.036	Harvie et al. (1984)
Na^+	Am^{+3}	0.1	Analog to Na^+/Cm^{+3} in Fanghanel and Kim (1998)
Na^+	Th^{+4}	0.42	Rai et al. (1997)
K^+	Ca^{+2}	0.032	Harvie et al. (1984)
K^+	H^+	0.005	Harvie et al. (1984)
K^+	Am^{+3}	0.1	Analog to Na^+/Cm^{+3} in Fanghanel and Kim (1998)
K^+	Th^{+4}	0.42	Analog to Na^+/Th^{+4} in Rai et al. (1997)
Ca^{+2}	Mg^{+2}	0.007	Harvie et al. (1984)
Ca^{+2}	H^+	0.092	Harvie et al. (1984)
Ca^{+2}	Am^{+3}	0.2	Analog to Ca^{+2}/Cm^{+3} in Fanghanel and Kim (1998)
Ca^{+2}	$AmCl^{+2}$	-0.014	Analog to $Ca^{+2}/CmCl^{+2}$ in Fanghanel and Kim (1998)[34]
Ca^{+2}	$AmCl_2^+$	-0.196	Analog to $Ca^{+2}/CmCl_2^+$ in Fanghanel and Kim (1998) [35]
Ca^{+2}	Th^{+4}	0.6	Analog to Mg^{+2}/Th^{+4} in Rai et al. (1997)
Mg^{+2}	H^+	0.10	Harvie et al. (1984)
Mg^{+2}	Am^{+3}	0.2	Analog to Ca^{+2}/Cm^{+3} in Fanghanel and Kim (1998)
Mg^{+2}	$AmCl^{+2}$	-0.014	Analog to $Ca^{+2}/CmCl^{+2}$ in Fanghanel and Kim (1998)
Mg^{+2}	$AmCl_2^+$	-0.196	Analog to $Ca^{+2}/CmCl_2^+$ in Fanghanel and Kim (1998)
Mg^{+2}	Th^{+4}	0.6	Rai et al. (1997)
H^+	Th^{+4}	0.6	Roy et al. (1992)
Cl^-	SO_4^{-2}	0.02	Harvie et al. (1984)
Cl-	OH^-	-0.050	Harvie et al. (1984)
Cl^-	HSO_4^-	-0.006	Harvie et al. (1984)
Cl-	HCO_3^-	0.03	Harvie et al. (1984)
Cl-	CO_3^{-2}	-0.02	Harvie et al. (1984)
Cl-	$H_2PO_4^-$	0.1	Pitzer and Silvester (1976)
Cl-	$B(OH)_4^-$	-0.065	Felmy and Weare (1986)

[34] Source information in data0.fm1 indicates that the value is in analogy to Mg in Fanghanel and Kim (1998), which is incorrect. Fanghanel and Kim (1998) is about Cm in $CaCl_2$ solution, not Mg solution.

[35] Source information in data0.fm1 indicates that the value is in analogy to Mg in Fanghanel and Kim (1998), which is incorrect. Fanghanel and Kim (1998) is about Cm in $CaCl_2$ solution, not Mg solution.

Cl^-	$B_3O_3(OH)_4^-$	0.12	Felmy and Weare (1986)
Cl^-	$B_4O_5(OH)_4^{-2}$	0.074	Felmy and Weare (1986)
Cl^-	$Acetate^-$	-0.09	Novak et al. (1996)
Cl^-	$Th(CO_3)_5^{-6}$	1.8	Moore et al. 1999 [36]; Felmy and Rai (1999), p.542
Cl^-	$NpO_2(OH)_2^-$	-0.24	Fanghanel et al. (1995)
Cl^-	$NpO_2CO_3^-$	-0.21	Fanghanel et al. (1995)
Cl^-	$NpO_2(CO_3)_2^{-3}$	-0.26	Fanghanel et al. (1995)
Cl^-	$NpO_2(CO_3)_3^{-5}$	-0.26	Fanghanel et al. (1995)
SO_4^{-2}	OH^-	-0.013	Harvie et al. (1984)
SO_4^{-2}	HCO_3^-	0.01	Harvie et al. (1984)
SO_4^{-2}	CO_3^{-2}	0.02	Harvie et al. (1984)
SO_4^{-2}	$B(OH)_4^-$	-0.012	Felmy and Weare (1986)
SO_4^{-2}	$B_3O_3(OH)_4^-$	0.1	Felmy and Weare (1986)
SO_4^{-2}	$B_4O_5(OH)_4^{-2}$	0.12	Felmy and Weare (1986)
OH^-	CO_3^{-2}	0.1	Harvie et al. (1984)
OH^-	ClO_4^-	-0.032	Pitzer (1991)
HCO_3	CO_3^{-2}	-0.04	Harvie et al. (1984)
HCO_3	$B_3O_3(OH)_4^-$	-0.1	Felmy and Weare (1986)
HCO_3^-	$B_4O_5(OH)_4^{-2}$	-0.087	Felmy and Weare (1986)
HCO_3	ClO_4	0.095	Neck et al. (1995)
CO_3^{-2}	ClO_4	0.21	Neck et al. (1995)
CO_3^{-2}	$NpO_2(CO_3)_3^{-5}$	-1.9	Neck et al. (1995)
ClO_4	$Th(CO_3)_5^{-6}$	5.5	Felmy et al. (1997)[37]
i	***j***	λ_{nc} **or** λ_{na}	
λ: neu -cat			
$CO_2(aq)$	H^+	0.0	By Harvie et al. (1984) convention
$CO_2(aq)$	Na^+	0.1	Harvie et al. (1984)
$CO_2(aq)$	K^+	0.051	Harvie et al. (1984)
$CO_2(aq)$	Ca^{+2}	0.183	Harvie et al. (1984)
$CO_2(aq)$	Mg^{+2}	0.183	Harvie et al. (1984)
$O_2(aq)$	Ca^{+2}	0.2497	Clegg and Brimblecombe (1990)
$O_2(aq)$	H^+	0.03528	Clegg and Brimblecombe (1990)
$O_2(aq)$	K^+	0.1519	Clegg and Brimblecombe (1990)
$O_2(aq)$	Mg^{+2}	0.2298	Clegg and Brimblecombe (1990)
$O_2(aq)$	Na^+	0.1602	Clegg and Brimblecombe (1990)
$B(OH)_3(aq)$	H^+	0.0	By Harvie et al. (1984) convention

[36] Source uncertain. Moore et al. (1999) does not contain this interaction parameter. Neither does Felmy et al. (1997).
[37] Proposed therein

$B(OH)_3(aq)$	Na^+	-0.097	Felmy and Weare (1986)[38]
$B(OH)_3(aq)$	K^+	-0.14	Felmy and Weare (1986)
$B(OH)_3(aq)$	$MgOH^+$	0.0	Required for populate zeta parameter. Currently not in use.
$B(OH)_3(aq)$	$AmCO_3^+$	0.0	Required for populate zeta parameter. Currently not in use.
$H_3PO_4(aq)$	H^+	0.29	Pitzer and Silvester (1976)
$H_3PO_4(aq)$	K^+	-0.07	Pitzer and Silvester (1976)
$Am(OH)_3(aq)$	H^+	0.0	By Harvie et al. (1984) convention
$Am(OH)_3(aq)$	Na^+	-0.2	Analog to $Cm(OH)_3(aq)/Na^+$ in Fanghanel and Kim (1998)
$Am(OH)_3(aq)$	K^+	-0.2	Analog to $Cm(OH)_3(aq)/Na^+$ in Fanghanel and Kim (1998)
λ: neu - ani			
$CO_2(aq)$	Cl^-	-0.005	Harvie et al. (1984)
$CO_2(aq)$	SO_4^{-2}	0.097	Harvie et al. (1984)
$CO_2(aq)$	HSO_4^-	-0.003	Harvie et al. (1984)
$O_2(aq)$	Cl^-	0.0	Clegg and Brimblecombe (1990), by convention
$O_2(aq)$	Br^-	-0.0347	Clegg and Brimblecombe (1990)
$O_2(aq)$	CO_3^{-2}	0.09648	Clegg and Brimblecombe (1990)
$O_2(aq)$	HCO_3^-	0.0854	Clegg and Brimblecombe (1990)[39]
$O_2(aq)$	NO_3^-	-0.0377	Clegg and Brimblecombe (1990)
$O_2(aq)$	OH^-	0.05222	Clegg and Brimblecombe (1990)[40]
$O_2(aq)$	SO_4^{-2}	0.08777	Clegg and Brimblecombe (1990)
$B(OH)_3(aq)$	Cl^-	0.091	Felmy and Weare (1986)
$B(OH)_3(aq)$	SO_4^{-2}	0.018	Felmy and Weare (1986)
$B(OH)_3(aq)$	$B_3O_3(OH)_4^-$	-0.2	Felmy and Weare (1986)
$NpO_2OH(aq)$	Cl^-	-0.19	Fanghanel et al. (1995)
$H_3PO_4(aq)$	Cl^-	0.0	Clegg and Brimblecombe (1990) convention; Pitzer and Silvester (1976)
$H_3PO_4(aq)$	$H_2PO_4^-$	-0.4	Pitzer and Silvester (1976)
CaOxalate(aq)	Cl^-	0.0189	Analog to MgOxalate(aq)/Cl^- in Giambalvo (2002, Org)
MgOxalate(aq)	Cl^-	0.0189	Giambalvo (2002, Org)
$Am(OH)_3(aq)$	Cl^-	-0.2	Analog to Cm(OH)3(aq)/Cl^- in Fanghanel and Kim (1998)
AmCitrate(aq)	Cl^-	-0.406	Choppin et al. (2001)

[38] Incorrect reference is cited in data0.fm1 for this pair. Correct one is Felmy and Weare (1986), not Harvie et al. (1984).
[39] Obtained from high pressure data
[40] The value listed in Clegg and Brimblecombe (1990) is 0.0500.

$Th(SO_4)_2(aq)$	Cl^-	0.29	Roy et al. (1992)[41]; Felmy and Rai (1992)
$Th(SO_4)_2(aq)$	HSO_4^-	0.68	Roy et al. (1992)[42] ; Felmy and Rai (1992)
ThEDTA(aq)	Cl^-	0.1111	Giambalvo (2002, Org)
NpO_2Acetate(aq)	Cl^-	-0.104	Giambalvo (2003, FMT, Release ...)
NpO_2Lactate(aq)	Cl^-	0.015	Choppin et al. (2001)
$CO_2(aq)$	$CO_2(aq)$	0.0	Template only. Currently not in use.
$B(OH)_3(aq)$	$B(OH)_3(aq)$	0.0	Template only. Currently not in use.
$CO_2(aq)$	$B(OH)_3(aq)$	0.0	Template only. Currently not in use.

i	*j*	*k*	$\psi_{cc'a}$ or $\psi_{aa'c}$	Source
Na^+	K^+	Cl^-	-0.0018	Harvie et al. (1984)
Na^+	K^+	SO_4^{-2}	-0.01	Harvie et al. (1984)
Na^+	K^+	HCO_3	-0.003	Harvie et al. (1984)
Na^+	K^+	CO_3^{-2}	0.003	Harvie et al. (1984)
Na^+	Ca^{+2}	Cl^-	-0.007	Harvie et al. (1984)
Na^+	Ca^{+2}	SO_4^{-2}	-0.055	Harvie et al. (1984)
Na^+	Mg^{+2}	Cl^-	-0.012	Harvie et al. (1984)
Na^+	Mg^{+2}	SO_4^{-2}	-0.015	Harvie et al. (1984)
Na^+	H^+	Cl^-	-0.004	Harvie et al. (1984)
Na^+	H^+	HSO_4	-0.0129	Harvie et al. (1984)
Na^+	H^+	ClO_4	-0.016	Neck et al. (1995)
Na^+	Th^{+4}	Cl^-	0.21	Rai et al. (1997)
K^+	Ca^{+2}	Cl^-	-0.025	Harvie et al. (1984)
K^+	Mg^{+2}	Cl^-	-0.022	Harvie et al. (1984)
K^+	Mg^{+2}	SO_4^{-2}	-0.048	Harvie et al. (1984)
K^+	H^+	Cl^-	-0.011	Harvie et al. (1984)
K^+	H^+	SO_4^{-2}	0.197	Harvie et al. (1984)
K^+	H^+	HSO_4	-0.0265	Harvie et al. (1984)
K^+	Th^{+4}	Cl^-	0.21	Analog to $Na^+/Th^{+4}/Cl^-$ in Rai et al. (1997)
Ca^{+2}	Mg^{+2}	Cl^-	-0.012	Harvie et al. (1984)
Ca^{+2}	Mg^{+2}	SO_4^{-2}	0.024	Harvie et al. (1984)[43]
Ca^{+2}	H^+	Cl^-	-0.015	Harvie et al. (1984)
Ca^{+2}	Th^{+4}	Cl^-	0.21	Analog to $Mg^{+2}/Th^{+4}/Cl^-$ in Rai et al. (1997)
Mg^{+2}	$MgOH^+$	Cl^-	0.028	Harvie et al. (1984)
Mg^{+2}	H^+	Cl^-	-0.011	Harvie et al. (1984)
Mg^{+2}	H^+	HSO_4	-0.0178	Harvie et al. (1984)
Mg^{+2}	Th^{+4}	Cl^-	0.21	Rai et al. (1997)
H^+	Th^{+4}	Cl^-	0.37	Roy et al. (1992)
aa'c			**psi (ψ)**	
Cl^-	SO_4^{-2}	Na^+	0.0014	Harvie et al. (1984)
Cl^-	SO_4^{-2}	Ca^{+2}	-0.018	Harvie et al. (1984)
Cl^-	SO_4^{-2}	Mg^{+2}	-0.004	Harvie et al. (1984)

[41] Reference cited for this pair is Roy et al. (1992) in data0.fm1. Roy et al. (1992) is about HCl-ThCl4-H2O system. No SO_4^{-2} is discusssed.

[42] Reference cited for this pair is Roy et al. (1992) in data0.fm1. Roy et al. (1992) is about HCl-ThCl4-H2O system. No SO_4^{-2} is discusssed.

[43] Reference is missing in data0.fm1 for this triplet. Harvie et al. (1984) contains the values for this triplet.

Cl^-	HSO_4	Na^+	-0.006	Harvie et al. (1984)
Cl^-	HSO_4	H^+	0.013	Harvie et al. (1984)
Cl^-	OH^-	Na^+	-0.006	Harvie et al. (1984)
Cl^-	OH^-	K^+	-0.006	Harvie et al. (1984)
Cl^-	OH^-	Ca^{+2}	-0.025	Harvie et al. (1984)
Cl^-	HCO_3	Na^+	-0.015	Harvie et al. (1984)
Cl^-	HCO_3	Mg^{+2}	-0.096	Harvie et al. (1984)
Cl^-	CO_3^{-2}	Na^+	0.0085	Harvie et al. (1984)
Cl^-	CO_3^{-2}	K^+	0.004	Harvie et al. (1984)
Cl^-	$B(OH)_4^-$	Na^+	-0.0073	Felmy and Weare (1986)
Cl^-	$B_3O_3(OH)_4$	Na^+	-0.024	Felmy and Weare (1986)
Cl^-	$B_4O_5(OH)_4^{-2}$	Na^+	0.026	Felmy and Weare (1986)
Cl^-	H_2PO_4	K^+	-0.01	Pitzer and Silvester (1976)
Cl^-	$Th(CO_3)_5^{-6}$	Na^+	0.3	Felmy and Rai (1999), p.542
Cl^-	$Th(CO_3)_5^{-6}$	K^+	0.3	Analog to Cl^-/ $Th(CO_3)_5^{-6}$/Na^+ in Felmy and Rai (1999)
Cl^-	$Acetate^-$	Na^+	0.01029	Novak et al. (1996)
SO_4^{-2}	HSO_4	Na^+	-0.0094	Harvie et al. (1984)
SO_4^{-2}	HSO_4	K^+	-0.0677	Harvie et al. (1984)
SO_4^{-2}	HSO_4	Mg^{+2}	-0.0425	Harvie et al. (1984)
SO_4^{-2}	OH^-	Na^+	-0.009	Harvie et al. (1984)
SO_4^{-2}	OH^-	K^+	-0.05	Harvie et al. (1984)
SO_4^{-2}	HCO_3	Na^+	-0.005	Harvie et al. (1984)
SO_4^{-2}	HCO_3	Mg^{+2}	-0.161	Harvie et al. (1984)
SO_4^{-2}	CO_3^{-2}	Na^+	-0.005	Harvie et al. (1984)
SO_4^{-2}	CO_3^{-2}	K^+	-0.009	Harvie et al. (1984)
OH^-	CO_3^{-2}	Na^+	-0.017	Harvie et al. (1984)
OH^-	CO_3^{-2}	K^+	-0.01	Harvie et al. (1984)
HCO_3	CO_3^{-2}	Na^+	0.002	Harvie et al. (1984)
HCO_3	CO_3^{-2}	K^+	0.012	Harvie et al. (1984)
HCO_3	ClO_4	Na^+	-0.01	Neck et al. (1995)
CO_3^{-2}	ClO_4	Na^+	-0.024	Neck et al. (1995)
nca, zeta			**zeta (ζ)**	
$O_2(aq)$	Ca^{+2}	Cl^-	-0.0169	Clegg and Brimblecombe (1990)
$O_2(aq)$	Ca^{+2}	NO_3^-	0.0	Clegg and Brimblecombe (1990)[44]
$O_2(aq)$	H^+	Cl^-	-0.0077	Clegg and Brimblecombe (1990)
$O_2(aq)$	K^+	Br^-	-0.00541	Clegg and Brimblecombe (1990)
$O_2(aq)$	K^+	Cl^-	-0.0211	Clegg and Brimblecombe (1990)
$O_2(aq)$	K^+	OH^-	-0.007064	Clegg and Brimblecombe (1990)
$O_2(aq)$	K^+	NO_3^-	-0.0281	Clegg and Brimblecombe (1990)
$O_2(aq)$	K^+	SO_4^{-2}	0.0	Clegg and Brimblecombe (1990)[45]
$O_2(aq)$	Na^+	Br^-	-0.00909	Clegg and Brimblecombe (1990)
$O_2(aq)$	Na^+	Cl^-	-0.009186	Clegg and Brimblecombe (1990)

[44] Not defined therein
[45] Not defined therein

$O_2(aq)$	Na^+	CO_3^{-2}	-0.0181	Clegg and Brimblecombe (1990)
$O_2(aq)$	Na^+	HCO_3^-	0.0	Clegg and Brimblecombe (1990)
$O_2(aq)$	Na^+	NO_3^-	-0.012	Clegg and Brimblecombe (1990)
$O_2(aq)$	Na^+	OH^-	-0.0125	Clegg and Brimblecombe (1990)
$O_2(aq)$	Na^+	SO_4^{-2}	-0.046	Clegg and Brimblecombe (1990)
$B(OH)_3(aq)$	Na^+	SO_4^{-2}	0.046	Felmy and Weare (1986)
$B(OH)_3(aq)$	H^+	Cl^-	-0.0102	Felmy and Weare (1986)
nnn'			**mu (μ)**	
$CO_2(aq)$	$CO_2(aq)$	$B(OH)_3(aq)$	0.0	template only

******End of Table III.1-2 *******

IV. IRON (Fe)

IV.1. Solubility Model of Ferrous Iron in NaCl and Na_2CO_3 Solutions

The solubilities of $Fe(OH)_2(s)$, $Fe_2Cl(OH)_3(s)$, $FeCO_3(s)$, and $Fe_2(OH)_2CO_3(s)$ in NaCl and Na_2CO_3 solutions were summarized by Kim et al. (2017).

Table IV.1-1 and Table IV.1-2 lists the 25 °C Log Ks and PIPs of Kim et al. (2017) that are validated with respect to the brine model in data0.fm1.

Table IV.1-1. Reactions and 25 °C Log K values.

Reaction	Log K (I = 0)	Reference
Aqueous Reaction		
$FeOH^+ + H^+ = Fe^{+2} + H_2O$	9.31	Shock et al. (1997)
$Fe(OH)_2(aq) + 2H^+ = Fe^{+2} + 2H_2O$	20.84	Lemire et al. (2013), Jang (2021, LogK)
$Fe(OH)_3^- + 3H^+ = Fe^{+2} + 3H_2O$	31.00	Baes and Mesmer (1976)
$Fe(OH)_4^{-2} + 4H^+ = Fe^{+2} + 4H_2O$	46.00	Baes and Mesmer (1976)
$FeCO_3(aq) + H^+ = Fe^{+2} + HCO_3^-$	4.83	Bruno et al. (1992)
$Fe(CO_3)_2^{-2} + 2H^+ = Fe^{+2} + 2HCO_3^-$	13.89	Kim et al. (2017)
Dissolution		
$Fe(OH)_2(s)$ (Ferrous Iron Hydroxide) + $2H^+ = Fe^{+2} + 2H_2O$	12.89	Kim et al. (2017)
$Fe_2Cl(OH)_3(s)$ (Hibbingite) + $3H^+ = 2Fe^{+2} + Cl^- + 3H_2O$	17.08	Kim et al. (2017)
$FeCO_3(s)$ (Siderite) + $H^+ = Fe^{2+} + HCO_3^-$	-0.12	Kim et al. (2017), Stumm and Morgan (1996)
$Fe_2(OH)_2CO_3(s)$ (Chukanovite) + $3H^+ = 2Fe^{2+} + HCO_3^- + 2H_2O$	12.32	Kim et al. (2017)

Table IV.1-2. 25 °C PIPs.

i	j	α_1/α_2[A]	$\beta^{(0)}$	$\beta^{(1)}$	$\beta^{(2)}$	C^φ	Reference
Fe^{+2}	Cl^-	2.0/12.0	0.37324	1.13499	0.0	-0.02152	Moog et al. (2004)
Na^+	$Fe(CO_3)_2^{-2}$	2.0/12.0	-0.230	6.26	0.0	0.0	Kim et al. (2017)
i	j	θ_{ij}	Reference	k	ψ_{ijk}	Reference	
Na^+	Fe^{+2}	0.10945	Moog et al. (2004)	Cl^-	-0.01605	Moog et al. (2004)	
Mg^{+2}	Fe^{+2}	0.14504	Moog et al. (2004)	Cl^-	-0.02985	Moog et al. (2004)	

IV.2. $Fe(OH)_2(s)/Fe_2Cl(OH)_3(s)$ - $Na_2H_2EDTA.2H_2O$ - NaCl - H_2O

IV.2.1. Chemical System

A mixture of ferrous iron hydroxide (FIH, $Fe(OH)_2(s)$) and hibbingite (HIBB, $Fe_2Cl(OH)_3(s)$) was added to duplicate NaCl solutions. The NaCl solutions were spiked with 0.040 M Na_2H_2EDTA. The six components of the system are Fe^{+2}, Na^+, Cl^-, $EDTA^{-4}$, H^+, and H_2O.

IV.2.2. Goals and Hypotheses

The goal was to test the accuracy of a literature-retrieved log $K(FeEDTA^{-2}) = -16.1$ (scaled to zero ionic strength; Morel and Hering, 1993) by solubility experiments in low to high ionic strength. The dissociation reaction of the $FeEDTA^{-2}$ complex is:

$$FeEDTA^{-2} = Fe^{+2} + EDTA^{-4};\ Log\ K = -16.1 \quad (1)$$

The hypothesis is that $EDTA^{-4}$ is an efficient chelator of Fe^{+2}. If so, at constant total dissolved EDTA (ΣEDTA), the total dissolved Fe (ΣFe) should be equivalent to ΣEDTA, independent of the solubility-limiting solid.

IV.2.3. Reactor Preparation

50 mL of 0.200 M Na_2H_2EDTA stock solution was mixed with 200 mL each of 0.010, 0.101, 0.976, 2.00, 3.00, 4.00, and 4.52 M NaCl solutions in individual Class A 250-mL volumetric flasks. Flasks were topped off with the respective NaCl solutions. Prior to use, the seven solutions were equilibrated with the internal gas (oxygen level less than 1 ppm) of the anaerobic glovebox for at least one hour using an electric air pump. The gravimetrically and volumetrically determined compositions of the background solutions are summarized in Table IV.2-1.

Table IV.2-1. Reactor description. Concentrations are in Molarity.

Reactor ID	Na_2H_2EDTA	NaCl	ΣNa	ΣCl	ΣEDTA	Density, g/mL	M:m, L/kg
Fe(OH)2-Na4EDTA-0.01(A,B)	0.040	0.008	0.088	0.008	0.040	1.010	1.004
Fe(OH)2-Na4EDTA-0.1(A,B)	0.040	0.081	0.16	0.081	0.040	1.013	1.006
Fe(OH)2-Na4EDTA-1(A,B)	0.040	0.78	0.86	0.78	0.040	1.039	1.021
Fe(OH)2-Na4EDTA-2(A,B)	0.040	1.60	1.68	1.60	0.040	1.069	1.039
Fe(OH)2-Na4EDTA-3(A,B)	0.040	2.40	2.48	2.40	0.040	1.099	1.057
Fe(OH)2-Na4EDTA-4(A,B)	0.040	3.20	3.28	3.20	0.040	1.129	1.077
Fe(OH)2-Na4EDTA-5(A,B)	0.040	3.62	3.70	3.62	0.040	1.159	1.096

The density of NaCl solutions was calculated using Equation (2):

$$\text{Density (g/mL)} = -0.0000 \times M_{NaCl}^2 + 0.0374 \times M_{NaCl} + 1.0009 \quad (2)$$

The polynomial of Equation (2) was obtained by regression of density and Molarity of NaCl solutions in Table I.4-1 using second order with respect to M_{NaCl}. The density of the 0.200 M Na_2H_2EDTA solution is 1.0445 g/mL. The density values in Table IV.2-1 were calculated using the density of the 0.200 M Na_2H_2EDTA solution and the density of each NaCl solution calculated using Equation (2).

M:m is the Molarity-to-molality conversion factor (Jang, 2020a);

$$M \times M{:}m \text{ (L-solution per kg-water)} = m \quad (3)$$

$$M{:}m \text{ (L-solution per kg-water)} = [\rho - \Sigma(0.001 \times FW_{solute} \times M_{solute}]^{-1} \quad (4),$$

where FM_{solute} stands for the formular weight of the solute in g/mol (e.g., for NaCl and Na_2H_2EDTA, FW = 58.44 and 336.2 g/mol).

The initial solid phase was synthesized by mixing 13.3530 grams of NaOH (0.333 moles) and 33.1869 grams of $FeCl_2.4H_2O$ (0.166 moles) with ~125 mL DDIW[46] in a 250-mL plastic bottle inside a glovebox (OH^-:Fe^{+2} = 2:1 with total added [NaOH] = [Cl^-] = ~2.6 M). Precipitation of ferrous solids occurred immediately. The solid was aged in the bottle for three days then filtered to drain the supernatant and dried; then gently ground inside the glovebox. Approximately 0.9 grams of the solid was put into 14 individual 50-mL glass serum bottles to prepare duplicates for each of the seven solutions made. Solution volume was ~50 mL for each of the 14 glass serum bottles. The serum bottles were sealed with rubber septa and aluminum crimps and kept inside gloveboxes.

IV.2.4. Data - Aqueous

IV.2.4.1. pHr

The recorded pHr values were stable over time (Table IV.2-2, Figure IV.2-1) with a maximum %2SD[47] of 2%. Statistics are displayed in Figure IV.2-1, and tabulated in Table IV.2-3. The pHr changed from 7.5 to 9.0 as ΣNa loading increased (Figure IV.2-2).

Table IV.2-2. Time-dependent measured pHr.

	Aging time (Days)	
Reactor ID	1000	2165
Fe(OH)2-Na4EDTA-0.01A	7.820	7.813
Fe(OH)2-Na4EDTA-0.01B	7.847	7.805
Fe(OH)2-Na4EDTA-0.1A	7.948	7.887
Fe(OH)2-Na4EDTA-0.1B	7.921	7.847
Fe(OH)2-Na4EDTA-1A	8.265	8.164

[46] Deoxygenated Deionized Water.
[47] SD: Standard Deviation

Fe(OH)2-Na4EDTA-1B	8.341	8.238
Fe(OH)2-Na4EDTA-2A	8.593	8.506
Fe(OH)2-Na4EDTA-2B	8.481	8.360
	Aging time (Days)	
Reactor ID	1001	2166
Fe(OH)2-Na4EDTA-3A	8.729	8.710
Fe(OH)2-Na4EDTA-3B	8.730	8.714
Fe(OH)2-Na4EDTA-4A	8.766	8.693
Fe(OH)2-Na4EDTA-4B	8.849	8.809
Fe(OH)2-Na4EDTA-5A	8.930	8.875
Fe(OH)2-Na4EDTA-5B	8.928	8.877

Figure IV.2-1. Time-dependent measured pHr. Solid black squares at 500 days are averages. Data labels are listed in the order of averages, 2SD, %2SD, and counts of measurements. Solid blue dots and circles are measurements made in duplicate (A and B in Table IV.2-2).

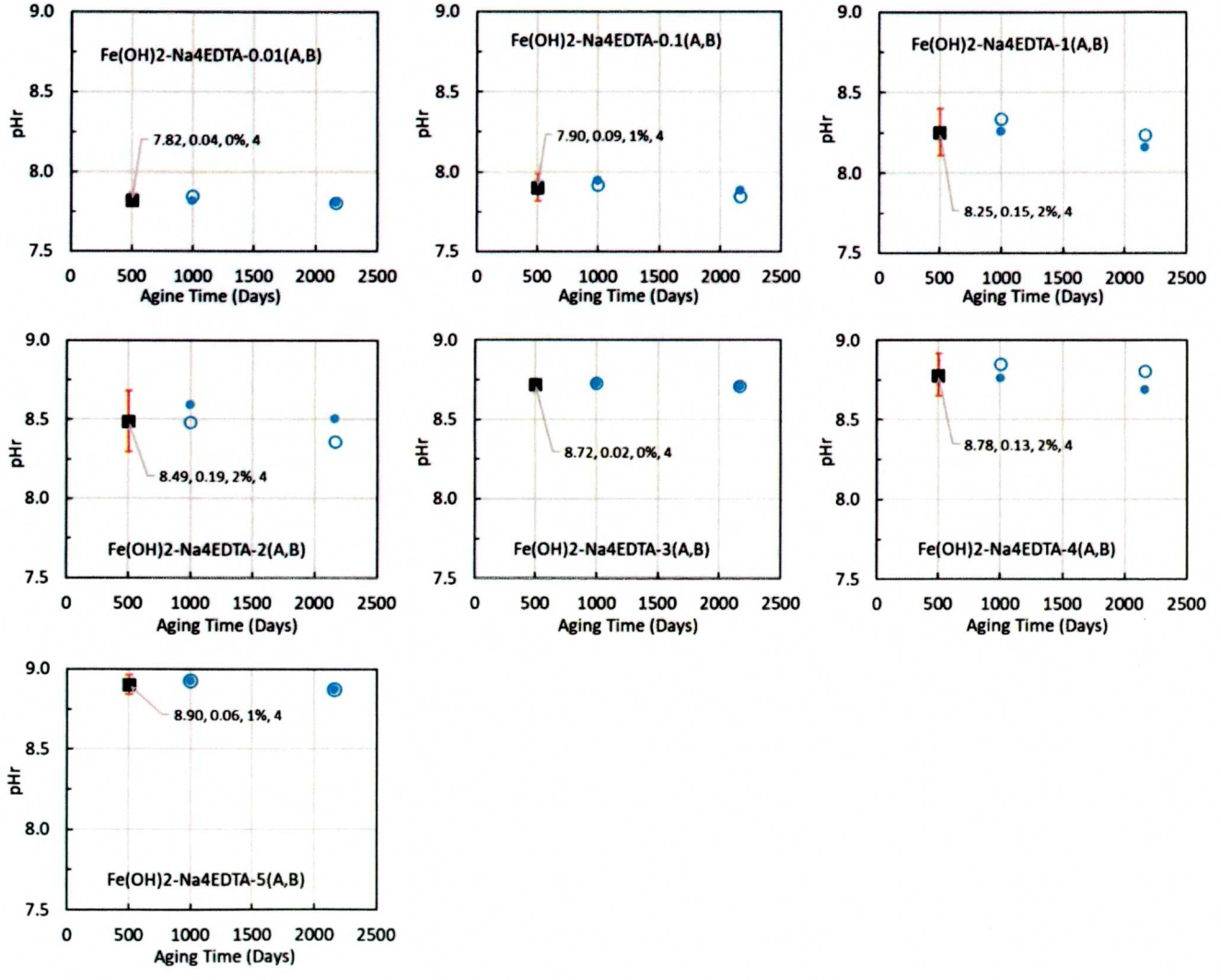

164 Table IV.2-3. Statistics of pHr measurements.

Reactor ID	Average	2SD	%2SD	Counts
Fe(OH)2-Na4EDTA-0.01(A,B)	7.82	0.04	0%	4
Fe(OH)2-Na4EDTA-0.1(A,B)	7.90	0.09	1%	4
Fe(OH)2-Na4EDTA-1(A,B)	8.25	0.15	2%	4
Fe(OH)2-Na4EDTA-2(A,B)	8.49	0.19	2%	4
Fe(OH)2-Na4EDTA-3(A,B)	8.72	0.02	0%	4
Fe(OH)2-Na4EDTA-4(A,B)	8.78	0.13	2%	4
Fe(OH)2-Na4EDTA-5(A,B)	8.90	0.06	1%	4

165

166 Figure IV.2-2. Change of pHr as a function of ΣNa loading.

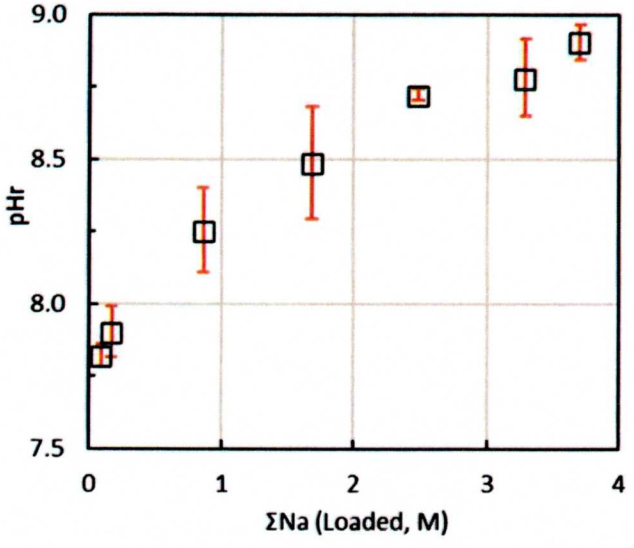

167

168 IV.2.4.2. ΣFe

169 pHr was measured on the 1000th day and 2166th day of aging (Table IV.2-2 and Figure IV.2-1).
170 Because the pHr's were stable, the pH-dependent EDTA reactions (5), (6), (7), and (8) were
171 assumed to be at equilibrium. No time-dependent measurements were made for ΣFe. Duplicate
172 measurements of ΣFe on the 1001st day of aging were precise, %2RG[48] being less than 12% (Table
173 IV.2-4). The measured ΣFe were corrected for the %Deviations seen in ΣNa measurements (Data
174 labels in Figure IV.2-5). ΣFe and ΣNa were measured using the same instrument, ICP-AES.

175 $$H_2EDTA^{-2} = HEDTA^{-3} + H^+ \quad (5)$$

176 $$H_3EDTA^{-} = H_2EDTA^{-2} + H^+ \quad (6)$$

177 $$Fe(OH)_2(s) + H_2EDTA^{-2} = FeEDTA^{-2} + 2H_2O \quad (7)$$

[48] RG: Range of two measurements

178 $$(1/2)Fe_2Cl(OH)_3(s) + H_2EDTA^{-2} = FeEDTA^{-2} + (3/2)H_2O + (1/2)H^+ + (1/2)Cl^- \quad (8)$$

179 The two data points in the green rectangle in Figure IV.2-3 were measured at low pHr (Figure
180 IV.2-2), where the solubility of $Fe(OH)_2(s)$ or $Fe_2Cl(OH)_3(s)$ exceeds ΣEDTA loading. Except for
181 these two data points, the corrected $\Sigma Fe \approx 0.04$ M, which is the loading of Na_2H_2EDTA (Figure
182 IV.2-3) confirming that $EDTA^{-4}$ completely chelated Fe^{+2}.

183 **Table IV.2-4. Measurements of ΣFe on the 1001th day (M).**

Fe(OH)2-Na4EDTA-	0.01(A,B)	0.1(A,B)	1(A,B)	2(A,B)	3(A,B)	4(A,B)	5(A,B)
	0.0531	0.0472	0.0381	0.0376	0.0368	0.0330	0.0339
	0.0501	0.0483	0.0390	0.0373	0.0364	0.0347	0.0333
Median:	0.0516	0.0478	0.0386	0.0375	0.0367	0.0339	0.0336
Corrected for bias	0.0483	0.0479	0.0406	0.0395	0.0396	0.0384	0.0374
2RG [D]:	0.0061	0.0021	0.0018	0.0005	0.0009	0.0034	0.0013
%2RG:	12%	4%	5%	1%	3%	10%	4%

184 [D] Twice the Range of two measurements.

185 Figure IV.2-3. A. Change in ΣFe as a function of ΣNa loading. B. %Deviation of ΣFe
186 from ΣEDTA as a function of ΣNa loading. Data points in the green rectangle
187 indicate the solubility of FIH exceeded available EDTA.

188

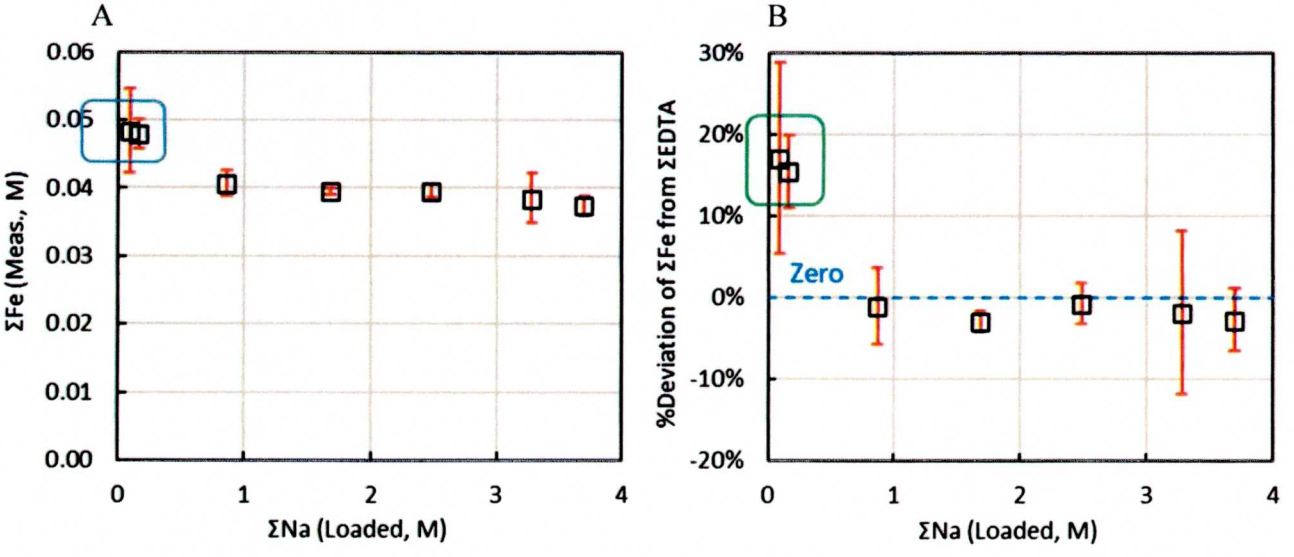

189

190 IV.2.4.3. ΣEDTA

191 ΣEDTA measurements accurately and precisely reproduced the loading of 0.04 M (Table IV.2-5;
192 Figure IV.2-4).

193 **Table IV.2-5. Measurements of ΣEDTA on the 1001th day (M).**

Fe(OH)2-Na4EDTA-	0.01(A,B)	0.1(A,B)	1(A,B)	2(A,B)	3(A,B)	4(A,B)	5(A,B)
	0.0408	0.0391	0.0403	0.0401	0.0412	0.0395	0.0401
	0.0397	0.0397	0.0393	0.0395	0.0399	0.0396	0.0403
Average:	0.040 for all 14 measurements						

2SD[A]:	0.001 for all 14 measurements
%2SD:	2% for all 14 measurements

[A] Twice the Standard Deviation

Figure IV.2-4. Accuracy and precision of ΣEDTA measurements as a function of ΣNa loading. The y-axis represents the %Deviation of the mean measured EDTA concentration from the expected amount. Error bars are ±two times the absolute difference of 2 measurements divided by the mean.

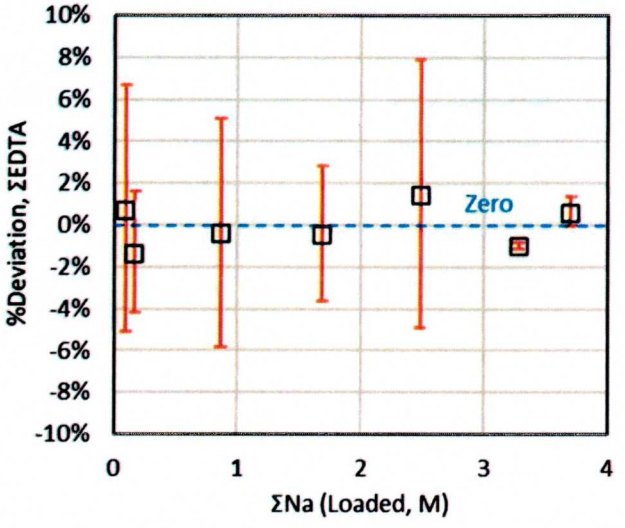

IV.2.4.4. ΣNa

ΣNa measurements are presented in Table IV.2-6. The accuracy and precision of the measurements are shown in Figure IV.2-5. ΣNa is considered a conservative/non-reactive component, and the loaded concentrations were known at each condition (Table IV.2-1).

Table IV.2-6. Measurements of ΣNa on the 1001th day (M).

Fe(OH)2-Na4EDTA-	0.01(A,B)	0.1(A,B)	1(A,B)	2(A,B)	3(A,B)	4(A,B)	5(A,B)
	0.0948	0.159	0.809	1.578	2.366	2.779	3.397
	0.0930	0.161	0.826	1.613	2.227	3.010	3.253
Mean:	0.094	0.161	0.818	1.596	2.297	2.895	3.325
2RG [D]:	0.003	0.005	0.035	0.070	0.278	0.461	0.287
%2RG:	4%	3%	4%	4%	12%	16%	9%

[D] Twice the Range of two measurements.

Figure IV.2-5. Accuracy and precision of ΣNa measurements. Data labels are %Deviation of averaged measurements from the ΣNa loading. Error bars are two times the absolute difference of 2 measurements divided by the mean.

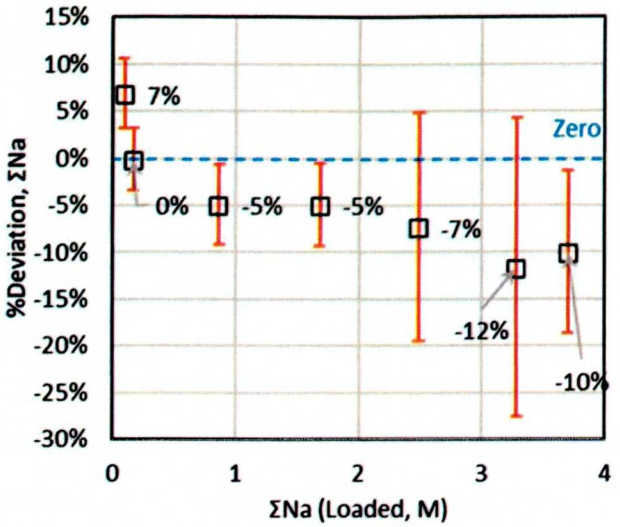

IV.2.4.5. ΣCl

Chloride is considered a conservative component, and the loaded concentrations were known at each condition (Table IV.2-1). The measurements are presented in Table IV.2-7. The accuracy and precision of the measurements are shown in Figure IV.2-6. Larger %Deviations in the area marked with the blue rectangle indicate the dissolution of hibbingite, $Fe_2Cl(OH)_3(s)$. Dissolution of hibbingite adds Cl^- to the solutions at lower loading of ΣCl.

Table IV.2-7. Measurements of ΣCl on the 3955th day (M).

Fe(OH)2-Na4EDTA-	0.01(A,B)	0.1(A,B)	1(A,B)	2(A,B)	3(A,B)	4(A,B)	5(A,B)
	0.0483	0.107	0.779	1.629	2.384	3.181	3.616
	0.0483	0.107	0.780	1.630	2.386	3.184	3.614
	0.0443	0.108	0.785	1.648	2.378	3.209	3.662
	0.0443	0.108	0.785	1.645	2.383	3.210	3.661
Median:	0.046	0.108	0.782	1.638	2.383	3.196	3.638
2RG [D]:	0.005	0.001	0.007	0.020	0.006	0.031	0.053
%2RG:	10%	1%	1%	1%	0%	1%	1%

[D] Twice the Range of two measurements.

Figure IV.2-6. Accuracy and precision of ΣCl measurements. A. whole range. B. Zoom-in of the area marked with yellow rectangle in A.

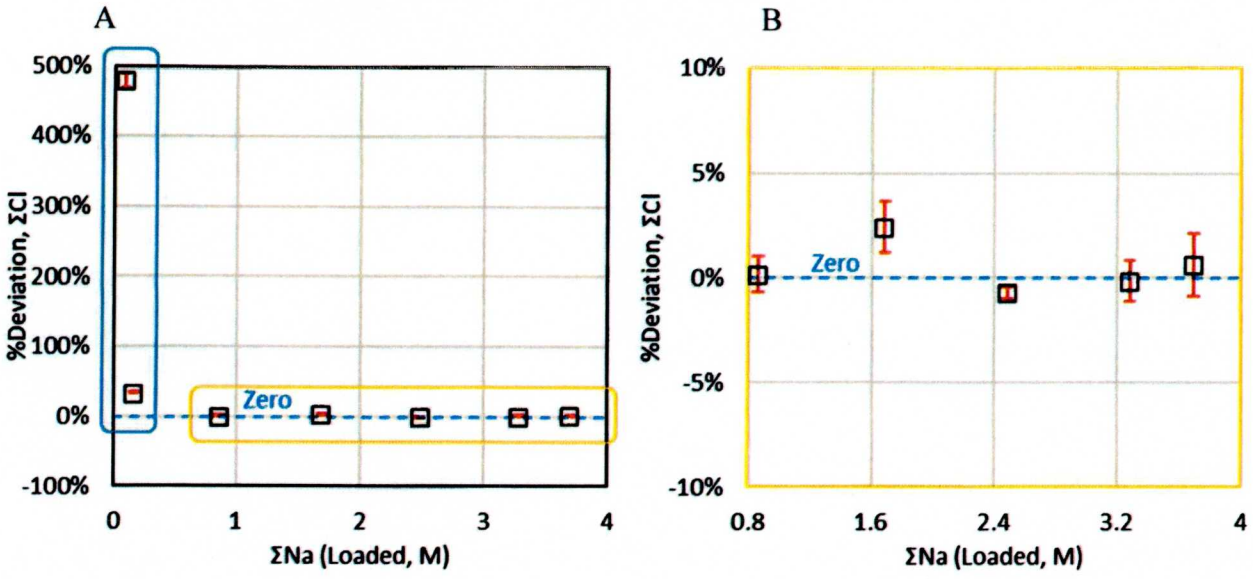

IV.2.5. Data - Solids

XRD scans are shown in Figure IV.2-7. The first two scans do not show the presence of hibbingite, which corroborates the observation made from ΣCl measurements (Section IV.2.4.5). The remaining five scans show the co-existence of hibbingite and ferrous iron hydroxide.

Figure IV.2-7. XRD scans of the solids collected at the end of experiments. Labels are the associated reactor IDs.

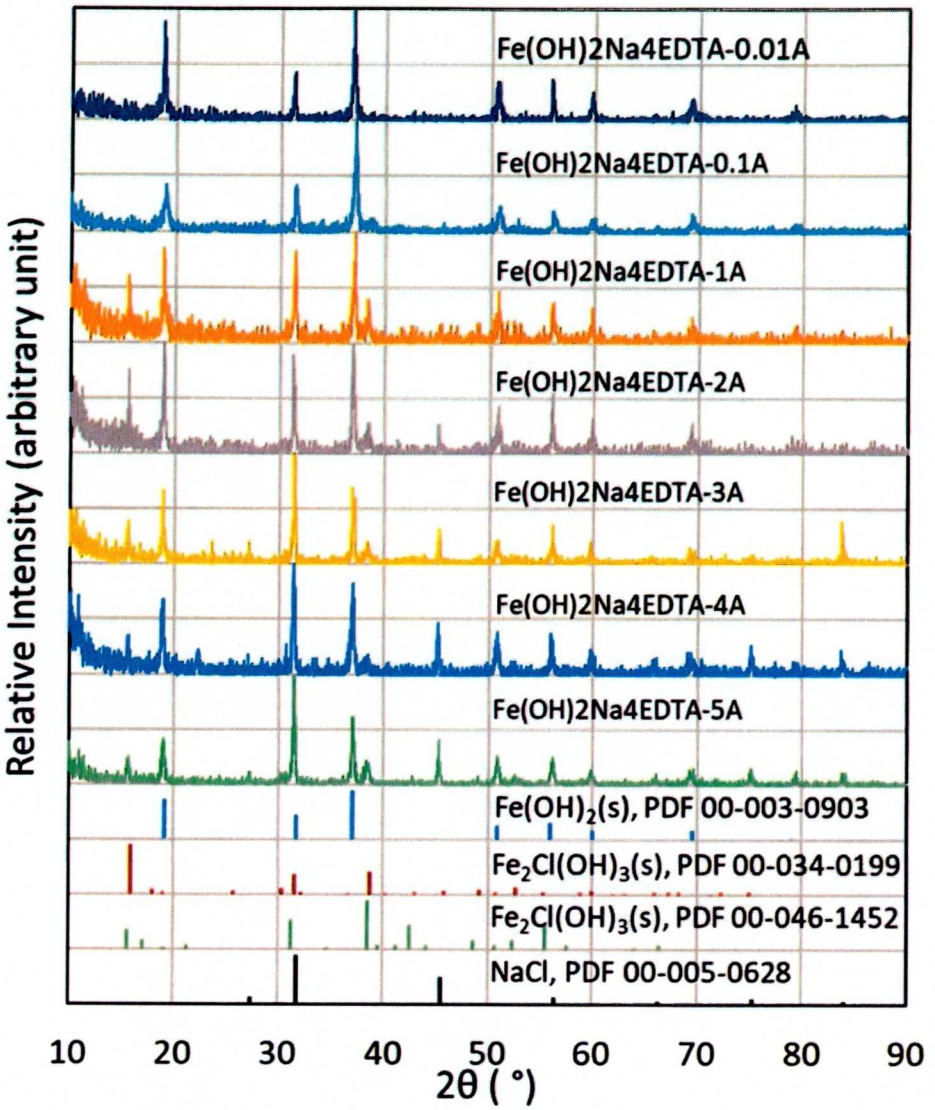

IV.2.6. Observations

pHr increased as NaCl loading increased. Measured ΣFe matched the loading of Na_2H_2EDTA when pHr > 8.0. Ferrous iron hydroxide and hibbingite co-existed when ΣCl > 0.7 M. EDTA was not consumed by microbes or light over the 1001 day reaction period.

IV.2.7. Model Parameterization: Pitzer Approach

Because the thermodynamic model uses molality, concentrations were converted from Molarity to molality using the M:m column in Table IV.2-1. The component concentrations in molality are shown in Table IV.2-8.

238 Table IV.2-8. Components concentrations are presented in molality.

Exp. ID	pmH	ΣFe	ΣEDTA[A]	ΣNa	ΣCl
Fe(OH)2-Na4EDTA-0.01(A,B)	7.72	0.0491 (±0.0058)	0.042 (±0.003)	*0.0895*	0.0471
Fe(OH)2-Na4EDTA-0.1(A,B)	7.81	0.0485 (±0.0021)	0.042 (±0.003)	*0.163*	0.109
Fe(OH)2-Na4EDTA-1(A,B)	8.28	0.0416 (±0.0020)	0.042 (±0.003)	*0.881*	*0.799*
Fe(OH)2-Na4EDTA-2(A,B)	8.66	0.0407 (±0.0005)	0.042 (±0.003)	*1.73*	*1.65*
Fe(OH)2-Na4EDTA-3(A,B)	9.04	0.0417 (±0.0011)	0.042 (±0.003)	*2.61*	*2.53*
Fe(OH)2-Na4EDTA-4(A,B)	9.24	0.0412 (±0.0041)	0.042 (±0.003)	*3.52*	*3.43*
Fe(OH)2-Na4EDTA-5(A,B)	9.43	0.0408 (±0.0016)	0.042 (±0.003)	*4.04*	*3.95*

239 [A] ΣEDTA are set to 0.042 m with 2SD = 0.003 m (7%). Numbers in italic mean the loadings by recipe.
240
241 Figure IV.2-8 shows that the selected log K for $FeEDTA^{-2}$ = -16.1 (Morel and Hering, 1993) predicts the
242 experimental results within the uncertainty, i.e. $EDTA^{-4}$ is completely chelated by Fe^{+2}. No further
243 fitting with PIPs is necessary.

244 Figure IV.2-8. Model calculation results. A. Whole range investigated (NaCl loading 0.09
245 to 4.0 m). B. Expansion of the green rectangle in A.

246

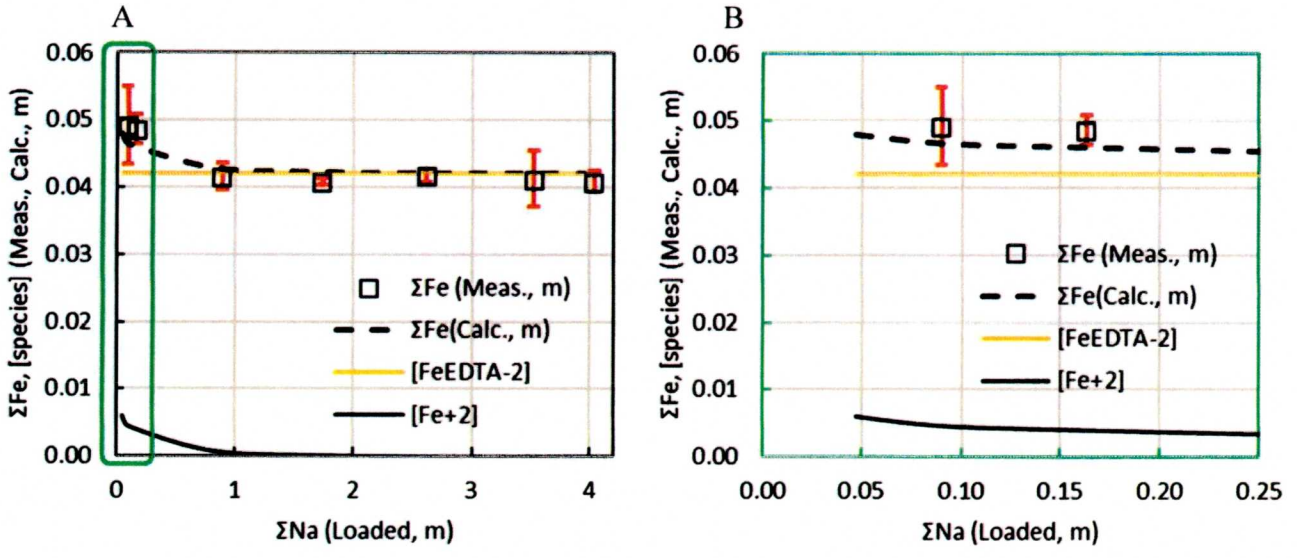

247

248 The model predicted activities corresponding to the stability field of FIH for the experiments where
249 HIBB disappeared at lower pHr (solid black line in Figure IV.2-9). For the remaining experiments
250 performed at higher pHr the calculated activities fall on the boundary of FIH and HIBB (solid blue
251 line in Figure IV.2-9). This is consistent with the minerals identified by XRD (Figure IV.2-7).

Figure IV.2-9. Stability of FIH and HIBB. The blue dashed line is the metastable extension of the phase boundary.

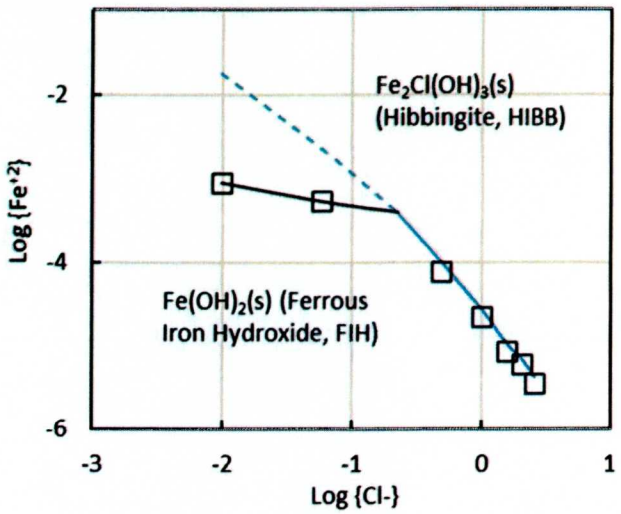

IV.2.8. Summary

The $FeEDTA^{-2}$ reaction and log K of -16.1 (Morel and Hering, 1993) effectively describes the experimental data. No further PIPs are needed to improve the thermodynamic model.

Table IV.2-9. Recommended reaction and the log K new for data0.fm1.

Reaction	LogK	Reference
$FeEDTA^{-2} = Fe^{+2} + EDTA^{-4}$	-16.1	Morel and Hering (1993)

IV.3. $FeCl_2.4H_2O$ - $Na_2EDTA.2H_2O$ - NaOH - H_2O

IV.3.1. Chemical System

The reaction of interest is Fe^{+2}-$EDTA^{-4}$ complexation in alkaline conditions. Formation of ferrous iron hydroxide (FIH) was induced by supersaturating solutions with respect to FIH by adding NaOH in excess to Fe:OH of 1:2. Solutions containing the prescribed mass of $FeCl_2.4H_2O$ and $Na_2H_2EDTA.2H_2O$ were spiked with NaOH. The six components of the system are Fe^{+2}, Na^+, Cl^-, $EDTA^{-4}$, H^+, and H_2O.

IV.3.2. Goals and Hypotheses

The goal of this section is to measure Fe^{+2}-$EDTA^{-4}$ complexation at high pHr.

IV.3.3. Reactor Preparation

Four chemicals, i.e., $Na_2H_2EDTA.2H_2O$, $FeCl_2.4H_2O$, Deoxygenated Deionized water, and NaOH were added to a 125-mL glass serum bottle in that order by the recipe (Table IV.3-1) to prepare reactors under six different conditions.

273 Table IV.3-1. Recipe and calculated solution properties.

Exp. ID	$Na_2H_2EDTA.2H_2O$ (gram)	$FeCl_2.4H_2O$ (gram)	NaOH (gram)	DDIW [A] (mL)	ΣNa (m)	ΣCl (m)	ΣEDTA (m)
FeEDTA-1	0.3728	11.9307	7.2017	100	1.75	1.15	0.010
FeEDTA-2	1.8658	11.9309	7.2070	100	1.83	1.15	0.048
FeEDTA-3	3.7275	11.9312	7.2028	100	1.92	1.15	0.096
FeEDTA-4	5.5870	11.9305	7.2043	100	2.01	1.15	0.144
FeEDTA-5	7.4430	11.9306	7.2020	100	2.10	1.15	0.191
FeEDTA-6	10.1453	11.9300	7.2021	100	2.23	1.14	0.260
Exp. ID	NaCl (m)	NaOH (m)	Density (g/mL)	m:M (kg/L)	ΣNa (M)	ΣCl (M)	ΣEDTA (M)
FeEDTA-1	1.15	0.60	1.059	0.9684	1.69	1.12	0.009
FeEDTA-2	1.15	0.67	1.066	0.9645	1.76	1.11	0.046
FeEDTA-3	1.15	0.77	1.074	0.9598	1.84	1.10	0.092
FeEDTA-4	1.15	0.86	1.082	0.9551	1.92	1.10	0.137
FeEDTA-5	1.15	0.95	1.091	0.9506	2.00	1.09	0.181
FeEDTA-6	1.14	1.09	1.102	0.9440	2.11	1.08	0.245

274 [A] Deoxygenated Deionized Water, density set to be (≡) 0.997 g/mL at Room Temperature and Pressure.

275

276 IV.3.4. Data - Aqueous: pHr, ΣFe, ΣEDTA, ΣNa, and ΣCl

277 pHr, ΣFe, ΣEDTA, ΣNa, and ΣCl measurements were made after 390 days[49] of aging. ΣEDTA was
278 measured in triplicate. The pHr remained stable at ~13 (Figure IV.3-1). A linear increase in ΣFe was
279 observed as a function of ΣNa loading (Figure IV.3-2). ΣNa loading is proportional to ΣEDTA
280 loading (Figure IV.3-2A). Because the ΣFe/ΣEDTA ratio was less than 73% (Figure IV.3-2B),
281 EDTA is not as effective a chelator at high pHr as at lower pHr . EDTA is a conservative
282 component; the accuracy and precision of the EDTA measurements are shown in Figure IV.3-3. The
283 accuracy of ΣCl is shown in Figure IV.3-4. Larger and consistently negative %Deviations were
284 observed for ΣNa (Figure IV.3-4).

285 Table IV.3-2. Solution Chemistry Measurements (M).

Exp. ID	pHr [A]	ΣFe	ΣEDTA	ΣNa	ΣCl
FeEDTA-1	13.02	0.0032	0.009	1.43	1.10
FeEDTA-2	12.93	0.026	0.045	1.41	1.11
FeEDTA-3	*13.30*	0.057	0.097	1.52	1.10
FeEDTA-4	*13.24*	0.092	0.137	1.60	1.10
FeEDTA-5	*13.14*	0.126	0.184	1.62	1.08
FeEDTA-6	13.06	0.178	0.243	1.71	1.08

286 [A] Some of the pHr values (in italic) are out of the calibration range and not used as input parameters in the model calculation.

[49] 391 days for FeEDTA-(1,2,6)

Figure IV.3-1. Change of pHr as a function of ΣNa loading.

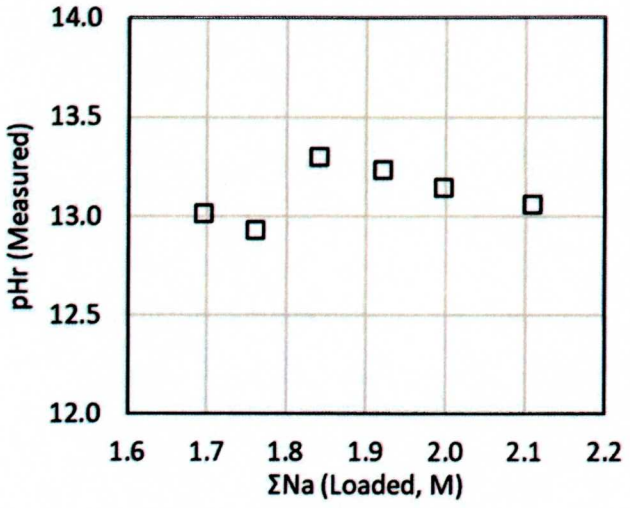

Figure IV.3-2. A. Change of ΣFe as a function of ΣNa loading. B. ΣFe are less than 73% of loaded ΣEDTA. Data labels in B describe the ratios of ΣFe/ΣEDTA in aqueous phase.

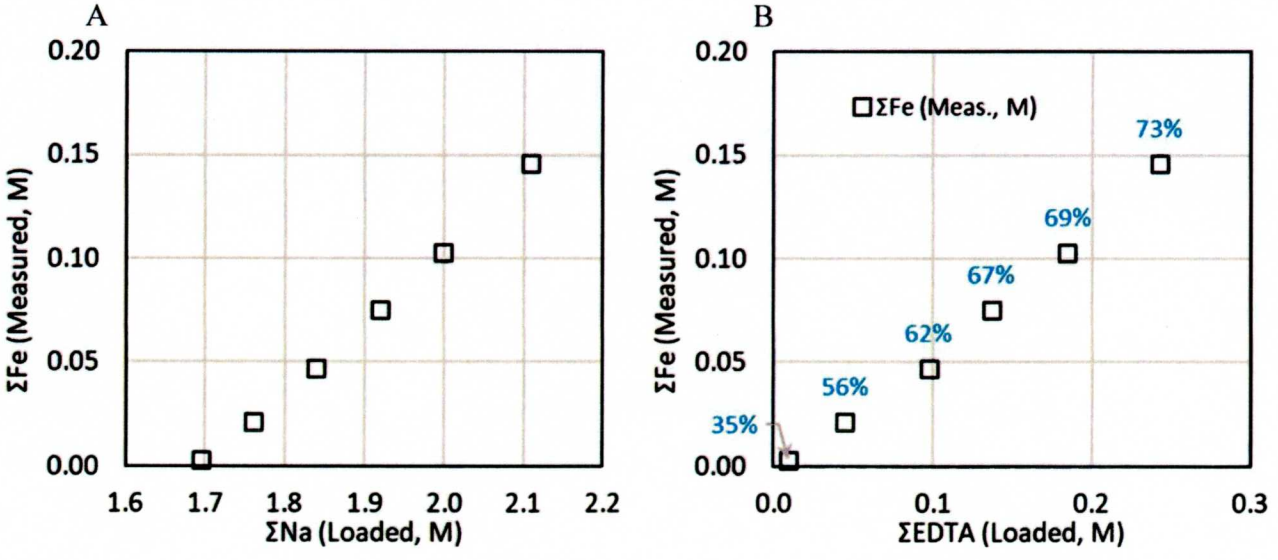

Figure IV.3-3. Accuracy and precision of ΣEDTA as a function of ΣNa loading.

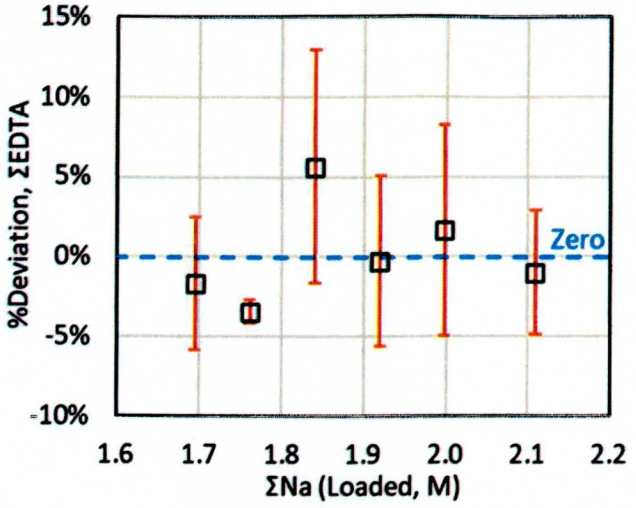

Figure IV.3-4. Accuracy of ΣNa and ΣCl as a function of ΣNa loading.

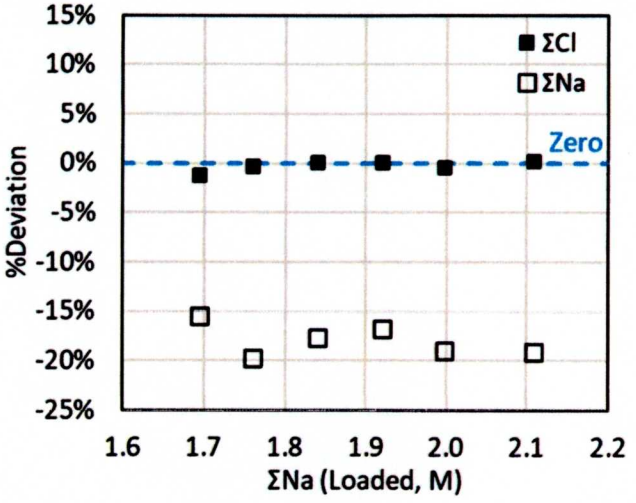

IV.3.5. Data - Solids

The experiments were designed to be within the stability of FIH as predicted by literature-retrieved thermodynamic quantities (Table IV.1-1; Table IV.1-2; Table IV.2-9). Solution chemistry measurements indicated that the FIH was stable after 390 days of aging (Figure IV.3-5B). Further analysis of solids by XRD was therefore not needed.

IV.3.6. Observations

Measurements of non-reactive/conservative components ΣCl and ΣEDTA demonstrated data quality. EDTA was not consumed for 390 days by microbes, or broken down by ambient laboratory light. Measurements of another non-reactive/conservative component, ΣNa, indicated lower accuracy of the instrument used.

IV.3.7. Model Parameterization: Pitzer Approach

The Molarities were converted to molality by applying M:m. By definition, M:m is the inverse of m:M in Table IV.3-1.

Table IV.3-3. Solution Chemistry Measurements (m).

Exp. ID	pmH	ΣFe	ΣEDTA	ΣNa	ΣCl
FeEDTA-1	13.11	2.73E-03(±3%)	*0.010*	*1.75*	*1.15*
FeEDTA-2	13.02	2.19E-02(±3%)	*0.048*	*1.83*	*1.15*
FeEDTA-3	13.38 [B]	4.89E-02(±3%)	*0.096*	*1.92*	*1.15*
FeEDTA-4	13.32 [B]	7.88E-02(±3%)	*0.144*	*2.01*	*1.15*
FeEDTA-5	13.22 [B]	1.09E-01(±3%)	*0.191*	*2.10*	*1.15*
FeEDTA-6	13.13	1.55E-01(±3%)	*0.260*	*2.23*	*1.14*

[B] Out of calibration range.
Italics are the concentrations by the loading (Table IV.3-1).

Figure IV.3-5A shows that the model accurately predicts $Fe(OH)_2(s)$ solubility in high pHr solutions. Figure IV.3-5B shows that the experiments remained in the $Fe(OH)_2(s)$ stability field, as planned.

Figure IV.3-5. A. Model calculation of Fe - EDTA complexation compared to the experimental data. B. Activity of Fe^{+2} plotted against hibbingite and FIH stability fields as a function of EDTA loading.

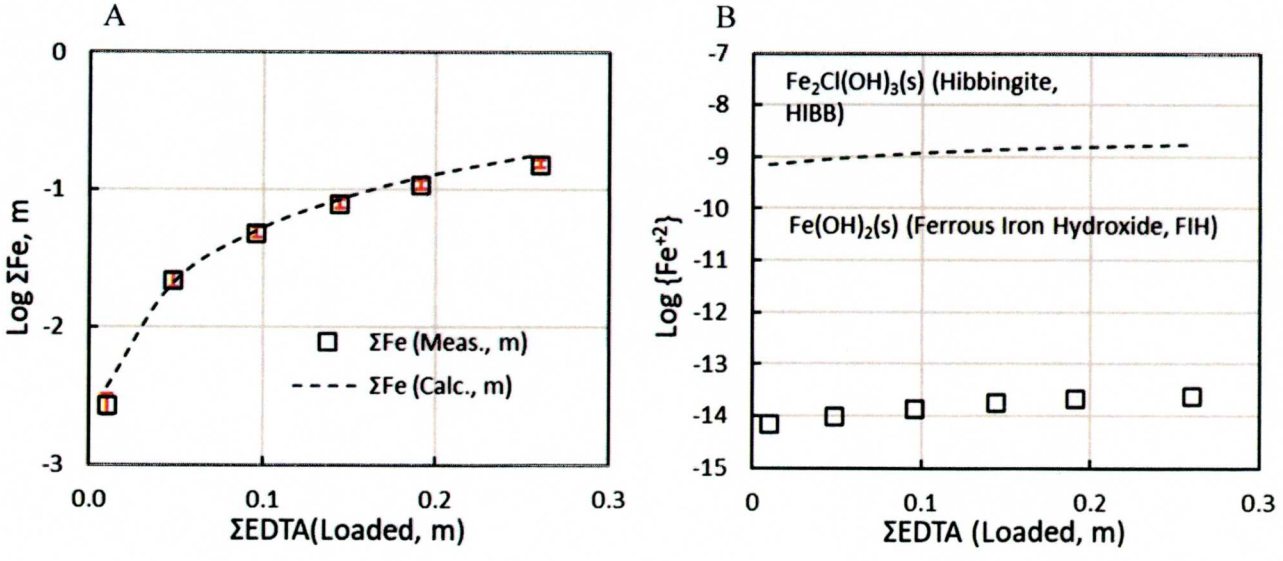

IV.3.8. Summary

No further fitting is necessary because the selected value in Table IV.2-9 matches the experimental observations, and is consistent with the log K for $Fe(OH)_2(s)$ of 12.89 in Table IV.1-1 to explain the incomplete chelation described in Figure IV.3-2B.

IV.4. $Fe(OH)_2(s)$ - $Na_3Citrate$ - NaCl - H_2O

IV.4.1. Chemical System

The solubility of $Fe(OH)_2(s)$ was measured in mixed salt solutions of trisodium citrate dihydrate, $Na_3Citrate.2H_2O$ (where $Citrate^{-3} = C_6H_5O_7^{-3}$), and NaCl. The loading of $Na_3Citrate.2H_2O$ ranged from 0.085 to 0.098 M. The loading of NaCl ranged from 0.1 to 4.9 M. The six components of this system are Fe^{+2}, Na^+, Cl^-, $Citrate^{-3}$, H^+, and H_2O.

IV.4.2. Goals and Hypotheses

The goal was to test the literature-retrieved Fe^{+2} - $Citrate^{-3}$ complexation reaction of Morel and Hering (1993): log K($FeCitrate^-$) = -5.7 (scaled to zero ionic strength) with $Fe(OH)_2(s)$ solubility experiments in low to high ionic strength solutions. The log K($FeCitrate^-$) is defined for the following dissociation reaction;

$$FeCitrate^- = Fe^{+2} + Citrate^{-3};\ Log\ K = -5.7 \quad (9)$$

IV.4.3. Reactor Preparation

The prescribed mass of the chemicals in Table IV.4-1 were mixed to prepare 12 reactors representing 6 experimental conditions in duplicate.

Table IV.4-1. Recipe and calculated solution properties.

Reactor ID	$Na_3Citrate.2H_2O$, gram	NaCl, gram	DI, mL	Slurry, mL [B]	Hydration Water in salt, g	H_2O, total, g
FeCitNa2-1-1	1.3267	0.2932	43	2.5	0.16	45.66
FeCitNa2-1-2	1.3172	0.296	44	2.5	0.16	46.66
FeCitNa2-2-1	1.3314	2.937	44	2.5	0.16	46.66
FeCitNa2-2-2	1.3604	2.9291	44	2.5	0.17	46.67
FeCitNa2-3-1	1.3537	5.8527	43	2.5	0.17	45.67
FeCitNa2-3-2	1.3322	5.8604	44	2.5	0.16	46.66
FeCitNa2-4-1	1.3507	8.7616	43	2.5	0.17	45.67
FeCitNa2-4-2	1.3509	8.7626	43	2.5	0.17	45.67
FeCitNa2-5-1	1.3348	11.6867	44	2.5	0.16	46.66
FeCitNa2-5-2	1.3191	11.6923	42	2.5	0.16	44.66
FeCitNa2-6-1	1.3331	14.613	45	2.5	0.16	47.66
FeCitNa2-6-2	1.3246	14.6108	43	2.5	0.16	45.66

Reactor ID	Na3Citrate, m	NaCl, m	Density, g/mL	M:m, L/kg	pmH[A]	ΣNa, M	ΣCitrate, M	ΣCl, M	I, M
FeCitNa2-1-1	9.88E-02	0.110	1.021	1.011	8.17	0.402	0.0978	0.109	0.695
FeCitNa2-1-2	9.60E-02	0.109	1.021	1.010	8.81	0.392	0.0950	0.107	0.678
FeCitNa2-2-1	9.70E-02	1.08	1.056	1.031	9.59	1.33	0.0941	1.04	1.61
FeCitNa2-2-2	9.91E-02	1.07	1.056	1.031	9.59	1.33	0.0962	1.04	1.62
FeCitNa2-3-1	1.01E-01	2.19	1.095	1.055	8.88	2.37	0.0956	2.08	2.65
FeCitNa2-3-2	9.71E-02	2.15	1.093	1.053	8.87	2.32	0.0922	2.04	2.59
FeCitNa2-4-1	1.01E-01	3.28	1.130	1.077	8.03	3.33	0.0933	3.05	3.61
FeCitNa2-4-2	1.01E-01	3.28	1.130	1.077	9.00	3.33	0.0934	3.05	3.61
FeCitNa2-5-1	9.73E-02	4.29	1.162	1.098	8.11	4.17	0.0886	3.90	4.43

FeCitNa2-5-2	1.00E-01	4.48	1.168	1.103	10.18	4.34	0.0911	4.06	4.61
FeCitNa2-6-1	9.51E-02	5.25	1.191	1.118	9.28	4.95	0.0850	4.69	5.20
FeCitNa2-6-2	9.86E-02	5.48	1.198	1.123	10.38	5.14	0.0878	4.87	5.40

[A] Calculated for the background solution without $Fe(OH)_2(s)$ addition.
[B] The slurry, i.e., $Fe(OH)_2(s)$ suspension, was dense enough to give excess $Fe(OH)_2(s)$ after 2.5-to-46 (i.e., ~18 times) dilution.

IV.4.4. Data - Aqueous

pHr was measured after 34 days of aging. ΣFe and ΣNa were measured after 49 days of aging (Table IV.4-2). pHr values were confined within 10.5 to 11.5 (Figure IV.4-1). Measured ΣFe was ~2 mM, and ΣFe/ΣCitrate ratios were less than 3% (Figure IV.4-2). The accuracy and precision of ΣNa measurements are shown in Figure IV.4-3. A larger %Deviation at low ΣNa loading occurred when Na concentrations were lower than, or close to, the detection limit. No correction was made for ΣFe based on the %Deviation of ΣNa measurements.

Table IV.4-2. Measurements of pHr, ΣFe, and ΣNa in M.

Reactor ID	pHr	ΣFe, M	ΣNa, M
FeCitNa2-1-1	11.37	3.50E-03	4.35E-01
FeCitNa2-1-2	11.04	2.04E-03	4.39E-01
FeCitNa2-2-1	11.29	3.30E-03	1.30E+00
FeCitNa2-2-2	10.85	1.82E-03	1.27E+00
FeCitNa2-3-1	11.21	3.09E-03	2.33E+00
FeCitNa2-3-2	10.68	1.50E-03	2.27E+00
FeCitNa2-4-1	11.14	2.70E-03	3.30E+00
FeCitNa2-4-2	10.66	1.42E-03	3.32E+00
FeCitNa2-5-1	11.08	2.35E-03	4.15E+00
FeCitNa2-5-2	10.55	1.20E-03	4.39E+00
FeCitNa2-6-1	11.02	2.12E-03	4.87E+00
FeCitNa2-6-2	10.49	9.99E-04	5.31E+00

Figure IV.4-1. pHr as a function of ΣNa loading.

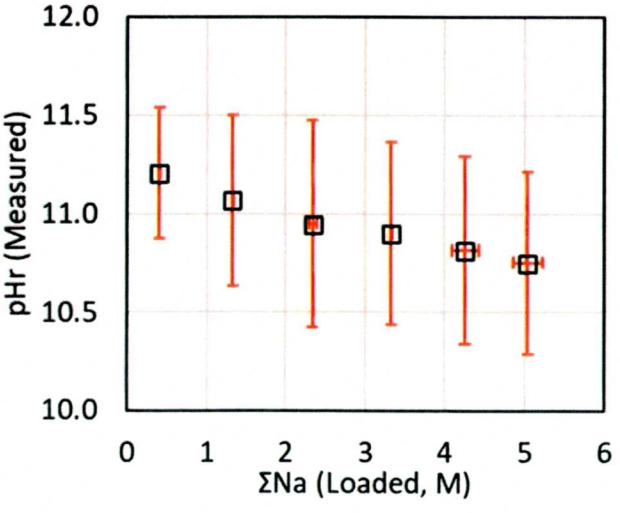

Figure IV.4-2. Change of ΣFe as a function of ΣNa loading. Data labels are ratios of ΣFe/ΣCitrate, meaning that ΣFe is less than 3% of the loaded ΣCitrate.

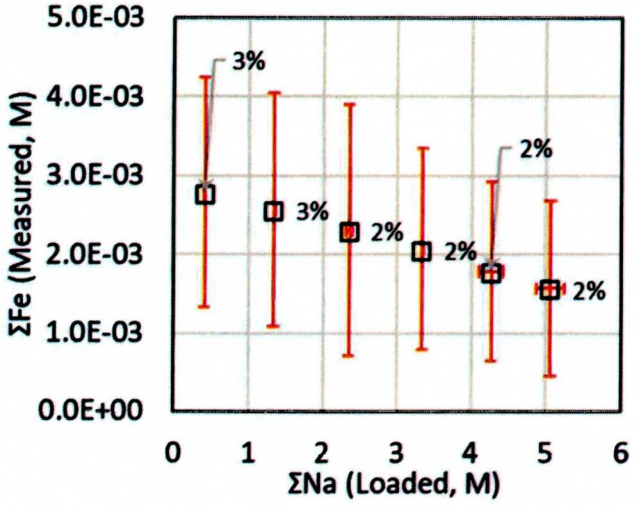

Figure IV.4-3. Accuracy and precision of ΣNa measurements.

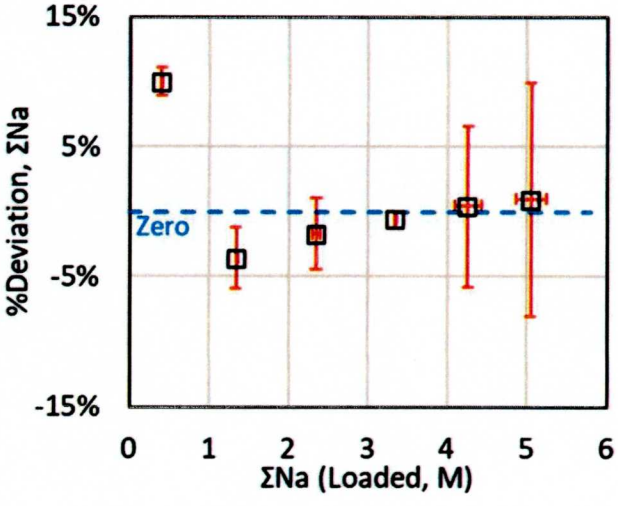

IV.4.5. Data - Solids

Experiments were performed at high pH where only $Fe(OH)_2(s)$ is stable. No solids other than $Fe(OH)_2(s)$ were observed in the XRD scans (Figure IV.4-4).

Figure IV.4-4. XRD scans for the solids collected at the end of experiments.

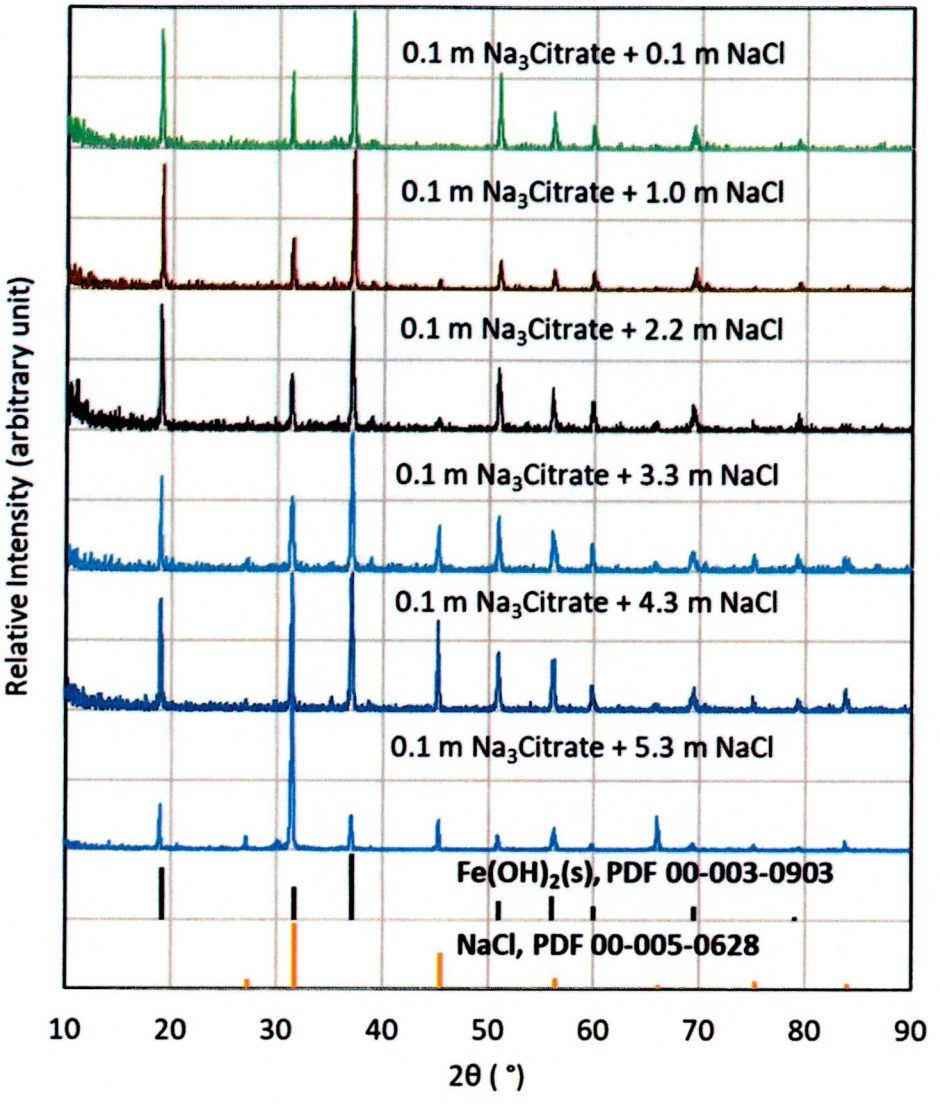

IV.4.6. Observations

ΣFe did not depend on ΣNa loading. The ΣNa measurements were accurate except at low ΣNa loading. Less than 3% of the loaded $Citrate^{-3}$ are chelated with Fe^{+2} (Figure IV.4-2).

IV.4.7. Model Parameterization: Pitzer Approach

Data0.fm1 does not contain Fe^{+2}-$Citrate^{-3}$ complexation reactions. So the log K for Reaction (9) (Morel and Hering, 1993) was tested against the experimental solubility measurements (Figure IV.4-5).

Table IV.4-3. Measured pmH and ΣFe in molality. ΣNa, ΣCitrate, ΣCl are the loadings.

Analyte	pmH			ΣFe			ΣNa		
Reactor ID	Median	RG	%RG	Median	RG	%RG	Median	RG	%RG
FeCitNa2-1-(1,2)	11.23	0.33	3%	2.80E-03	1.47E-03	53%	4.01E-01	9.59E-03	2%

FeCitNa2-2-(1,2)	11.25	0.44	4%	2.63E-03	1.53E-03	58%	1.37E+00	3.12E-03	0%
FeCitNa2-3-(1,2)	11.30	0.54	5%	2.42E-03	1.68E-03	69%	2.47E+00	5.22E-02	2%
FeCitNa2-4-(1,2)	11.42	0.48	4%	2.22E-03	1.38E-03	62%	3.59E+00	4.74E-04	0%
FeCitNa2-5-(1,2)	11.49	0.50	4%	1.96E-03	1.26E-03	64%	4.68E+00	1.85E-01	4%
FeCitNa2-6-(1,2)	11.56	0.50	4%	1.75E-03	1.25E-03	72%	5.65E+00	2.14E-01	4%
Analyte	ΣCitrate			ΣCl					
Reactor ID	Median	RG	%RG	Median	RG	%RG			
FeCitNa2-1-(1,2)	9.74E-02	2.77E-03	3%	1.09E-01	1.37E-03	1%			
FeCitNa2-2-(1,2)	9.80E-02	2.09E-03	2%	1.08E+00	3.13E-03	0%			
FeCitNa2-3-(1,2)	9.89E-02	3.58E-03	4%	2.17E+00	4.15E-02	2%			
FeCitNa2-4-(1,2)	1.01E-01	8.62E-07	0%	3.28E+00	3.77E-04	0%			
FeCitNa2-5-(1,2)	9.88E-02	2.71E-03	3%	4.38E+00	1.77E-01	4%			
FeCitNa2-6-(1,2)	9.68E-02	3.06E-03	3%	5.36E+00	2.05E-01	4%			

Figure IV.4-5. Application of log K(FeCitrate$^-$) = -5.7 to predict the dissolved ΣFe.

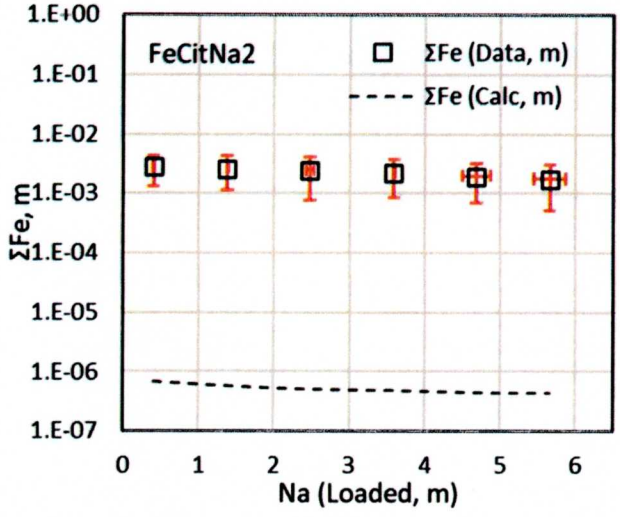

IV.4.8. Summary

The orders of magnitude difference between measured and calculated ΣFe in Figure IV.4-5 is so large that it cannot be closed by minor adjustment of the FeCitrate$^-$ complexation constant, or by using PIPs.

IV.5. $Fe(OH)_2(s)$ - MgHCitrate - NaCl - H_2O

IV.5.1. Chemical System

The solubility of ferrous iron hydroxide, $Fe(OH)_2(s)$, was measured in sodium chloride solutions spiked with ΣMg = 0.0442 M and ΣCitrate = 0.0526 M.

IV.5.2. Goals and Hypotheses

The aim is to better fit the $Fe(OH)_2(s)$ solubility data in mixed solutions of MgHCitrate and NaCl. Our hypothesis is that closing the orders of magnitude gap between measured and model-calculated concentrations (Figure IV.4-5) requires an additional Fe^{+2}-Citrate^{-3} complexation reaction.

IV.5.3. Reactor Preparation

MgFeCit-1-(1,2,3,4): 42 mL of 0.100 m (0.099 M) of NaCl solution + 5 mL of Mg-Cit stock solution + 3 mL of $Fe(OH)_2(s)$ suspension was mixed. The $Fe(OH)_2(s)$ suspension was dense enough to give excess $Fe(OH)_2(s)$ after 3-to-50 (i.e., 16.7 times) dilution. The Mg-Cit stock solution contains 0.442 M Mg and 0.526 M Citrate. For MgFeCit-(2,3,4,5,6)-(1,2,3), 42 mL of 1.00, 2.00, 3.00, 4.00, and 5.00 m NaCl solution was mixed with 5 mL of Mg-Cit stock solution + 3 mL of $Fe(OH)_2(s)$ suspension. The 1.00, 2.00, 3.00, 4.00, and 5.00 m NaCl solutions are equivalent to 0.9803, 1.921, 2.825, 3.693, and 4.528 M. Concentrations of components in the background solutions are listed in the Table below.

Table IV.5-1. Recipe and calculated solution properties for Mg and Fe-Citrate complexation experiments.

	M				m		
Reactor ID	NaCl	Mg	Cit	M:m[A]	NaCl	Mg	Cit
MgFeCit-1-(1~4)	8.39E-02	4.42E-02	5.26E-02	1.0008	8.40E-02	4.42E-02	5.26E-02
MgFeCit-2-(1~3)	8.23E-01	4.42E-02	5.26E-02	1.0166	8.37E-01	4.49E-02	5.35E-02
MgFeCit-3-(1~3)	1.61E+00	4.42E-02	5.26E-02	1.0340	1.67E+00	4.57E-02	5.44E-02
MgFeCit-4-(1~3)	2.37E+00	4.42E-02	5.26E-02	1.0513	2.49E+00	4.65E-02	5.53E-02
MgFeCit-5-(1~3)	3.10E+00	4.42E-02	5.26E-02	1.0684	3.31E+00	4.72E-02	5.62E-02
MgFeCit-6-(1~3)	3.80E+00	4.42E-02	5.26E-02	1.0855	4.13E+00	4.80E-02	5.71E-02

[A] $M:m\ (L/kg) = 0.0005 \times M^2 + 0.0208 \times M + 0.9991$.

IV.5.4. Data - Aqueous

IV.5.4.1. pHr

pHr was recorded three times (Table IV.5-2; Figure IV.5-1). Scatter in the measurements was less than 11% as %2SD (Table IV.5-3). Averaged pHr's were between 7.5 and 8.0 (Figure IV.5-2).

Table IV.5-2. Time-dependent measurements of pHr (DSP = Days Since Preparation, i.e., aging time in days).

MgFeCit-1-1		MgFeCit-1-2		MgFeCit-1-3		MgFeCit-1-4		MgFeCit-2-1		MgFeCit-2-2	
DSP	pHr	DSP	pHr	DSP	pHr	DSP	pHr	DSP	pHr	DSP	pHr
3	7.60	3	7.60	3	7.18	1	6.95	9	7.82	9	7.77
63	8.17	63	8.20	63	8.22	55	7.94	63	7.98	63	7.98
1162	8.13	1162	8.12	1162	8.23	1155	8.23	1162	7.92	1162	7.90
MgFeCit-2-3		MgFeCit-3-1		MgFeCit-3-2		MgFeCit-3-3		MgFeCit-4-1		MgFeCit-4-2	
DSP	pHr	DSP	pHr	DSP	pHr	DSP	pHr	DSP	pHr	DSP	pHr
9	7.40	9	7.84	9	7.83	9	7.83	9	7.74	9	7.74
63	8.05	63	7.86	63	7.86	63	7.94	64	7.74	64	7.75
1162	7.99	1162	7.77	1162	7.77	1163	7.90	1163	7.75	1163	7.73

MgFeCit-4-3		MgFeCit-5-1		MgFeCit-5-2		MgFeCit-5-3		MgFeCit-6-1		MgFeCit-6-2	
DSP	pHr	DSP	pHr	DSP	pHr	DSP	pHr	DSP	pHr	DSP	pHr
9	7.75	10	7.64	10	7.67	10	7.67	10	7.63	10	7.63
64	7.80	64	7.67	64	7.66	64	7.70	64	7.62	64	7.62
1163	7.79	1163	7.63	1163	7.63	1163	7.63	1163	7.60	1163	7.60

MgFeCit-6-3	
DSP	pHr
10	7.63
64	7.66
1163	7.59

409

410 Figure IV.5-1. Time-dependent measurement results of pHr.

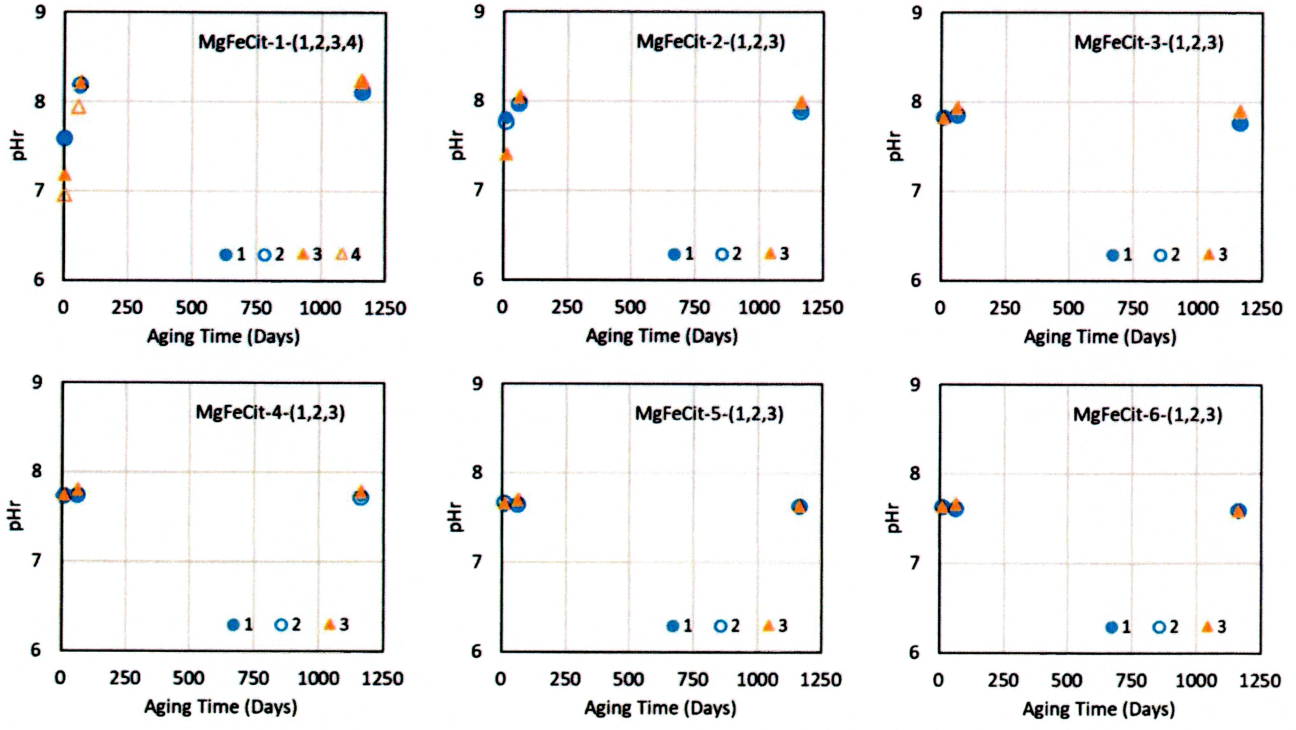

411

412

413

414 Table IV.5-3. Statistics of pHr measurements.

pHr	Average	SD	2SD	%SD	%2SD	Counts
MgFeCit-1-(1~4)	7.88	0.45	0.89	6%	11%	12
MgFeCit-2-(1~3)	7.87	0.19	0.39	2%	5%	9
MgFeCit-3-(1~3)	7.84	0.05	0.11	1%	1%	9
MgFeCit-4-(1~3)	7.75	0.02	0.05	0%	1%	9
MgFeCit-5-(1~3)	7.66	0.02	0.05	0%	1%	9
MgFeCit-6-(1~3)	7.62	0.02	0.05	0%	1%	9

415

Figure IV.5-2. Change of pHr as a function of ΣNa loading.

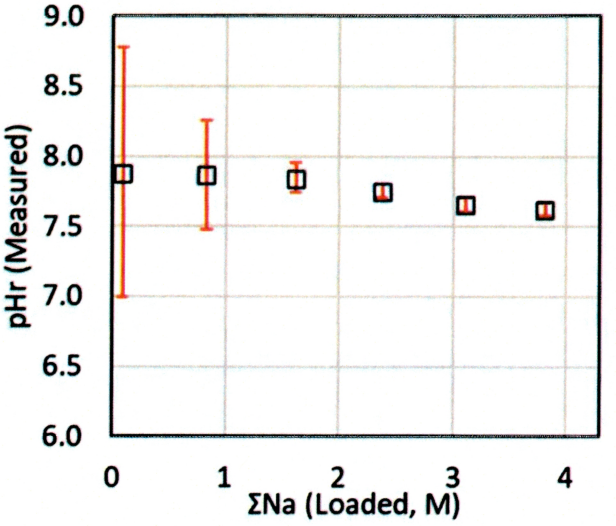

IV.5.4.2. ΣFe

ΣFe measurements are summarized in Table IV.5-4. Three measurement techniques showed agreement: ICP-AES, Ferrozine for ferrous iron, and Ferrozine for total dissolved iron (Figure IV.5-3). The scatter of the measurements was less than 13% as %2SD (Table IV.5-5). Averaged ΣFe ranges from 0.05 to 0.06 M (Figure IV.5-4). The ratios of ΣFe to ΣCitrate loading are displayed as data labels in Figure IV.5-4 and are close to 100%. Unlike in experiments performed at higher pH (Section IV.4; Data labels in Figure IV.4-2), $Citrate^{-3}$ effectively extracts Fe^{+2} into solution at circumneutral pHr. The ratios exceeding 100% of the loaded ΣCitrate are thought to be experimental uncertainty.

Table IV.5-4. Time-dependent measurements of ΣFe in M (DSP = Days Since Preparation, i.e., aging time in days).

MgFeCit-1-1		MgFeCit-1-2		MgFeCit-1-3		MgFeCit-1-4		MgFeCit-2-1		MgFeCit-2-2	
DSP	ΣFe	DSP	ΣFe	DSP	ΣFe	DSP	ΣFe	DSP	ΣFe	DSP	ΣFe
65	5.73E-02	65	5.75E-02	65	5.71E-02	57	5.66E-02	65	5.60E-02	65	5.79E-02
65	*5.81E-02*	*65*	*5.81E-02*	*65*	*5.78E-02*	*57*	*5.66E-02*	*65*	*5.68E-02*	*65*	*5.87E-02*
65	5.86E-02	65	5.83E-02	65	5.76E-02	57	5.63E-02	65	5.46E-02	65	5.69E-02
MgFeCit-2-3		MgFeCit-3-1		MgFeCit-3-2		MgFeCit-3-3		MgFeCit-4-1		MgFeCit-4-2	
DSP	ΣFe	DSP	ΣFe	DSP	ΣFe	DSP	ΣFe	DSP	ΣFe	DSP	ΣFe
65	5.69E-02	65	5.70E-02	65	5.76E-02	65	5.81E-02	65	5.70E-02	65	5.79E-02
65	*5.78E-02*	*65*	*5.76E-02*	*65*	*5.75E-02*	*65*	*5.80E-02*	*65*	*5.75E-02*	*65*	*5.76E-02*
65	5.60E-02	65	5.40E-02	65	5.43E-02	65	5.44E-02	65	5.32E-02	65	5.34E-02
MgFeCit-4-3		MgFeCit-5-1		MgFeCit-5-2		MgFeCit-5-3		MgFeCit-6-1		MgFeCit-6-2	
DSP	ΣFe	DSP	ΣFe	DSP	ΣFe	DSP	ΣFe	DSP	ΣFe	DSP	ΣFe
65	5.67E-02	65	5.53E-02	65	5.78E-02	65	5.79E-02	65	5.57E-02	65	5.52E-02

65	*5.67E-02*	*65*	*5.51E-02*	*65*	*5.76E-02*	*65*	*5.78E-02*	*65*	*5.54E-02*	*65*	*5.52E-02*
65	5.28E-02	65	5.05E-02	65	4.89E-02	65	5.14E-02	65	4.89E-02	65	4.92E-02

MgFeCit-6-3	
DSP	ΣFe
65	5.57E-02
65	*5.51E-02*
65	4.90E-02

Values in normal Times New Roman fonts were obtained by Ferrozine technique for dissolved ferrous iron; values in italic fonts were obtained by Ferrozine technique for dissolved total iron; values underlined were obtained by ICP-AES for dissolved total iron.

Figure IV.5-3. Time-dependent measurements of ΣFe. Different colors and symbols indicate the results of different ΣFe measurement techniques.

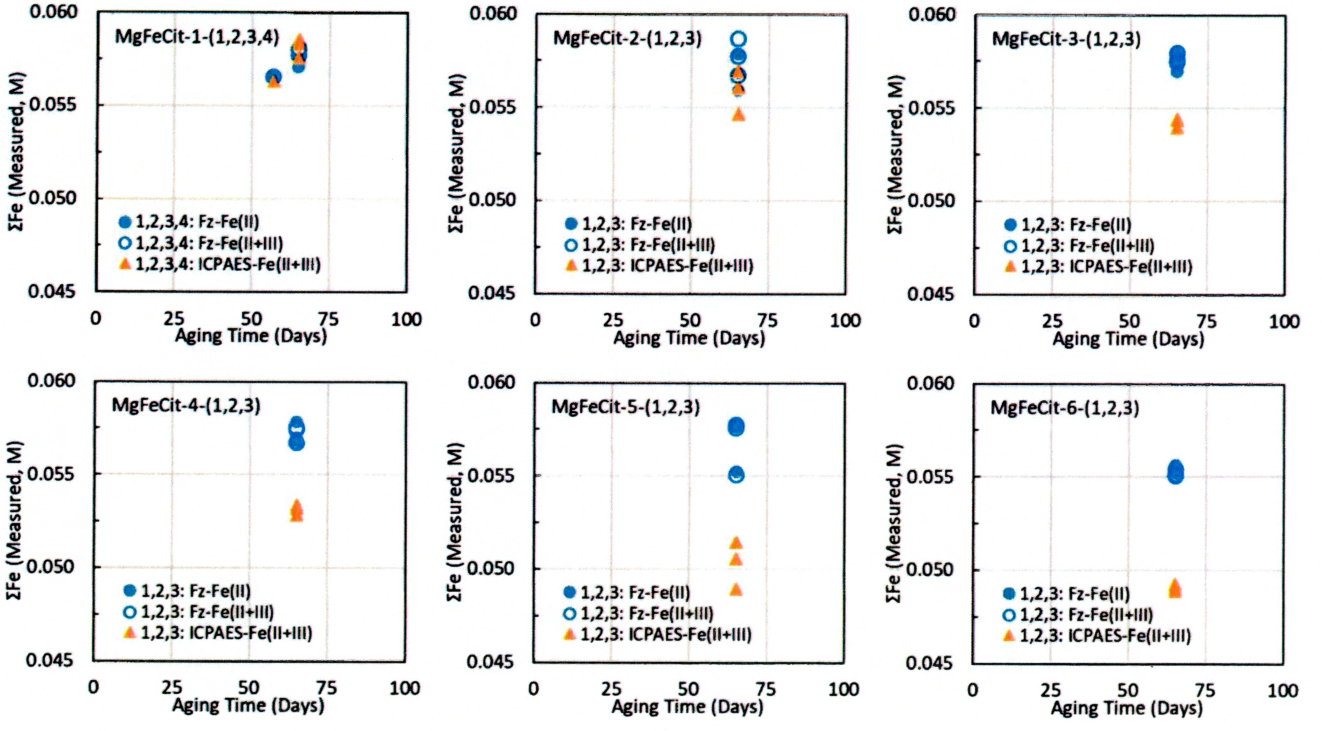

Table IV.5-5. Statistics of ΣFe measurements.

ΣFe, M	Average	SD	2SD	%SD	%2SD	Counts
MgFeCit-1-(1~4)	5.75E-02	7.22E-04	1.44E-03	1%	3%	12
MgFeCit-2-(1~3)	5.68E-02	1.23E-03	2.46E-03	2%	4%	9
MgFeCit-3-(1~3)	5.65E-02	1.75E-03	3.50E-03	3%	6%	9
MgFeCit-4-(1~3)	5.59E-02	2.10E-03	4.20E-03	4%	8%	9
MgFeCit-5-(1~3)	5.47E-02	3.53E-03	7.06E-03	6%	13%	9
MgFeCit-6-(1~3)	5.33E-02	3.18E-03	6.36E-03	6%	12%	9

Figure IV.5-4. Change of ΣFe as a function of ΣNa loading. Data labels are the ratio of ΣFe/ΣCitrate.

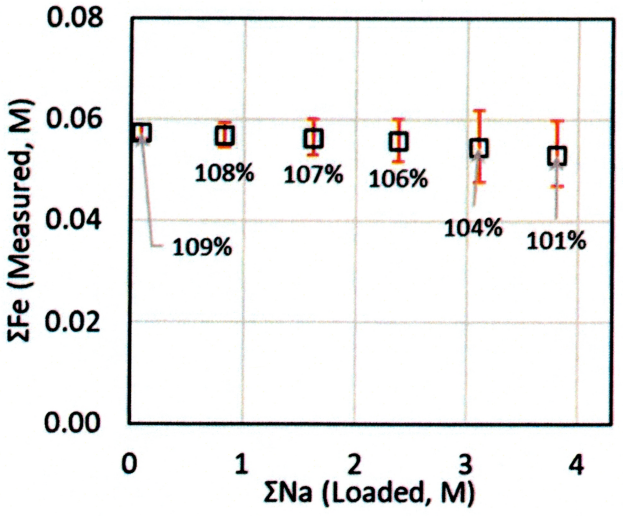

IV.5.4.3. ΣCitrate

Citrate measurements are summarized in Table IV.5-6. Two measurement techniques (IC and coulometer) showed agreement (Figure IV.5-5): the scatter of the measurements was less than 7% as %2SD (Table IV.5-7). The accuracy and precision of Citrate measurements are shown in Figure IV.5-6. The loaded ΣCitrate was confirmed by measurement. We have demonstrated through different set of experiments that the microbial consumption of Citrate was effectively suppressed under our laboratory practice (e.g., use of filtered DI water, use of brand-new supplies for repeated sampling) for up to 900 days (Figure IV.5-7).

Table IV.5-6. Time-dependent measurements of ΣCitrate (DSP = Days Since Preparation, i.e., aging time in days).

MgFeCit-1-1		MgFeCit-1-2		MgFeCit-1-3		MgFeCit-1-4		MgFeCit-2-1		MgFeCit-2-2	
DSP	ΣCitrate	DSP	ΣCitrate	DSP	ΣCitrate	DSP	ΣCitrate	DSP	ΣCitrate	DSP	ΣCitrate
65	5.40E-02	65	5.41E-02	65	5.26E-02	57	5.48E-02	65	5.35E-02	65	5.45E-02
65	*5.29E-02*							*65*	*5.10E-02*		
MgFeCit-2-3		MgFeCit-3-1		MgFeCit-3-2		MgFeCit-3-3		MgFeCit-4-1		MgFeCit-4-2	
DSP	ΣCitrate	DSP	ΣCitrate	DSP	ΣCitrate	DSP	ΣCitrate	DSP	ΣCitrate	DSP	ΣCitrate
65	5.56E-02	65	5.41E-02	65	5.34E-02	65	5.46E-02	65	5.37E-02	65	5.42E-02
		65	*5.14E-02*					*65*	*5.29E-02*		
MgFeCit-4-3		MgFeCit-5-1		MgFeCit-5-2		MgFeCit-5-3		MgFeCit-6-1		MgFeCit-6-2	
DSP	ΣCitrate	DSP	ΣCitrate	DSP	ΣCitrate	DSP	ΣCitrate	DSP	ΣCitrate	DSP	ΣCitrate
65	5.48E-02	65	5.36E-02	65	5.58E-02	65	5.44E-02	65	5.10E-02	65	5.19E-02
		65	*5.11E-02*					*65*	*5.04E-02*		
MgFeCit-6-3											
DSP	ΣCitrate										

65	5.28E-02

Values in italic fonts were obtained by coulometer

Figure IV.5-5. Time-dependent measurements of ΣCitrate.

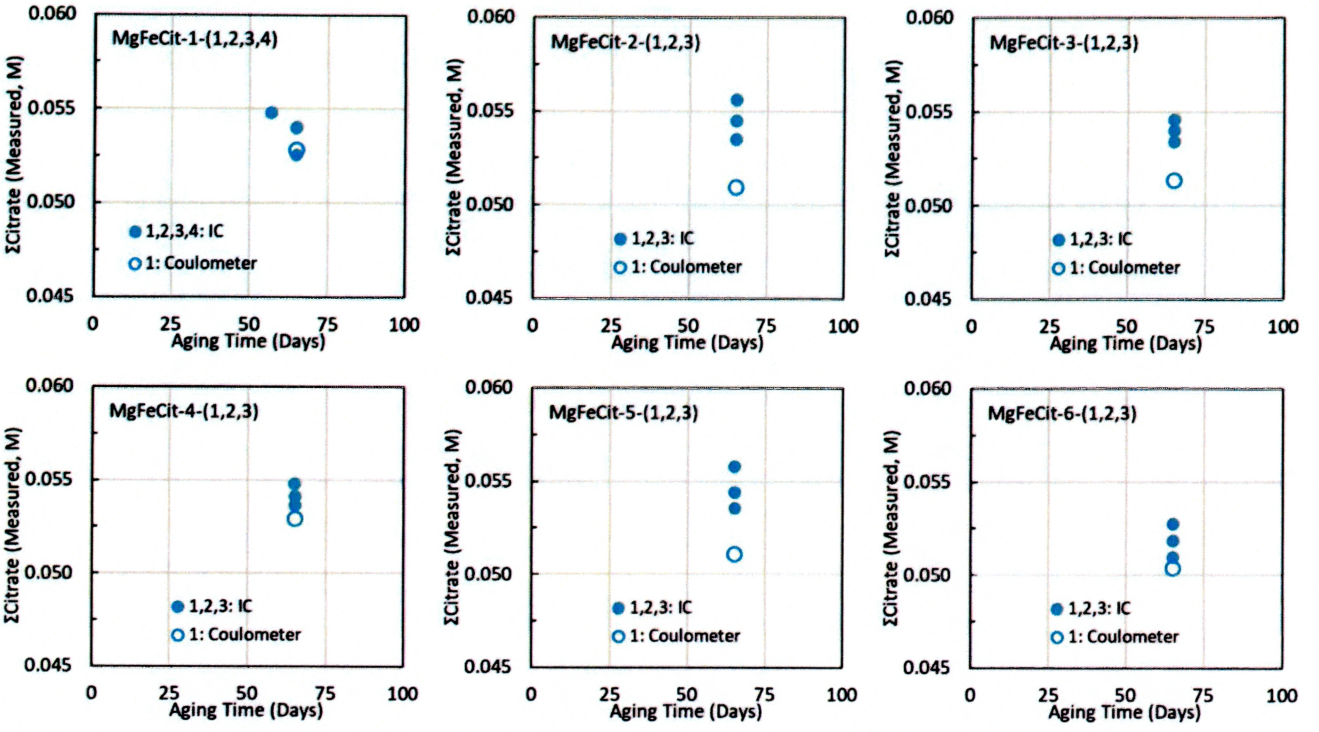

Table IV.5-7. Statistics of ΣCitrate measurements.

ΣCitrate, M	Average	2SD	%2SD	%Deviation	Counts
MgFeCit-1-(1~4)	5.37E-02	1.86E-03	3%	2%	5
MgFeCit-2-(1~3)	5.37E-02	3.96E-03	7%	2%	4
MgFeCit-3-(1~3)	5.34E-02	2.84E-03	5%	1%	4
MgFeCit-4-(1~3)	5.39E-02	1.59E-03	3%	2%	4
MgFeCit-5-(1~3)	5.38E-02	3.94E-03	7%	2%	4
MgFeCit-6-(1~3)	5.15E-02	2.09E-03	4%	-2%	4

458 Figure IV.5-6. Accuracy and precision of ΣCitrate measurements.

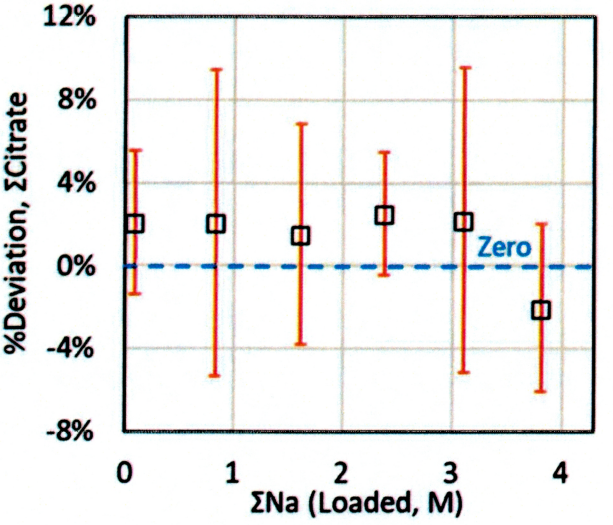

459

460 Figure IV.5-7. Time-dependent measurements of ΣCitrate for more than 900 days. The
461 last panel demonstrates the accuracy and precision of ΣCitrate measurements by
462 IC.

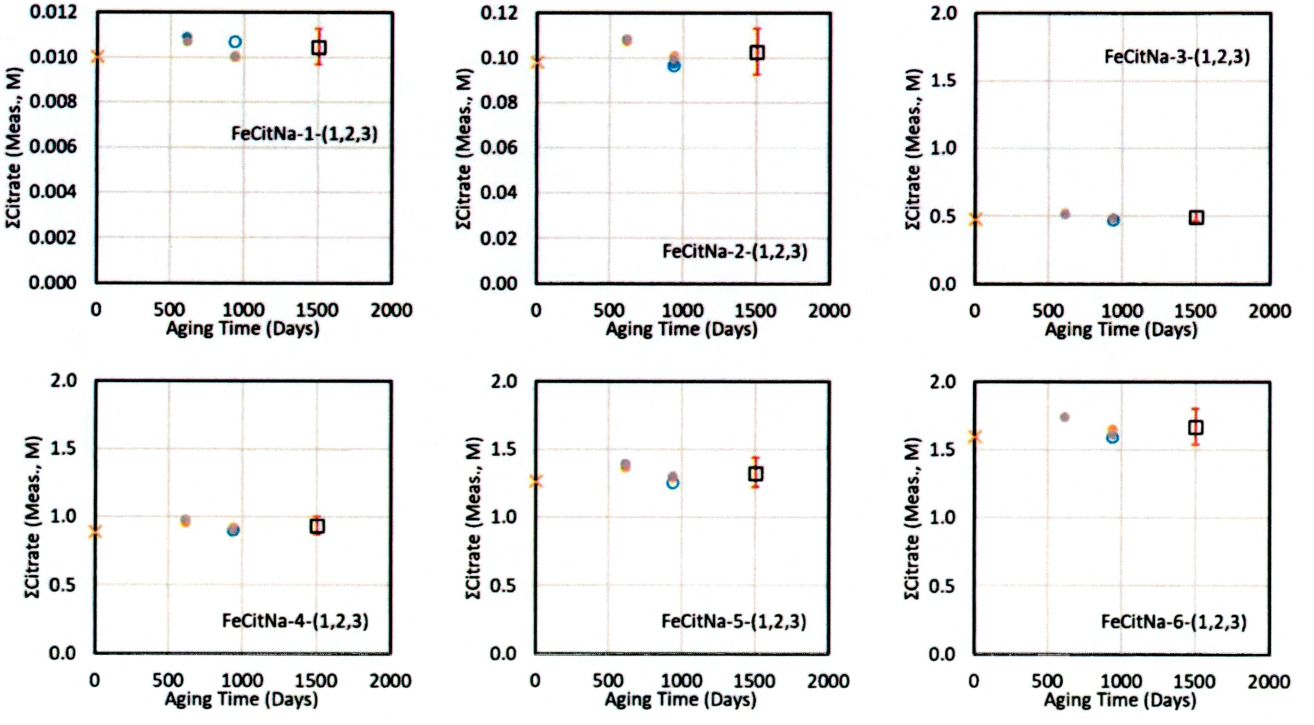

463

464

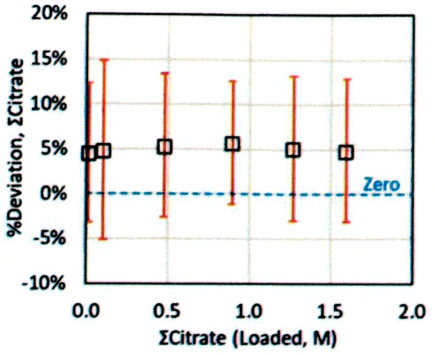

IV.5.4.4. ΣMg

Measurements of ΣMg are summarized in Table IV.5-8. The scatter of the measurements was less than 6% (maximum %2SD, i.e., precision; Table IV.5-9). %Deviation of the measurements from the loading reached 30+% (Figure IV.5-8).

Table IV.5-8. Measurements of ΣMg on 57 or 65 days of aging (DSP = Days Since Preparation, i.e., Aging time in days).

MgFeCit-1-1		MgFeCit-1-2		MgFeCit-1-3		MgFeCit-1-4		MgFeCit-2-1		MgFeCit-2-2	
DSP	ΣMg	DSP	ΣMg	DSP	ΣMg	DSP	ΣMg	DSP	ΣMg	DSP	ΣMg
65	4.92E-02	65	4.92E-02	65	4.86E-02	57	4.83E-02	65	5.30E-02	65	5.48E-02
MgFeCit-2-3		MgFeCit-3-1		MgFeCit-3-2		MgFeCit-3-3		MgFeCit-4-1		MgFeCit-4-2	
DSP	ΣMg	DSP	ΣMg	DSP	ΣMg	DSP	ΣMg	DSP	ΣMg	DSP	ΣMg
65	5.45E-02	65	5.66E-02	65	5.70E-02	65	5.62E-02	65	5.81E-02	65	5.90E-02
MgFeCit-4-3		MgFeCit-5-1		MgFeCit-5-2		MgFeCit-5-3		MgFeCit-6-1		MgFeCit-6-2	
DSP	ΣMg	DSP	ΣMg	DSP	ΣMg	DSP	ΣMg	DSP	ΣMg	DSP	ΣMg
65	5.78E-02	65	5.87E-02	65	5.60E-02	65	5.94E-02	65	5.70E-02	65	5.71E-02
MgFeCit-6-3											
DSP	ΣMg										
65	5.72E-02										

Table IV.5-9. Statistics of ΣMg measurements.

ΣMg, M	Average	SD	2SD	%SD	%2SD	Counts
MgFeCit-1-(1~4)	4.88E-02	4.54E-04	9.08E-04	1%	2%	4
MgFeCit-2-(1~3)	5.41E-02	9.80E-04	1.96E-03	2%	4%	3
MgFeCit-3-(1~3)	5.66E-02	3.92E-04	7.85E-04	1%	1%	3
MgFeCit-4-(1~3)	5.83E-02	6.30E-04	1.26E-03	1%	2%	3
MgFeCit-5-(1~3)	5.80E-02	1.78E-03	3.56E-03	3%	6%	3
MgFeCit-6-(1~3)	5.71E-02	1.04E-04	2.07E-04	0%	0%	3

475 Figure IV.5-8. Accuracy and precision of ΣMg measurements as a function of ΣNa
476 loading.

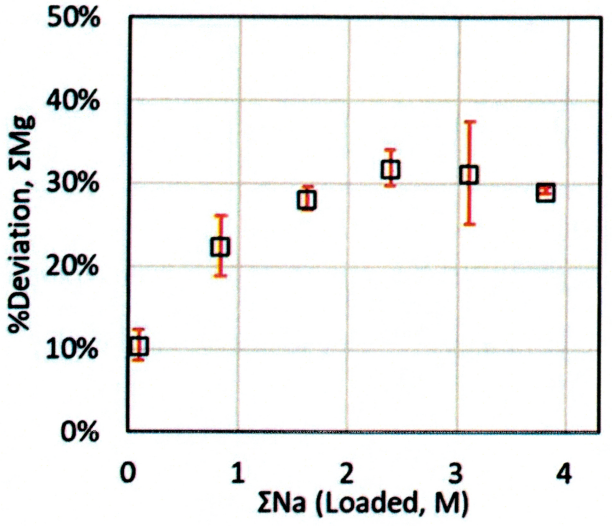

477

478 IV.5.4.5. ΣNa

479 Measurements of ΣNa are summarized in Table IV.5-10. The scatter of the measurements was less
480 than 7% (maximum %2SD, i.e., precision; Table IV.5-11). The accuracy and precision of the
481 measurements are shown in Figure IV.5-9.

482 Table IV.5-10. Measurements of ΣNa on 57 or 65 days of aging (DSP = Days Since
483 Preparation, i.e., Aging time in days).

MgFeCit-1-1		MgFeCit-1-2		MgFeCit-1-3		MgFeCit-1-4		MgFeCit-2-1		MgFeCit-2-2	
DSP	ΣNa	DSP	ΣNa	DSP	ΣNa	DSP	ΣNa	DSP	ΣNa	DSP	ΣNa
65	8.53E-02	65	4.92E-02	65	8.35E-02	57	8.13E-02	65	7.83E-01	65	8.00E-01
MgFeCit-2-3		MgFeCit-3-1		MgFeCit-3-2		MgFeCit-3-3		MgFeCit-4-1		MgFeCit-4-2	
DSP	ΣNa	DSP	ΣNa	DSP	ΣNa	DSP	ΣNa	DSP	ΣNa	DSP	ΣNa
65	8.26E-01	65	1.57E+00	65	1.57E+00	65	1.54E+00	65	2.30E+00	65	2.30E+00
MgFeCit-4-3		MgFeCit-5-1		MgFeCit-5-2		MgFeCit-5-3		MgFeCit-6-1		MgFeCit-6-2	
DSP	ΣNa	DSP	ΣNa	DSP	ΣNa	DSP	ΣNa	DSP	ΣNa	DSP	ΣNa
65	2.29E+00	65	2.88E+00	65	2.78E+00	65	2.99E+00	65	3.50E+00	65	3.44E+00
MgFeCit-6-3											
DSP	ΣNa										
65	3.51E+00										

484

485 Table IV.5-11. Statistics of ΣNa measurements.

ΣNa, M	Average	SD	2SD	%SD	%2SD	Counts
MgFeCit-1-(1~4)	8.36E-02	1.68E-03	3.36E-03	2%	4%	4
MgFeCit-2-(1~3)	8.03E-01	2.19E-02	4.38E-02	3%	5%	3
MgFeCit-3-(1~3)	1.56E+00	1.76E-02	3.52E-02	1%	2%	3
MgFeCit-4-(1~3)	2.30E+00	4.35E-03	8.70E-03	0%	0%	3

MgFeCit-5-(1~3)	2.89E+00	1.02E-01	2.04E-01	4%	7%	3
MgFeCit-6-(1~3)	3.48E+00	3.45E-02	6.90E-02	1%	2%	3

Figure IV.5-9. Accuracy and precision of ΣNa measurements.

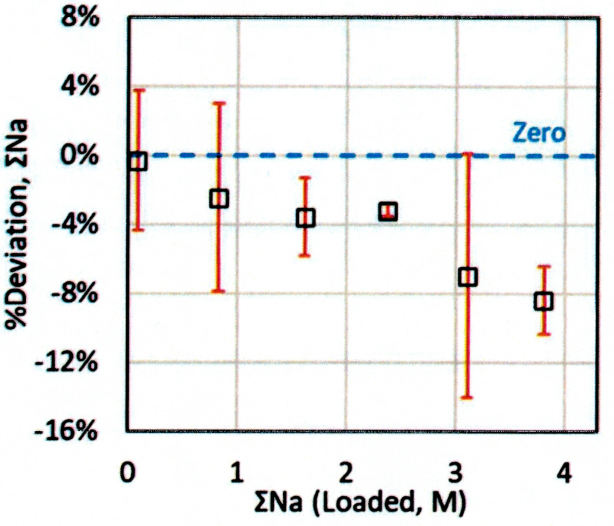

IV.5.4.6. ΣCl

Not measured.

IV.5.5. Data - Solids

$Fe(OH)_2(s)$ was observed in the XRD scans. No other solids than NaCl were identified (Figure IV.5-10).

494 Figure IV.5-10. XRD scans for the solids collected at the end of the experiments of this
495 section.

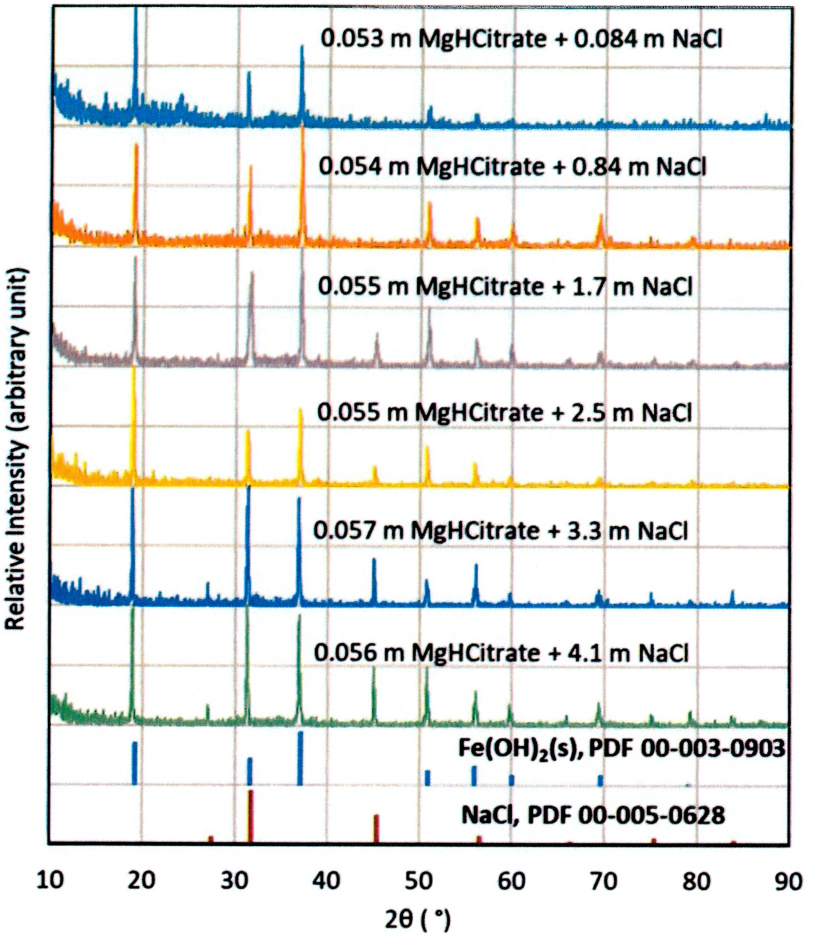

496

497

498 IV.5.6. Observations

499 Experiments were performed at pHr 7.5 - 8.0. Average ΣFe was 0.05 - 0.06 M. Over this pHr range
500 Citrate is an effective Fe^{+2} chelator. No iron solid other than $Fe(OH)_2(s)$ was observed in the XRD
501 scans. Presence of NaCl can be explained by the evaporation of background solution captured in the
502 pore space of collected solids.

503 IV.5.7. Model Parameterization: Pitzer Approach

504 In Table IV.5-12, the concentrations are presented in molality scale.

505 Table IV.5-13 summarizes Fe^{+2}-$Citrate^{-3}$ complexation reactions selected from the literature. The log
506 Ks from Morel and Hering (1993) are used below as they are scaled to zero ionic strength.

507 Figure IV.5-11 demonstrates that the model calculations using the selected reactions underestimate
508 measured $Fe(OH)_2(s)$ solubilities in Sections IV.4 and IV.5 (this section). Specifically, the orders of

magnitude difference between measured and calculated ΣFe in Figure IV.5-11A (i.e., Figure IV.4-5) is too large to be explained by ionic interaction or reasonable modification of the log K($FeCitrate^-$) from its literature value.

Instead, a new reaction for Fe^{+2} - $Citrate^{-3}$ complexation is added, $FeOHCitrate^{-2}$, which is presumed to be stable at high pH and is a chemical analogue to the Cu^{+2}-$Citrate^{-3}$ complex of Morel and Hering (1993); $CuOHCitrate^{-2}$ (Table IV.5-14). Use of the new species with the log K fitted to 2.24 greatly improves the model prediction of the solubility data (Figure IV.5-12).

Table IV.5-12. Concentrations in molality for model calculations. The pmH and ΣFe are measured. ΣNa, ΣMg, ΣCitrate, and ΣCl are the loading.

Analyte	pmH (Meas.)			ΣFe (Meas., m)		
Reactor ID	Average	2SD	%2SD	Average	2SD	%2SD
MgFeCit-1-(1~4)	7.85	0.89	11%	5.75E-02	1.44E-03	3%
MgFeCit-2-(1~3)	7.97	0.39	5%	5.78E-02	2.50E-03	4%
MgFeCit-3-(1~3)	8.08	0.11	1%	5.84E-02	3.62E-03	6%
MgFeCit-4-(1~3)	8.13	0.05	1%	5.87E-02	4.41E-03	8%
MgFeCit-5-(1~3)	8.16	0.05	1%	5.84E-02	7.54E-03	13%
MgFeCit-6-(1~3)	8.25	0.05	1%	5.78E-02	6.91E-03	12%
Reactor ID	ΣNa	ΣCl	ΣMg	ΣCitrate		
MgFeCit-1-(1~4)	8.40E-02	8.40E-02	4.42E-02	5.26E-02		
MgFeCit-2-(1~3)	8.37E-01	8.37E-01	4.49E-02	5.35E-02		
MgFeCit-3-(1~3)	1.67E+00	1.67E+00	4.57E-02	5.44E-02		
MgFeCit-4-(1~3)	2.49E+00	2.49E+00	4.65E-02	5.53E-02		
MgFeCit-5-(1~3)	3.31E+00	3.31E+00	4.72E-02	5.62E-02		
MgFeCit-6-(1~3)	4.13E+00	4.13E+00	4.80E-02	5.71E-02		

Table IV.5-13. Literature-retrieved reactions and their log Ks.

Reaction	Log K (I= 0)	Log K_{app}	References
$FeCitrate^- = Fe^{+2} + Citrate^{-3}$	-5.7		Morel and Hering (1993)
		-4.4 (20 °C, 0.1)	Martell and Smith (1977)
		-3.1 (1 M NaClO4)	Lerman and Childs (1973)
$FeHCitrate(aq) = Fe^{+2} + H^+ + Citrate^{-3}$	-9.9		Morel and Hering (1993)
		-8.5 (1 M NaClO4)	Lerman and Childs (1973)
$FeHCitrate(aq) = Fe^{+2} + HCitrate^{-2}$		-2.65 (20 °C, 0.1)	Martell and Smith (1977)

Figure IV.5-11. Application of literature-retrieved thermodynamic quantities in Table IV.5-13. A. Same as Figure IV.4-5. B. Data of this section (IV.5).

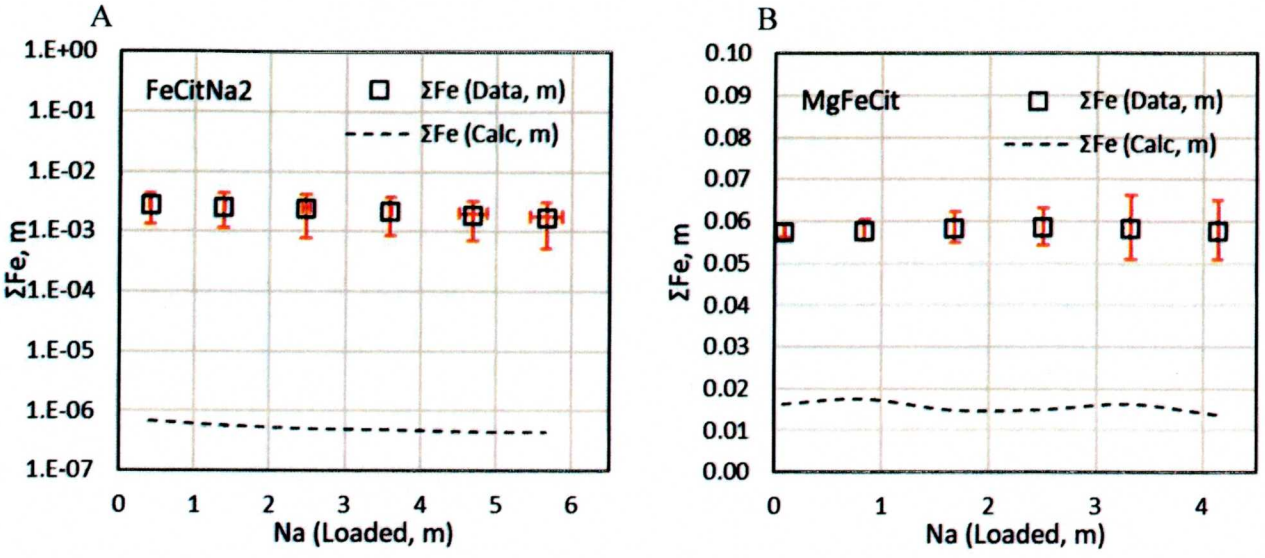

Table IV.5-14. New required reaction to better delineate the measurements in Figure IV.5-11.

Reaction	Log K (I= 0)	References
$FeOHCitrate^{-2} + H^{+} = Fe^{+2} + Citrate^{-3} + H_2O$[A]	2.24	This section

[A] By analogy with Cu^{+2} in Morel and Hering (1993), i.e., $CuOHCitrate^{-2}$.

Figure IV.5-12. Introduction of new reaction (Table IV.5-14).

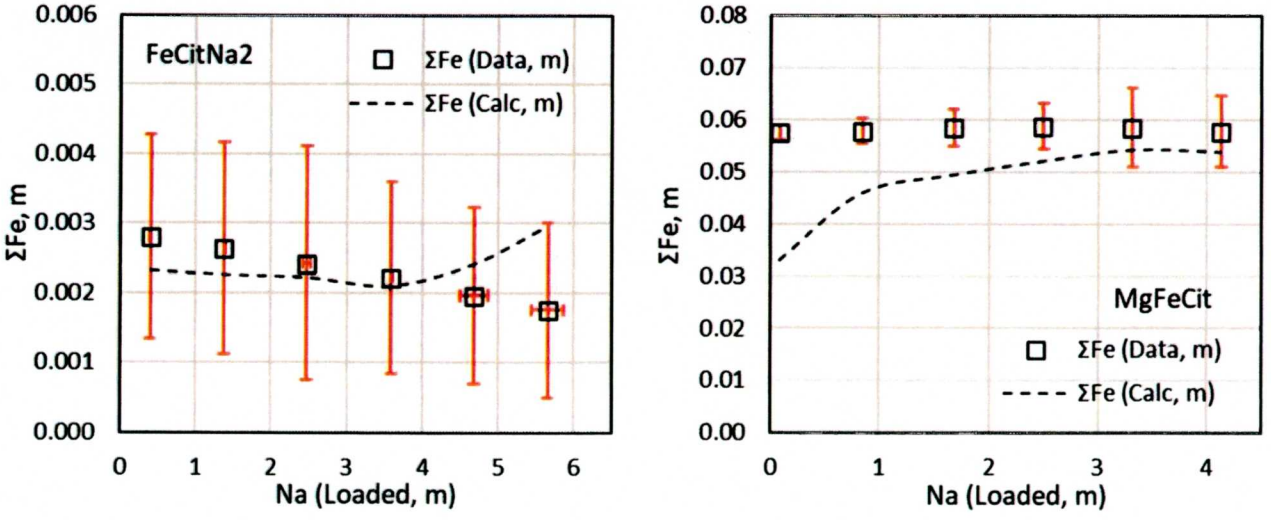

IV.5.8. Summary

A model based on literature log K($FeCitrate^{-}$) = -5.7 could not accurately predict measured $Fe(OH)_2(s)$ solubilities; so a new complex, $FeOHCitrate^{-2}$ with its log K fitted to 2.24 (Table IV.5-14), was shown to better fit the data. No new PIPs were necessary.

V. LEAD (Pb)

V.1. $PbCl_2(s) - H_2O$

V.1.1. Chemical System

Excess $PbCl_2(s)$ (cotunnite) was added to water. The four components in this system are Pb^{+2}, Cl^-, H^+, and H_2O.

V.1.2. Goals and Hypotheses

The goal of this experiment was to confirm that the dissolved total concentration of Pb (ΣPb) at equilibrium with three $PbCl_2(s)$ solids of different purity and/or LOT numbers is the same.

V.1.3. Reactor Preparation

Three different $PbCl_2(s)$'s were used to prepare the reactors listed in Table V.1-1. One $PbCl_2(s)$ is from Acros Organics (99%, LOT A0387918).[50] The other two are from Alfa Aesar; 99.999%, LOT Z31E012 and 99.999%, LOT 23244. XRD scans for two commercial $PbCl_2(s)$ are presented in Figure V.1-1.

Table V.1-1. Recipe for PbCl2DI series.

Reactor ID	$PbCl_2(s)$, LOT Number, %Purity	$PbCl_2(s)$, gram	DDI water, mL
PbCl2DI-1-1	A0387918, 99%	1.0008	50
PbCl2DI-1-2	A0387918, 99%	4.9999	50
PbCl2DI-1-3	A0387918, 99%	15.0012	50
PbCl2DI-2-1	Z31E012, 99.999%	1.0007	50
PbCl2DI-2-2	Z31E012, 99.999%	5.0006	50
PbCl2DI-2-3	Z31E012, 99.999%	15.0001	50
PbCl2DI-3-1	23244, 99.999%	1.0003	50
PbCl2DI-3-2	23244, 99.999%	5.0006	50
PbCl2DI-3-3	23244, 99.999%	14.9999	50

[50] Acros Organics (2017)

549 Figure V.1-1. XRD scans of the commercial $PbCl_2$(s).

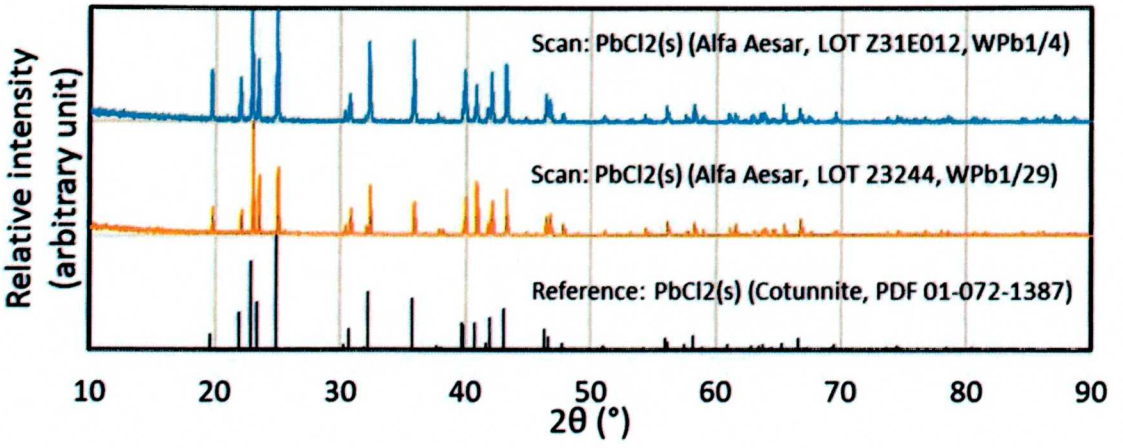

550

551 V.1.4. Data - Aqueous

552 V.1.4.1. pHr

553 pHr measurements are shown in Table V.1-2. Scatters observed in Figure V.1-2 are less than 0.05
554 pH units (2SD of 27 measurements; Table V.1-3). Data from experiments with three solid:solution
555 ratios do not show significant differences.

556 Table V.1-2. Time-dependent measurements of pHr (DSP = Days Since Preparation, i.e.,
557 Aging time in days).

PbCl2DI-1-1		PbCl2DI-1-2		PbCl2DI-1-3	
DSP	pHr	DSP	pHr	DSP	pHr
29	3.97	29	3.97	29	3.958
65	3.96	65	3.96	65	3.942
98	3.98	98	3.99	98	3.993
PbCl2DI-2-1		PbCl2DI-2-2		PbCl2DI-2-3	
DSP	pHr	DSP	pHr	DSP	pHr
29	3.953	29	3.953	29	3.94
65	3.935	65	3.93	65	3.918
98	3.988	98	3.982	98	3.974
PbCl2DI-3-1		PbCl2DI-3-2		PbCl2DI-3-3	
DSP	pHr	DSP	pHr	DSP	pHr
29	3.937	29	3.935	29	3.942
65	3.921	65	3.916	65	3.915
98	3.951	98	3.937	98	3.976

558

559 Figure V.1-2. pHr and aging time. A. $PbCl_2$(s) from Acros Organics, LOT A0387918, at
560 three different solid:solution ratios. B. $PbCl_2$(s) from Alfa Aesar, LOT Z31E012,
561 at three different solid:solution ratios. C. $PbCl_2$(s) from Alfa Aesar, LOT 23244,
562 at three different solid:solution ratios.

563

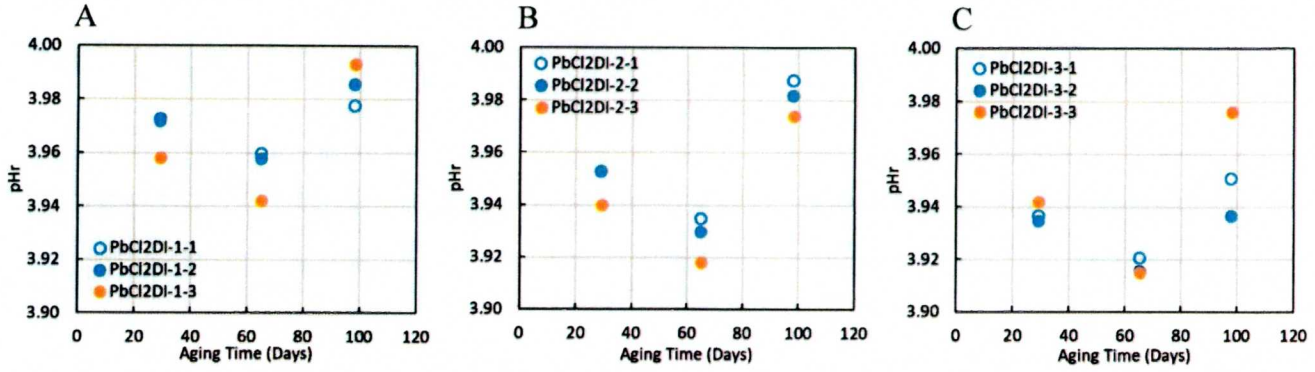

564

565 Table V.1-3. Statistics of pHr measurements.

	Average	SD	2SD	%SD	%2SD	Counts
pHr	3.95	0.02	0.05	1%	1%	27

566

567 V.1.4.2. ΣPb

568 ΣPb measurements are tabulated in Table V.1-4. The scatter observed in Figure V.1-3 is within
569 10% (%2SD of 27 measurements; Table V.1-5).

570 Table V.1-4. Time-dependent measurements of ΣPb (M) (DSP = Days Since Preparation,
571 i.e., Aging time in days).

PbCl2DI-1-1		PbCl2DI-1-2		PbCl2DI-1-3	
DSP	ΣPb	DSP	ΣPb	DSP	ΣPb
30	4.49E-02	30	4.01E-02	30	4.04E-02
65	3.61E-02	65	4.28E-02	65	3.95E-02
98	3.72E-02	98	3.72E-02	98	3.73E-02
PbCl2DI-2-1		PbCl2DI-2-2		PbCl2DI-2-3	
DSP	ΣPb	DSP	ΣPb	DSP	ΣPb
30	4.00E-02	30	3.90E-02	30	4.08E-02
65	3.88E-02	65	3.85E-02	65	3.96E-02
98	3.74E-02	98	3.73E-02	98	3.77E-02
PbCl2DI-3-1		PbCl2DI-3-2		PbCl2DI-3-3	
DSP	ΣPb	DSP	ΣPb	DSP	ΣPb
30	3.86E-02	30	4.03E-02	30	4.16E-02
65	3.93E-02	65	3.96E-02	65	3.96E-02
98	3.86E-02	98	3.71E-02	98	3.93E-02

572

Figure V.1-3. ΣPb over aging time. A. $PbCl_2$(s) from Acros Organics, LOT AO387918. B. $PbCl_2$(s) from Alfa Aesar, LOT Z31E012. C. $PbCl_2$(s) from Alfa Aesar, LOT 23244.

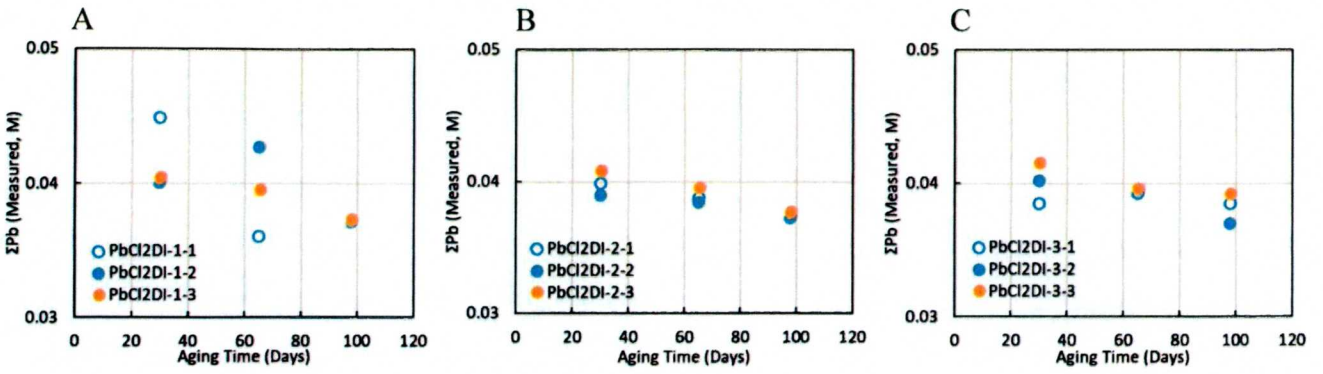

Table V.1-5. Statistics of ΣPb measurements (M).

	Average	SD	2SD	%SD	%2SD	Counts
ΣPb	3.92E-02	1.90E-03	3.81E-03	5%	10%	27

V.1.4.3. ΣCl

ΣCl measurements are tabulated in Table V.1-6. Scatter observed in Figure V.1-4 is within 7% (%2SD of 27 measurements; Table V.1-7).

Table V.1-6. Time-dependent measurements of ΣCl in M (DSP = Days Since Preparation, i.e., Aging time in days).

PbCl2DI-1-1		PbCl2DI-1-2		PbCl2DI-1-3	
DSP	ΣCl	DSP	ΣCl	DSP	ΣCl
30	8.30E-02	30	8.37E-02	30	8.48E-02
65	7.76E-02	65	7.88E-02	65	7.92E-02
98	7.70E-02	98	7.83E-02	98	7.70E-02
PbCl2DI-2-1		PbCl2DI-2-2		PbCl2DI-2-3	
DSP	ΣCl	DSP	ΣCl	DSP	ΣCl
30	8.08E-02	30	8.27E-02	30	8.31E-02
65	7.85E-02	65	7.86E-02	65	7.83E-02
98	7.78E-02	98	7.90E-02	98	7.92E-02
PbCl2DI-3-1		PbCl2DI-3-2		PbCl2DI-3-3	
DSP	ΣCl	DSP	ΣCl	DSP	ΣCl
30	8.33E-02	30	9.03E-02	30	8.34E-02
65	7.91E-02	65	7.97E-02	65	7.87E-02
98	7.90E-02	98	7.98E-02	98	7.98E-02

Figure V.1-4. ΣCl measurements over aging time. A. $PbCl_2$(s) from Acros Organics, LOT AO387918. B. $PbCl_2$(s) from Alfa Aesar, LOT Z31E012. C. $PbCl_2$(s) from Alfa Aesar, LOT 23244.

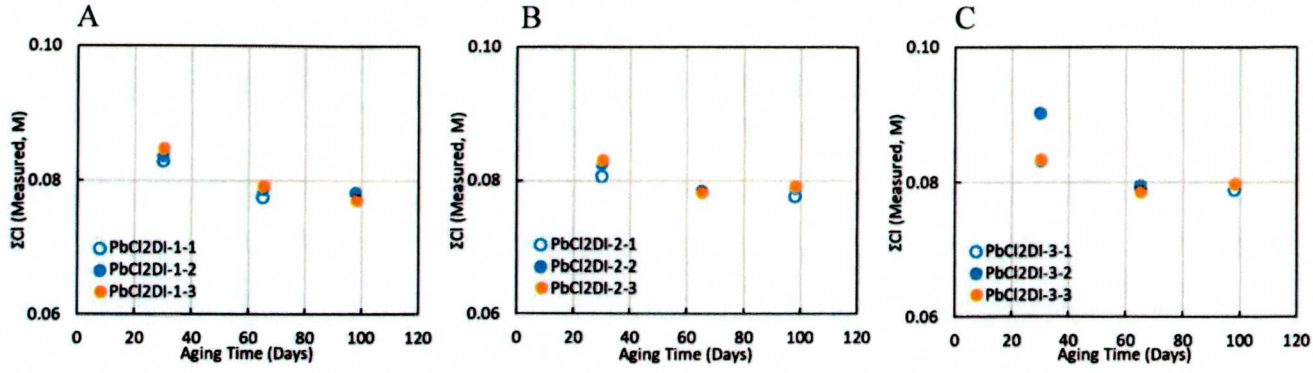

Table V.1-7. Statistics of ΣCl measurements (M).

	Average	SD	2SD	%SD	%2SD	Counts
ΣCl	8.04E-02	3.00E-03	6.00E-03	4%	7%	27

V.1.5. Data - Solids

Solids collected from the nine reactors after the third sampling (98 days) were examined by XRD (Figure V.1-5). $PbCl_2$(s) (cotunnite) was identified. No other solids were found. Maturing of $PbCl_2$(s) along minor crystalline structure(s) was observed in the reactor PbCl2DI-2-3.

Figure V.1-5. XRD scans for the solids collected from the nine reactors.

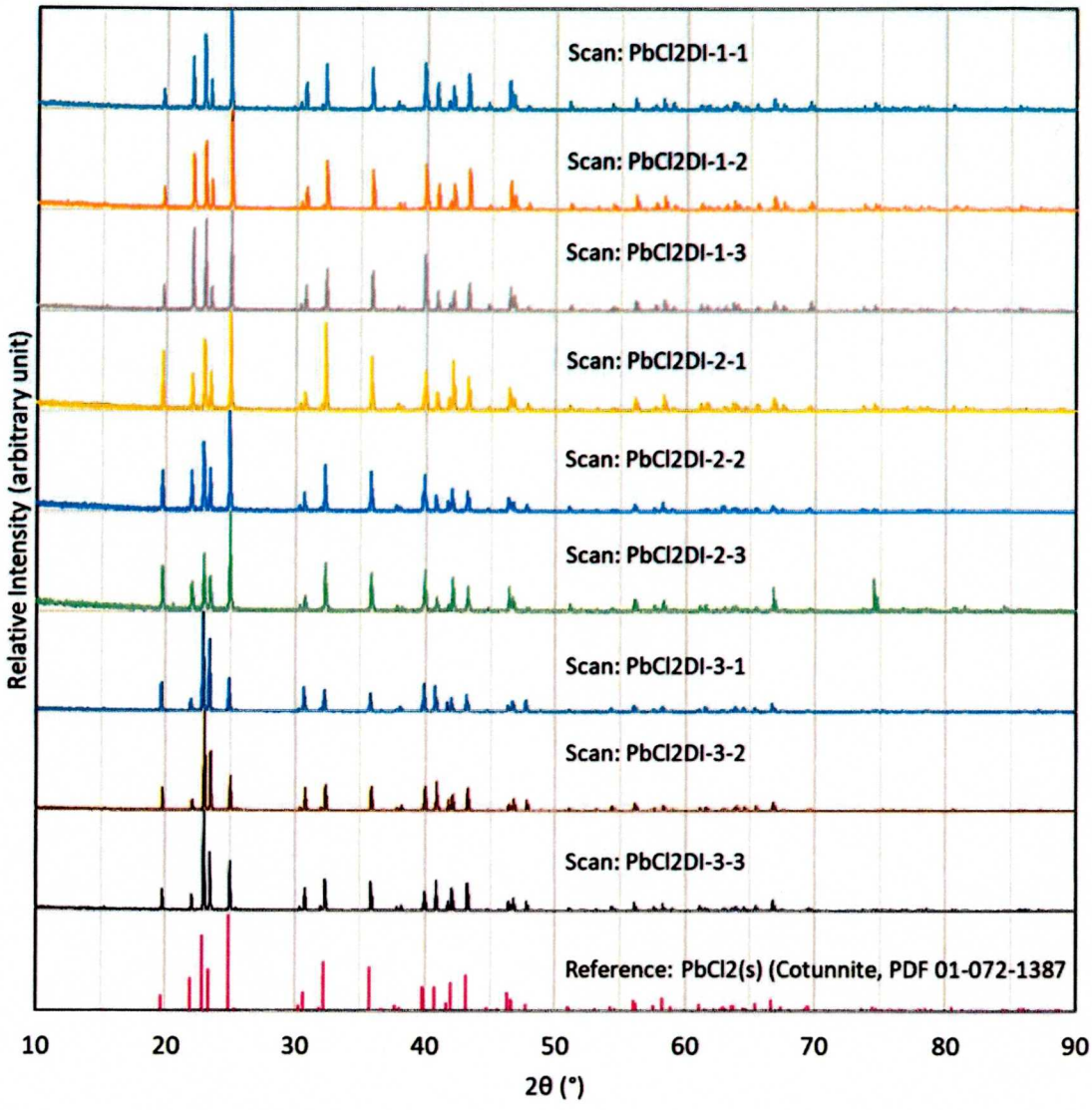

V.1.6. Observations

An increase of particle size was observed in all reactors. Trend of decreases in ΣPb (Figure V.1-3) and ΣCl (Figure V.1-4) and growth of minor peaks observed in PbCl2DI-2-3 could be attributed to particle size growth.

V.1.7. Model Parameterization: Pitzer Approach

Experiments were performed at low ionic strength. Thus, pHr ≡[51] pmH, and Molarity ≡ molality.

The measurements in Table V.1-8 are used in Sections V.2, V.3, and V.4 to check the accuracy of the literature-retrieved log K of $PbCl_2$(s), which is -4.83 (Edwards et al., 1992).

[51] meaning "equated to".

607 Table V.1-8. Measurements in molality.

molality	Average	SD	2SD	%SD	%2SD	Counts
pmH	3.95	0.02	0.05	1%	1%	27
ΣCl	8.04E-02	3.00E-03	6.00E-03	4%	7%	27
ΣPb	3.92E-02	1.90E-03	3.81E-03	5%	10%	27

608

609 V.1.8. Summary

610 The solubility of $PbCl_2(s)$ of three LOT numbers (Table V.1-1) was compared. No significant
611 difference was identified, within the precision of our laboratory operation.

612 ## V.2. $PbCl_2(s)$ - HCl - H_2O

613 V.2.1. Chemical System

614 The solubility of $PbCl_2(s)$ was measured in aqueous solutions containing HCl from 0.1 to 6.0 M. The
615 four components of this system are Pb^{+2}, Cl^-, H^+ , and H_2O.

616 V.2.2. Goals and Hypotheses

617 The goal was to confirm how the common-ion effect is expressed in the dissolved concentration of
618 Pb in the HCl solutions when the solubility limiting solid is $PbCl_2(s)$. The common-ion is chloride.

619 V.2.3. Reactor Preparation

620 6.0 grams of $PbCl_2(s)$ were added to each of 18 reactors representing 9 experimental conditions (HCl
621 concentration) in duplicate. The HCl solutions were prepared by the recipes in Table V.2-1.

622 Table V.2-1. Recipe and calculated solution properties.

Reactor ID	6.0 M HCl	DI, mL	$PbCl_2(s)$, gram
PbCl2HCl-1-1	0.75	44.3	6.0
PbCl2HCl-1-2	0.75	44.3	6.0
PbCl2HCl-2-1	1.50	43.5	6.0
PbCl2HCl-2-2	1.50	43.5	6.0
PbCl2HCl-3-1	3.75	41.3	6.0
PbCl2HCl-3-2	3.75	41.3	6.0
PbCl2HCl-4-1	7.50	37.5	6.0
PbCl2HCl-4-2	7.50	37.5	6.0
PbCl2HCl-5-1	15.0	30.0	6.0
PbCl2HCl-5-2	15.0	30.0	6.0
PbCl2HCl-6-1	22.5	22.5	6.0
PbCl2HCl-6-2	22.5	22.5	6.0
PbCl2HCl-7-1	30.0	15.0	6.0
PbCl2HCl-7-2	30.0	15.0	6.0
PbCl2HCl-8-1	37.5	7.5	6.0

PbCl2HCl-8-2	37.5	7.5	6.0
PbCl2HCl-9-1	45.0	0.00	6.0
PbCl2HCl-9-2	45.0	0.00	6.0
Solution properties	M:m, L/kg	Density, g/mL	pH
PbCl2HCl-1-(1,2)	1.0006	1.0033	0.53
PbCl2HCl-2-(1,2)	1.0019	1.0056	0.49
PbCl2HCl-3-(1,2)	1.0058	1.0126	0.38
PbCl2HCl-4-(1,2)	1.0124	1.0243	0.19
PbCl2HCl-5-(1,2)	1.0259	1.0476	-0.17
PbCl2HCl-6-(1,2)	1.0398	1.0710	-0.52
PbCl2HCl-7-(1,2)	1.0542	1.0943	-0.85
PbCl2HCl-8-(1,2)	1.0690	1.1176	-1.17
PbCl2HCl-9-(1,2)	1.0842	1.1410	-1.47

Recipe reference: Scientific Notebook WIPP-Pb-1, page 94

V.2.4. Data - Aqueous

V.2.4.1. pHr

Time-dependent pHr is tabulated in Table V.2-2. The scatter observed in Figure V.2-1 is less than 27% (maxium %2SD observed in PbCl2HCl-7-(1,2); Table V.2-3). Change of pHr as a function of HCl loading is shown in Figure V.2-2.

Table V.2-2. Time-dependent pHr (DSP = Days Since Preparation, i.e., Aging time in days).

pHr	DSP		
Reactor ID	51	83	119
PbCl2HCl-1-1	1.12	1.13	1.14
PbCl2HCl-1-2	1.12	1.15	1.15
PbCl2HCl-2-1	0.82	0.86	0.84
PbCl2HCl-2-2	0.83	0.86	0.85
PbCl2HCl-3-1	0.43	0.46	0.48
PbCl2HCl-3-2	0.41	0.45	0.48
PbCl2HCl-4-1	0.10	0.12	0.17
PbCl2HCl-4-2	0.08	0.10	0.16
PbCl2HCl-5-1	-0.30	-0.27	-0.19
PbCl2HCl-5-2	-0.30	-0.27	-0.17
PbCl2HCl-6-1	-0.56	-0.50	-0.37
PbCl2HCl-6-2	-0.56	-0.52	-0.42
PbCl2HCl-7-1	-0.83	-0.73	-0.59
PbCl2HCl-7-2	-0.80	-0.73	-0.61
PbCl2HCl-8-1	-0.99	-0.97	-0.79
PbCl2HCl-8-2	-0.99	-0.95	-0.78
PbCl2HCl-9-1	-1.15	-1.09	-0.97
PbCl2HCl-9-2	-1.13	-1.10	-0.96

631

632 Figure V.2-1. Time-dependent pHr.

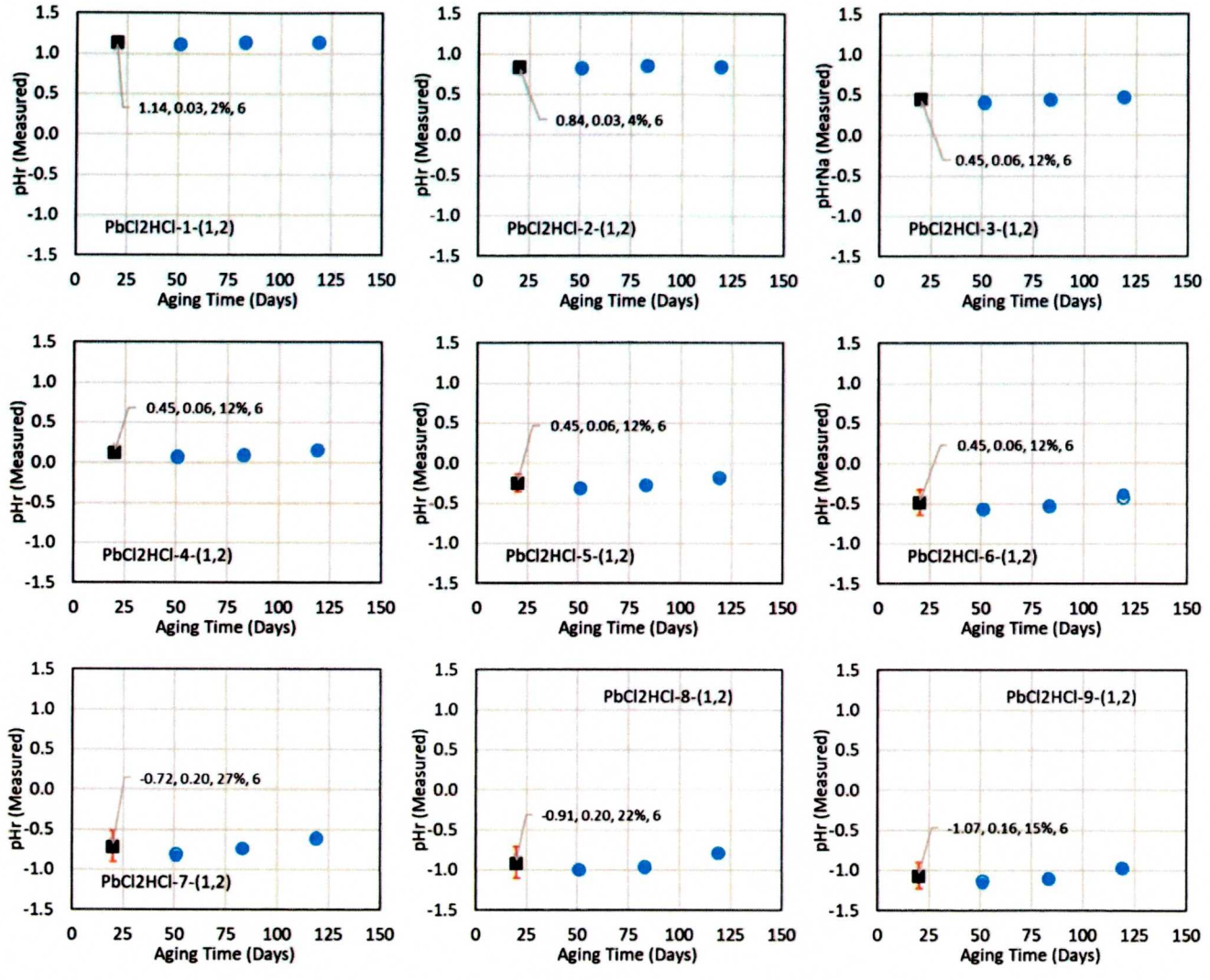

633

634

635

636 Table V.2-3. Statistics of pHr.

Reactor ID	Average	2SD	%2SD	Counts
PbCl2HCl-1-(1,2)	1.14	0.03	2%	6
PbCl2HCl-2-(1,2)	0.84	0.03	4%	6
PbCl2HCl-3-(1,2)	0.45	0.06	12%	6
PbCl2HCl-4-(1,2)	0.12	0.07	59%	6
PbCl2HCl-5-(1,2)	-0.25	0.11	45%	6
PbCl2HCl-6-(1,2)	-0.49	0.16	32%	6
PbCl2HCl-7-(1,2)	-0.72	0.20	27%	6
PbCl2HCl-8-(1,2)	-0.91	0.20	22%	6
PbCl2HCl-9-(1,2)	-1.07	0.16	15%	6

637

638 Figure V.2-2. Change of pHr as a function of HCl loading.

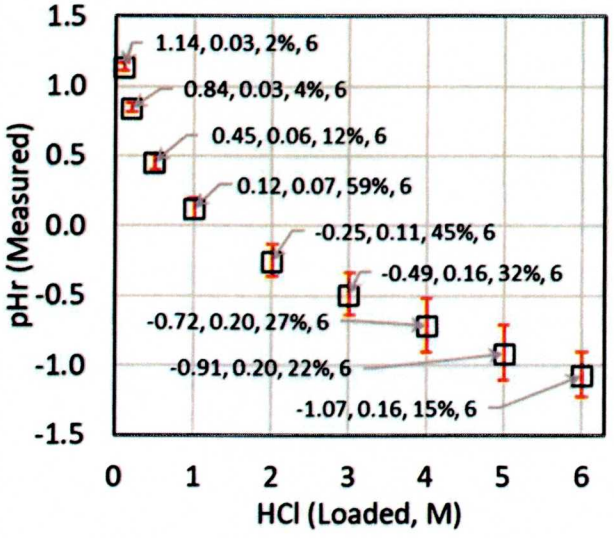

639

640 V.2.4.2. ΣPb

641 Time-dependent measurements of ΣPb are listed in Table V.2-4. The scatter observed in Figure
642 V.2-3 is less than 15% (maximum %2SD observed in PbCl2HCl-9-(1,2); Table V.2-5). Figure
643 V.2-4 displays the change of ΣPb as a function of HCl loading.

644 Table V.2-4. Time-dependent ΣPb (M).

ΣPb	DSP		
Reactor ID	51	83	119
PbCl2HCl-1-1	1.46E-02	1.31E-02	1.43E-02
PbCl2HCl-1-2	1.53E-02	1.29E-02	1.46E-02
PbCl2HCl-2-1	9.14E-03	7.90E-03	8.56E-03
PbCl2HCl-2-2	9.08E-03	7.93E-03	8.34E-03
PbCl2HCl-3-1	4.65E-03	4.50E-03	4.67E-03
PbCl2HCl-3-2	4.68E-03	4.38E-03	4.64E-03
PbCl2HCl-4-1	3.75E-03	3.59E-03	3.70E-03
PbCl2HCl-4-2	3.71E-03	3.62E-03	3.77E-03
PbCl2HCl-5-1	4.67E-03	4.41E-03	4.47E-03
PbCl2HCl-5-2	4.64E-03	4.34E-03	4.39E-03
PbCl2HCl-6-1	6.91E-03	6.20E-03	6.39E-03
PbCl2HCl-6-2	6.91E-03	6.25E-03	6.44E-03
PbCl2HCl-7-1	1.10E-02	9.91E-03	1.04E-02
PbCl2HCl-7-2	1.05E-02	9.69E-03	1.03E-02
PbCl2HCl-8-1	1.84E-02	1.63E-02	1.76E-02
PbCl2HCl-8-2	1.83E-02	1.64E-02	1.74E-02
PbCl2HCl-9-1	3.10E-02	2.57E-02	2.87E-02
PbCl2HCl-9-2	3.04E-02	2.67E-02	3.03E-02

645

646 Figure V.2-3. Time-dependent ΣPb in duplicate reactors.

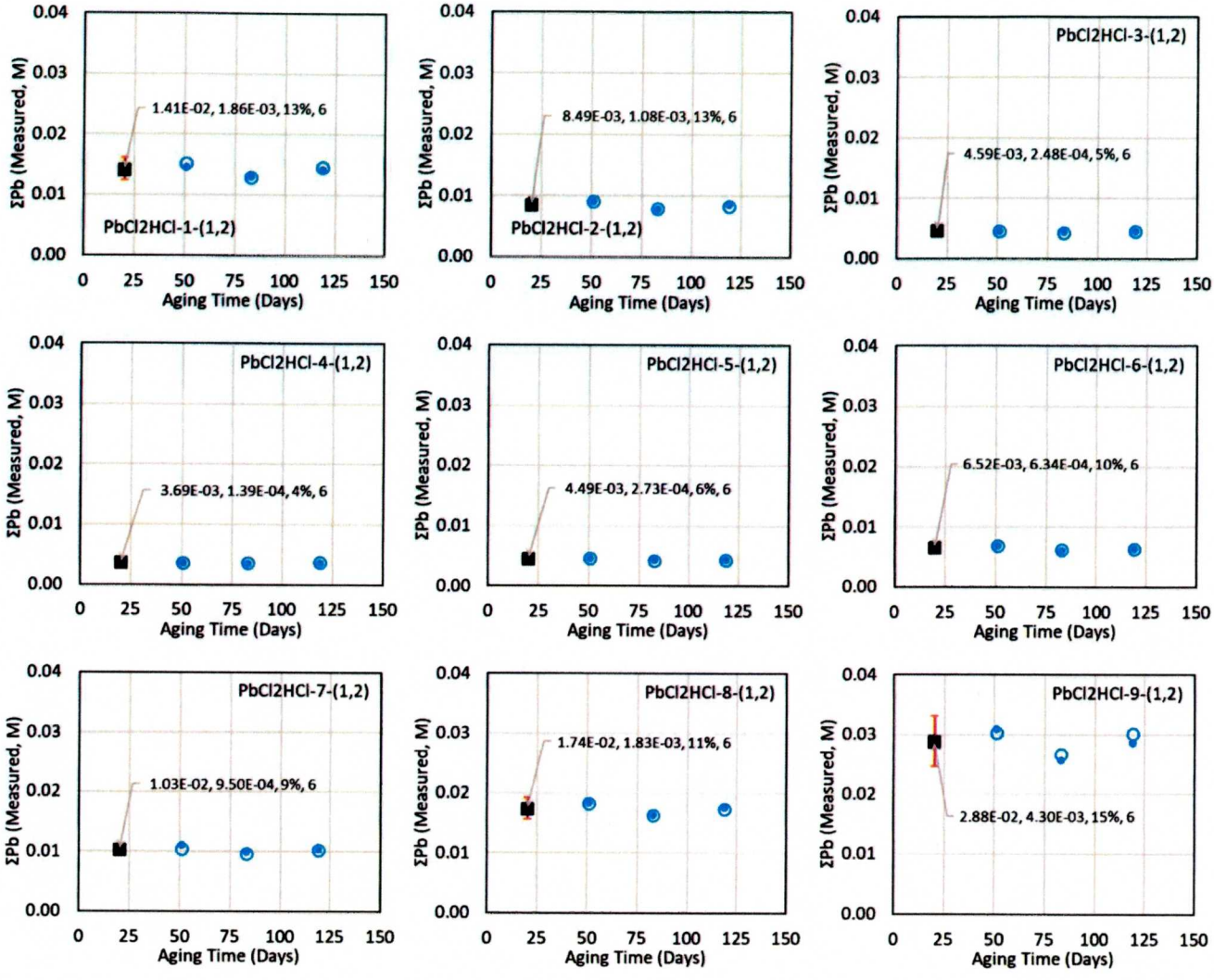

647

648

649

650

651 Table V.2-5. Statistics of ΣPb.

Reactor ID	Average	2SD	%2SD	Counts
PbCl2HCl-1-(1,2)	1.41E-02	1.86E-03	13%	6
PbCl2HCl-2-(1,2)	8.49E-03	1.08E-03	13%	6
PbCl2HCl-3-(1,2)	4.59E-03	2.48E-04	5%	6
PbCl2HCl-4-(1,2)	3.69E-03	1.39E-04	4%	6
PbCl2HCl-5-(1,2)	4.49E-03	2.73E-04	6%	6
PbCl2HCl-6-(1,2)	6.52E-03	6.34E-04	10%	6
PbCl2HCl-7-(1,2)	1.03E-02	9.50E-04	9%	6
PbCl2HCl-8-(1,2)	1.74E-02	1.83E-03	11%	6
PbCl2HCl-9-(1,2)	2.88E-02	4.30E-03	15%	6

652

Figure V.2-4. ΣPb as a function of HCl loading.

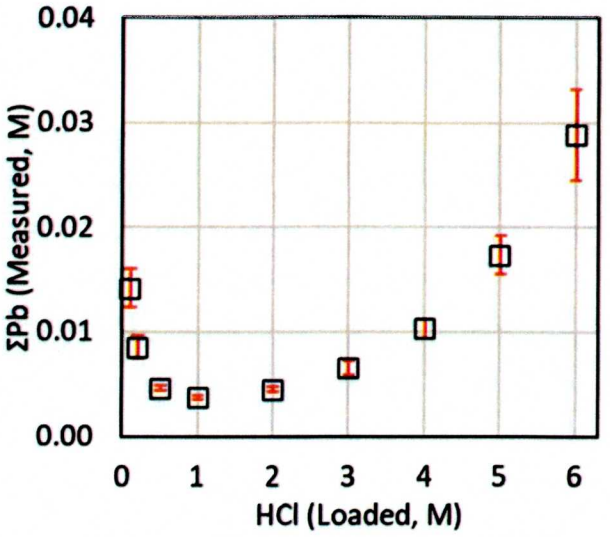

V.2.4.3. ΣCl

Time-dependent measurements of ΣCl are listed in Table V.2-6. The scatters observed in Figure V.2-5 are less than 18% (maximum %2SD observed in PbCl2HCl-1-(1,2); Table V.2-7). The change of ΣCl as a function of HCl loading is shown in Figure V.2-6.

Table V.2-6. Time-dependent measurements of ΣCl in M (DSP = Days Since Preparation, i.e., Aging time in days).

PbCl2HCl-1-1		PbCl2HCl-1-2		PbCl2HCl-2-1		PbCl2HCl-2-2		PbCl2HCl-3-1		PbCl2HCl-3-2	
DSP	ΣCl, M	DSP	ΣCl, M	DSP	ΣCl, M	DSP	ΣCl, M	DSP	ΣCl, M	DSP	ΣCl, M
51	1.63E-01	51	1.66E-01	51	2.37E-01	51	2.41E-01	51	4.93E-01	51	4.97E-01
83	1.44E-01	83	1.39E-01	83	2.20E-01	83	2.19E-01	83	5.09E-01	83	5.14E-01
PbCl2HCl-4-1		PbCl2HCl-4-2		PbCl2HCl-5-1		PbCl2HCl-5-2		PbCl2HCl-6-1		PbCl2HCl-6-2	
DSP	ΣCl, M	DSP	ΣCl, M	DSP	ΣCl, M	DSP	ΣCl, M	DSP	ΣCl, M	DSP	ΣCl, M
51	9.51E-01	51	1.00E+00	51	1.99E+00	51	1.95E+00	51	2.97E+00	51	2.96E+00
83	9.99E-01	83	1.07E+00	83	2.13E+00	83	2.11E+00	83	3.11E+00	83	3.12E+00
PbCl2HCl-7-1		PbCl2HCl-7-2		PbCl2HCl-8-1		PbCl2HCl-8-2		PbCl2HCl-9-1		PbCl2HCl-9-2	
DSP	ΣCl, M	DSP	ΣCl, M	DSP	ΣCl, M	DSP	ΣCl, M	DSP	ΣCl, M	DSP	ΣCl, M
51	3.97E+00	51	3.97E+00	51	5.01E+00	51	4.96E+00	*51*	*5.96E+00*	*51*	*5.95E+00*
83	4.22E+00	83	4.11E+00	83	5.14E+00	83	5.27E+00	51	5.63E+00	51	5.67E+00
								83	6.27E+00	83	6.06E+00

Italics in red fonts: flagged by lab, but are consistent with other valid measurements. Not included in calculating the statistics presented in Table V.2-7.

Figure V.2-5. Time-dependent ΣCl. Solid black squares and red error bars are averages and 2SD. Orange dots and circles are those in red-italic in Table V.2-6.

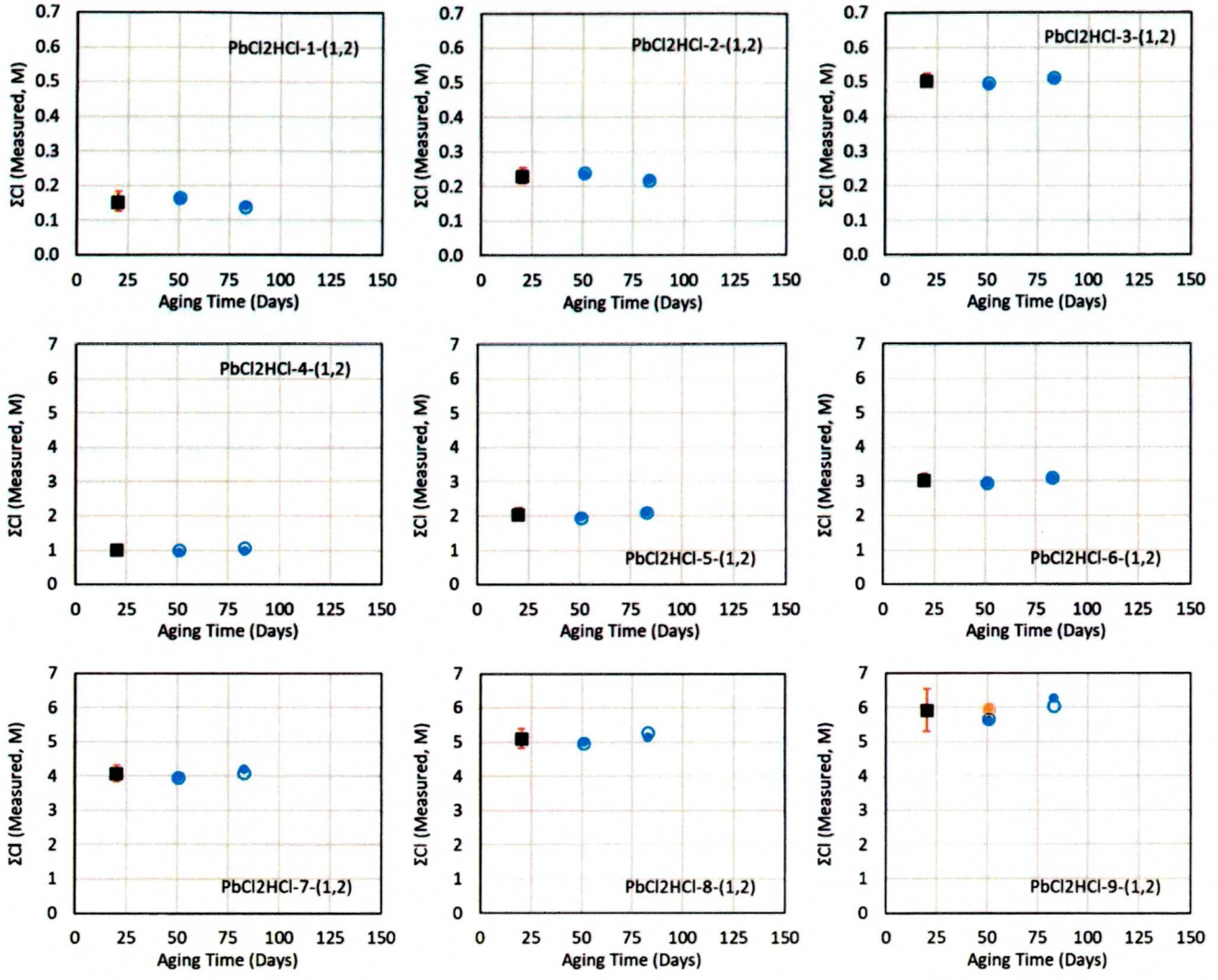

Table V.2-7. Statistics of ΣCl.

Reactor ID	Average	2SD	%2SD	Counts
PbCl2HCl-1-(1,2)	1.53E-01	2.77E-02	18%	4
PbCl2HCl-2-(1,2)	2.29E-01	2.21E-02	10%	4
PbCl2HCl-3-(1,2)	5.03E-01	1.93E-02	4%	4
PbCl2HCl-4-(1,2)	1.00E+00	9.65E-02	10%	4
PbCl2HCl-5-(1,2)	2.05E+00	1.79E-01	9%	4
PbCl2HCl-6-(1,2)	3.04E+00	1.71E-01	6%	4
PbCl2HCl-7-(1,2)	4.07E+00	2.42E-01	6%	4
PbCl2HCl-8-(1,2)	5.10E+00	2.81E-01	6%	4
PbCl2HCl-9-(1,2)	5.91E+00	6.16E-01	10%	4

673 Figure V.2-6. Accuracy and precision of ΣCl measurements as a function of HCl loading.
674 Larger %Deviations exceeding the 2SDs are indicative of the dissolution of
675 $PbCl_2(s)$, i.e., $\Sigma Cl = [HCl]_{Loaded} + 2 \times [PbCl_2(s)]_{Dissolved}$.

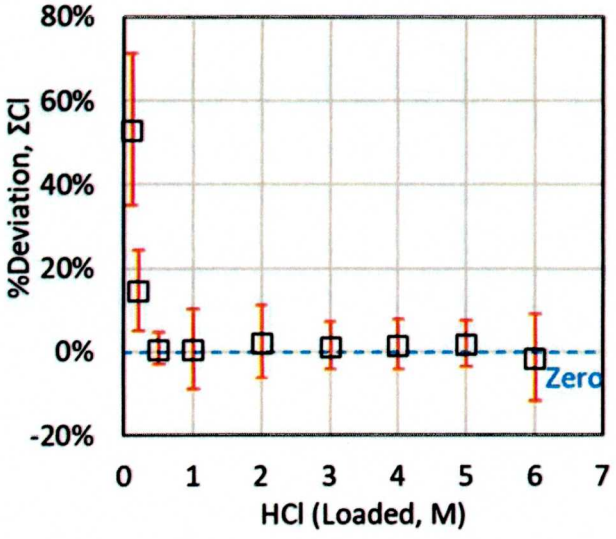

676

677 V.2.5. Data - Solids

678 No solid characterization has been done as of 7/31/2021.

679 V.2.6. Observations

680 Particle size growth was observed. The common ion effect was observed, that is, the depression of
681 ΣPb, followed by an increase (Figure V.2-4), is consistent with the literature-retrieved experimental
682 data collected in Jang (2021a).

683 V.2.7. Model Parameterization: Pitzer Approach

684 Molarity was converted to molality in Table V.2-8. The model in Jang (2021a) was adopted (Table
685 V.2-9, Table V.2-10), and the model predictions compared against the measurements in Figure V.2-7.
686 The solubility data in Section V.1 (i.e., Table V.1-8) is included in this model parameterization. The
687 data point represents the dissolved total concentration of Pb in the absence of loaded Cl.

688 Table V.2-8. Measurements in molality.

Reactor ID	ΣCl, m	2SD	ΣPb, m	2SD
PbCl2DI-(1,2,3)-(1,2,3)[A]	8.04E-02	6.00E-03	3.92E-02	3.81E-03
PbCl2HCl-1-(1,2)	1.53E-01	2.77E-02	1.42E-02	1.86E-03
PbCl2HCl-2-(1,2)	2.30E-01	2.21E-02	8.51E-03	1.08E-03
PbCl2HCl-3-(1,2)	5.06E-01	1.94E-02	4.61E-03	2.49E-04
PbCl2HCl-4-(1,2)	1.02E+00	9.77E-02	3.74E-03	1.41E-04
PbCl2HCl-5-(1,2)	2.10E+00	1.84E-01	4.60E-03	2.80E-04
PbCl2HCl-6-(1,2)	3.16E+00	1.78E-01	6.78E-03	6.59E-04
PbCl2HCl-7-(1,2)	4.29E+00	2.55E-01	1.09E-02	1.00E-03

PbCl2HCl-8-(1,2)	5.45E+00	3.00E-01	1.86E-02	1.96E-03
PbCl2HCl-9-(1,2)	6.40E+00	6.68E-01	3.12E-02	4.66E-03

[A] Data from Table V.1-8.

Table V.2-9. Reactions and Log Ks (Jang, 2021a).

Reaction	Log K	Reference
Aqueous reactions		
$PbCl^+ = Pb^{2+} + Cl^-$	-1.48±0.01	Millero and Byrne (1984) (6 m)[A]
$PbCl_2(aq) = Pb^{2+} + 2Cl^-$	-2.03±0.01	Millero and Byrne (1984) (6 m)[A]
$PbCl_3^- = Pb^{2+} + 3Cl^-$	-1.86±0.01	Millero and Byrne (1984) (6 m)[A]
Dissolution		
$PbCl_2(s)$ (cotunnite) $= Pb^{2+} + 2Cl^-$	-4.83	Edwards et al. (1992)[A]

[A] Validated for chloride concentrations up to 6 m (Jang, 2021a).

Table V.2-10. PIPs (Jang, 2021a).

i	j	α_1/α_2[A]	$\beta^{(0)}$	$\beta^{(1)}$	$\beta^{(2)}$	C^φ	Source
H^+	$PbCl_3^-$	2.0/12.0	0.1077	0.0425	0.00	-0.0035	Jang (2021. Revisit ...) (6 m)[B]

[A] α_1 and α_2 are pre-set constants used in the Pitzer activity coefficient equation. α_1 and α_2 apply for only cation-anion binary pair. α_2 is only used for 2:2 electrolytes and multivalent ions. α_2 is not applied when $\beta^{(2)}$ is zero or not used. The unit for α_1 and α_2 is $kg^{1/2} \cdot mol^{-1/2}$.

[B] Valid for chloride concentrations up to 6 m.

Figure V.2-7. ΣPb vs. ΣCl in molality. The open diamond is the results from Section V.1 with uncertainty shown. A. Whole range investigated. B. Zoom-in view of the area marked with the green rectangle in A.

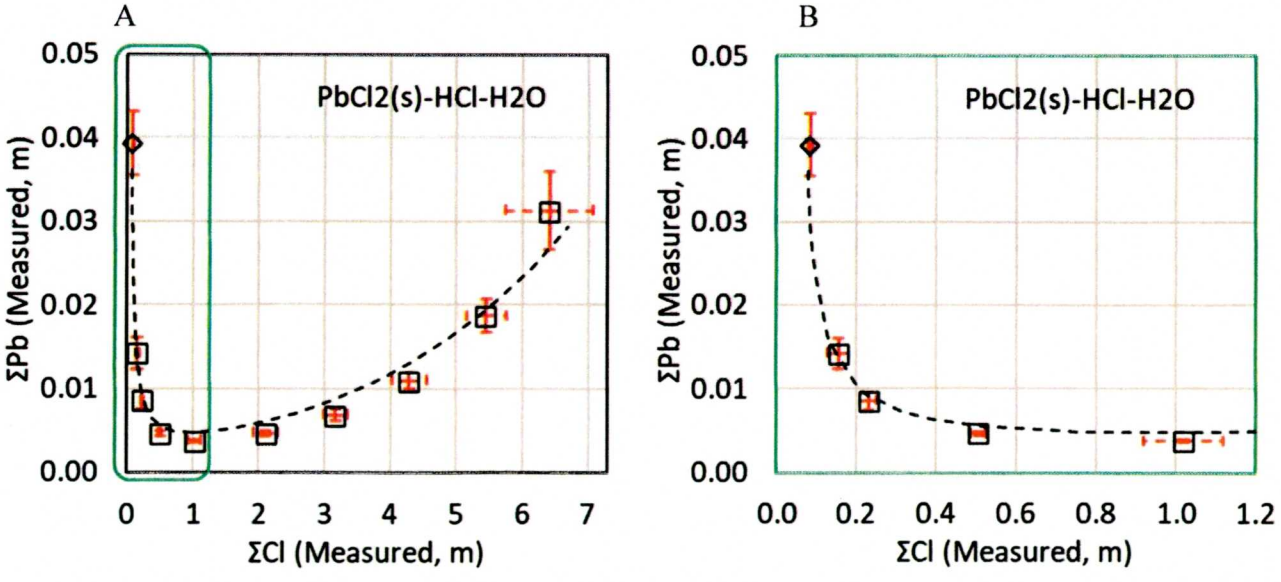

V.2.8. Summary

The model adopted from Jang (2021a) accurately predicts the measurements within the uncertainty. There is no need to further fit the model.

Thermodynamic quantities in Table V.2-9 and Table V.2-10 are the recommended new additions to data0.fm1.

V.3. $PbCl_2$(s) - NaCl - H_2O

V.3.1. Chemical System

The solubility of $PbCl_2$(s) was measured in 0.1 to 6.5 m NaCl solutions. The five components of this system are Pb^{+2}, Na^+, Cl^-, H^+ , and H_2O.

V.3.2. Goals and Hypotheses

The goal was to accurately model how Na^+ affects the solubility of $PbCl_2$(s).

V.3.3. Reactor Preparation

The 18 clean 50-mL glass serum bottles were prepared. Upon completion of the recipe in Table V.3-1, they represent 9 NaCl loadings (0.1, 0.2, 0.5, 1.0, 2.0, 3.1, 4.3, 5.6, 6.5 m) and each had a duplicate. 3.0 grams of solid $PbCl_2$(s) was weighed and placed in each bottle, then sealed using a rubber seal. 18 clean plastic conical tubes were prepared to make NaCl solutions nine different concentrations in duplicate by mixing the prescribed mass of NaCl and 45 mL DI water degassed in N_2 filled glovebox.

Table V.3-1. Recipe and calculated solution properties.

Reactor ID	NaCl, g	DI water, mL	NaCl, m	PbCl2, gram
PbCl2NaCl-1-1	0.2629	45.0	0.100	3.0
PbCl2NaCl-1-2	0.2630	45.0	0.100	3.0
PbCl2NaCl-2-1	0.5260	45.0	0.201	3.0
PbCl2NaCl-2-2	0.5262	45.0	0.201	3.0
PbCl2NaCl-3-1	1.3152	45.0	0.502	3.0
PbCl2NaCl-3-2	1.3149	45.0	0.502	3.0
PbCl2NaCl-4-1	2.6303	45.0	1.003	3.0
PbCl2NaCl-4-2	2.6301	45.0	1.003	3.0
PbCl2NaCl-5-1	5.2605	45.0	2.006	3.0
PbCl2NaCl-5-2	5.2600	45.0	2.006	3.0
PbCl2NaCl-6-1	8.1520	45.0	3.109	3.0
PbCl2NaCl-6-2	8.1523	45.0	3.109	3.0
PbCl2NaCl-7-1	11.3103	45.0	4.314	3.0
PbCl2NaCl-7-2	11.3101	45.0	4.314	3.0
PbCl2NaCl-8-1	14.7304	45.0	5.618	3.0
PbCl2NaCl-8-2	14.7305	45.0	5.618	3.0
PbCl2NaCl-9-1	17.0900	45.0	6.518	3.0
PbCl2NaCl-9-2	17.0903	45.0	6.518	3.0

Solution properties	M:m, L/kg	Density, g/mL (calculated)	NaCl, M	pH
PbCl2NaCl-1-(1,2)	1.0012	1.005	0.100	6.99
PbCl2NaCl-2-(1,2)	1.0033	1.008	0.200	6.98
PbCl2NaCl-3-(1,2)	1.0096	1.019	0.497	6.97
PbCl2NaCl-4-(1,2)	1.0201	1.038	0.983	6.94
PbCl2NaCl-5-(1,2)	1.0412	1.073	1.927	6.87
PbCl2NaCl-6-(1,2)	1.0644	1.110	2.921	6.78
PbCl2NaCl-7-(1,2)	1.0897	1.148	3.959	6.67
PbCl2NaCl-8-(1,2)	1.1171	1.188	5.029	6.54
PbCl2NaCl-9-(1,2)	1.1360	1.214	5.738	6.44

V.3.4. Data - Aqueous

V.3.4.1. pHr

Time-dependent pHr is tabulated in Table V.3-2, and displayed in Figure V.3-1. The observed scatters are within the maximum %2SD of 2% (Table V.3-3). Figure V.3-2 show the change in pHr as a function of NaCl loading.

Table V.3-2. Time-dependent pHr (DSP = Days Since Preparation, i.e., Aging time in days).

PbCl2NaCl-1-1		PbCl2NaCl-1-2		PbCl2NaCl-2-1		PbCl2NaCl-2-2		PbCl2NaCl-3-1		PbCl2NaCl-3-2	
DSP	pHr	DSP	pHr	DSP	pHr	DSP	pHr	DSP	pHr	DSP	pHr
75	4.295	75	4.353	75	4.519	75	4.537	75	4.854	75	4.882
117	4.38	117	4.37	117	4.57	117	4.58	117	4.92	117	4.91
154	4.34	154	4.37	154	4.58	154	4.6	154	4.92	154	4.88
PbCl2NaCl-4-1		PbCl2NaCl-4-2		PbCl2NaCl-5-1		PbCl2NaCl-5-2		PbCl2NaCl-6-1		PbCl2NaCl-6-2	
DSP	pHr	DSP	pHr	DSP	pHr	DSP	pHr	DSP	pHr	DSP	pHr
75	5.120	75	5.187	75	5.315	75	5.419	75	5.551	75	5.546
117	5.16	117	5.19	117	5.44	117	5.41	117	5.56	117	5.56
154	5.17	154	5.2	154	5.45	154	5.46	154	5.53	154	5.56
PbCl2NaCl-7-1		PbCl2NaCl-7-2		PbCl2NaCl-8-1		PbCl2NaCl-8-2		PbCl2NaCl-9-1		PbCl2NaCl-9-2	
DSP	pHr	DSP	pHr	DSP	pHr	DSP	pHr	DSP	pHr	DSP	pHr
75	5.645	75	5.71	75	5.849	75	5.870	75	5.929	75	5.932
117	5.67	117	5.7	117	5.93	117	5.86	117	6.03	117	6.04
154	5.66	154	5.73	154	5.82	154	5.83	154	5.95	154	5.91

731 Figure V.3-1. Time-dependent pHr.

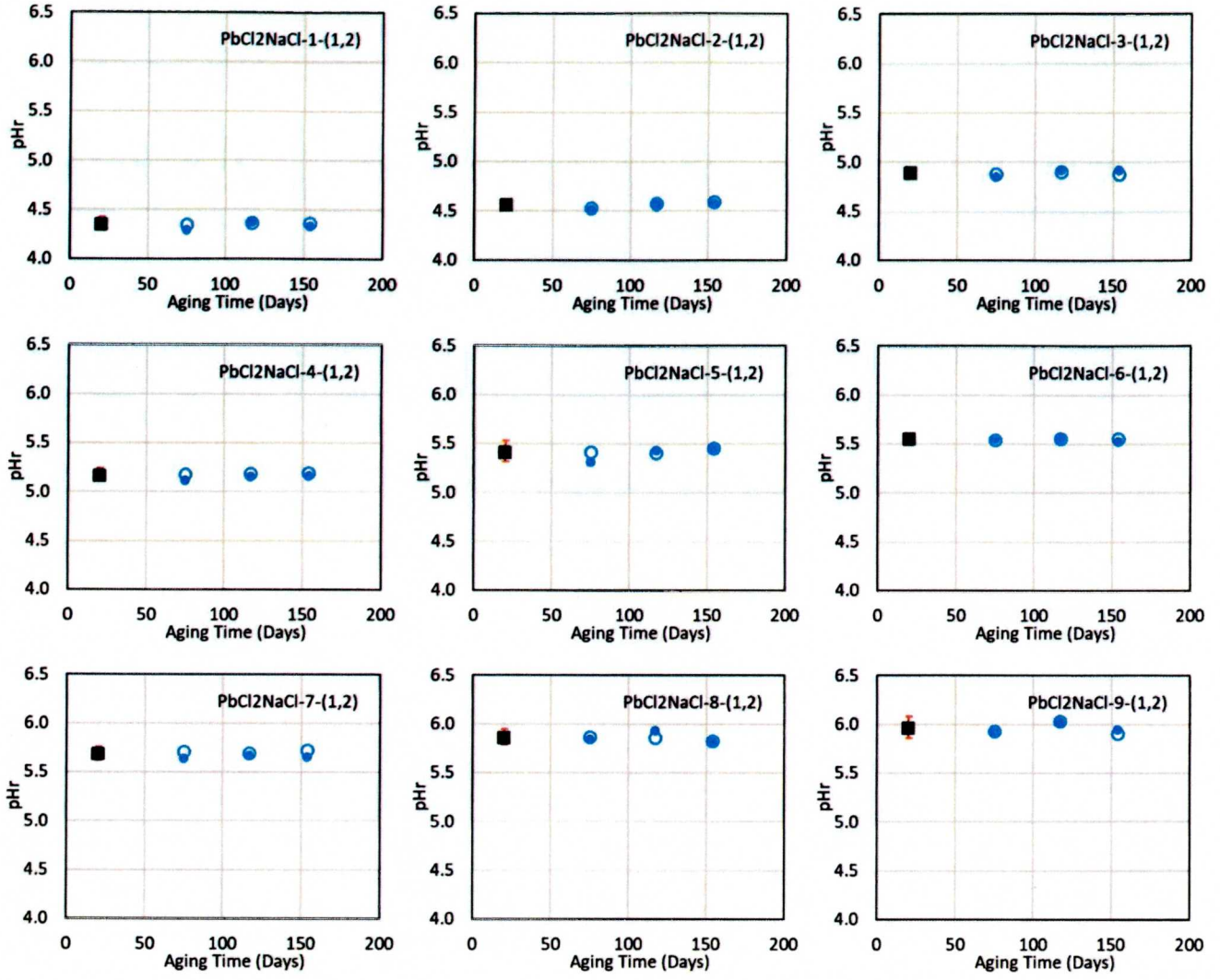

732

733

734

735

736 Table V.3-3. Statistics of pHr measurements.

Reactor ID	Average	2SD	%2SD	Counts
PbCl2NaCl-1-(1,2)	4.35	0.06	1%	6
PbCl2NaCl-2-(1,2)	4.56	0.06	1%	6
PbCl2NaCl-3-(1,2)	4.89	0.05	1%	6
PbCl2NaCl-4-(1,2)	5.17	0.06	1%	6
PbCl2NaCl-5-(1,2)	5.42	0.11	2%	6
PbCl2NaCl-6-(1,2)	5.55	0.02	0%	6
PbCl2NaCl-7-(1,2)	5.69	0.07	1%	6
PbCl2NaCl-8-(1,2)	5.86	0.08	1%	6
PbCl2NaCl-9-(1,2)	5.97	0.11	2%	6

737

738 Figure V.3-2. pHr as a function of NaCl loading.

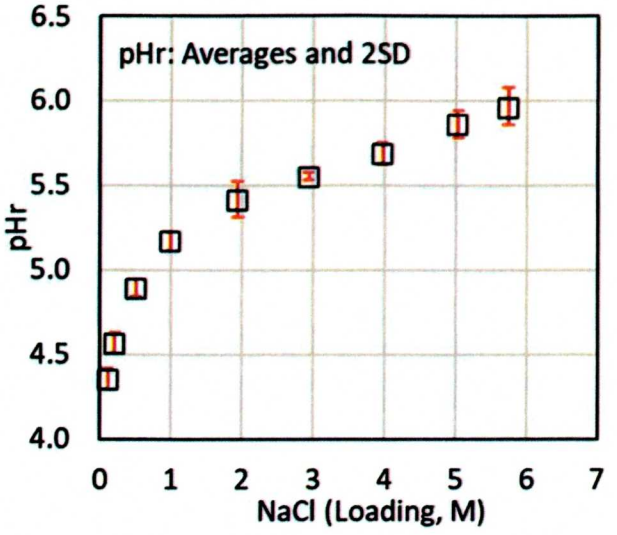

739

740 V.3.4.2. ΣPb

741 Time-dependent measurements of ΣPb are tabulated in Table V.3-4, and displayed in Figure V.3-3.
742 The observed scatter is within the maximum %2SD of 86% (Table V.3-5). The change in ΣPb as a
743 function of NaCl loading is shown in Figure V.3-4.

744 Table V.3-4. Time-dependent ΣPb in M (DSP = Days Since Preparation, i.e., Aging time
745 in days).

PbCl2NaCl-1-1		PbCl2NaCl-1-2		PbCl2NaCl-2-1		PbCl2NaCl-2-2		PbCl2NaCl-3-1		PbCl2NaCl-3-2	
DSP	ΣPb, M	DSP	ΣPb, M	DSP	ΣPb, M	DSP	ΣPb, M	DSP	ΣPb, M	DSP	ΣPb, M
75	1.59E-02	75	2.31E-02	75	9.17E-03	75	9.50E-03	75	5.86E-03	75	5.98E-03
117	1.54E-02	117	1.48E-04	117	9.82E-03	117	9.71E-03	117	6.21E-03	117	6.06E-03
154	1.22E-02	117	1.54E-02	154	7.47E-03	154	7.58E-03	154	4.62E-03	154	4.55E-03
		154	1.21E-02								
PbCl2NaCl-4-1		PbCl2NaCl-4-2		PbCl2NaCl-5-1		PbCl2NaCl-5-2		PbCl2NaCl-6-1		PbCl2NaCl-6-2	
DSP	ΣPb, M	DSP	ΣPb, M	DSP	ΣPb, M	DSP	ΣPb, M	DSP	ΣPb, M	DSP	ΣPb, M
75	5.41E-03	75	5.32E-03	75	7.58E-03	75	7.63E-03	75	1.42E-02	75	1.39E-02
117	5.86E-03	117	5.62E-03	117	8.42E-03	117	8.25E-03	117	1.50E-02	117	1.47E-02
154	4.19E-03	154	4.33E-03	154	6.37E-03	154	6.31E-03	154	1.14E-02	154	1.14E-02
PbCl2NaCl-7-1		PbCl2NaCl-7-2		PbCl2NaCl-8-1		PbCl2NaCl-8-2		PbCl2NaCl-9-1		PbCl2NaCl-9-2	
DSP	ΣPb, M	DSP	ΣPb, M	DSP	ΣPb, M	DSP	ΣPb, M	DSP	ΣPb, M	DSP	ΣPb, M
75	2.93E-02	75	2.87E-02	75	6.11E-02	75	6.14E-02	75	8.84E-02	75	8.84E-02
117	2.95E-02	117	2.92E-02	75	6.29E-02	117	6.30E-02	75	8.22E-02	117	6.84E-02
154	2.28E-02	154	2.33E-02	117	6.71E-02	154	5.25E-02	117	7.28E-02	154	5.54E-02
				154	5.10E-02			154	5.38E-02		

746 Red fonts: Flagged by lab (Saturated within auto integration window (code 4)); Values in underlined fonts: instrumental
747 reading exceeded the calibration range, but the values are consistent with other valid values. They are included to strenthen
748 the statistics. This is an example of the need to establish low detection limit, linear calibration range, and upper detection
749 limit (i.e., saturation) to prevent *a priori* discarding potentially useful measurements. Similar finding is reported in Jang et al.
750 (2021, GEOC-21-03).

Figure V.3-3. Time-dependent ΣPb in duplicate reactors.

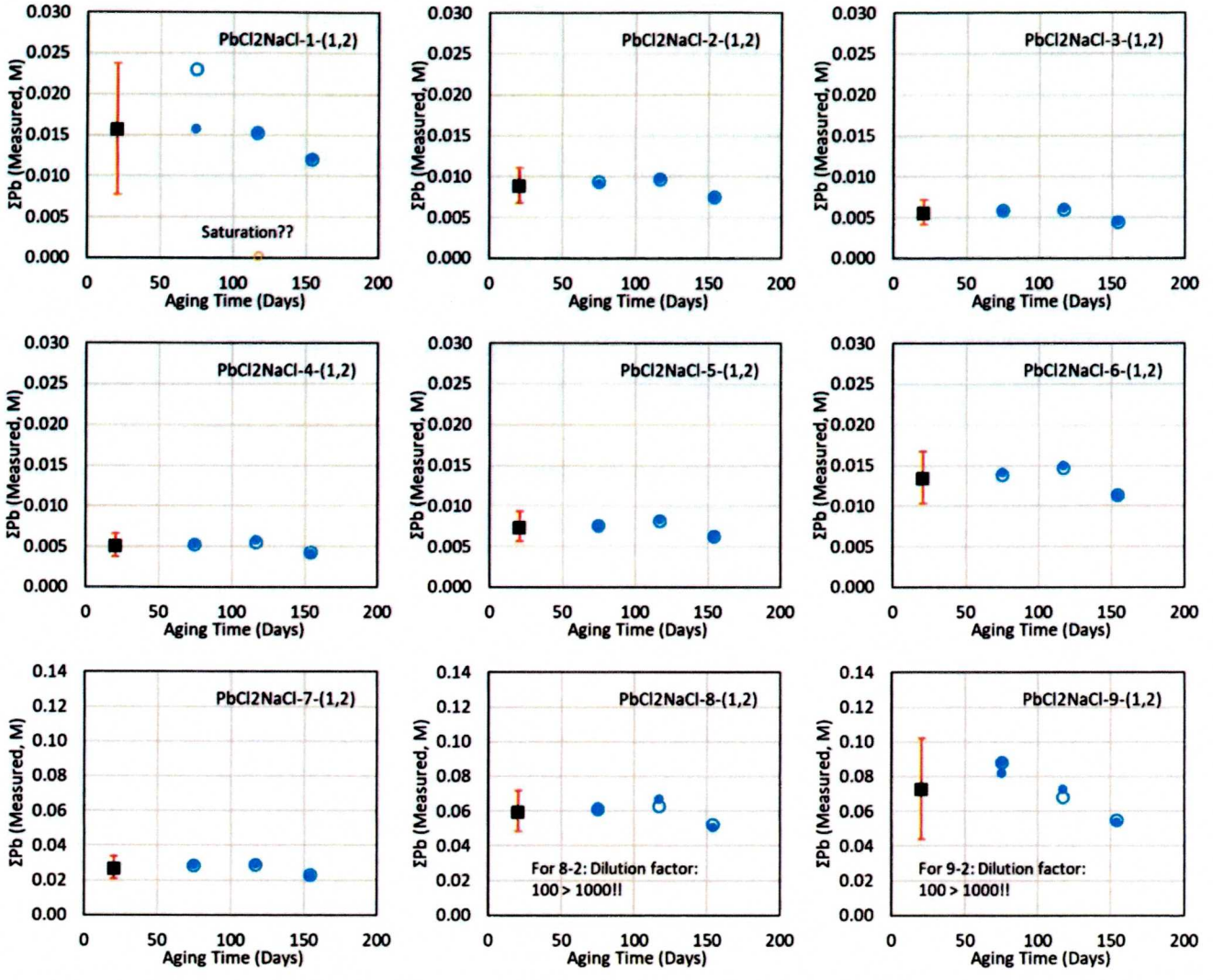

Table V.3-5. Statistics of ΣPb (M).

Reactor ID	Average	SD	2SD	%2SD	Counts
PbCl2NaCl-1-(1,2)	1.57E-02	4.01E-03	8.02E-03	51%	6
PbCl2NaCl-2-(1,2)	8.87E-03	1.07E-03	2.14E-03	24%	6
PbCl2NaCl-3-(1,2)	5.55E-03	7.55E-04	1.51E-03	27%	6
PbCl2NaCl-4-(1,2)	5.12E-03	6.96E-04	1.39E-03	27%	6
PbCl2NaCl-5-(1,2)	7.43E-03	9.06E-04	1.81E-03	24%	6
PbCl2NaCl-6-(1,2)	1.34E-02	1.63E-03	3.25E-03	24%	6
PbCl2NaCl-7-(1,2)	2.71E-02	3.18E-03	6.37E-03	23%	6
PbCl2NaCl-8-(1,2)	5.99E-02	5.91E-03	1.18E-02	20%	7
PbCl2NaCl-9-(1,2)	7.28E-02	1.45E-02	2.90E-02	40%	7

757 Figure V.3-4. ΣPb as a function of NaCl loading.

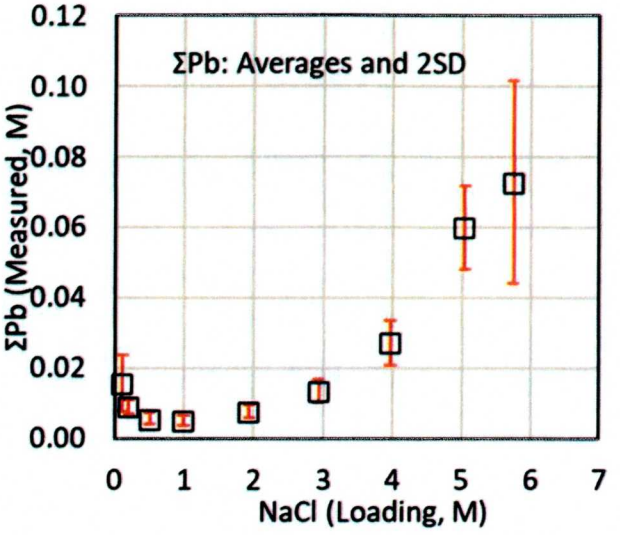

758

759 V.3.4.3. ΣNa

760 Time-dependent measurements of ΣNa are tabulated in Table V.3-6, and displayed in Figure V.3-5.
761 The observed scatters are within the maximum %2SD of 45% (Table V.3-7). Figure V.3-6 shows
762 the accuracy and precision of ΣNa. The %Deviation of ΣNa measurements reached -19%.

763 Table V.3-6. Time-dependent measurements of ΣNa.

PbCl2NaCl-1-1		PbCl2NaCl-1-2		PbCl2NaCl-2-1		PbCl2NaCl-2-2		PbCl2NaCl-3-1		PbCl2NaCl-3-2	
DSP	ΣNa, M	DSP	ΣNa, M	DSP	ΣNa, M	DSP	ΣNa, M	DSP	ΣNa, M	DSP	ΣNa, M
75	7.37E-02	75	7.85E-02	75	1.59E-01	75	1.60E-01	75	4.36E-01	75	4.35E-01
117	8.82E-02	117	8.62E-02	117	1.64E-01	117	1.66E-01	117	4.27E-01	117	4.25E-01
154	8.49E-02	154	8.62E-02	154	1.65E-01	154	1.70E-01	154	4.29E-01	154	4.33E-01
PbCl2NaCl-4-1		PbCl2NaCl-4-2		PbCl2NaCl-5-1		PbCl2NaCl-5-2		PbCl2NaCl-6-1		PbCl2NaCl-6-2	
DSP	ΣNa, M	DSP	ΣNa, M	DSP	ΣNa, M	DSP	ΣNa, M	DSP	ΣNa, M	DSP	ΣNa, M
75	7.33E-01	75	7.29E-01	75	1.56E+00	75	1.56E+00	75	2.42E+00	75	2.42E+00
117	8.47E-01	117	8.33E-01	117	1.59E+00	117	1.58E+00	117	2.44E+00	117	2.40E+00
154	8.35E-01	154	8.34E-01	154	1.63E+00	154	1.62E+00	154	2.45E+00	154	2.48E+00
PbCl2NaCl-7-1		PbCl2NaCl-7-2		PbCl2NaCl-8-1		PbCl2NaCl-8-2		PbCl2NaCl-9-1		PbCl2NaCl-9-2	
DSP	ΣNa, M	DSP	ΣNa, M	DSP	ΣNa, M	DSP	ΣNa, M	DSP	ΣNa, M	DSP	ΣNa, M
75	2.40E+00	75	2.43E+00	75	3.29E+00	75	3.31E+00	75	3.80E+00	75	3.87E+00
117	4.00E+00	117	4.09E+00	117	4.83E+00	117	4.84E+00	117	5.31E+00	117	4.99E+00
154	3.34E+00	154	3.37E+00	154	4.28E+00	154	4.39E+00	154	4.86E+00	154	4.93E+00

764

765 Figure V.3-5. Time-dependent ΣNa. Solid black squares and red error bars are averages
766 and 2SDs. For the first six panels, the error bars are smaller than the solid black
767 squares.

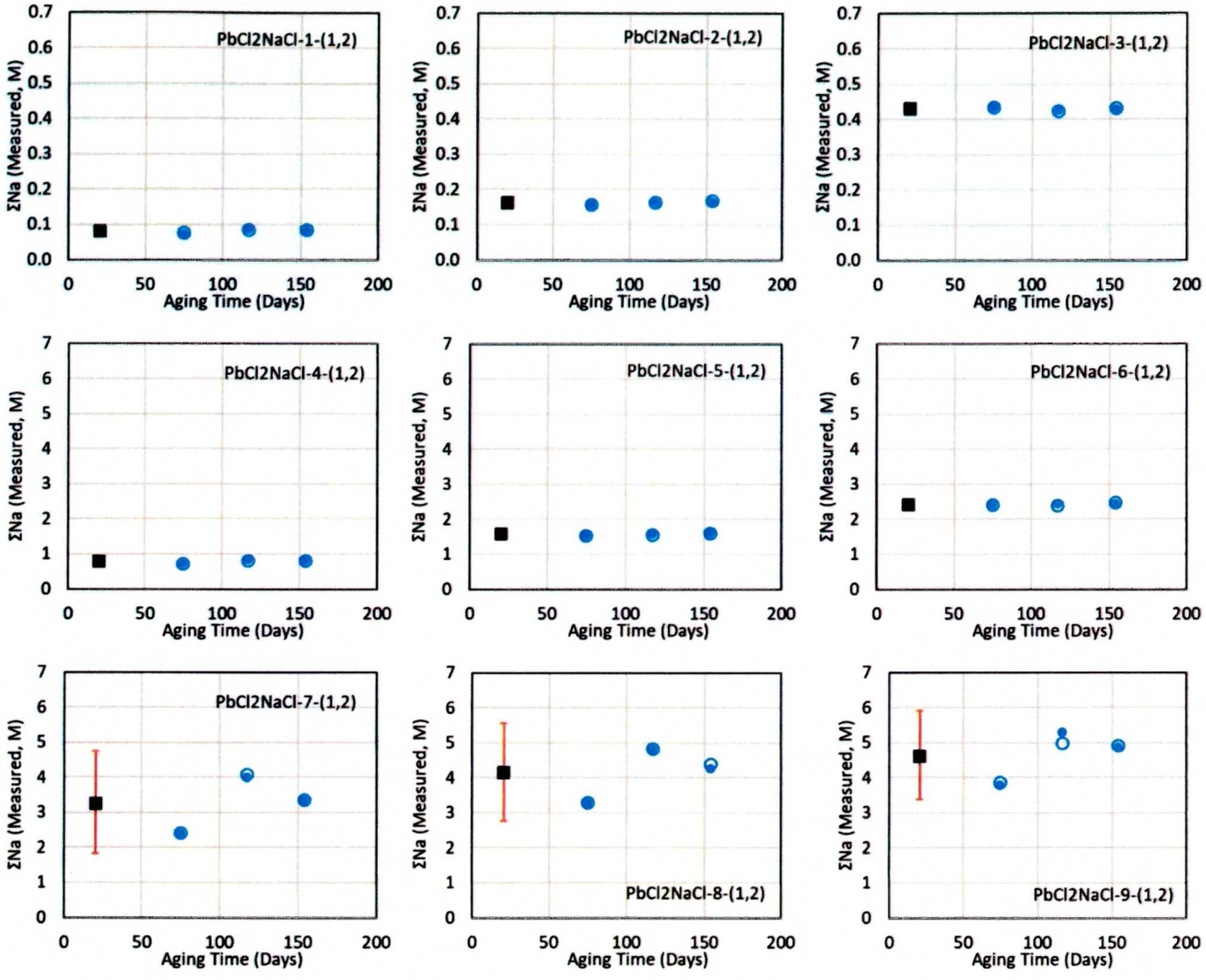

768

769

770

771 Table V.3-7. Statistics of ΣNa (M).

Reactor ID	Average	2SD	%2SD	%Deviation	Counts
PbCl2NaCl-1-(1,2)	8.29E-02	1.12E-02	14%	-17%	6
PbCl2NaCl-2-(1,2)	1.64E-01	7.99E-03	5%	-18%	6
PbCl2NaCl-3-(1,2)	4.31E-01	9.33E-03	2%	-13%	6
PbCl2NaCl-4-(1,2)	8.02E-01	1.10E-01	14%	-18%	6
PbCl2NaCl-5-(1,2)	1.59E+00	5.86E-02	4%	-18%	6
PbCl2NaCl-6-(1,2)	2.44E+00	5.82E-02	2%	-17%	6
PbCl2NaCl-7-(1,2)	3.27E+00	1.47E+00	45%	-17%	6
PbCl2NaCl-8-(1,2)	4.16E+00	1.40E+00	34%	-17%	6
PbCl2NaCl-9-(1,2)	4.63E+00	1.27E+00	27%	-19%	6

772

773 Figure V.3-6. Accuracy and precision of ΣNa measurements as a function of NaCl
774 loading.

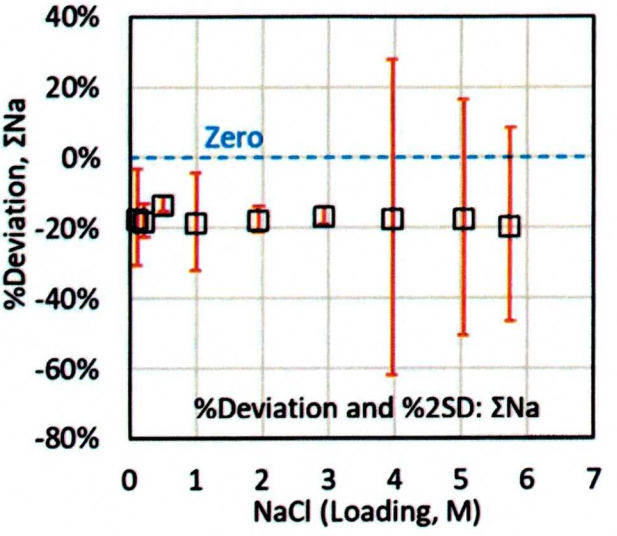

775

776 V.3.4.4. ΣCl

777 Time-dependent measurements of ΣCl are tabulated in Table V.3-8, and displayed in Figure V.3-7.
778 The observed scatters are within the maximum %2SD of 11% (Table V.3-9). The accuracy and
779 precision of ΣCl measurements are shown in Figure V.3-8. The larger %Deviation exceeding
780 the %2SD at lowest loading of NaCl indicates that the dissolution of $PbCl_2$(s) added Cl^- over and
781 above that from NaCl loading.

782 Table V.3-8. Time-dependent measurements of ΣCl.

PbCl2NaCl-1-1		PbCl2NaCl-1-2		PbCl2NaCl-2-1		PbCl2NaCl-2-2		PbCl2NaCl-3-1		PbCl2NaCl-3-2	
DSP	ΣCl, M	DSP	ΣCl, M	DSP	ΣCl, M	DSP	ΣCl, M	DSP	ΣCl, M	DSP	ΣCl, M
75	1.18E-01	75	1.28E-01	75	2.00E-01	75	2.11E-01	75	4.29E-01	75	4.66E-01
117	1.25E-01	117	1.24E-01	117	2.04E-01	117	2.03E-01	117	4.70E-01	117	4.81E-01
154	1.23E-01	154	1.26E-01	154	2.05E-01	154	2.05E-01	154	4.94E-01	154	5.06E-01
PbCl2NaCl-4-1		PbCl2NaCl-4-2		PbCl2NaCl-5-1		PbCl2NaCl-5-2		PbCl2NaCl-6-1		PbCl2NaCl-6-2	
DSP	ΣCl, M	DSP	ΣCl, M	DSP	ΣCl, M	DSP	ΣCl, M	DSP	ΣCl, M	DSP	ΣCl, M
75	8.95E-01	75	9.50E-01	75	1.82E+00	75	1.86E+00	75	2.82E+00	75	2.86E+00
117	8.94E-01	117	9.19E-01	117	1.78E+00	117	1.79E+00	117	2.73E+00	117	2.83E+00
154	9.36E-01	154	9.54E-01	154	1.81E+00	154	1.83E+00	154	2.81E+00	154	2.86E+00
PbCl2NaCl-7-1		PbCl2NaCl-7-2		PbCl2NaCl-8-1		PbCl2NaCl-8-2		PbCl2NaCl-9-1		PbCl2NaCl-9-2	
DSP	ΣCl, M	DSP	ΣCl, M	DSP	ΣCl, M	DSP	ΣCl, M	DSP	ΣCl, M	DSP	ΣCl, M
75	3.80E+00	75	3.82E+00	75	4.84E+00	75	4.89E+00	75	5.41E+00	75	5.47E+00
117	3.89E+00	117	3.84E+00	117	4.97E+00	117	4.92E+00	117	5.57E+00	117	5.48E+00
154	3.86E+00	154	3.91E+00	154	5.21E+00	154	5.25E+00	154	5.50E+00	154	5.45E+00

783

Figure V.3-7. Time-dependent measurements of ΣCl. Solid black squares and red error bars are averages and 2SD.

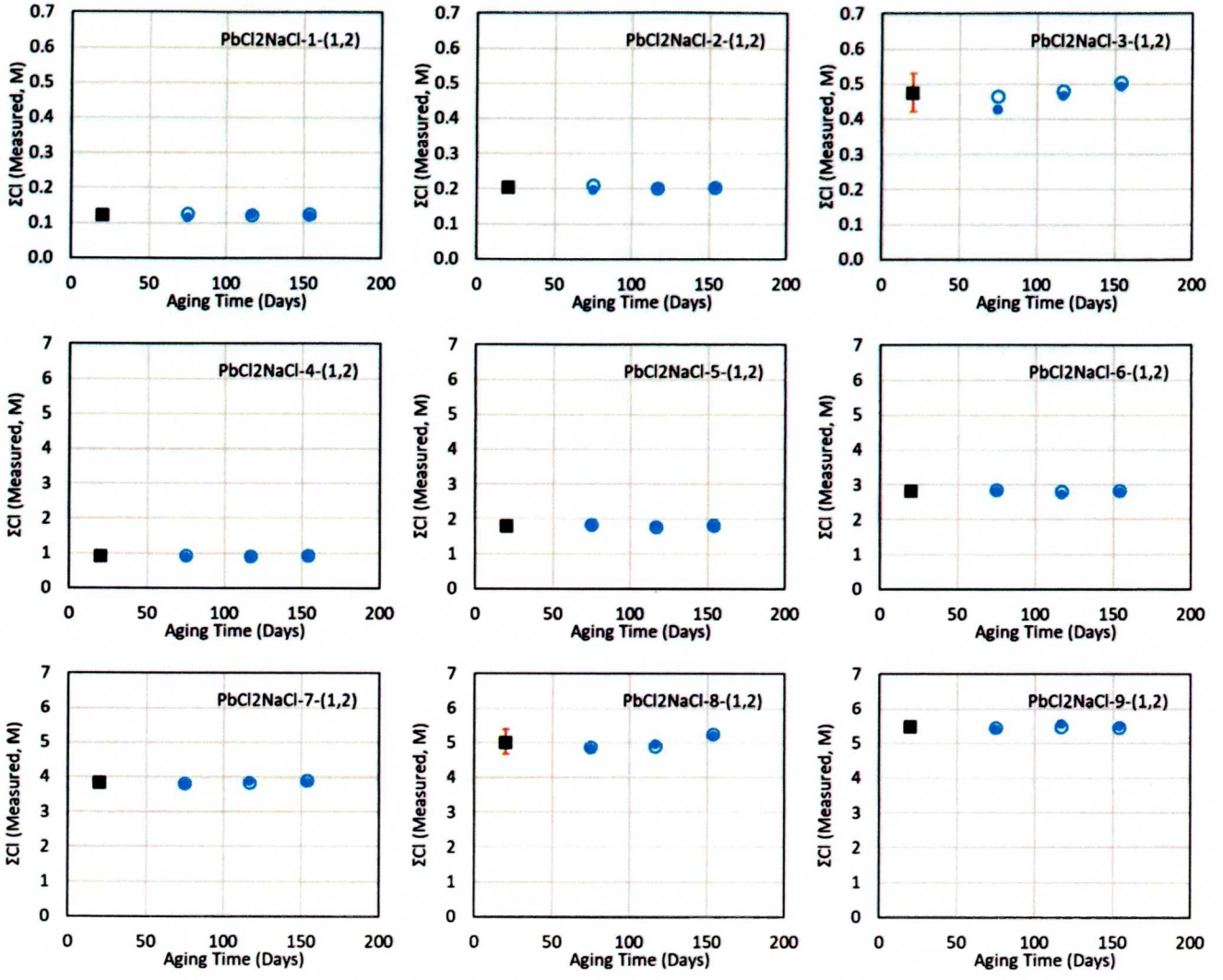

Table V.3-9. Statistics of ΣCl measurements (M).

Reactor ID	Average	2SD	%2SD	%Deviation	Counts
PbCl2NaCl-1-(1,2)	1.24E-01	7.06E-03	6%	24%	6
PbCl2NaCl-2-(1,2)	2.05E-01	7.63E-03	4%	2%	6
PbCl2NaCl-3-(1,2)	4.74E-01	5.34E-02	11%	-5%	6
PbCl2NaCl-4-(1,2)	9.25E-01	5.30E-02	6%	-6%	6
PbCl2NaCl-5-(1,2)	1.81E+00	5.73E-02	3%	-6%	6
PbCl2NaCl-6-(1,2)	2.82E+00	9.23E-02	3%	-3%	6
PbCl2NaCl-7-(1,2)	3.85E+00	7.73E-02	2%	-3%	6
PbCl2NaCl-8-(1,2)	5.01E+00	3.46E-01	7%	0%	6
PbCl2NaCl-9-(1,2)	5.48E+00	1.09E-01	2%	-5%	6

Figure V.3-8. Accuracy and precision of ΣCl measurements as a function of HCl loading. Larger %Deviations exceeding the 2SDs are consistent with dissolution of $PbCl_2(s)$, i.e., $\Sigma Cl = [NaCl]_{Loaded} + 2 \times [PbCl_2(s)]_{Dissolved}$.

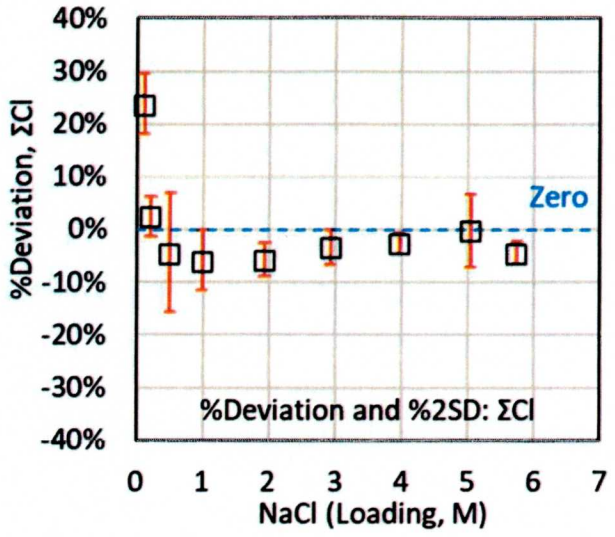

V.3.5. Data - Solids

Not obtained yet

V.3.6. Observations

The presence of Na^+ increased the dissolved total concentration of Pb (ΣPb) at similar loading of Cl (compare Figure V.2-4 and Figure V.3-4). The increase can be attributed to the influence of Na^+ on speciation of dissolved lead.

V.3.7. Model Parameterization: Pitzer Approach

The molalities of components are in Table V.3-10. The solubility data in Section V.1 (i.e., Table V.1-8) is included in this model parameterization. The data point represents the dissolved total concentration of Pb in the absence of loaded Cl. Application of the same set of reactions and PIPs as in Table V.2-9 and Table V.2-10 resulted in Figure V.3-9(A,B). Larger differences in measured and calculated ΣPb at ΣCl > 1 m indicate the need of new PIP for the species pair $Na^+/PbCl_3^-$. Fitting of $\beta^{(0)}$ for the species pair $Na^+/PbCl_3^-$ achieved a satisfactory fit to the data (Figure V.3-9, C and D).

Table V.3-10. Concentrations in molality (m, mol/kg)

Measurements	pmH		ΣPb, m	
Reactor ID	avg	2SD	avg	2SD
PbCl2DI-(1,2,3)-(1,2,3)[A]	3.95	0.05	3.92E-02	3.81E-03
PbCl2NaCl-1-(1,2)	4.27	0.06	1.57E-02	8.03E-03
PbCl2NaCl-2-(1,2)	4.50	0.06	8.90E-03	2.15E-03
PbCl2NaCl-3-(1,2)	4.88	0.05	5.60E-03	1.52E-03
PbCl2NaCl-4-(1,2)	5.24	0.06	5.22E-03	1.42E-03
PbCl2NaCl-5-(1,2)	5.65	0.11	7.73E-03	1.89E-03

Measurements	pmH		ΣPb, m	
Reactor ID	avg	2SD	avg	2SD
PbCl2NaCl-6-(1,2)	5.95	0.03	1.43E-02	3.46E-03
PbCl2NaCl-7-(1,2)	6.26	0.07	2.95E-02	6.94E-03
PbCl2NaCl-8-(1,2)	6.62	0.09	6.69E-02	1.32E-02
PbCl2NaCl-9-(1,2)	6.84	0.13	8.27E-02	3.29E-02
Measurements	ΣNa, m		ΣCl, m	
Reactor ID	avg	2SD	avg	2SD
PbCl2DI-(1,2,3)-(1,2,3)[A]	NA	NA	8.04E-02	6.00E-03
PbCl2NaCl-1-(1,2)	8.30E-02	1 12E-02	1.24E-01	7.07E-03
PbCl2NaCl-2-(1,2)	1.64E-01	8.01E-03	2.05E-01	7.66E-03
PbCl2NaCl-3-(1,2)	4.35E-01	9 42E-03	4 79E-01	5.39E-02
PbCl2NaCl-4-(1,2)	8.18E-01	1.13E-01	9 43E-01	5.41E-02
PbCl2NaCl-5-(1,2)	1.65E+00	6.10E-02	1.89E+00	5.97E-02
PbCl2NaCl-6-(1,2)	2.59E+00	6.19E-02	3.00E+00	9.83E-02
PbCl2NaCl-7-(1,2)	3.56E+00	1.60E+00	4.20E+00	8.42E-02
PbCl2NaCl-8-(1,2)	4.64E+00	1.56E+00	5.60E+00	3.87E-01
PbCl2NaCl-9-(1,2)	5.26E+00	1 44E+00	6.22E+00	1.23E-01

[A] Data from Table V 1-8.

Figure V.3-9. A and B: Application of model in Table V.2-9 and Table V.2-10. C and D: Fitting of the model using PIP(Na^+/$PbCl_3^-$). B and D are zoom-in views of A and B, respectively.

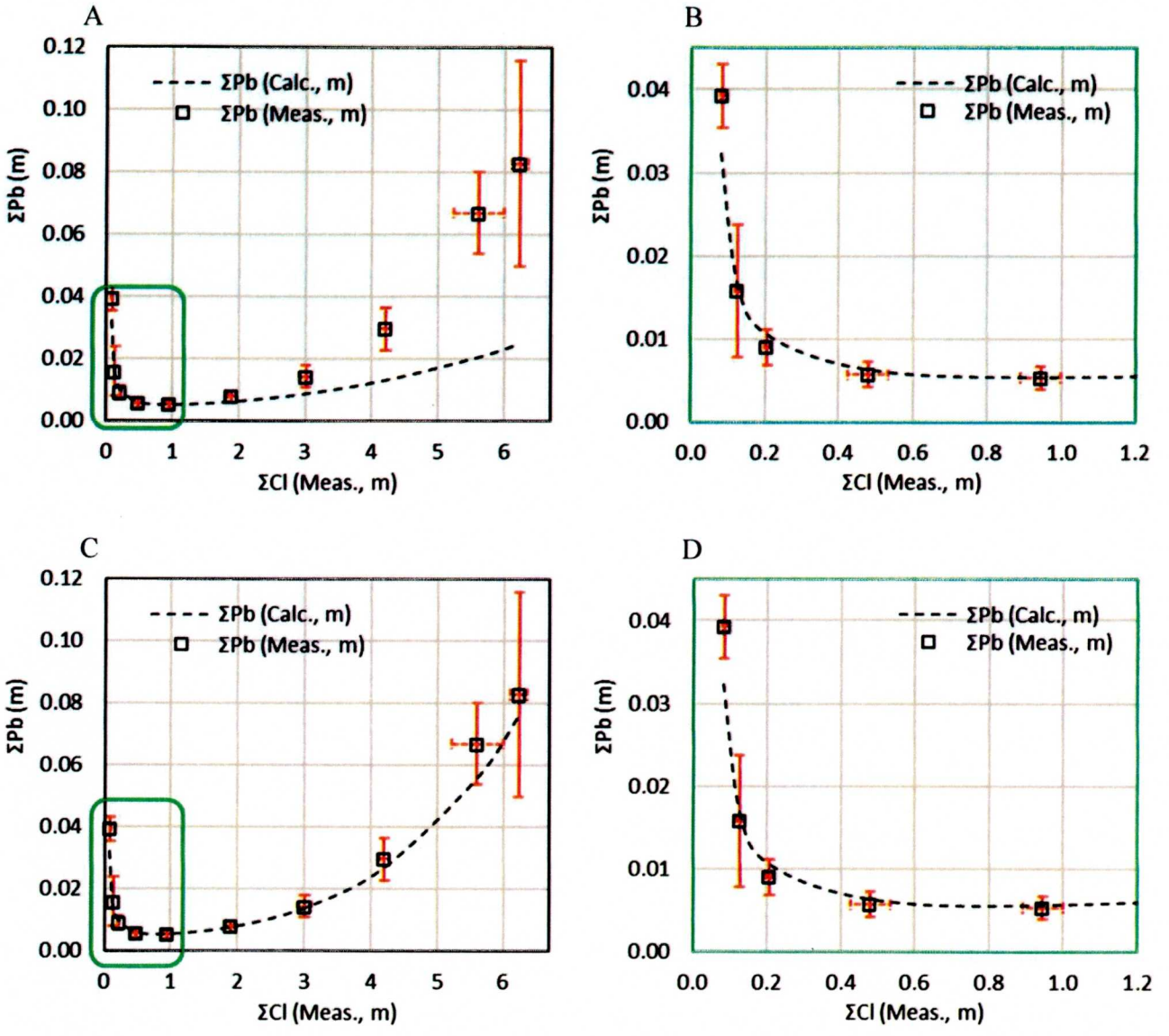

V.3.8. Summary

Below is the recommended new addition to data0.fm1 (Table V.3-11). Our solubility data are consistent with literature data where $PbCl_2$(s) is the solubility-limiting phase (Figure V.3-10). The XRD characterization of our solids will be reported later when the XRD scans are available.

Table V.3-11. Recommended new addition to data0.fm1.

i	j	α_1/α_2[A]	$\beta^{(0)}$	$\beta^{(1)}$	$\beta^{(2)}$	C^{φ}	Source
Na^+	$PbCl_3^-$	2.0/12.0	-0.10025	0.0	0.0	0.0	This section

[A] α_1 and α_2 are pre-set constants used in the Pitzer activity coefficient equation. α_1 and α_2 apply for only cation-anion binary pair. α_2 is only used for 2:2 electrolytes and multivalent ions. α_2 is not applied when $\beta^{(2)}$ is zero or not used. The unit for α_1 and α_2 is $kg^{1/2} \cdot mol^{-1/2}$.

Figure V.3-10. Comparison of our data (x SNL WIPP) with selected literature data. A. Whole range investigated. B. Zoom-in of the area marked with green rectangle in A.

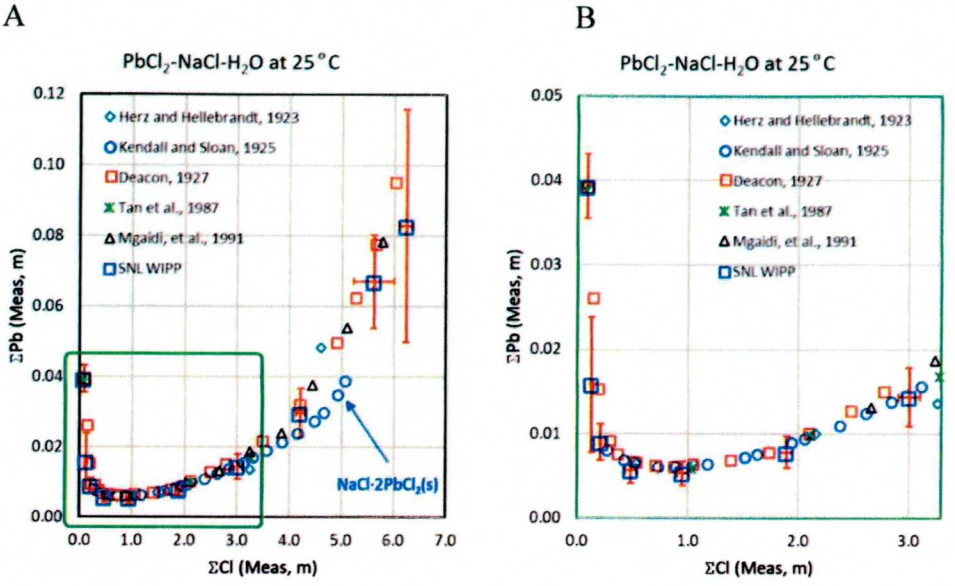

V.4. $PbCl_2$(s) - $MgCl_2$ - H_2O

V.4.1. Chemical System

The solubility of $PbCl_2$(s) was measured in 0.05 to 3.0 m $MgCl_2$. This is a 5 component system: Pb^{+2} - Mg^{+2} - Cl^- - H^+ - H_2O.

V.4.2. Goals and Hypotheses

The goal is to accurately model how Mg^{+2} influences the solubility of $PbCl_2$(s).

V.4.3. Reactor Preparation

6.0 grams of $PbCl_2$(s) was mixed with the $MgCl_2$ solutions prepared by the recipes in Table V.4-1. Hydration water of the salt, $MgCl_2.6H_2O$, was accounted for in calculating the molality of $MgCl_2$.

Table V.4-1. Recipe and calculated solution properties.

Reactor ID	$MgCl_2.6H_2O$, gram	DI, mL	DI, gram	Hydration H_2O in the salt, g	Total H_2O, g	MgCl2, m	$PbCl_2$(s)
PbCl2MgCl2-1-1	0.4588	44.8	44.6	0.2	44.9	0.0503	6.0
PbCl2MgCl2-1-2	0.4587	44.8	44.6	0.2	44.9	0.0503	6.0
PbCl2MgCl2-2-1	0.9150	44.5	44.4	0.5	44.9	0.100	6.0
PbCl2MgCl2-2-2	0.9152	44.5	44.4	0.5	44.9	0.100	6.0
PbCl2MgCl2-3-1	2.7455	43.5	43.4	1.5	44.9	0.301	6.0
PbCl2MgCl2-3-2	2.7459	43.5	43.4	1.5	44.9	0.301	6.0
PbCl2MgCl2-4-1	4.5746	42.6	42.4	2.4	44.9	0.501	6.0
PbCl2MgCl2-4-2	4.574	42.6	42.4	2.4	44.9	0.501	6.0

PbCl2MgCl2-5-1	9.1499	40.1	40.0	4.9	44.9	1.00	6.0
PbCl2MgCl2-5-2	9.1496	40.1	40.0	4.9	44.9	1.00	6.0
PbCl2MgCl2-6-1	13.728	37.7	37.6	7.3	44.9	1.50	6.0
PbCl2MgCl2-6-2	13.7287	37.7	37.6	7.3	44.9	1.50	6.0
PbCl2MgCl2-7-1	18.308	35.3	35.2	9.7	44.9	2.01	6.0
PbCl2MgCl2-7-2	18.3083	35.3	35.2	9.7	44.9	2.01	6.0
PbCl2MgCl2-8-1	22.8735	32.9	32.8	12.2	44.9	2.51	6.0
PbCl2MgCl2-8-2	22.8736	32.9	32.8	12.2	44.9	2.51	6.0
PbCl2MgCl2-9-1	27.4561	30.4	30.3	14.6	44.9	3.01	6.0
PbCl2MgCl2-9-2	27.4565	30.4	30.3	14.6	44.9	3.01	6.0

Properties	pH	Density, g/mL	M:m, L/kg	MgCl2, M
PbCl2MgCl2-1-(1,2)	6.77	1.0040	1.0008	0.050
PbCl2MgCl2-2-(1,2)	6.74	1.0071	1.0025	0.100
PbCl2MgCl2-3-(1,2)	6.62	1.0191	1.0094	0.298
PbCl2MgCl2-4-(1,2)	6.50	1.0310	1.0162	0.493
PbCl2MgCl2-5-(1,2)	6.22	1.0601	1.0334	0.970
PbCl2MgCl2-6-(1,2)	5.95	1.0882	1.0506	1.432
PbCl2MgCl2-7-(1,2)	5.71	1.1155	1.0678	1.878
PbCl2MgCl2-8-(1,2)	5.48	1.1418	1.0849	2.310
PbCl2MgCl2-9-(1,2)	5.27	1.1672	1.1021	2.728

840

841 V.4.4. Data - Aqueous

842 V.4.4.1. pHr

843 Time-dependent measurements of pHr are tabulated in Table V.4-2, and displayed in Figure V.4-1.
844 The observed scatter is within the maximum %2SD of 4% (Table V.4-3). The change of pHr as a
845 function of $MgCl_2$ loading is presented in Figure V.4-2.

846 Table V.4-2. Time-dependent measurement of pHr (DSP = Days Since Preparation, i.e.,
847 Aging time in days).

PbCl2MgCl2-1-1		PbCl2MgCl2-1-2		PbCl2MgCl2-2-1		PbCl2MgCl2-2-2		PbCl2MgCl2-3-1		PbCl2MgCl2-3-2	
DSP	pHr	DSP	pHr	DSP	pHr	DSP	pHr	DSP	pHr	DSP	pHr
63	4.31	63	4.35	63	4.51	63	4.54	63	4.91	63	4.94
93	4.26	93	4.31	93	4.57	93	4.55	93	4.89	93	4.96
129	4.28	129	4.27	129	4.48	129	4.5	129	4.85	129	4.85
PbCl2MgCl2-4-1		PbCl2MgCl2-4-2		PbCl2MgCl2-5-1		PbCl2MgCl2-5-2		PbCl2MgCl2-6-1		PbCl2MgCl2-6-2	
DSP	pHr	DSP	pHr	DSP	pHr	DSP	pHr	DSP	pHr	DSP	pHr
63	5.13	63	5.07	63	5.44	63	5.36	63	5.56	63	5.49
93	5.12	93	5.16	93	5.38	93	5.34	93	5.43	93	5.43
129	5.06	129	5.02	129	5.26	129	5.29	129	5.43	129	5.45
PbCl2MgCl2-7-1		PbCl2MgCl2-7-2		PbCl2MgCl2-8-1		PbCl2MgCl2-8-2		PbCl2MgCl2-9-1		PbCl2MgCl2-9-2	
DSP	pHr	DSP	pHr	DSP	pHr	DSP	pHr	DSP	pHr	DSP	pHr
63	5.67	63	5.67	63	5.38	63	5.57	63	5.41	63	5.41

93	5.59	93	5.53	93	5.53	93	5.47	93	5.25	93	5.22
129	5.54	129	5.57	129	5.5	129	5.48	129	5.28	129	5.17

848

849 Figure V.4-1. Time-dependent measurement of pHr.

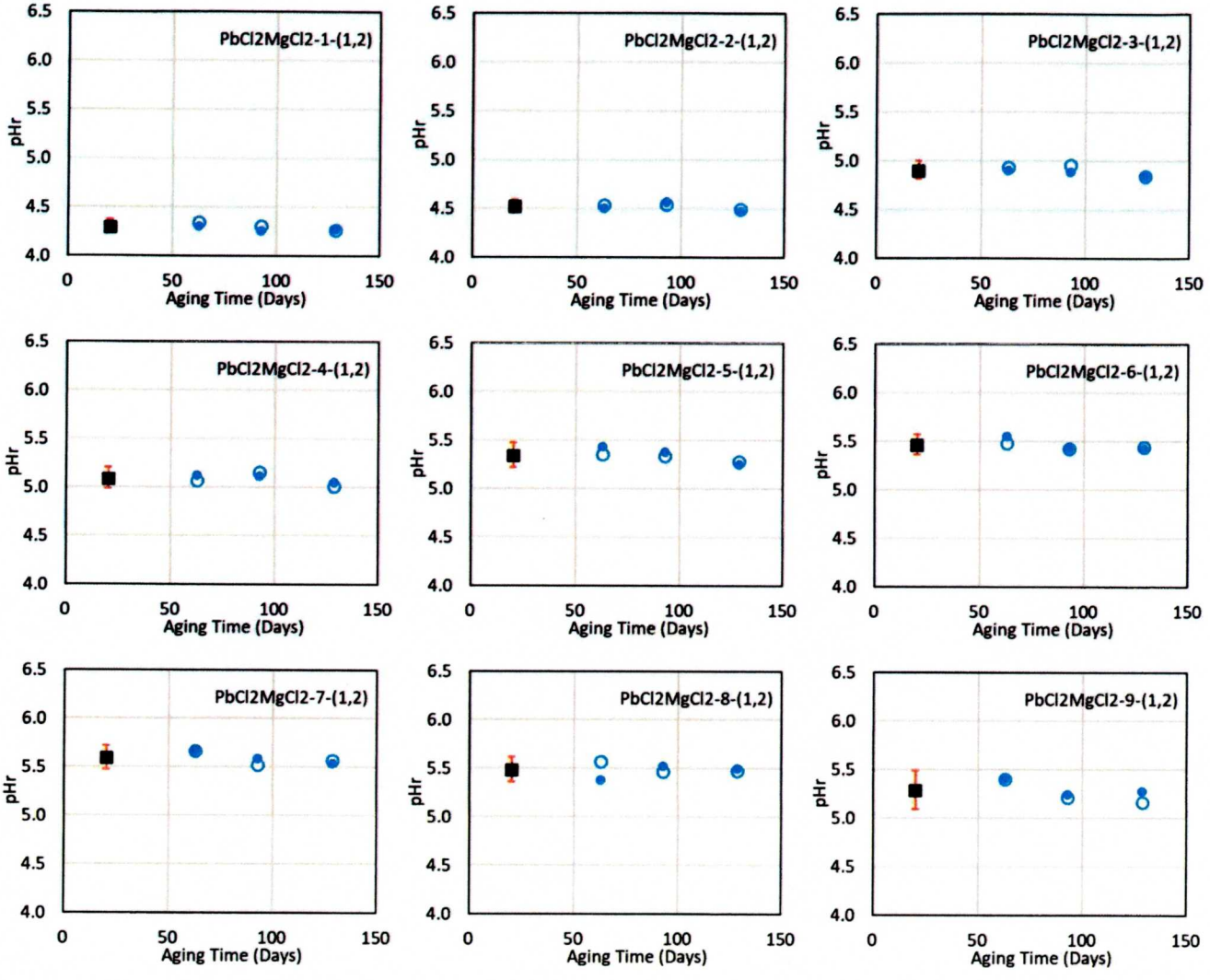

850

851

852

853 Table V.4-3. Statistics of pHr measurements.

Reactor ID	Average	2SD	%2SD	Counts
PbCl2MgCl2-1-(1,2)	4.30	0.07	2%	6
PbCl2MgCl2-2-(1,2)	4.53	0.07	1%	6
PbCl2MgCl2-3-(1,2)	4.90	0.09	2%	6
PbCl2MgCl2-4-(1,2)	5.09	0.10	2%	6
PbCl2MgCl2-5-(1,2)	5.35	0.13	2%	6
PbCl2MgCl2-6-(1,2)	5.47	0.10	2%	6
PbCl2MgCl2-7-(1,2)	5.60	0.12	2%	6
PbCl2MgCl2-8-(1,2)	5.49	0.13	2%	6
PbCl2MgCl2-9-(1,2)	5.29	0.20	4%	6

854

Figure V.4-2. Change of pHr as a function of $MgCl_2$ loading.

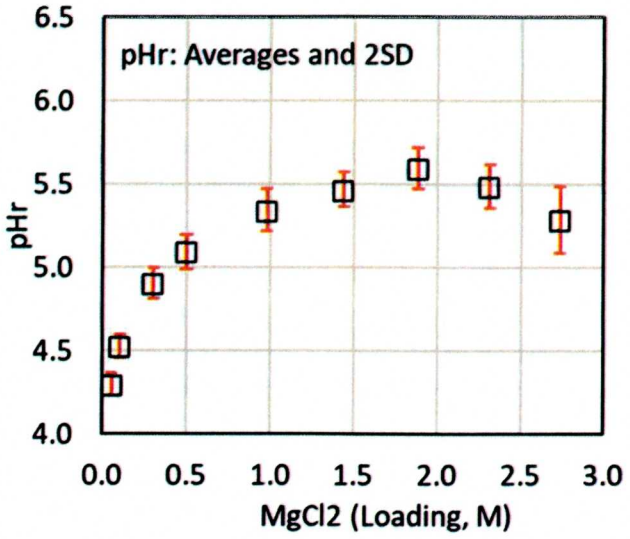

V.4.4.2. ΣPb

Time-dependent ΣPb is tabulated in Table V.4-4, and displayed in Figure V.4-3. The observed scatter is within the maximum %2SD of 18% (Table V.4-5). Figure V.4-4 shows the change of ΣPb as a function of $MgCl_2$ loading.

Table V.4-4. Time-dependent ΣPb in M (DSP = Days Since Preparation, i.e., Aging time in days).

PbCl2MgCl2-1-1		PbCl2MgCl2-1-2		PbCl2MgCl2-2-1		PbCl2MgCl2-2-2		PbCl2MgCl2-3-1		PbCl2MgCl2-3-2	
DSP	ΣPb	DSP	ΣPb	DSP	ΣPb	DSP	ΣPb	DSP	ΣPb	DSP	ΣPb
63	1.51E-02	63	1.54E-02	63	8.86E-03	63	8.76E-03	63	4.77E-03	63	4.82E-03
93	1.64E-02	93	1.68E-02	93	1.01E-02	93	9.61E-03	93	5.10E-03	93	5.28E-03
129	1.68E-02	129	1.73E-02	129	1.05E-02	129	1.05E-02	129	5.42E-03	129	5.30E-03
PbCl2MgCl2-4-1		PbCl2MgCl2-4-2		PbCl2MgCl2-5-1		PbCl2MgCl2-5-2		PbCl2MgCl2-6-1		PbCl2MgCl2-6-2	
DSP	ΣPb	DSP	ΣPb	DSP	ΣPb	DSP	ΣPb	DSP	ΣPb	DSP	ΣPb
63	4.30E-03	63	4.35E-03	63	4.86E-03	63	4.67E-03	63	6.86E-03	63	6.80E-03
93	4.52E-03	93	4.53E-03	93	5.24E-03	93	5.56E-03	93	7.77E-03	93	7.86E-03
129	5.08E-03	129	4.94E-03	129	5.80E-03	129	5.68E-03	129	8.54E-03	129	7.96E-03
PbCl2MgCl2-7-1		PbCl2MgCl2-7-2		PbCl2MgCl2-8-1		PbCl2MgCl2-8-2		PbCl2MgCl2-9-1		PbCl2MgCl2-9-2	
DSP	ΣPb	DSP	ΣPb	DSP	ΣPb	DSP	ΣPb	DSP	ΣPb	DSP	ΣPb
63	1.08E-02	63	1.07E-02	63	1.89E-02	63	1.71E-02	63	2.82E-02	63	2.71E-02
93	1.17E-02	93	1.20E-02	93	1.92E-02	93	1.88E-02	93	3.00E-02	93	3.12E-02
129	1.18E-02	129	1.20E-02	129	1.93E-02	129	1.85E-02	129	3.00E-02	129	3.07E-02

Figure V.4-3. Time-dependent ΣPb in duplicate reactors.

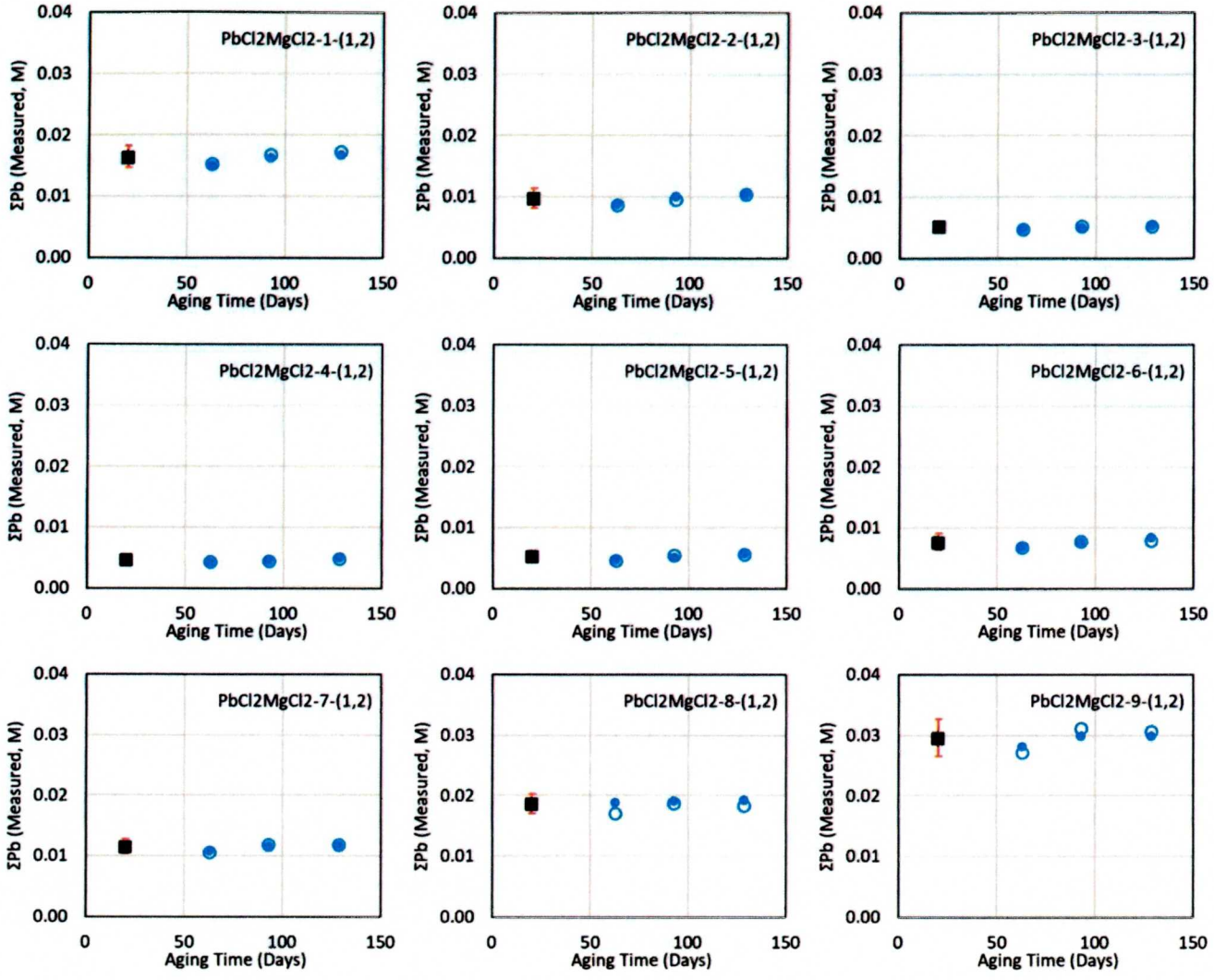

Table V.4-5. Statistics of ΣPb measurements in M.

Reactor ID	Average	2SD	%2SD	Counts
PbCl2MgCl2-1-(1,2)	1.63E-02	1.77E-03	11%	6
PbCl2MgCl2-2-(1,2)	9.73E-03	1.58E-03	16%	6
PbCl2MgCl2-3-(1,2)	5.11E-03	5.39E-04	11%	6
PbCl2MgCl2-4-(1,2)	4.62E-03	6.39E-04	14%	6
PbCl2MgCl2-5-(1,2)	5.30E-03	9.20E-04	17%	6
PbCl2MgCl2-6-(1,2)	7.63E-03	1.36E-03	18%	6
PbCl2MgCl2-7-(1,2)	1.15E-02	1.14E-03	10%	6
PbCl2MgCl2-8-(1,2)	1.86E-02	1.60E-03	9%	6
PbCl2MgCl2-9-(1,2)	2.95E-02	3.12E-03	11%	6

Figure V.4-4. Change of ΣPb as a function of $MgCl_2$ loading.

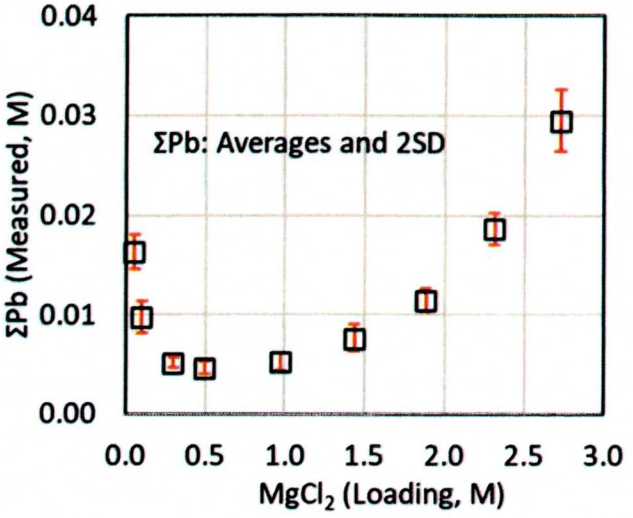

V.4.4.3. ΣMg

Time-dependent ΣMg is tabulated in Table V.4-6, and displayed in Figure V.4-5. The observed scatter is within the maximum %2SD of 5%, except one that is 78% of %2SD (Table V.4-7; the value in green fonts), which seems to be due to dilution error. Figure V.4-6 shows the accuracy and precision of ΣMg measurements.

Table V.4-6. Time-dependent ΣMg in M (DSP = Days Since Preparation, i.e., Aging time in days).

PbCl2MgCl2-1-1		PbCl2MgCl2-1-2		PbCl2MgCl2-2-1		PbCl2MgCl2-2-2		PbCl2MgCl2-3-1		PbCl2MgCl2-3-2	
DSP	ΣMg	DSP	ΣMg	DSP	ΣMg	DSP	ΣMg	DSP	ΣMg	DSP	ΣMg
63	4.85E-02	63	5.03E-02	63	1.01E-01	63	9.60E-02	63	2.91E-01	63	2.95E-02
93	5.16E-02	63	4.99E-02	93	1.02E-01	93	1.03E-01	93	3.02E-01	63	2.95E-01
129	4.95E-02	93	5.16E-02	129	1.02E-01	129	1.02E-01	129	2.95E-01	93	3.04E-01
		129	5.04E-02							129	2.93E-01
PbCl2MgCl2-4-1		PbCl2MgCl2-4-2		PbCl2MgCl2-5-1		PbCl2MgCl2-5-2		PbCl2MgCl2-6-1		PbCl2MgCl2-6-2	
DSP	ΣMg	DSP	ΣMg	DSP	ΣMg	DSP	ΣMg	DSP	ΣMg	DSP	ΣMg
63	4.77E-01	63	4.85E-01	63	1.16E+00	63	1.20E+00	63	1.22E+00	63	1.22E+00
93	5.07E-01	93	5.06E-01	63	9.78E-01	63	9.92E-01	63	1.45E+00	63	1.46E+00
129	4.93E-01	129	4.81E-01	93	9.94E-01	93	9.90E-01	93	1.51E+00	93	1.49E+00
				129	9.99E-01	129	9.84E-01	129	1.48E+00	129	1.46E+00
PbCl2MgCl2-7-1		PbCl2MgCl2-7-2		PbCl2MgCl2-8-1		PbCl2MgCl2-8-2		PbCl2MgCl2-9-1		PbCl2MgCl2-9-2	
DSP	ΣMg	DSP	ΣMg	DSP	ΣMg	DSP	ΣMg	DSP	ΣMg	DSP	ΣMg
63	1.22E+00	63	1.22E+00	63	1.22E+00	63	1.22E+00	63	1.22E+00	63	1.22E+00
63	1.92E+00	63	1.92E+00	63	2.36E+00	63	2.36E+00	63	2.67E+00	63	2.79E+00
93	1.98E+00	93	1.90E+00	93	2.42E+00	93	2.38E+00	93	2.79E+00	93	2.87E+00
129	1.90E+00	129	1.88E+00	129	2.38E+00	129	2.40E+00	129	2.77E+00	129	2.82E+00

Green: Concentration calculated by potentially incorrect dilution factor, but valid record under SNL WIPP QA, so included in the statistics. No justification present to exclude the record. Red: flagged by lab, not included to calculate the statistics.

Figure V.4-5. Time-dependent ΣMg. Solid black squares and red error bars are averages and 2SD. The data marked with green oval in the third panel is the value in green fonts in Table V.4-6.

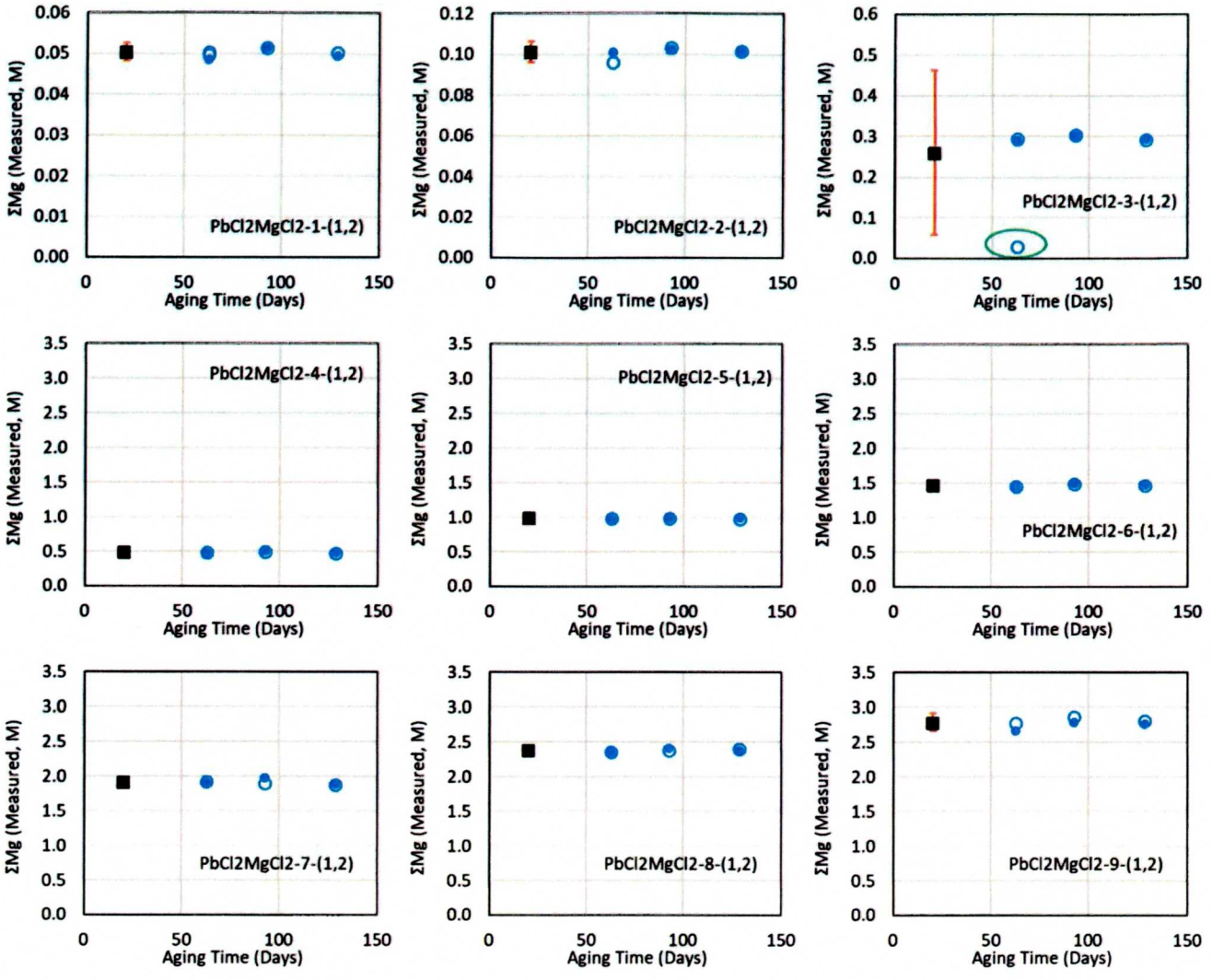

Table V.4-7. Statistics of ΣMg measurements (M).

Reactor ID	Average	2SD	%2SD	%Deviation	Counts
PbCl2MgCl2-1-(1,2)	5.03E-02	2.16E-03	4%	0%	7
PbCl2MgCl2-2-(1,2)	1.01E-01	5.17E-03	5%	1%	6
PbCl2MgCl2-3-(1,2)	2.58E-01	2.02E-01	78%	-13%	7
PbCl2MgCl2-4-(1,2)	4.92E-01	2.56E-02	5%	0%	6
PbCl2MgCl2-5-(1,2)	9.89E-01	1.48E-02	1%	2%	6
PbCl2MgCl2-6-(1,2)	1.47E+00	3.97E-02	3%	3%	6
PbCl2MgCl2-7-(1,2)	1.92E+00	6.52E-02	3%	2%	6
PbCl2MgCl2-8-(1,2)	2.38E+00	4.69E-02	2%	3%	6
PbCl2MgCl2-9-(1,2)	2.78E+00	1.29E-01	5%	2%	6

Figure V.4-6. Accuracy and precision of ΣMg as a function of $MgCl_2$ loading.

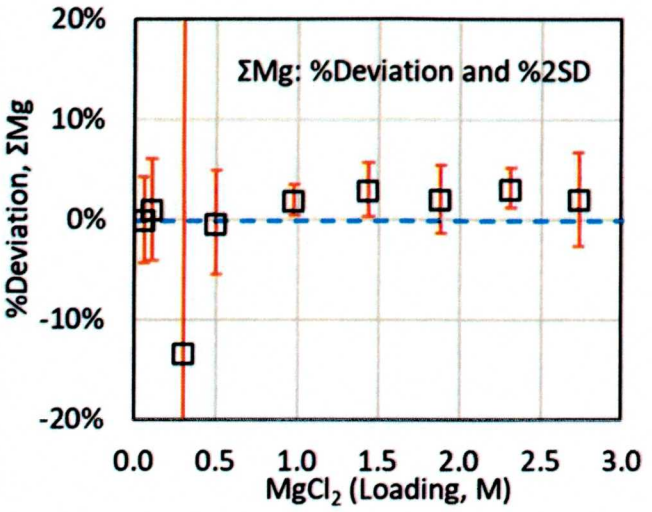

V.4.4.4. ΣCl

Time-dependent measurements of ΣCl are tabulated in Table V.4-8, and displayed in Figure V.4-7. The observed scatters are within the maximum %2SD of 18% (Table V.4-9). The accuracy and precision of ΣCl as a function of $MgCl_2$ loading is shown in Figure V.4-8. The large %Deviation exceeding the %2SD indicates that the dissolution of $PbCl_2$(s) increased the ΣCl above the loading.

Table V.4-8. Time-dependent measurements of ΣCl in M (DSP = Days Since Preparation, i.e., Aging time in days).

PbCl2MgCl2-1-1		PbCl2MgCl2-1-2		PbCl2MgCl2-2-1		PbCl2MgCl2-2-2		PbCl2MgCl2-3-1		PbCl2MgCl2-3-2	
DSP	ΣCl	DSP	ΣCl	DSP	ΣCl	DSP	ΣCl	DSP	ΣCl	DSP	ΣCl
63	1.56E-01	63	1.50E-01	63	2.09E-01	63	2.11E-01	63	5.14E-01	63	5.51E-01
93	1.66E-01	93	1.58E-01	93	2.46E-01	93	2.44E-01	93	6.25E-01	93	6.09E-01
PbCl2MgCl2-4-1		PbCl2MgCl2-4-2		PbCl2MgCl2-5-1		PbCl2MgCl2-5-2		PbCl2MgCl2-6-1		PbCl2MgCl2-6-2	
DSP	ΣCl	DSP	ΣCl	DSP	ΣCl	DSP	ΣCl	DSP	ΣCl	DSP	ΣCl
63	9.01E-01	63	8.99E-01	63	1.86E+00	63	1.87E+00	63	2.82E+00	63	2.83E+00
93	1.01E+00	93	1.02E+00	93	1.98E+00	93	1.99E+00	93	2.94E+00	93	2.95E+00
PbCl2MgCl2-7-1		PbCl2MgCl2-7-2		PbCl2MgCl2-8-1		PbCl2MgCl2-8-2		PbCl2MgCl2-9-1		PbCl2MgCl2-9-2	
DSP	ΣCl	DSP	ΣCl	DSP	ΣCl	DSP	ΣCl	DSP	ΣCl	DSP	ΣCl
63	3.75E+00	63	3.68E+00	63	4.63E+00	63	4.56E+00	63	4.89E+00	63	4.80E+00
93	3.82E+00	93	3.85E+00	93	4.76E+00	93	4.74E+00	93	5.66E+00	93	5.68E+00
								93	5.75E+00	93	5.79E+00

Figure V.4-7. Time-dependent measurements of ΣCl. Solid black squares and red error bars are averages and 2SDs.

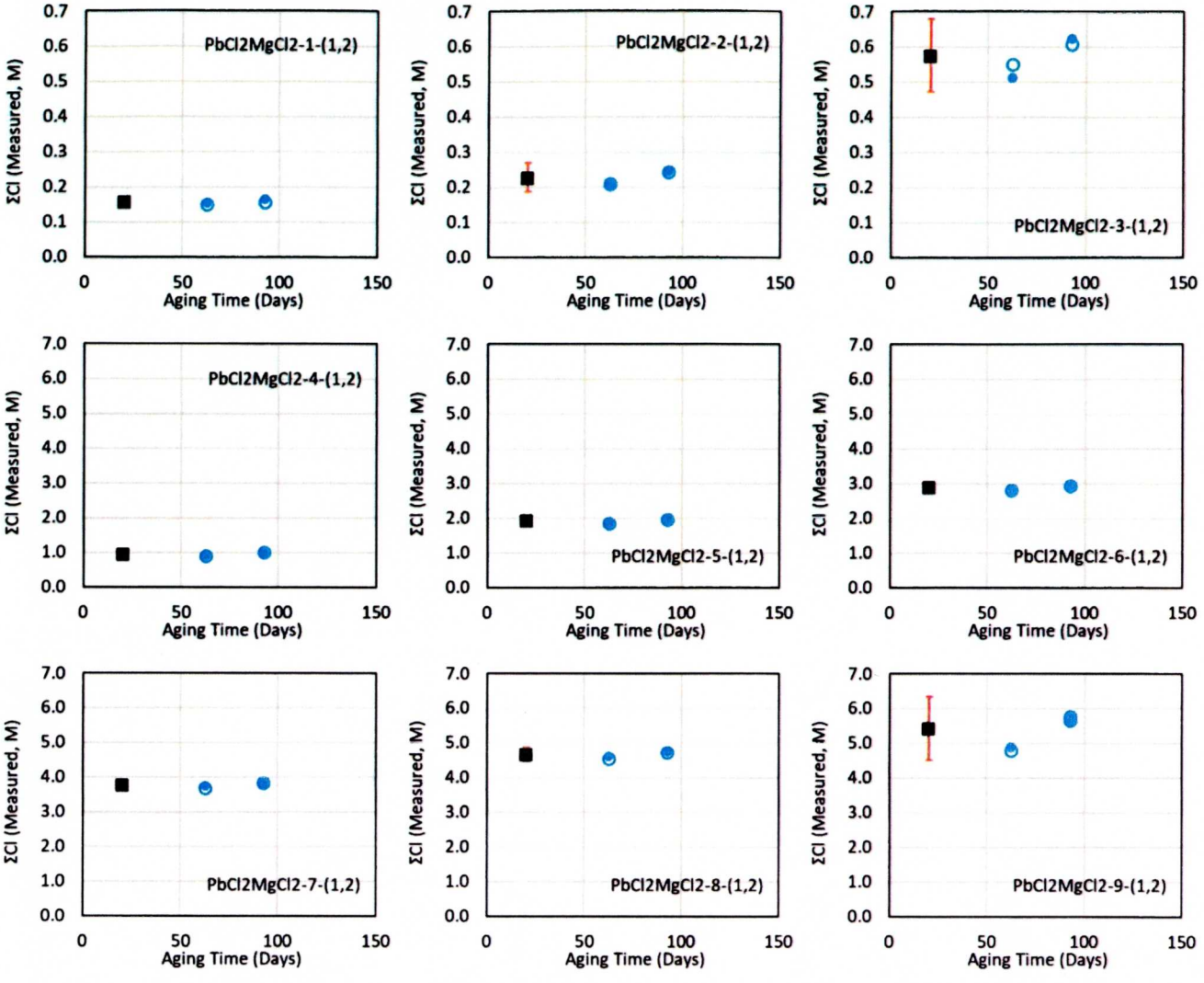

Table V.4-9. Statistics of ΣCl measurements in M.

Reactor ID	Average	2SD	%2SD	%Deviation	Counts
PbCl2MgCl2-1-(1,2)	1.57E-01	1.26E-02	8%	57%	4
PbCl2MgCl2-2-(1,2)	2.27E-01	4.07E-02	18%	14%	4
PbCl2MgCl2-3-(1,2)	5.75E-01	1.03E-01	18%	-4%	4
PbCl2MgCl2-4-(1,2)	9.55E-01	1.28E-01	13%	-3%	4
PbCl2MgCl2-5-(1,2)	1.93E+00	1.37E-01	7%	-1%	4
PbCl2MgCl2-6-(1,2)	2.89E+00	1.37E-01	5%	1%	4
PbCl2MgCl2-7-(1,2)	3.78E+00	1.52E-01	4%	1%	4
PbCl2MgCl2-8-(1,2)	4.67E+00	1.92E-01	4%	1%	4
PbCl2MgCl2-9-(1,2)	5.43E+00	9.11E-01	17%	-1%	6

Figure V.4-8. Accuracy and precision of ΣCl as a function of $MgCl_2$ loading. Larger %Deviations exceeding the 2SDs are consistent with dissolution of $PbCl_2(s)$, i.e., $\Sigma Cl = 2 \times [MgCl_2]_{Loaded} + 2 \times [PbCl_2(s)]_{Dissolved}$.

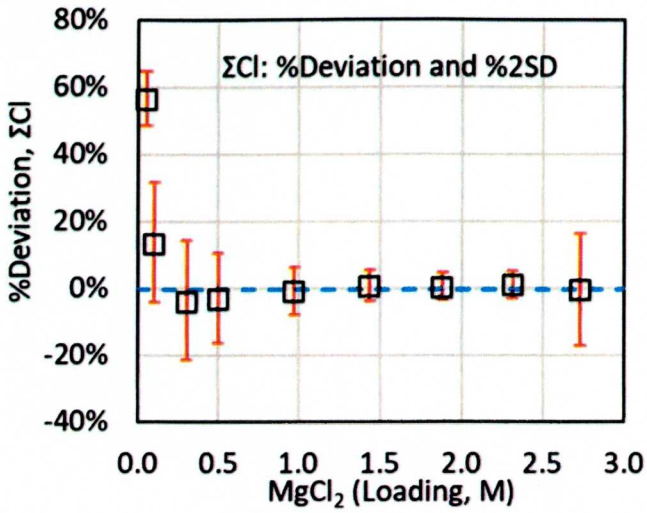

V.4.5. Data - Solids

No data yet.

V.4.6. Observations

The common-ion effect is apparent in this $MgCl_2$ experiment: The solubility of $PbCl_2(s)$ in $MgCl_2$ solution is similar to its solubility in HCl solutions (compare Figure V.2-4 and Figure V.4-4), but the solubility is lower than the solubility seen in the NaCl experiment (compare Figure V.2-4 and Figure V.4-4).

V.4.7. Model Parameterization: Pitzer Approach

Concentrations are converted to molality in Table V.4-10. The solubility data in Section V.1 (i.e., Table V.1-8) is used in this model parameterization to estimate dissolved Pb in the absence of loaded Cl. Application of the same set of reactions and PIPs as in Table V.2-9 and Table V.2-10 is shown in Figure V.4-9(A,B). Larger differences in measured and calculated ΣPb at ΣCl > 1 m indicate the need for new PIP for the species pair $Mg^{+2}/PbCl_3^-$. Fitting of $\beta^{(0)}$ for the species pair $Mg^{+2}/PbCl_3^-$ greatly improves the fit (Figure V.4-9, C and D).

Table V.4-10. Concentrations in molality (m, mol/kg)

	pmH		ΣPb, m	
Reactor ID	avg	2SD	avg	2SD

PbCl2DI-(1,2,3)-(1,2,3)	3.95	0.05	3.92E-02	3.81E-03
PbCl2MgCl2-1-(1,2)	4.22	0.07	1.63E-02	1.77E-03
PbCl2MgCl2-2-(1,2)	4.46	0.07	9.76E-03	1.58E-03
PbCl2MgCl2-3-(1,2)	4.92	0.09	5.16E-03	5.44E-04
PbCl2MgCl2-4-(1,2)	5.20	0.11	4.69E-03	6.49E-04
PbCl2MgCl2-5-(1,2)	5.65	0.14	5.48E-03	9.51E-04
PbCl2MgCl2-6-(1,2)	5.96	0.11	8.02E-03	1.42E-03
PbCl2MgCl2-7-(1,2)	6.28	0.14	1.23E-02	1.22E-03
PbCl2MgCl2-8-(1,2)	6.35	0.15	2.02E-02	1.73E-03
PbCl2MgCl2-9-(1,2)	6.33	0.24	3.25E-02	3.44E-03
	ΣMg, m		ΣCl, m	
Reactor ID	avg	2SD	avg	2SD
PbCl2DI-(1,2,3)-(1,2,3)	NA	NA	8.04E-02	6.00E-03
PbCl2MgCl2-1-(1,2)	5.03E-02	2.16E-03	1.58E-01	1.26E-02
PbCl2MgCl2-2-(1,2)	1.01E-01	5.19E-03	2.28E-01	4.08E-02
PbCl2MgCl2-3-(1,2)	2.61E-01	2.04E-01	5.80E-01	1.04E-01
PbCl2MgCl2-4-(1,2)	5.00E-01	2.60E-02	9.71E-01	1.30E-01
PbCl2MgCl2-5-(1,2)	1.02E+00	1.53E-02	1.99E+00	1.42E-01
PbCl2MgCl2-6-(1,2)	1.55E+00	4.17E-02	3.03E+00	1.44E-01
PbCl2MgCl2-7-(1,2)	2.05E+00	6.96E-02	4.03E+00	1.62E-01
PbCl2MgCl2-8-(1,2)	2.58E+00	5.09E-02	5.07E+00	2.09E-01
PbCl2MgCl2-9-(1,2)	3.07E+00	1.43E-01	5.98E+00	1.00E+00

929

Figure V.4-9. A and B: Application of model in Table V.2-9 and Table V.2-10. C and D: Fitting of the model using PIP($Mg^{+2}/PbCl_3^-$). B and D are zoom-in views of the areas marked with green rectangles in A and B, respectively.

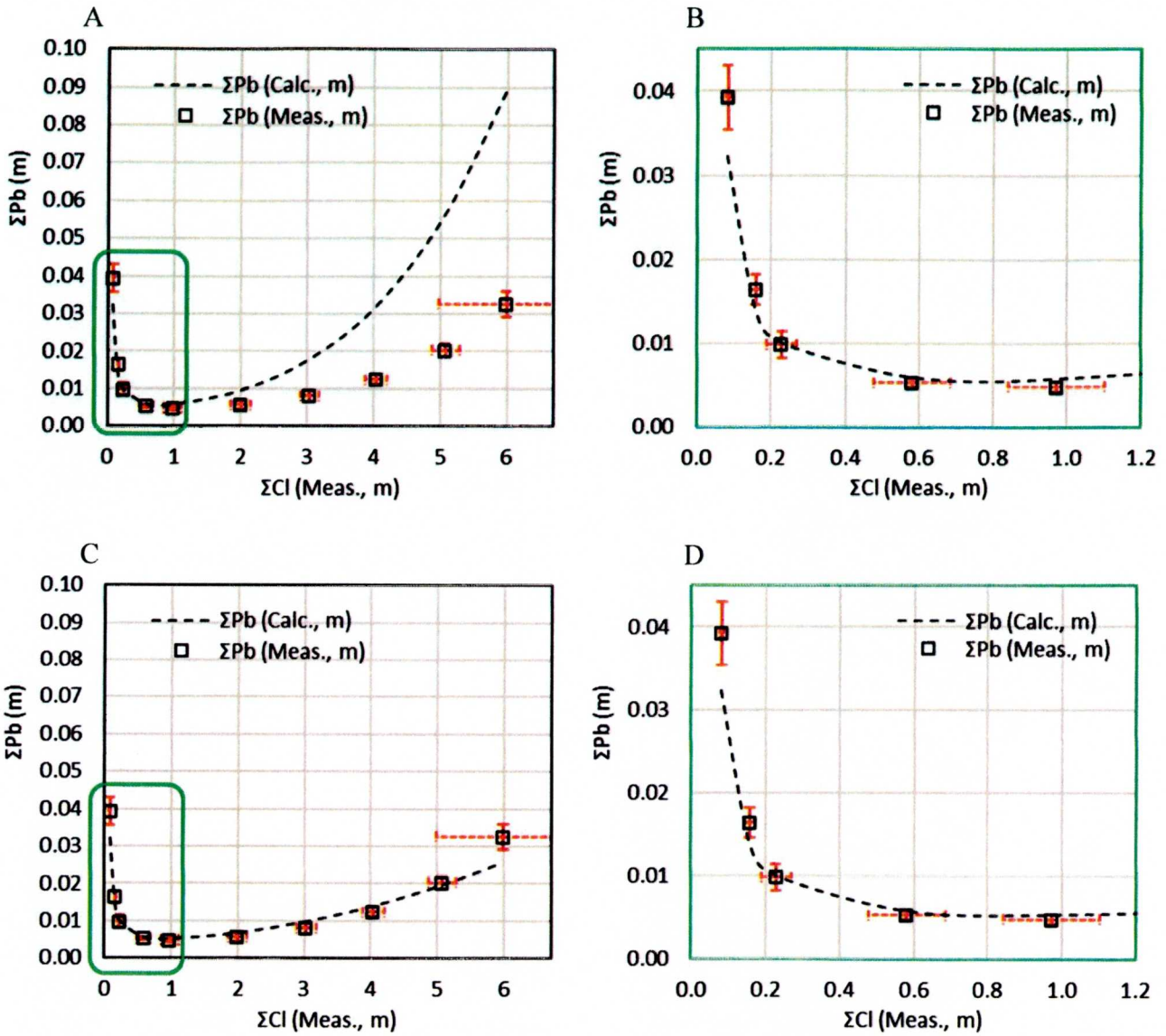

V.4.8. Summary

Table V.4-11. Recommended new addition to data0.fm1.

i	j	α_1/α_2[A]	$\beta^{(0)}$	$\beta^{(1)}$	$\beta^{(2)}$	C^{φ}	Source
Mg^{+2}	$PbCl_3^-$	2.0/12.0	0.23015	0.0	0.0	0.0	This section

[A] α_1 and α_2 are pre-set constants used in the Pitzer activity coefficient equation. α_1 and α_2 apply for only cation-anion binary pair. α_2 is only used for 2:2 electrolytes and multivalent ions. α_2 is not applied when $\beta^{(2)}$ is zero or not used. The unit for α_1 and α_2 is $kg^{1/2} \cdot mol^{-1/2}$.

VI. MAGNESIUM (Mg)

VI.1. $MgOxalate.2H_2O(s)$ - $Na_2Oxalate$ - H_2O

This section contains a refinement of the analysis presented in Jang (2020b).

VI.1.1. Chemical System

Excess $MgOxalate.2H_2O(s)$ (glushinskite) was added to solutions of incrementally higher concentrations of $Na_2Oxalate$.

VI.1.2. Goals and Hypotheses

The goal is to accurately model how the common-ion effect impacts the solubility of $MgOxalate.2H_2O(s)$, the common-ion being $Oxalate^{-2}$.

VI.1.3. Reactor Preparation

1.0 gram of $MgOxalate.2H_2O(s)$ was added to solutions of $Na_2Oxalate$ prepared by the recipes in Table VI.1-1. Preparation of the reactors was conducted in a N_2-filled glovbox to prevent possible interference of $CO_2(g)$. Serum bottles with rubber seals and aluminum crimps were used to preserve the reactor. Sampling, pHr recording, and dilution were conducted in the glovebox.

Table VI.1-1. Recipe and calculated solution properties.

Reactor ID	$Na_2Oxalate$, gram	DI, mL	Oxalate, m	Na, m	$MgOxalate.2H_2O$, gram	
MgOxNa2Ox-1	0.0000	50.0	0.0000	0.0000	1.0000	
MgOxNa2Ox-2	0.0067	50.0	0.0010	0.0020	1.0041	
MgOxNa2Ox-3	0.0670	50.0	0.0100	0.0201	1.0051	
MgOxNa2Ox-4	0.1340	50.0	0.0201	0.0401	1.0010	
MgOxNa2Ox-5	0.2010	50.0	0.0301	0.0602	1.0043	
MgOxNa2Ox-6	0.2680	50.0	0.0401	0.0802	1.0026	
MgOxNa2Ox-7	0.3350	50.0	0.0502	0.1003	1.0022	
MgOxNa2Ox-8	0.6700	50.0	0.1003	0.2006	1.0000	
MgOxNa2Ox-9	1.3400	50.0	0.2006	0.4012	1.0000	
MgOxNa2Ox-10	2.1440	50.0	0.3210	0.6419	1.0029	
Solution properties	pH	Density, g/mL	M:m, L/kg	Na, M	Oxalate, M	I, M
MgOxNa2Ox-1	6.43	1.001	0.999	0.000	0.000	0.000
MgOxNa2Ox-2	7.59	1.001	0.999	0.002	0.001	0.003
MgOxNa2Ox-3	8.00	1.002	1.000	0.020	0.010	0.030
MgOxNa2Ox-4	8.11	1.003	1.000	0.040	0.020	0.060
MgOxNa2Ox-5	8.17	1.004	1.001	0.060	0.030	0.090
MgOxNa2Ox-6	8.21	1.004	1.001	0.080	0.040	0.120
MgOxNa2Ox-7	8.24	1.005	1.002	0.100	0.050	0.150
MgOxNa2Ox-8	8.34	1.010	1.004	0.200	0.100	0.301
MgOxNa2Ox-9	8.43	1.018	1.009	0.398	0.199	0.602
MgOxNa2Ox-10	8.49	1.028	1.015	0.633	0.316	0.960

958

959 VI.1.4. Data - Aqueous

960 VI.1.4.1. pHr

961 Time-dependent pHr is tabulated in Table VI.1-2, and displayed in Figure VI.1-1. The observed
962 scatter is within the maximum %2SD of 6% (Table VI.1-3). The change in pHr as a function of
963 ΣOxalate loading is shown in Figure VI.1-2.

964 **Table VI.1-2. Time-dependent measurements of pHr (DSP = Days Since Preparation, i.e.,**
965 **Aging time in days).**

MgOxNa2Ox-1		MgOxNa2Ox-2		MgOxNa2Ox-3		MgOxNa2Ox-4		MgOxNa2Ox-5	
DSP	pHr	DSP	pHr	DSP	pHr	DSP	pHr	DSP	pHr
211	8.163	211	8.156	211	8.223	211	8.280	211	8.363
239	8.569	239	8.441	239	8.172	239	8.223	239	8.291
820	8.598	820	8.648	820	8.289	820	8.347	820	8.382
MgOxNa2Ox-6		MgOxNa2Ox-7		MgOxNa2Ox-8		MgOxNa2Ox-9		MgOxNa2Ox-10	
DSP	pHr	DSP	pHr	DSP	pHr	DSP	pHr	DSP	pHr
211	8.371	211	8.405	211	8.474	211	8.507	211	8.536
239	8.320	239	8.325	239	8.397	239	8.455	239	8.489
820	8.382	820	8.368	820	8.402	820	8.510	820	8.530

966

967 **Figure VI.1-1. Time-dependent measurements of pHr.**

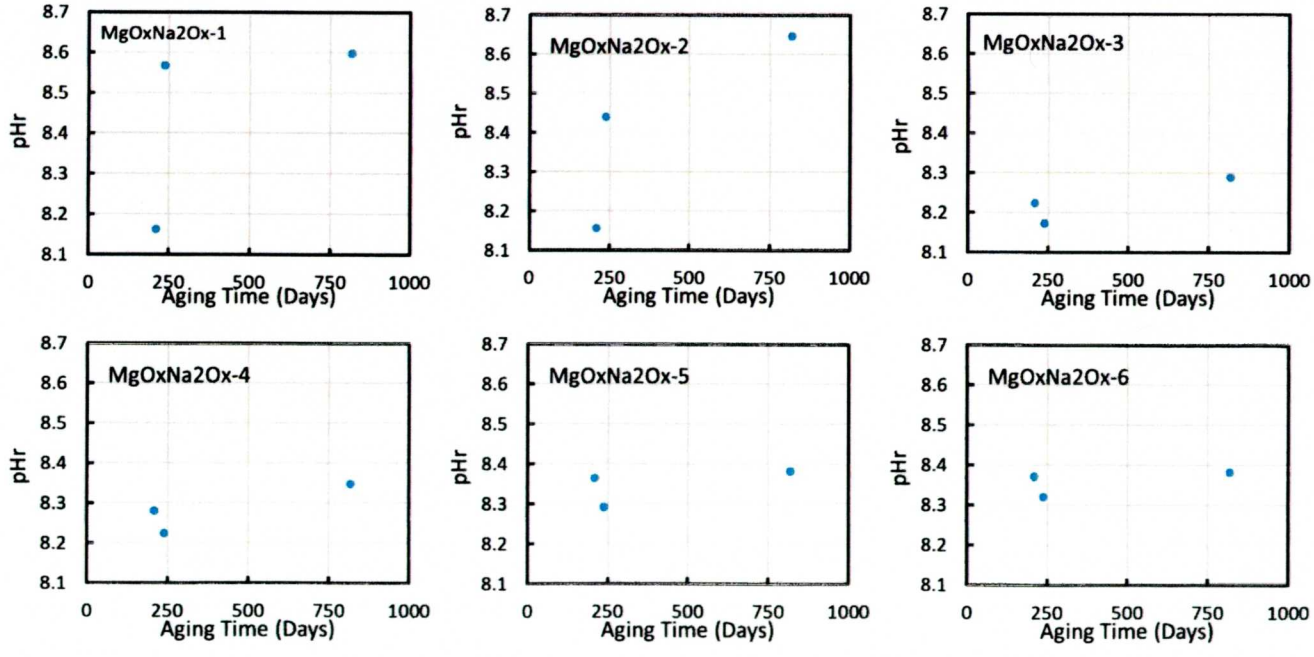

968

969

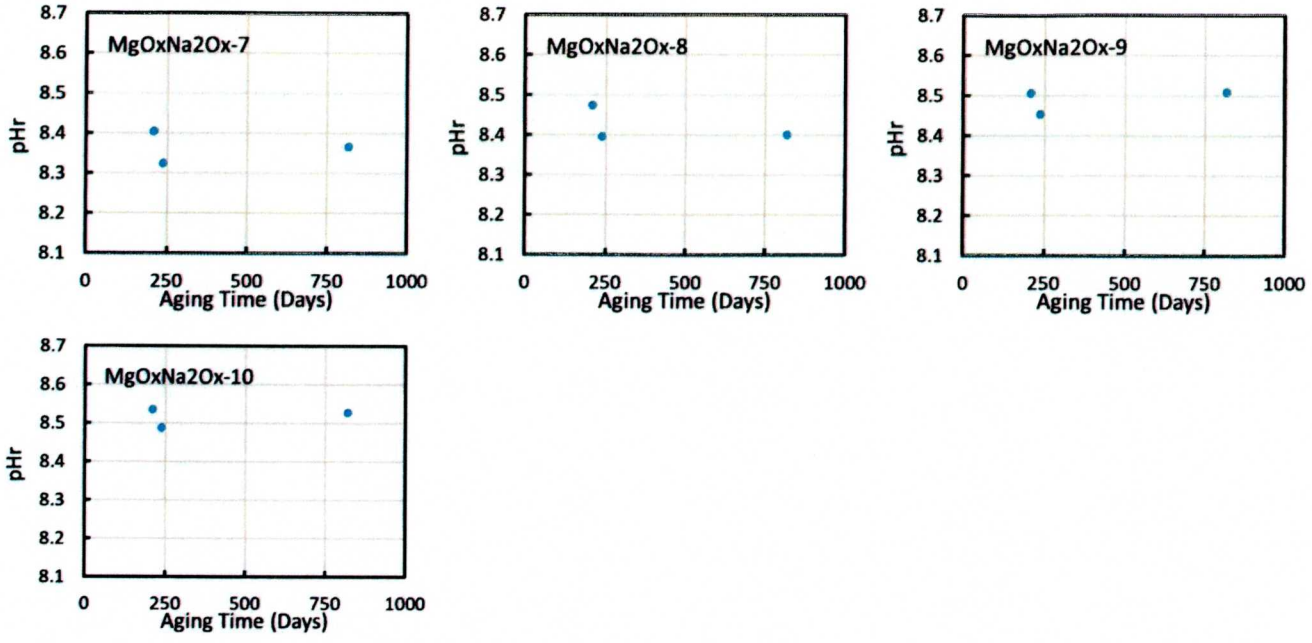

Table VI.1-3. Statistics of pHr measurements.

Reactor ID	Average	2SD	%2SD	Counts
MgOxNa2Ox-1	8.44	0.49	6%	3
MgOxNa2Ox-2	8.42	0.49	6%	3
MgOxNa2Ox-3	8.23	0.12	1%	3
MgOxNa2Ox-4	8.28	0.12	1%	3
MgOxNa2Ox-5	8.35	0.10	1%	3
MgOxNa2Ox-6	8.36	0.07	1%	3
MgOxNa2Ox-7	8.37	0.08	1%	3
MgOxNa2Ox-8	8.42	0.09	1%	3
MgOxNa2Ox-9	8.49	0.06	1%	3
MgOxNa2Ox-10	8.52	0.05	1%	3

Figure VI.1-2. Change of pHr as a function of Na_2Oxalate loading.

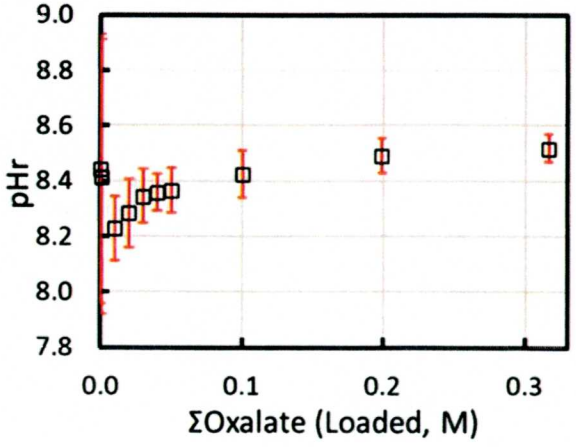

976 VI.1.4.2. ΣMg

977 The time-dependent measurement of ΣMg is shown in Table VI.1-4, and displayed in Figure VI.1-3.
978 The observed scatter is within the maximum %2SD of 16% (Table VI.1-5). Figure VI.1-4 shows
979 the change of ΣMg as a function of Na_2Oxalate loading.

980 Table VI.1-4. Time-dependent measurements of ΣMg in M (DSP = Days Since
981 Preparation, i.e., Aging time in days).

MgOxNa2Ox-1		MgOxNa2Ox-2		MgOxNa2Ox-3		MgOxNa2Ox-4		MgOxNa2Ox-5	
DSP	ΣMg	DSP	ΣMg	DSP	ΣMg	DSP	ΣMg	DSP	ΣMg
211	2.88E-03	211	2.38E-03	211	2.36E-03	211	2.68E-03	211	2.85E-03
239	2.78E-03	239	2.37E-03	239	2.46E-03	239	2.72E-03	239	3.11E-03
820	2.56E-03	820	2.21E-03	820	2.27E-03	820	2.67E-03	820	2.92E-03
MgOxNa2Ox-6		MgOxNa2Ox-7		MgOxNa2Ox-8		MgOxNa2Ox-9		MgOxNa2Ox-10	
DSP	ΣMg	DSP	ΣMg	DSP	ΣMg	DSP	ΣMg	DSP	ΣMg
211	3.61E-03	211	3.55E-03	211	5.99E-03	211	1.16E-02	211	1.46E-02
239	3.47E-03	239	3.87E-03	239	6.29E-03	239	1.10E-02	239	1.71E-02
820	3.21E-03	820	3.41E-03	820	5.48E-03	820	1.05E-02	820	1.65E-02

982

983 Figure VI.1-3. Time-dependent measurements of ΣMg.

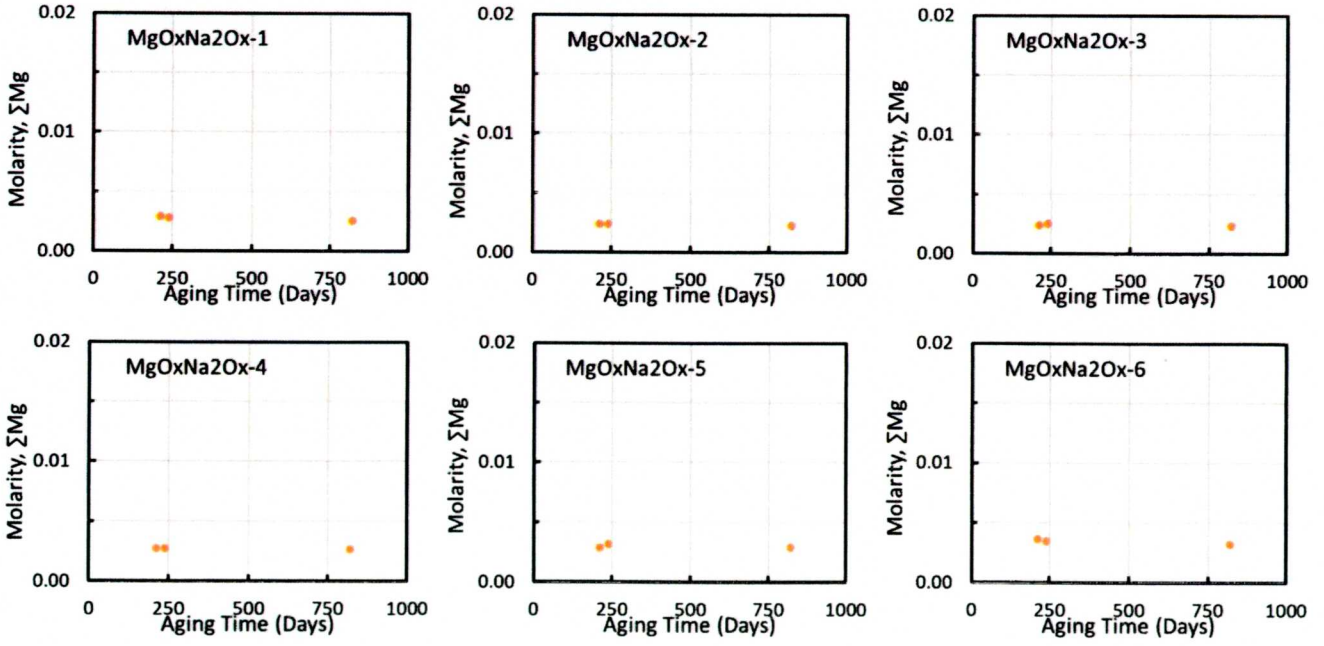

984

985

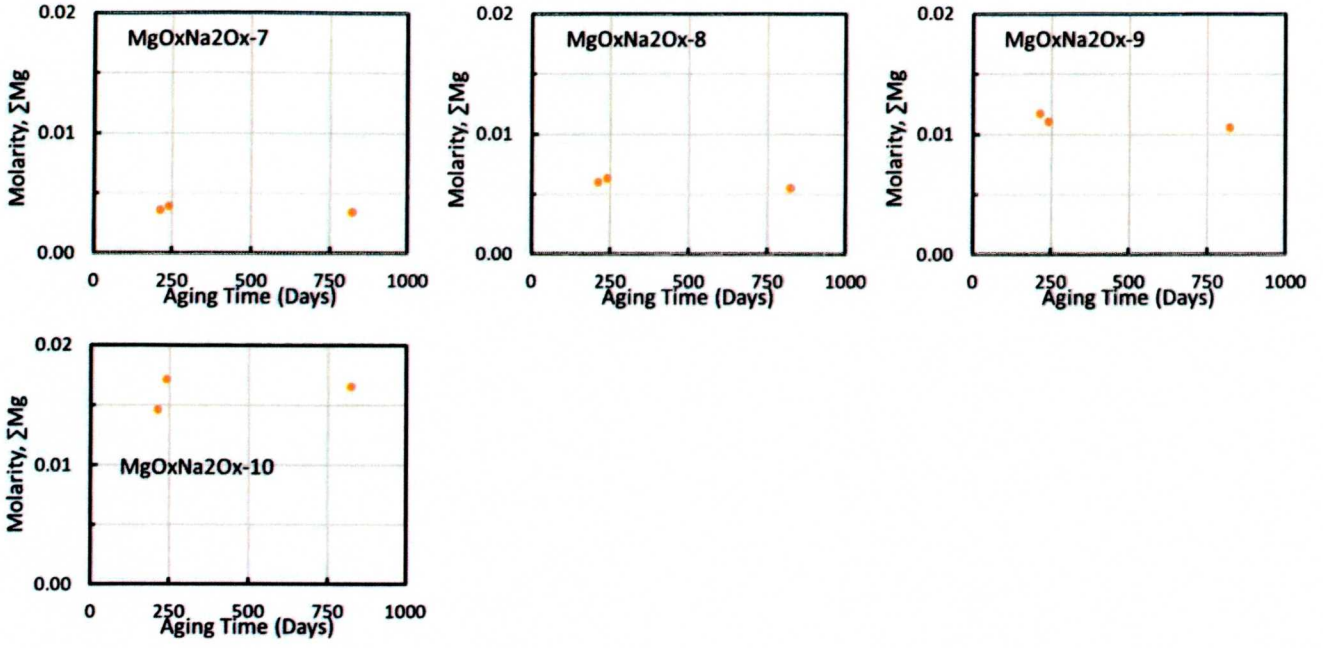

Table VI.1-5. Statistics of measured ΣMg in M.

Reactor ID	Average	2SD	%2SD	Counts
MgOxNa2Ox-1	2.74E-03	3.24E-04	12%	3
MgOxNa2Ox-2	2.32E-03	1.83E-04	8%	3
MgOxNa2Ox-3	2.36E-03	1.94E-04	8%	3
MgOxNa2Ox-4	2.69E-03	5.05E-05	2%	3
MgOxNa2Ox-5	2.96E-03	2.69E-04	9%	3
MgOxNa2Ox-6	3.43E-03	4.09E-04	12%	3
MgOxNa2Ox-7	3.61E-03	4.68E-04	13%	3
MgOxNa2Ox-8	5.92E-03	8.19E-04	14%	3
MgOxNa2Ox-9	1.10E-02	1.12E-03	10%	3
MgOxNa2Ox-10	1.61E-02	2.64E-03	16%	3

Figure VI.1-4. Change of ΣMg as a function of Na_2Oxalate loading. A. Whole range. B. Zoom-in of the area marked with green rectangle in A.

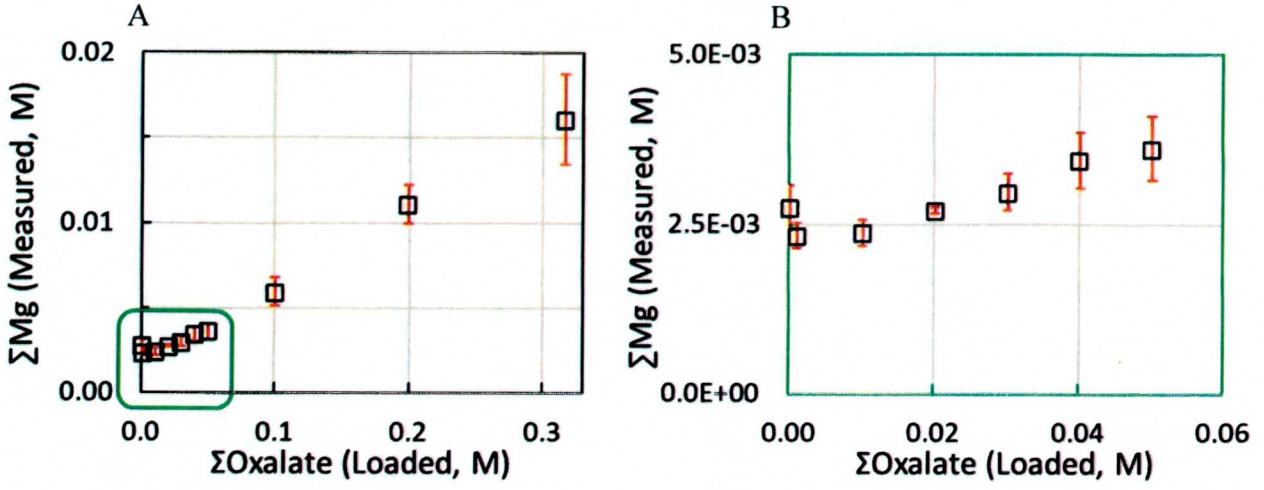

VI.1.4.3. ΣOxalate

Time-dependent measurements of ΣOxalate are tabulated in Table VI.1-6, and displayed in Figure VI.1-5. The observed scatter is within %2SD of 61%, except one (Table VI.1-7). Figure VI.1-6 demonstrates the accuracy and precision of ΣOxalate. Dissolution of MgOxalate.$2H_2O$(s) significantly increased ΣOxalate above the loading of Oxalate when the loading was less than 0.01 M (Figure VI.1-6, C).

Table VI.1-6. Time-dependent ΣOxalate in M (DSP = Days Since Preparation, i.e., Aging time in days).

MgOxNa2Ox-1		MgOxNa2Ox-2		MgOxNa2Ox-3		MgOxNa2Ox-4		MgOxNa2Ox-5	
DSP	ΣOxalate	DSP	ΣOxalate	DSP	ΣOxalate	DSP	ΣOxalate	DSP	ΣOxalate
820	BD	211	3.95E-03	211	6.19E-03	211	2.28E-02	211	3.35E-02
1066	6.52E-03	211	1.64E-03	211	9.39E-03	239	2.17E-02	239	3.16E-02
1066	6.56E-03	239	1.56E-03	211	1.45E-02	820	2.01E-02	820	3.05E-02
1066	6.64E-03	239	4.09E-03	239	8.91E-03				
1066	3.96E-03	820	1.57E-03	239	1.31E-02				
1066	3.93E-03			239	1.38E-02				
1066	3.97E-03			820	8.78E-03				
1066	7.20E-03								
1066	7.09E-03								
1066	7.19E-03								
1066	3.67E-03								
1066	3.67E-03								
1066	3.66E-03								
MgOxNa2Ox-6		MgOxNa2Ox-7		MgOxNa2Ox-8		MgOxNa2Ox-9		MgOxNa2Ox-10	
DSP	ΣOxalate	DSP	ΣOxalate	DSP	ΣOxalate	DSP	ΣOxalate	DSP	ΣOxalate
211	4.45E-02	211	5.15E-02	211	1.07E-01	211	2.00E-01	211	2.84E-01

239	4.06E-02	239	5.22E-02	239	9.95E-02	239	2.65E-01	239	1.92E-01
820	4.11E-02	820	5.23E-02	820	1.03E-01	820	2.11E-01	820	2.95E-01

Red fonts: Flagged by lab, not used in calculating the statistics.

Figure VI.1-5. Time-dependent ΣOxalate. The blue x on the vertical axis is the loading of $Na_2Oxalate$.

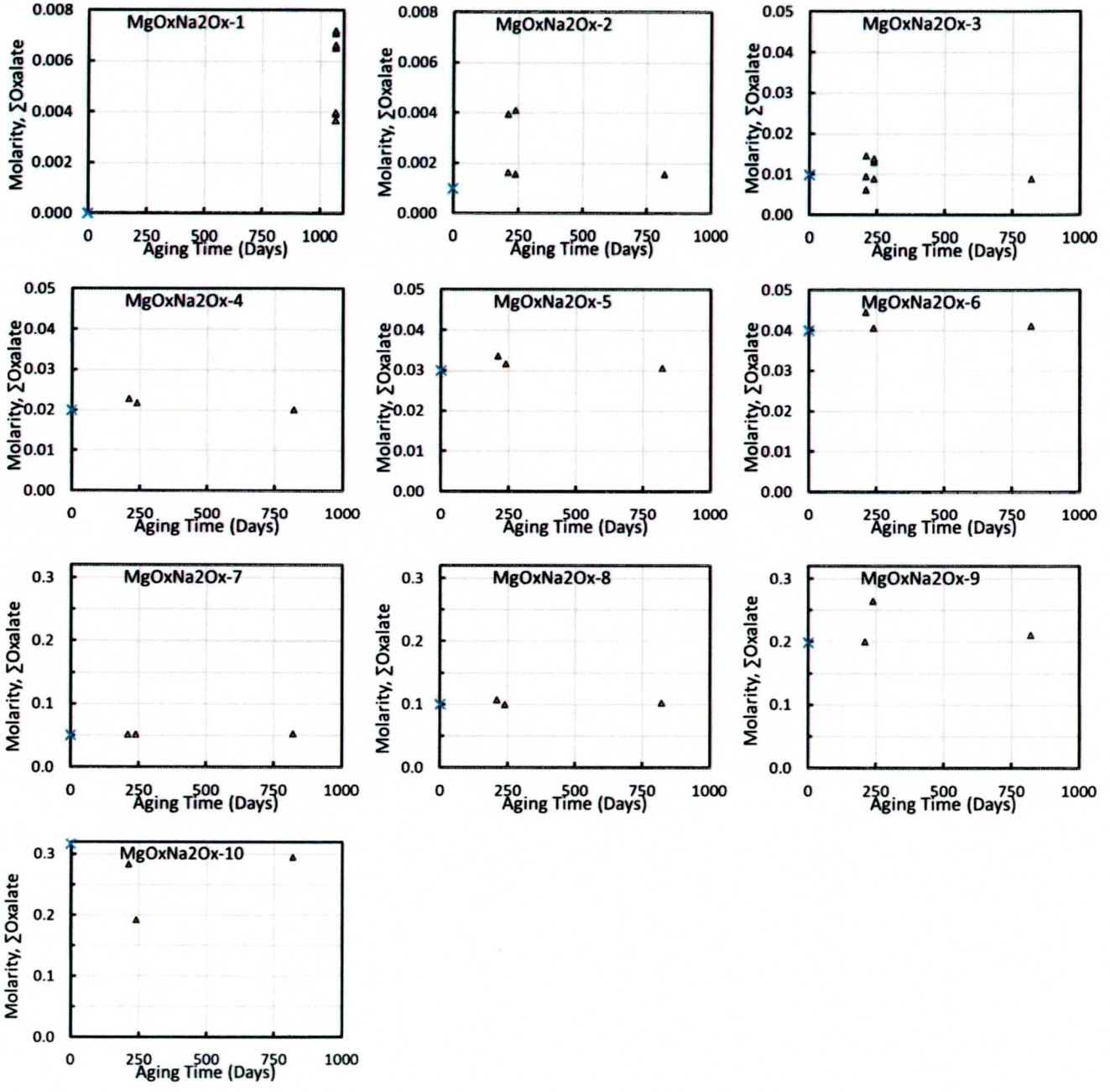

Table VI.1-7. Statistics of measurements of ΣOxalate in M.

Reactor ID	Average	2SD	%2SD	%Deviation	Counts
MgOxNa2Ox-1	*5.34E-03*	*3.23E-03*	*61%*	*NA*	*12*
MgOxNa2Ox-2	2.56E-03	2.67E-03	104%	155%	5
MgOxNa2Ox-3	9.27E-03	4.95E-03	53%	-8%	5

MgOxNa2Ox-4	2.15E-02	2.78E-03	13%	7%	3
MgOxNa2Ox-5	3.19E-02	3.08E-03	10%	6%	3
MgOxNa2Ox-6	4.21E-02	4.26E-03	10%	5%	3
MgOxNa2Ox-7	5.20E-02	8.82E-04	2%	4%	3
MgOxNa2Ox-8	1.03E-01	8.08E-03	8%	3%	3
MgOxNa2Ox-9	2.25E-01	6.93E-02	31%	13%	3
MgOxNa2Ox-10	2.57E-01	1.13E-01	44%	-19%	3

Italic: dissolution of MgOxalate.2H_2O(s) resulted in non-zero ΣOxalate.

Figure VI.1-6. Accuracy and precision of ΣOxalate measurements as a function of Na_2Oxalate loading. A. Whole range. B. Zoom-in view of the area marked with the green rectangle in A. C. Dissolution of MgOxalate.2H_2O(s) significantly increased the ΣOxalate at the lower loadings of Na_2Oxalate. Blue dashed lines in A and B are lines of slope = 1. Blue dashed line in C represents %Deviation = 0.

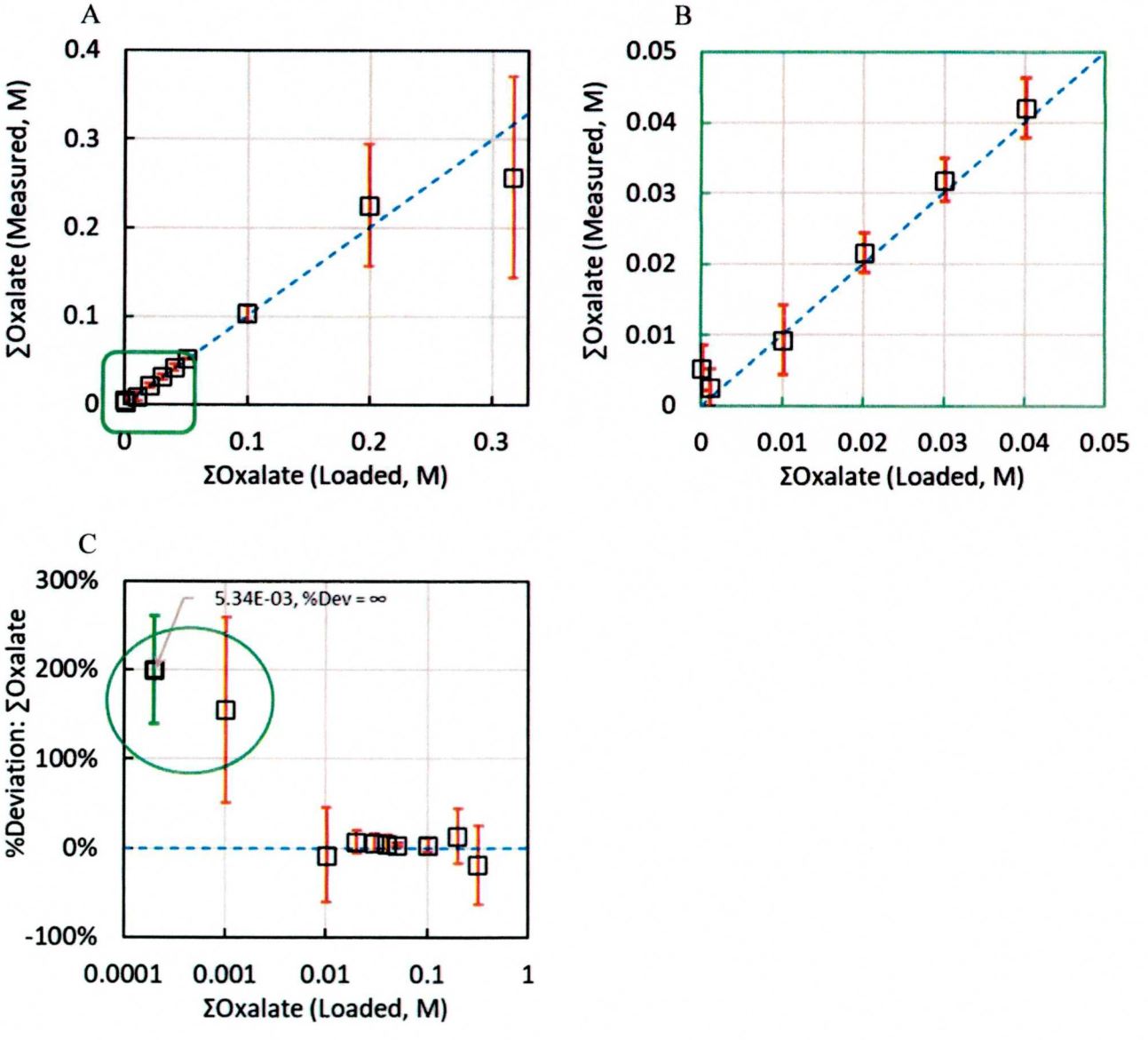

1021 VI.1.4.4. ΣNa

1022 Time-dependent measurements of ΣNa are tabulated in Table VI.1-8, and displayed in Figure
1023 VI.1-7. The observed scatters are significant, indicating that the ΣNa measurements were affected
1024 by the low precision of the instrument, ICP-AES (Table VI.1-9); the instrument detected ΣNa even
1025 from the sample where no Na was added. Figure VI.1-8 displays the data quality of ΣNa
1026 measurements.

1027 **Table VI.1-8. Time-dependent ΣNa in M (DSP = Days Since Preparation, i.e., Aging time**
1028 **in days).**

MgOxNa2Ox-1		MgOxNa2Ox-2		MgOxNa2Ox-3		MgOxNa2Ox-4		MgOxNa2Ox-5	
DSP	ΣNa	DSP	ΣNa	DSP	ΣNa	DSP	ΣNa	DSP	ΣNa
211	1.81E-04	211	4.13E-03	211	1.12E-02	211	1.18E-01	211	1.34E-01
239	1.77E-04	239	4.11E-03	239	1.92E-02	239	4.05E-02	239	5.87E-02
820	1.31E-01	820	1.36E-01	820	1.44E-01	820	1.58E-01	820	1.74E-01
820	1.32E-02	820	1.51E-02	820	2.91E-02	820	4.13E-02	820	5.61E-02
820	1.25E-03	820	3.99E-03						
MgOxNa2Ox-6		MgOxNa2Ox-7		MgOxNa2Ox-8		MgOxNa2Ox-9		MgOxNa2Ox-10	
DSP	ΣNa	DSP	ΣNa	DSP	ΣNa	DSP	ΣNa	DSP	ΣNa
211	1.47E-01	211	1.73E-01	211	2.46E-01	211	4.72E-01	211	5.39E-01
239	7.68E-02	239	9.53E-02	239	2.43E-01	239	4.13E-01	239	5.57E-01
820	1.96E-01	820	2.03E-01	820	2.88E-01	820	4.36E-01	820	5.56E-01
820	7.62E-02	820	8.73E-02	820	1.69E-01	820	3.31E-01	820	4.92E-01

1029 Red fonts: Flagged by lab, not used in calculating the statistics.

1030

Figure VI.1-7. Time-dependent measurements of ΣNa. The pink rectangles mark the data flagged by the lab and not used in calculating the statistics. The orange x on the vertical axis is the initial loading of ΣNa.

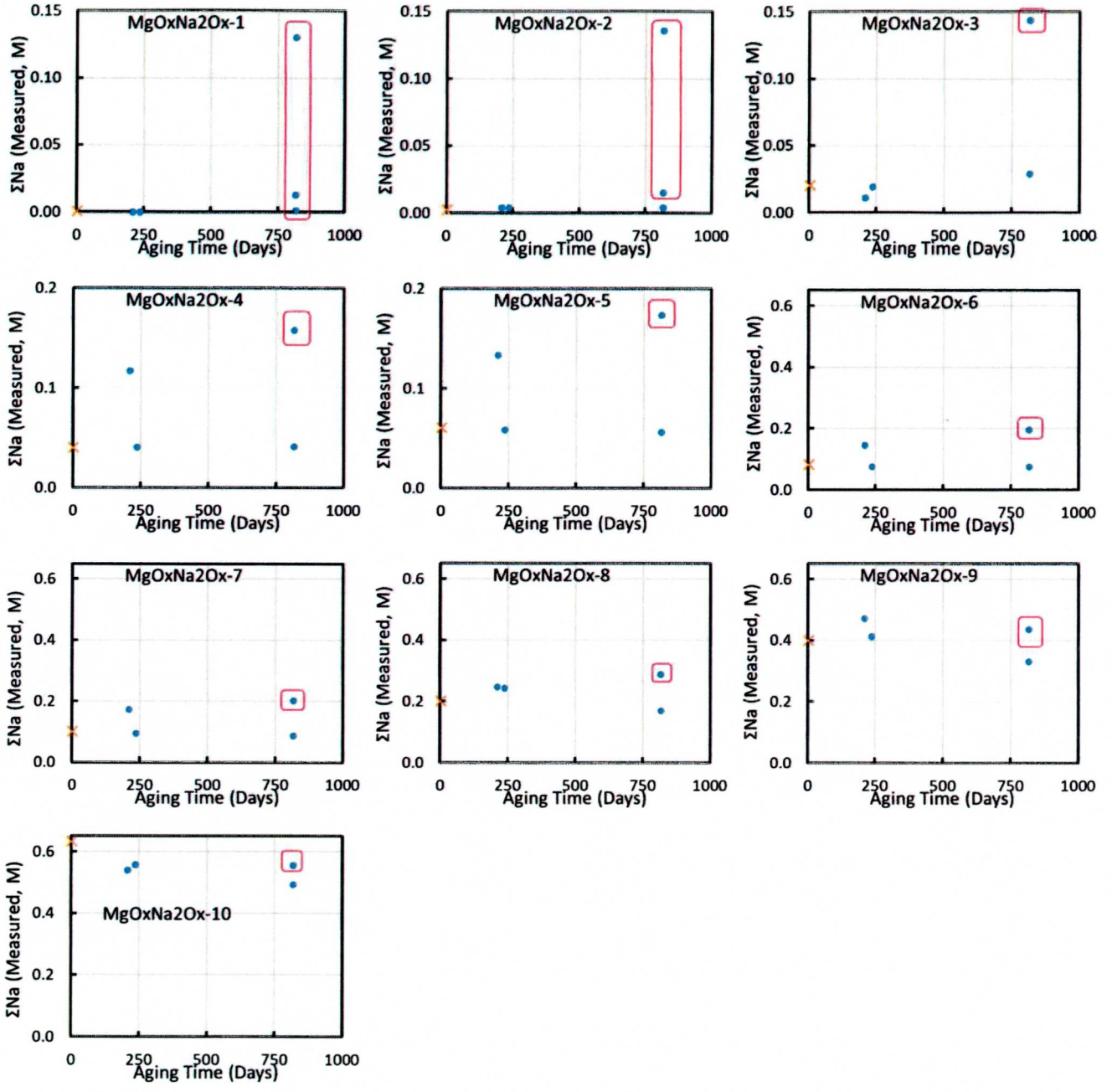

Table VI.1-9. Statistics of ΣNa measurements (M).

Reactor ID	Average	2SD	%2SD	%Deviation	Counts
MgOxNa2Ox-1	*1.79E-04*	5.91E-06	3%	∞	*2*
MgOxNa2Ox-2	4.08E-03	1.49E-04	4%	103%	3
MgOxNa2Ox-3	1.98E-02	1.79E-02	90%	-1%	3
MgOxNa2Ox-4	6.65E-02	8.87E-02	133%	66%	3
MgOxNa2Ox-5	8.29E-02	8.82E-02	106%	38%	3

MgOxNa2Ox-6	9.99E-02	8.12E-02	81%	25%	3
MgOxNa2Ox-7	1.18E-01	9.45E-02	80%	18%	3
MgOxNa2Ox-8	2.20E-01	8.69E-02	40%	10%	3
MgOxNa2Ox-9	4.05E-01	1.41E-01	35%	2%	3
MgOxNa2Ox-10	5.29E-01	6.72E-02	13%	-16%	3

Italic: Considering the loading of Na_2Oxalate = 0 for MgOxNa_2Ox-1, this number may be close to the low detection limit of our ICP-AES for Na.

Figure VI.1-8. Accuracy and precision of ΣNa measurements as a function of Na_2Oxalate loading.

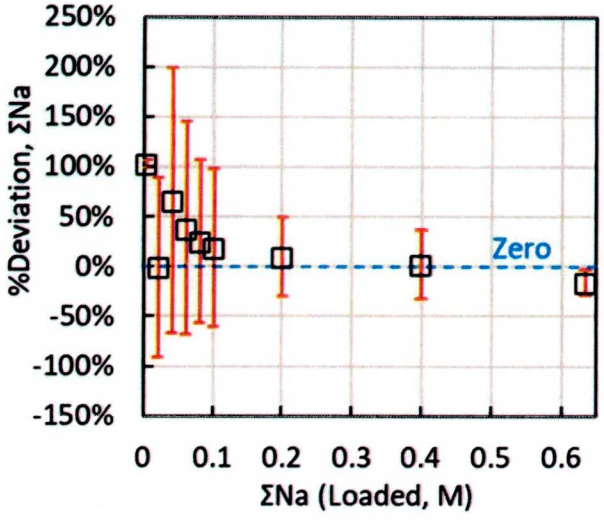

VI.1.5. Data - Solids

The solids collected at the end of experiments were examined by XRD (Figure VI.1-9). Growths of a few minor peaks were noticed from the experiments conducted at higher Na_2Oxalate loadings (MgOxNa_2Ox-(4~10), i.e., peaks surrounded by blue dashed rectangles in Figure VI.1-9).

Figure VI.1-9. XRD scans for the solids collected at the end of the experiments. Growth of a few minor peaks were noticed and marked with blue dashed rectangles.

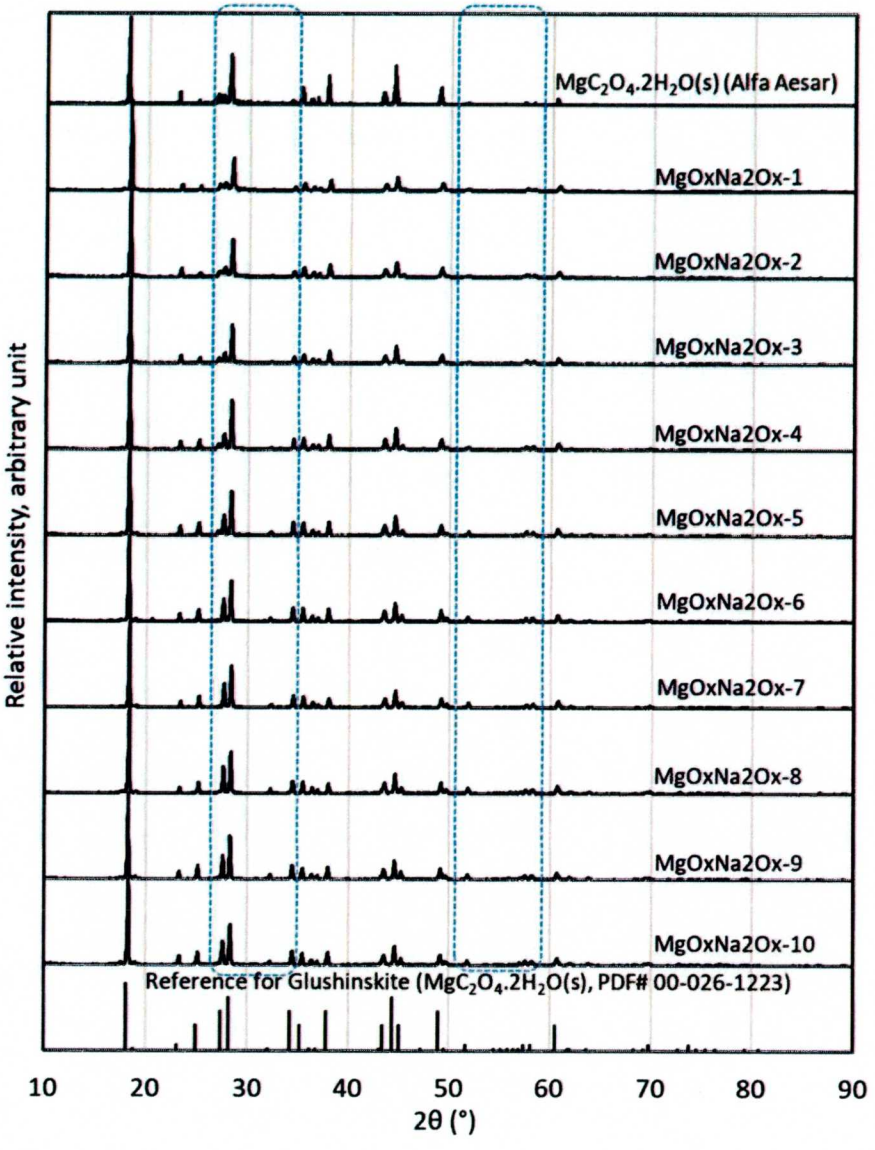

VI.1.6. Observations

The common-ion effect of $Oxalate^{-2}$ on the solubility of $MgOxalate.2H_2O(s)$ is seen in the data. In Figure VI.1-4, a slight depression of ΣMg was observed, followed by an increase. The increase indicates that additional species to those in data0.fm1 may be required to model the observation.

Although an increase of crystallinity, i.e., growth of a few minor peaks, was observed from the XRD scans (Figure VI.1-9), the curvature of solubility in Figure VI.1-4 is smooth without inflection point(s) that could indicate the change of solubility-limiting solid.

VI.1.7. Model Parameterization: Pitzer Approach

The concentrations were converted to molality (Table VI.1-10). To describe the increase of ΣMg at the $Na_2Oxalate$ loading ≥ 0.02 M, a new species $Mg(Oxalate)_2^{-2}$ and its log K were imported from Martell and Smith (1977) (Table VI.1-11). The solubility constant for $MgOxalate.2H_2O(s)$ was imported from Hummel et al. (2005) as an initial guess (Table VI.1-11). When the model parameters in Table VI.1-11 were applied to calculate the solubility, overestimation was observed (Figure VI.1-10; A and B). The overestimation exceeded the uncertainties associated with ΣMg over the entire range. A downward shift of the solubility line can be achieved by adjusting the log K to smaller (i.e., more negative to make the solid less soluble). When the log K is fitted to -6.49, the model calculation described the observation within the uncertainty (Figure VI.1-10; C and D). The fitted log K = -6.49 is within the uncertainty of Hummel et al. (2005), -6.4 ± 0.2.

Table VI.1-10. Concentrations in molality (m, mol/kg).

Reactor ID	ΣOxalate			ΣMg		
	Average	2SD	%2SD	Average	2SD	%2SD
MgOxNa2Ox-1	5.33E-03	3.23E-03	61%	2.74E-03	3.24E-04	12%
MgOxNa2Ox-2	2.56E-03	2.67E-03	104%	2.32E-03	1.83E-04	8%
MgOxNa2Ox-3	9.27E-03	4.95E-03	53%	2.36E-03	1.94E-04	8%
MgOxNa2Ox-4	2.15E-02	2.78E-03	13%	2.69E-03	5.05E-05	2%
MgOxNa2Ox-5	3.19E-02	3.09E-03	10%	2.96E-03	2.69E-04	9%
MgOxNa2Ox-6	4.21E-02	4.26E-03	10%	3.43E-03	4.09E-04	12%
MgOxNa2Ox-7	5.21E-02	8.83E-04	2%	3.62E-03	4.69E-04	13%
MgOxNa2Ox-8	1.04E-01	8.12E-03	8%	5.94E-03	8.22E-04	14%
MgOxNa2Ox-9	2.27E-01	6.99E-02	31%	1.11E-02	1.13E-03	10%
MgOxNa2Ox-10	2.61E-01	1.15E-01	44%	1.63E-02	2.68E-03	16%
Reactor ID	ΣNa			pmH		
	Average	2SD	%2SD	Average	2SD	%2SD
MgOxNa2Ox-1	5.36E-04	1.24E-03	231%	8.34	0.48	6%
MgOxNa2Ox-2	4.07E-03	1.49E-04	4%	8.31	0.49	6%
MgOxNa2Ox-3	1.98E-02	1.79E-02	90%	8.13	0.12	1%
MgOxNa2Ox-4	6.65E-02	8.87E-02	133%	8.19	0.12	1%
MgOxNa2Ox-5	8.29E-02	8.82E-02	106%	8.26	0.09	1%
MgOxNa2Ox-6	1.00E-01	8.13E-02	81%	8.27	0.07	1%
MgOxNa2Ox-7	1.19E-01	9.46E-02	80%	8.29	0.08	1%
MgOxNa2Ox-8	2.20E-01	8.73E-02	40%	8.37	0.09	1%
MgOxNa2Ox-9	4.09E-01	1.42E-01	35%	8.49	0.06	1%
MgOxNa2Ox-10	5.37E-01	6.82E-02	13%	8.59	0.05	1%

Table VI.1-11. Reactions and their Log Ks.

Reaction	LogK	Reference
Aqueous reactions		
$Mg(Oxalate)_2^{-2} = Mg^{+2} + 2Oxalate^{-2}$	-4.94	Martell and Smith (1977) [B]
Dissolution		
$MgOxalate.2H_2O(s)$ (Glushinskite) $= Mg^{+2} + Oxalate^{-2} + 2H_2O$	-6.4±0.2	Hummel et al. (2005)
	-6.49	This section

[A] $Oxalate^{-2} = C_2O_4^{-2}$ (88.0 g/mol).

[B] Listed in Martell and Smith (1977) is log ^cK = -4.24 at I = 0.1, where ^cK is a conditional equilibrium constant expressed as a quotient of concentrations. The value in Table above is an extrapolation of log ^cK = -4.24 to zero ionic strength using Davies activity coefficient equation provided in Stumm and Morgan (1996).

Figure VI.1-10. A and B: Before fitting the log K (Residual = 0.084). C and D: After fitting the log K (Residual = 0.003). B and D are magnifications of the areas marked with green rectangles in A and C, respectively.

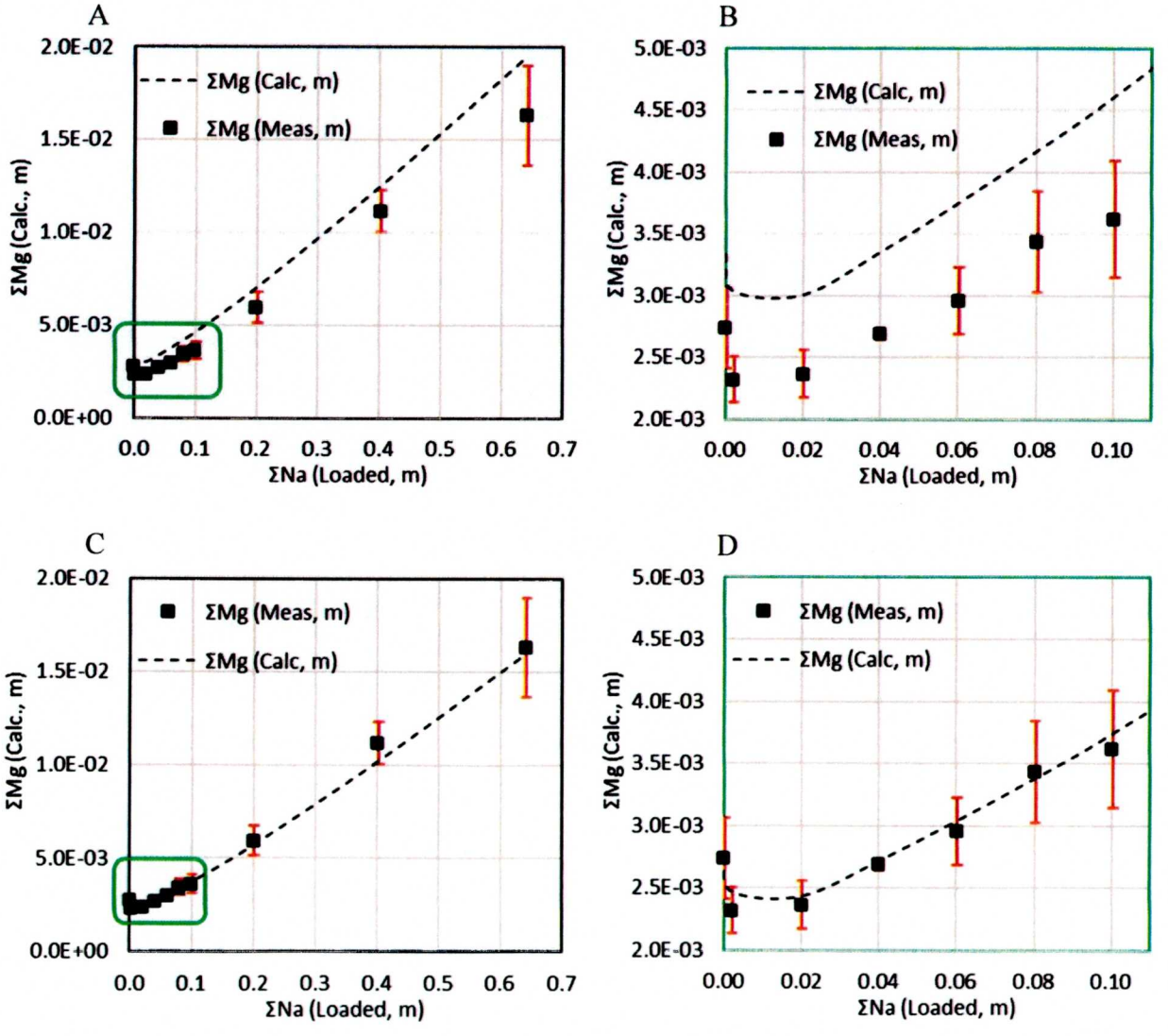

VI.1.8. Summary

One of the reasons Hummel et al. (2005) assigned a relatively large uncertainty to their log K was that the references they reviewed did not address slow kinetics of solubility equilibrium of MgOxalate.$2H_2O$(s). We aged our experiments for more than 800 days to make our data inclusive for the slow kinetics of the solubility equilibrium. The observed increase in crystallinity corroborates the derived log K, which is more negative than the value suggested by Hummel et al. (2005).

Table VI.1-12. Recommended new addition to data0.fm1.

Reaction	Log K	Source
$Mg(Oxalate)_2^{-2} = Mg^{+2} + 2Oxalate^{-2}$	-4.94	Martell and Smith (1977)
$MgOxalate.2H_2O(s)$ (Glushinskite) $= Mg^{+2} + Oxalate^{-2} + 2H_2O$	-6.49	This section

VII. NEODYMIUM (Nd)

VII.1. $Nd(OH)_3(s)$ - $MgCl_2$ - H_2O

VII.1.1. Chemical System

Excess $Nd(OH)_3(s)$ was added to $MgCl_2$ solutions. The five components of this system are Nd^{+3}, Mg^{+2}, Cl^-, H^+, and H_2O.

VII.1.2. Goals and Hypotheses

The goal was to test if our current model accurately predicts the solubility of $Nd(OH)_3(s)$ as a function of $MgCl_2$.

VII.1.3. Reactor Preparation

0.36 grams of $Nd(OH)_3(s)$ was mixed with $MgCl_2$ solutions prepared by the recipes in Table VII.1-1. The experiments were prepared and conducted in $CO_2(g)$-minimal glovebox.

Table VII.1-1. Recipe and calculated solution properties.

Reactor ID	$MgCl_2.6H_2O$, g	DI, g	Hyd. H_2O	H_2O.Total	$MgCl_2$, m	$MgCl_2$, M
Nd(OH)3-0.01 Mg-(1,2)	1.0705	500.01	0.57	500.58	0.0105	1.05E-02
Nd(OH)3-0.1 Mg-(1,2)	10.1675	500.00	5.40	505.40	0.0990	9.87E-02
Nd(OH)3-1.0 Mg-(1,2)	101.65	504.60	54.00	558.60	0.895	8.69E-01
Nd(OH)3-1.5 Mg-(1,2)	152.47	500.00	81.00	581.00	1.29	1.24E+00
Nd(OH)3-2.0 Mg-(1,2)	203.33	500.01	108.02	608.03	1.64	1.56E+00
Nd(OH)3-2.5 Mg-(1,2)	254.12	500.00	135.00	635.00	1.97	1.85E+00
Reactor ID	M:m, L/kg	Density g/mL	Density meas.	%Dev	pH	M:m, L/kg
Nd(OH)3-0.01 Mg-(1,2)	0.9994	1.002	1.001	0%	6.80	0.9994
Nd(OH)3-0.1 Mg-(1,2)	1.0024	1.007	1.006	0%	6.75	1.0024
Nd(OH)3-1.0 Mg-(1,2)	1.0297	1.054	1.065	1%	6.29	1.0297

Nd(OH)3-1.5 Mg-(1,2)	1.0432	1.076	1.099	2%	6.08	1.0432
Nd(OH)3-2.0 Mg-(1,2)	1.0554	1.096	1.115	2%	5.90	1.0554
Nd(OH)3-2.5 Mg-(1,2)	1.0664	1.113	1.138	2%	5.74	1.0664

1106

1107 VII.1.4. Data - Aqueous

1108 VII.1.4.1. pHr

1109 Time-dependent pHr is tabulated in Table VII.1-2, and displayed in Figure VII.1-1. The observed
1110 scatter is within the maximum %2SD of 3% (Table VII.1-3). Figure VII.1-2 shows the change of
1111 pHr as a function of $MgCl_2$ loading.

1112 Table VII.1-2. Time-dependent measurements of pHr: Table 3-24 of Kirkes and Hora
1113 (2020).

pHr	DSP				
Reactor ID	671	986	1874	1972	2082
Nd(OH)3-0.01 Mg-1	8.88	9.02	8.95	8.94	8.90
Nd(OH)3-0.01 Mg-2	8.84	8.99	8.99	9.03	8.80
Nd(OH)3-0.1 Mg-1	8.71	8.81	8.88	8.93	8.81
Nd(OH)3-0.1 Mg-2	8.74	8.87	8.90	8.95	8.72
Nd(OH)3-1.0 Mg-1	7.99	8.13	8.15	8.22	7.98
Nd(OH)3-1.0 Mg-2	8.06	8.18	8.22	8.29	8.08
Nd(OH)3-1.5 Mg-1	7.75	7.89	7.94	7.94	7.85
Nd(OH)3-1.5 Mg-2	7.77	7.89	7.95	7.99	7.76
Nd(OH)3-2.0 Mg-1	7.54	7.68	7.75	7.80	7.59
Nd(OH)3-2.0 Mg-2	7.52	7.65	7.70	7.74	7.53
Nd(OH)3-2.5 Mg-1	7.35	7.49	7.58	7.57	7.45
Nd(OH)3-2.5 Mg-2	7.32	7.47	7.55	7.57	7.40

1114

Figure VII.1-1. Time-dependent pHr.

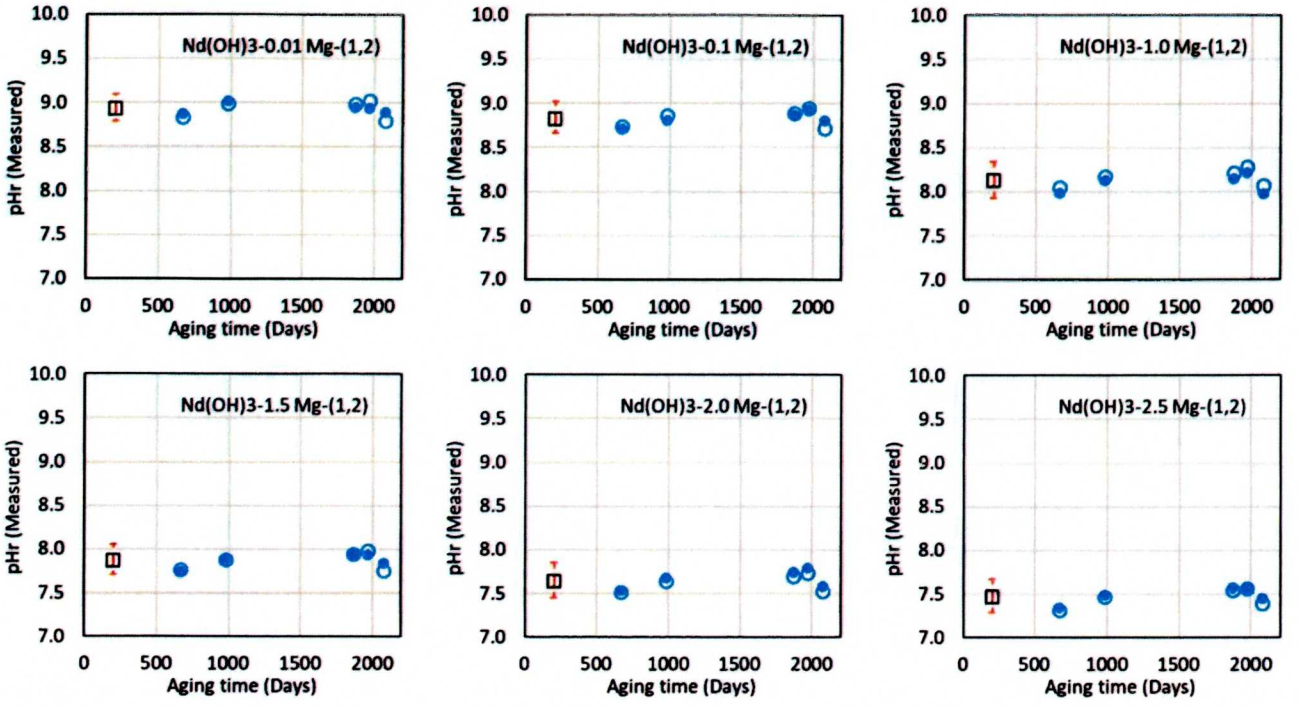

Table VII.1-3. Statistics of measurements of pHr.

Reactor ID	Average	2SD	%2SD	Count
Nd(OH)3-0.01 Mg-(1,2)	8.93	0.15	2%	10
Nd(OH)3-0.1 Mg-(1,2)	8.83	0.17	2%	10
Nd(OH)3-1.0 Mg-(1,2)	8.13	0.20	3%	10
Nd(OH)3-1.5 Mg-(1,2)	7.87	0.17	2%	10
Nd(OH)3-2.0 Mg-(1,2)	7.65	0.20	3%	10
Nd(OH)3-2.5 Mg-(1,2)	7.48	0.19	3%	10

Figure VII.1-2. Change of pHr as a function of $MgCl_2$ loading.

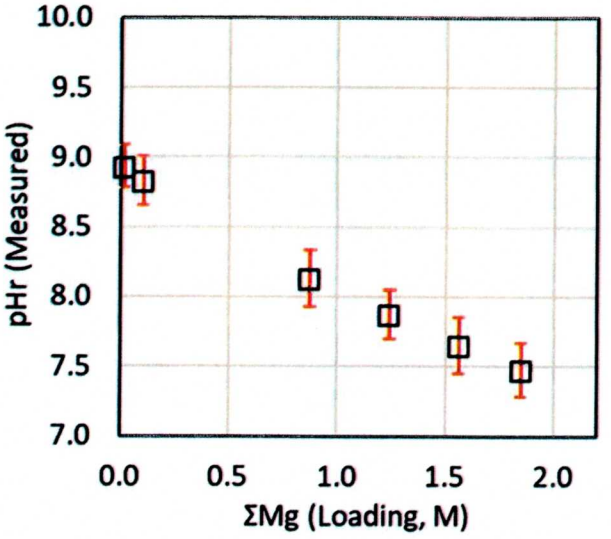

VII.1.4.2. ΣNd

Time-dependent measurements of ΣNd are tabulated in Table VII.1-4, and displayed in Figure VII.1-3. The data marked with green ovals in the first and fifth panels in Figure VII.1-3 are outliers based on the statistics in the upper half of Table VII.1-5 (open squares and red dashed error bars in Figure VII.1-3). In the lower half of Table VII.1-5, the once-reduced statistics excluding the data in green ovals are tabulated for the first and fifth panels of Figure VII.1-3 (solid squares and red error bars). The observed scatter is within a maximum 36% of %2SD, except the first two data points (Table VII.1-5). Figure VII.1-4 displays the change in ΣNd as a function of $MgCl_2$ loading. The first two data points marked with a red oval would not be used in model parameterization.

Table VII.1-4. Time-dependent measurements of ΣNd in M (DSP = Days Since Preparation, i.e., Aging time in days). Data from Kirkes and Hora (2020).

ΣNd, M	DSP			
Reactor ID	671	986	1874	1972
Nd(OH)3-0.01 Mg-1	1.92E-07	1.60E-08	2.87E-07	2.13E-07
Nd(OH)3-0.01 Mg-2	3.10E-08	4.67E-08	2.52E-07	2.75E-06
Nd(OH)3-0.1 Mg-1	2.82E-07	6.09E-08	3.78E-07	1.44E-07
Nd(OH)3-0.1 Mg-2	1.06E-07	5.77E-08	3.25E-07	6.80E-08
Nd(OH)3-1.0 Mg-1	3.79E-06	3.21E-06	4.05E-06	3.41E-06
Nd(OH)3-1.0 Mg-2	2.92E-06	2.61E-06	2.87E-06	2.43E-06
Nd(OH)3-1.5 Mg-1	8.96E-06	9.42E-06	8.83E-06	7.68E-06
Nd(OH)3-1.5 Mg-2	8.39E-06	8.04E-06	8.53E-06	7.34E-06
Nd(OH)3-2.0 Mg-1	1.71E-05	1.56E-05	1.81E-05	1.59E-05
Nd(OH)3-2.0 Mg-2	2.03E-05	3.52E-05	2.32E-05	1.95E-05
Nd(OH)3-2.5 Mg-1	2.89E-05	2.63E-05	2.82E-05	2.60E-05
Nd(OH)3-2.5 Mg-2	2.66E-05	2.91E-05	3.02E-05	2.69E-05

Red fonts: Valid data under SNL WIPP QA, however, can be considered outliers. Marked with green ovals in the Figure below.

1135 Figure VII.1-3. Time-dependent ΣNd: Table 3-25 in Kirkes and Hora (2020).

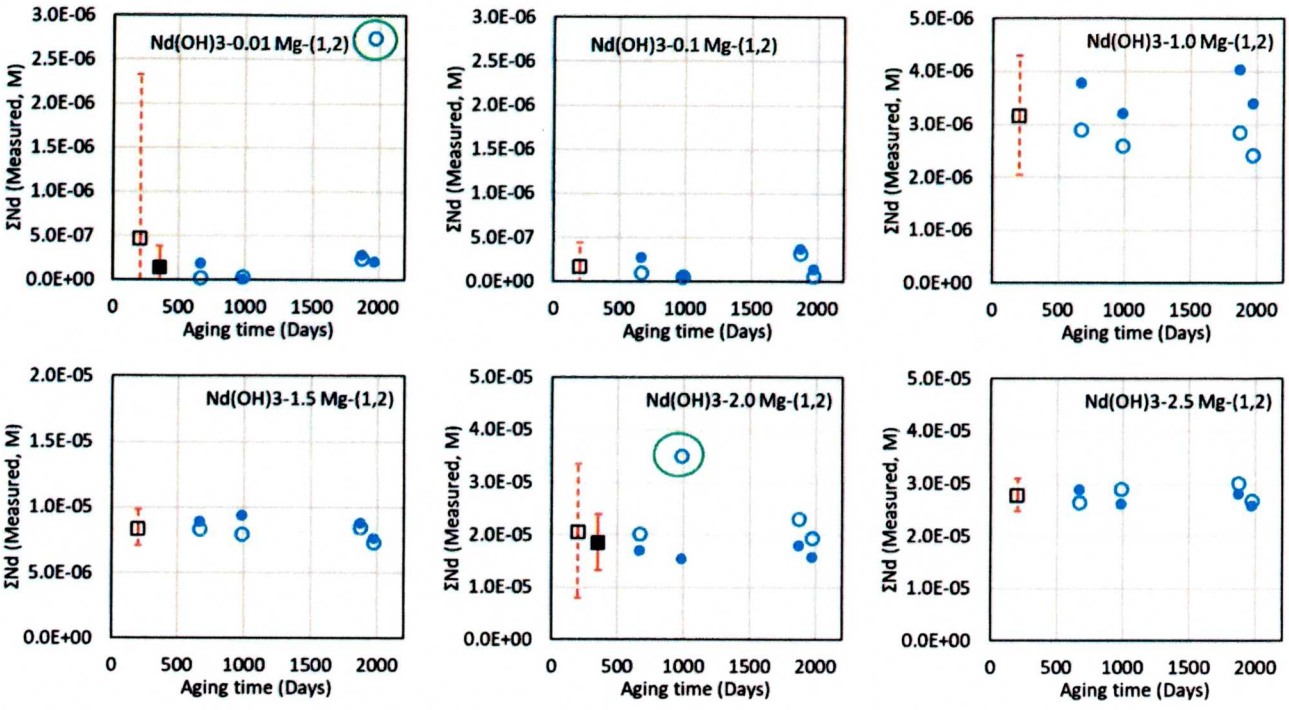

1136

1137

1138 Table VII.1-5. Statistics of measurements of ΣNd.

All valid measurements				
Reactor ID	Average	2SD	%2SD	Count
Nd(OH)3-0.01 Mg-(1,2)	4.73E-07	1.85E-06	391%	8
Nd(OH)3-0.1 Mg-(1,2)	1.78E-07	2.61E-07	147%	8
Nd(OH)3-1.0 Mg-(1,2)	3.16E-06	1.13E-06	36%	8
Nd(OH)3-1.5 Mg-(1,2)	8.40E-06	1.38E-06	16%	8
Nd(OH)3-2.0 Mg-(1,2)	2.06E-05	1.28E-05	62%	8
Nd(OH)3-2.5 Mg-(1,2)	2.78E-05	3.08E-06	11%	8
Reduced				
Reactor ID	Average	2SD	%2SD	Count
Nd(OH)3-0.01 Mg-(1,2)	1.48E-07	2.28E-07	154%	7
Nd(OH)3-0.1 Mg-(1,2)	*1.78E-07*	*2.61E-07*	*147%*	*8*
Nd(OH)3-1.0 Mg-(1,2)	*3.16E-06*	*1.13E-06*	*36%*	*8*
Nd(OH)3-1.5 Mg-(1,2)	*8.40E-06*	*1.38E-06*	*16%*	*8*
Nd(OH)3-2.0 Mg-(1,2)	1.85E-05	5.39E-06	29%	7
Nd(OH)3-2.5 Mg-(1,2)	*2.78E-05*	*3.08E-06*	*11%*	*8*

1139 Blue italic fonts mean that the statistics are kept the same as in the upper half of the Table.

Figure VII.1-4. ΣNd as a function of $MgCl_2$ loading.

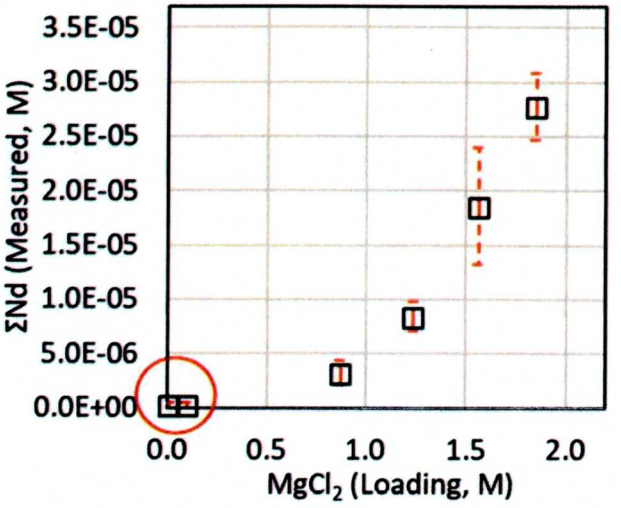

VII.1.4.3. ΣMg

Time-dependent ΣMg is shown in Table VII.1-6, and displayed in Figure VII.1-5. The observed scatter is within the maximum %2SD of 19% (Table VII.1-7). Figure VII.1-6 displays the accuracy and precision of our ΣMg measurements.

Table VII.1-6. Time-dependent ΣMg in M (DSP = Days Since Preparation, i.e., Aging time in days). Data from Table 3-26 in Kirkes and Hora (2020).

ΣMg, M	DSP				
Reactor ID	671	986	1874	1972	2082
Nd(OH)3-0.01 Mg-1	1.02E-02	1.03E-02	1.03E-02	8.44E-03	8.91E-03
Nd(OH)3-0.01 Mg-2	1.07E-02	1.04E-02	1.05E-02	8.46E-03	8.92E-03
Nd(OH)3-0.1 Mg-1	9.61E-02	9.57E-02	9.72E-02	8.13E-02	8.55E-02
Nd(OH)3-0.1 Mg-2	9.61E-02	9.37E-02	9.59E-02	8.00E-02	8.64E-02
Nd(OH)3-1.0 Mg-1	8.82E-01	8.52E-01	9.03E-01	7.45E-01	7.83E-01
Nd(OH)3-1.0 Mg-2	8.87E-01	8.48E-01	8.46E-01	7.46E-01	7.86E-01
Nd(OH)3-1.5 Mg-1	1.28E+00	1.24E+00	1.28E+00	1.05E+00	1.12E+00
Nd(OH)3-1.5 Mg-2	1.15E+00	1.25E+00	1.27E+00	1.03E+00	1.12E+00
Nd(OH)3-2.0 Mg-1	1.59E+00	1.59E+00	1.64E+00	1.33E+00	1.39E+00
Nd(OH)3-2.0 Mg-2	1.58E+00	1.56E+00	1.64E+00	1.35E+00	1.49E+00
Nd(OH)3-2.5 Mg-1	1.95E+00	1.87E+00	1.98E+00	1.59E+00	1.75E+00
Nd(OH)3-2.5 Mg-2	1.85E+00	1.83E+00	1.99E+00	1.58E+00	1.71E+00

Figure VII.1-5. Time-dependent ΣMg.

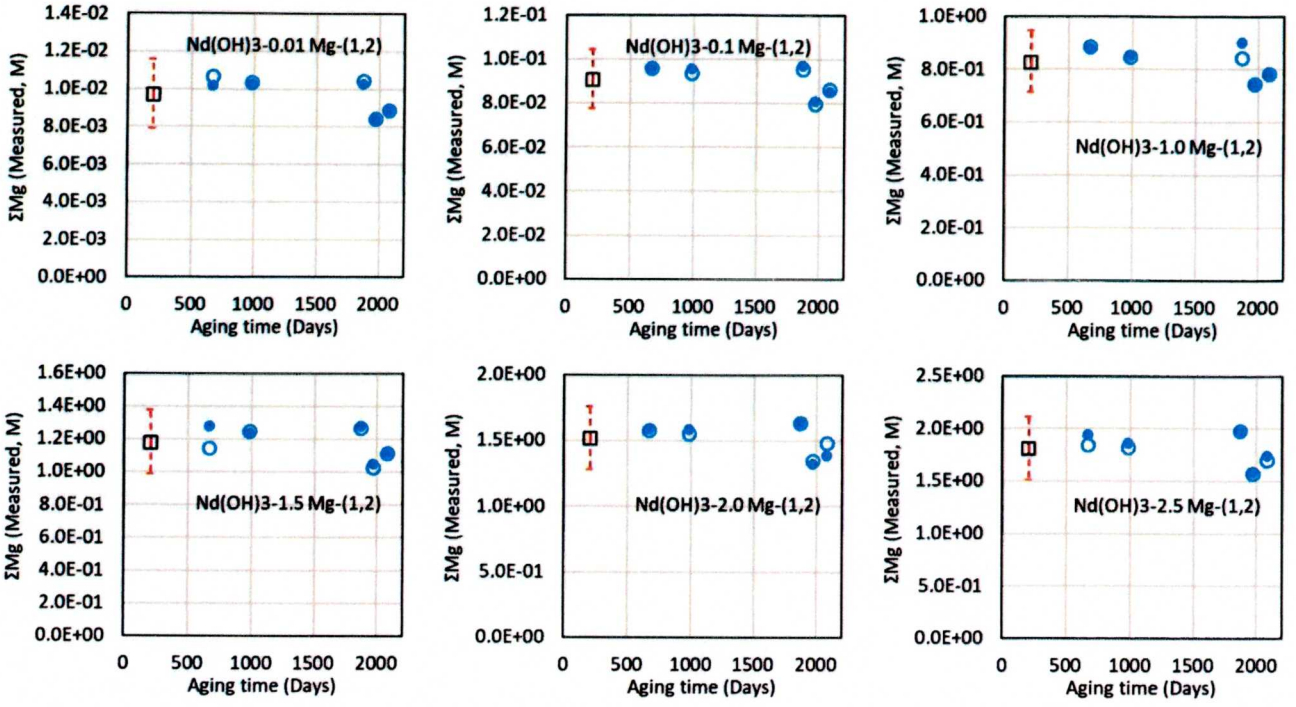

Table VII.1-7. Statistics of measurements of ΣMg (M).

Reactor ID	Average	2SD	%2SD	%Deviation	Count
Nd(OH)3-0.01 Mg-(1,2)	9.71E-03	1.82E-03	19%	-8%	10
Nd(OH)3-0.1 Mg-(1,2)	9.08E-02	1.35E-02	15%	-8%	10
Nd(OH)3-1.0 Mg-(1,2)	8.28E-01	1.17E-01	14%	-5%	10
Nd(OH)3-1.5 Mg-(1,2)	1.18E+00	1.93E-01	16%	-5%	10
Nd(OH)3-2.0 Mg-(1,2)	1.52E+00	2.37E-01	16%	-3%	10
Nd(OH)3-2.5 Mg-(1,2)	1.81E+00	2.99E-01	17%	-2%	10

Figure VII.1-6. Accuracy and precision of ΣMg measurements as a function of $MgCl_2$ loading.

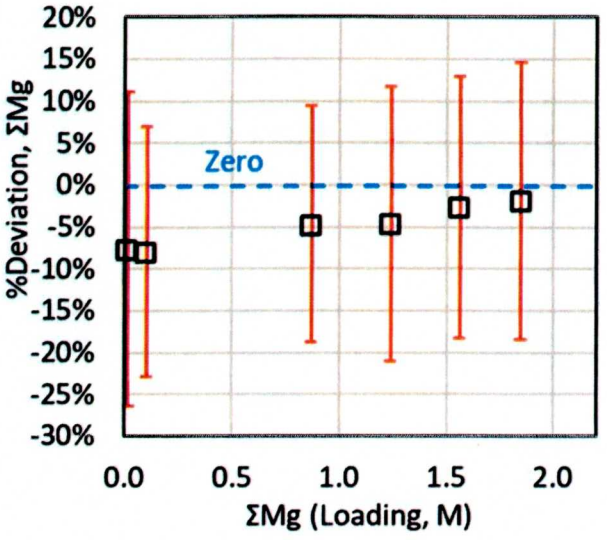

VII.1.4.4. ΣCl

Time-dependent measurements of ΣCl are tabulated in Table VII.1-8, and displayed in Figure VII.1-7. The observed scatter is within maximum %2SD of 9% (Table VII.1-9). Figure VII.1-8 displays the accuracy and precision of our ΣCl measurements. It is unclear why the last three data points show %Deviations larger than the %2SDs.

Table VII.1-8. Time-dependent ΣCl in M (DSP = Days Since Preparation, i.e., Aging time in days). Data from Table 3-27 in Kirkes and Hora (2020).

ΣCl, M	DSP				
Reactor ID	671	986	1874	1972	2082
Nd(OH)3-0.01 Mg-1	2.14E-02	2.20E-02	2.16E-02	2.25E-02	2.05E-02
Nd(OH)3-0.01 Mg-2	2.11E-02	2.21E-02	2.04E-02	2.14E-02	2.01E-02
Nd(OH)3-0.1 Mg-1	2.04E-01	2.12E-01	2.02E-01	2.06E-01	2.03E-01
Nd(OH)3-0.1 Mg-2	2.03E-01	2.05E-01	1.94E-01	2.07E-01	2.04E-01
Nd(OH)3-1.0 Mg-1	1.87E+00	1.96E+00	1.78E+00	1.87E+00	1.89E+00
Nd(OH)3-1.0 Mg-2	1.88E+00	1.97E+00	1.69E+00	1.87E+00	1.88E+00
Nd(OH)3-1.5 Mg-1	2.69E+00	2.78E+00	2.57E+00	2.66E+00	2.68E+00
Nd(OH)3-1.5 Mg-2	2.69E+00	2.71E+00	2.47E+00	2.66E+00	2.68E+00
Nd(OH)3-2.0 Mg-1	3.32E+00	3.45E+00	3.18E+00	3.33E+00	3.38E+00
Nd(OH)3-2.0 Mg-2	3.32E+00	3.47E+00	3.18E+00	3.36E+00	3.33E+00
Nd(OH)3-2.5 Mg-1	4.01E+00	4.10E+00	3.75E+00	4.06E+00	4.02E+00
Nd(OH)3-2.5 Mg-2	3.98E+00	4.11E+00	3.78E+00	4.04E+00	4.03E+00

Figure VII.1-7. Time-dependent ΣCl.

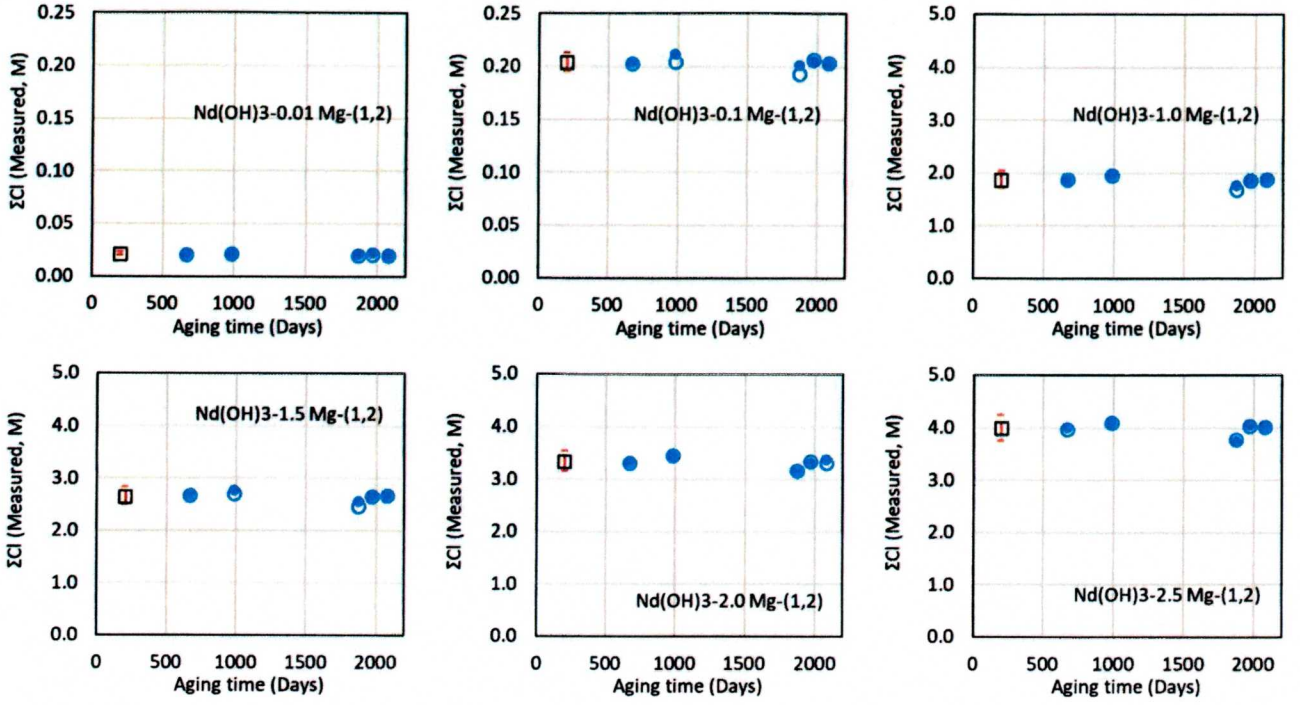

Table VII.1-9. Statistics of ΣCl measurements (M).

Reactor ID	Average	2SD	%2SD	%Deviation	Count
Nd(OH)3-0.01 Mg-(1,2)	2.13E-02	1.58E-03	7%	1%	10
Nd(OH)3-0.1 Mg-(1,2)	2.04E-01	9.04E-03	4%	3%	10
Nd(OH)3-1.0 Mg-(1,2)	1.87E+00	1.62E-01	9%	7%	10
Nd(OH)3-1.5 Mg-(1,2)	2.66E+00	1.68E-01	6%	7%	10
Nd(OH)3-2.0 Mg-(1,2)	3.33E+00	1.92E-01	6%	7%	10
Nd(OH)3-2.5 Mg-(1,2)	3.99E+00	2.48E-01	6%	8%	10

Figure VII.1-8. Accuracy and precision of ΣCl measurements as a function of $MgCl_2$ loading.

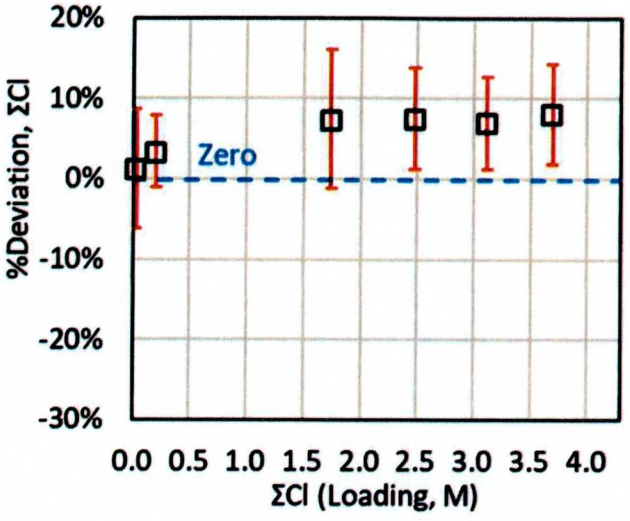

VII.1.5. Data - Solids

Solids collected at the end of the experiments were examined by XRD (Figure VII.1-9). $Nd(OH)_3(s)$ was identified. Unidentified peaks were observed from scan Nd(OH)3-2.5-Mg-1. It is unclear if they match with NdOOH(s).

Figure VII.1-9. XRD scans of solids collected at the end of experiments.

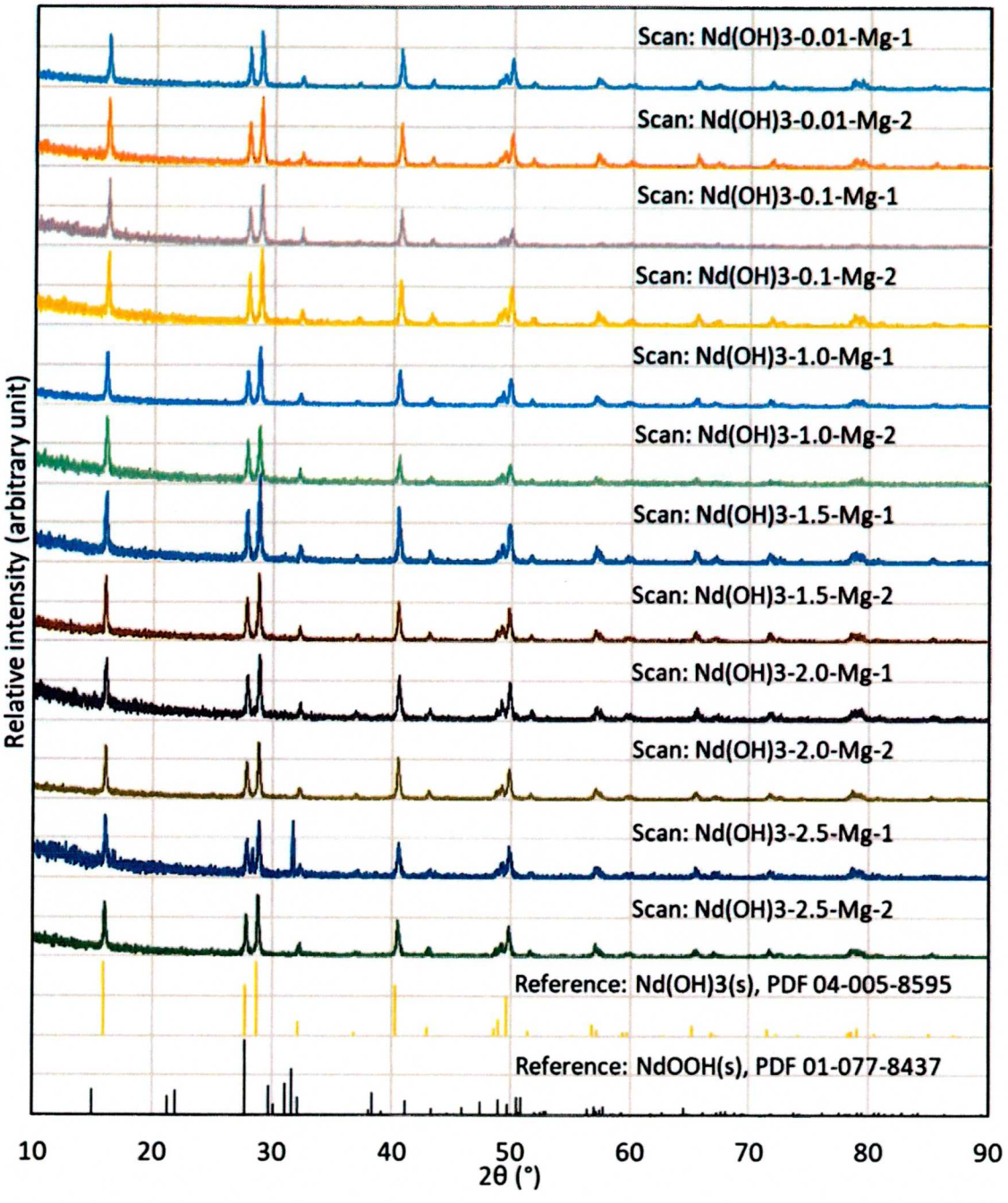

VII.1.6. Observations

The scatter of time-dependent measurements of aqueous components is within reasonable 2SD values. No systematic changes of concentrations were observed as a function of time. Therefore, the 2SDs quantify the precision of our measurements. Within the 2SDs, the experiments appear to have reached equilibrium. XRD scans showed only $Nd(OH)_3(s)$.

VII.1.7. Model Parameterization

Measurements were converted to molalities in Table VII.1-10, and plotted in Figure VII.1-10.

Table VII.1-10. Concentrations in molality.

ΣMg, m	ΣCl, m	pmH	ΣNd, m
8.95E-01	1.79E+00	8.39	3.26E-06
1.29E+00	2.58E+00	8.29	8.76E-06
1.64E+00	3.29E+00	8.20	2.18E-05
1.97E+00	3.94E+00	8.15	2.96E-05

The dominant aqueous species is $Nd(OH)_2^+$ which increases as ΣMg loading increases and the pHr decreases.[52] Among the three solubility constants (K) retrieved from literature for the dissolution of $Nd(OH)_3(s)$, i.e., $Nd(OH)_3(s) + 3H^+ = Nd^{+3} + 3H_2O$, the application of log K = 16.9 (Guillaumont et al., 2003) with relevant thermodynamic in the quantities in data0.fm1 results in Saturation Indexes (SIs) closest to zero. Use of the other log Ks, 14.49 (data0.fm1) and 15.6 (Guillaumont et al. 2003) resulted in the SI deviating from zero.

Interaction of $Nd(OH)_2^+$ with the major anion, Cl^-, is accounted for by PIP($Nd(OH)_2^+/Cl^-$) in data0.fm1. The other species that can interact with $Nd(OH)_2^+$ is Mg^{+2} because it is the major cation to potentially influence the Nd speciation. Fitting was performed on PIP($Nd(OH)_2^+/Mg^{+2}$) with log K of $Nd(OH)_3(s)$ set to 16.9 (Guillaumont et al., 2003). The fitting resulted in PIP($Nd(OH)_2^+/Mg^{+2}$) = 0.302. Nd is an analog of Am in data0.fm1, therefore, the new PIP($Nd(OH)_2^+/Mg^{+2}$) will be considered to represent PIP($Am(OH)_2^+/Mg^{+2}$) in data0.fm1. Model predictions after fitting are much better, and are compared in Figure VII.1-10.

[52] This behavior is worth noting and will be discussed in future reports. Analysis of this behavior in this report is intended to be consistent with the thermodynamic quantities in data0.fm1.

Figure VII.1-10. Model predictions. A. Before fitting, and B. After fitting. The two data points marked in red ovals were not considered in model parameterization due to larger uncertainty.

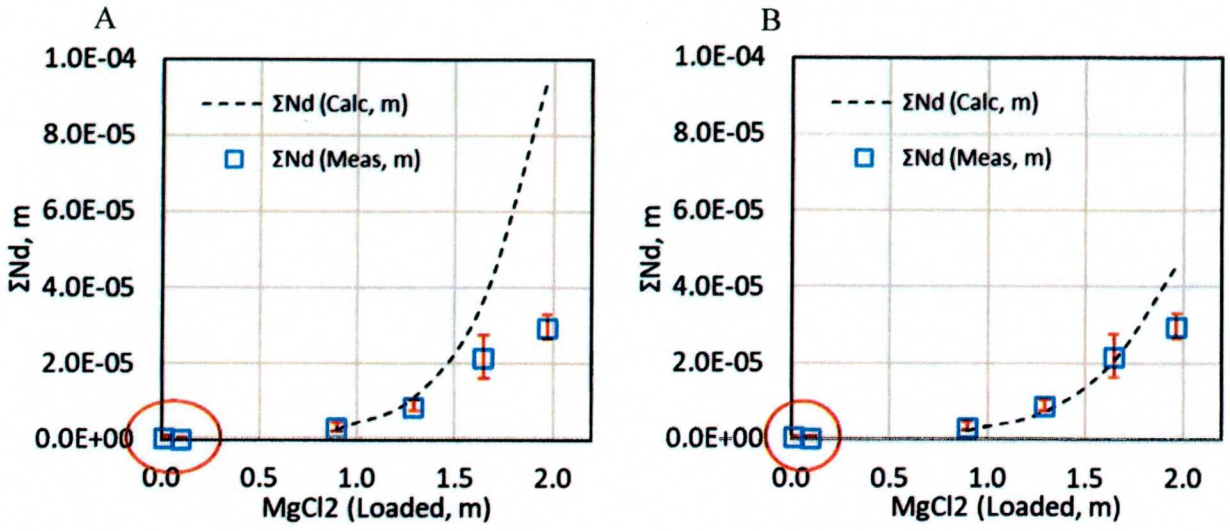

VII.1.8. Summary

$PIP(Nd(OH)_2^+/Mg^{+2}) = PIP(Am(OH)_2^+/Mg^{+2}) = 0.302$ is the recommended new addition to data0.fm1.

VIII. BORON (B)

VIII.1. $Na_2B_4O_7(s)$ - $Nd(OH)_3(s)$ - NaCl - H_2O

VIII.1.1. Chemical System

$Na_2B_4O_7(s)$ and $Nd(OH)_3(s)$ were added to solutions of incrementally increased NaCl. The six components of this system are Nd^{+3}, $B(OH)_4^-$, Na^+, Cl^-, H^+, and H_2O.

VIII.1.2. Goals and Hypotheses

The goal of this experiment was to validate the borate speciation model currently in data0.fm1.

VIII.1.3. Reactor Preparation

10.0 to 10.6 grams of $Na_2B_4O_7$ and 0.34 to 0.36 grams of $Nd(OH)_3(s)$ were added to 100 mL of NaCl solutions prepared by the recipes in Table VIII.1-1.

Table VIII.1-1. Recipe and calculated solution properties.

Reactor ID	NaCl, g	DI, g	NaCl, m	M:m, L/kg	NaCl, M	I,M	A
Nd(OH)3-0.01B-(1,2)	0.1462	250.00	1.00E-02	0.9993	1.00E-02	1.00E-02	-0.10
Nd(OH)3-0.1B-(1,2)	1.4614	250.01	1.00E-01	1.0012	9.99E-02	9.99E-02	-0.08
Nd(OH)3-1.0B-(1,2)	14.6138	250.01	1.00E+00	1.0201	9.81E-01	9.81E-01	0.08
Nd(OH)3-2.0B-(1,2)	29.2248	250.01	2.00E+00	1.0411	1.92E+00	1.92E+00	0.25

Nd(OH)3-3.0B-(1,2)	43.8327	250.02	3.00E+00	1.0621	2.82E+00	2.82E+00	0.41
Nd(OH)3-4.0B-(1,2)	58.4457	250.01	4.00E+00	1.0831	3.69E+00	3.69E+00	0.57
Nd(OH)3-5.0B-(1,2)	73.0307	249.99	5.00E+00	1.1041	4.53E+00	4.53E+00	0.72

	Density ,g/mL		
	calc	meas	%Dev
Nd(OH)3-0.01B-(1,2)	1.001	1.027	3%
Nd(OH)3-0.1B-(1,2)	1.005	1.028	2%
Nd(OH)3-1.0B-(1,2)	1.038	1.049	1%
Nd(OH)3-2.0B-(1,2)	1.073	1.083	1%
Nd(OH)3-3.0B-(1,2)	1.107	1.115	1%
Nd(OH)3-4.0B-(1,2)	1.139	1.145	1%
Nd(OH)3-5.0B-(1,2)	1.170	1.178	1%

VIII.1.4. Data - Aqueous

This set of experiments was originally initiated to examine the influence of borate on the speciation of dissolved Nd. However, ΣNd measurements showed 2SD values (i.e., precision) exceeding the averages, making the 95% confidence interval extending to negative concentration range. We believe this is because the dissolved total concentrations of Nd were close to, or lower than, the low detection limit of the instrument used (ICP-MS). So the results of ΣNd measurements are not analyzed in this report.

VIII.1.4.1. pHr

The recorded pHr showed scatter (Table VIII.1-2; Figure VIII.1-1). The observed scatters were within 2% of maximum %2SD (Table VIII.1-3). The change of pHr as a function of NaCl loading is shown in Figure VIII.1-2.

Table VIII.1-2. Time-dependent pHr: Table 3-18 of Kirkes and Hora (2020).

pHr	DSP			
Set-up ID	412	1176	1218	1972
Nd(OH)3-0.01B-1	9.30	9.25	9.33	9.35
Nd(OH)3-0.01B-2	9.28	9.25	9.32	9.34
Nd(OH)3-0.1B-1	9.21	9.18	9.24	9.27
Nd(OH)3-0.1B-2	9.19	9.18	9.21	9.28
Nd(OH)3-1.0B-1	8.85	8.82	8.86	8.96
Nd(OH)3-1.0B-2	8.85	8.82	8.87	8.95
Nd(OH)3-2.0B-1	8.65	8.62	8.67	8.76
Nd(OH)3-2.0B-2	8.64	8.61	8.63	8.75
Nd(OH)3-3.0B-1	8.49	8.46	8.48	8.62
Nd(OH)3-3.0B-2	8.50	8.46	8.49	8.62
Nd(OH)3-4.0B-1	8.34	8.34	8.39	8.50
Nd(OH)3-4.0B-2	8.37	8.33	8.36	8.50
Nd(OH)3-5.0B-1	8.24	8.23	8.25	8.40
Nd(OH)3-5.0B-2	8.23	8.23	8.25	8.38

Figure VIII.1-1. Time-dependent pHr.

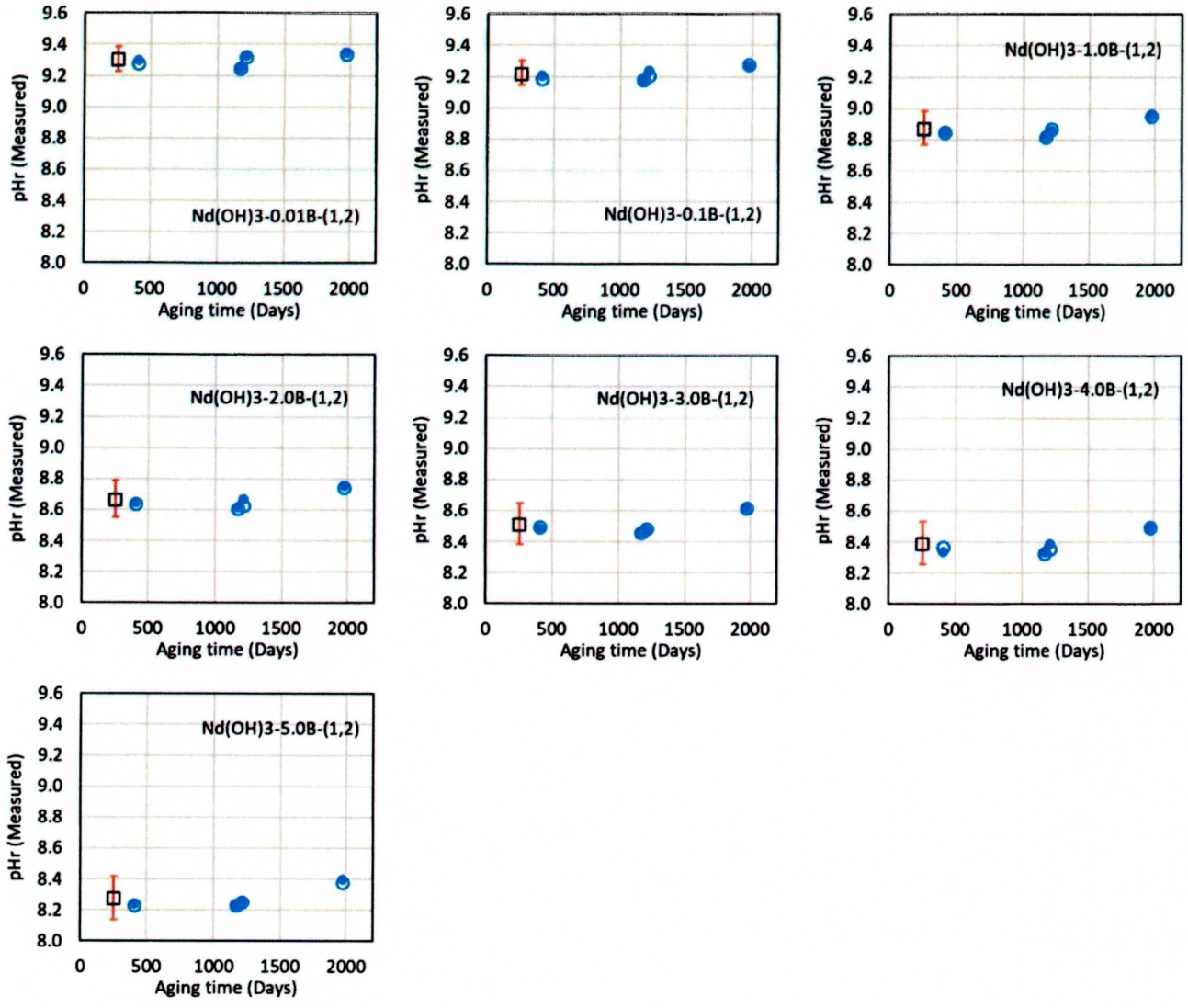

Table VIII.1-3. Statistics of measurements of pHr.

Reactor ID	Average	2SD	%2SD	Count
Nd(OH)3-0.01B-(1,2)	9.30	0.08	1%	8
Nd(OH)3-0.1B-(1,2)	9.22	0.08	1%	8
Nd(OH)3-1.0B-(1,2)	8.87	0.11	1%	8
Nd(OH)3-2.0B-(1,2)	8.67	0.12	1%	8
Nd(OH)3-3.0B-(1,2)	8.52	0.13	2%	8
Nd(OH)3-4.0B-(1,2)	8.39	0.14	2%	8
Nd(OH)3-5.0B-(1,2)	8.28	0.14	2%	8

Figure VIII.1-2. pHr as a function of NaCl loading.

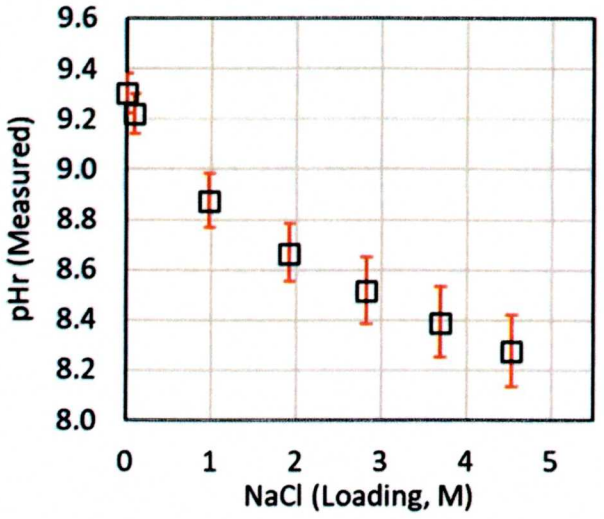

VIII.1.4.2. ΣB

The measurements of ΣB showed scatter (Table VIII.1-4; Figure VIII.1-3) within the maximum %2SD of 23% (Table VIII.1-5). ΣB as a function of NaCl loading is shown in Figure VIII.1-4. ΣB loading was conducted by adding >10 grams of $Na_2B_4O_7$ (formula weight = 201.22 g/mol) to 100 mL of solution (Section VIII.1.3). Thus, the loading of ΣB was greater than 1.9 (= 10/201.22/0.1×4) M. The observed ΣB are always less than the half of the minimum ΣB loading of 1.9 M, indicating that the dissolution of loaded $Na_2B_4O_7$ was not complete.

Table VIII.1-4. Time-dependent ΣB in M (DSP = Days Since Preparation, i.e., Aging time in days). Data from Table 3-22 of Kirkes and Hora (2020).

ΣB, M	DSP			
Set-up ID	412	1176	1218	1972
Nd(OH)3-0.01B-1	5.62E-01	6.05E-01	6.66E-01	6.28E-01
Nd(OH)3-0.01B-2	5.40E-01	5.96E-01	6.51E-01	6.34E-01
Nd(OH)3-0.1B-1	4.07E-01	5.15E-01	5.77E-01	5.54E-01
Nd(OH)3-0.1B-2	4.63E-01	5.08E-01	5.63E-01	5.65E-01
Nd(OH)3-1.0B-1	2.27E-01	2.52E-01	2.75E-01	2.66E-01
Nd(OH)3-1.0B-2	2.29E-01	2.57E-01	2.77E-01	2.70E-01
Nd(OH)3-2.0B-1	1.85E-01	2.12E-01	2.32E-01	2.11E-01
Nd(OH)3-2.0B-2	1.82E-01	2.10E-01	2.28E-01	2.09E-01
Nd(OH)3-3.0B-1	2.09E-01	1.90E-01	2.03E-01	1.98E-01
Nd(OH)3-3.0B-2	1.82E-01	2.07E-01	2.09E-01	1.98E-01
Nd(OH)3-4.0B-1	1.63E-01	1.97E-01	1.79E-01	1.91E-01
Nd(OH)3-4.0B-2	1.68E-01	1.91E-01	1.77E-01	1.89E-01
Nd(OH)3-5.0B-1	1.65E-01	1.98E-01	2.09E-01	1.83E-01
Nd(OH)3-5.0B-2	1.69E-01	2.00E-01	2.09E-01	1.80E-01

Figure VIII.1-3. Time-dependent ΣB.

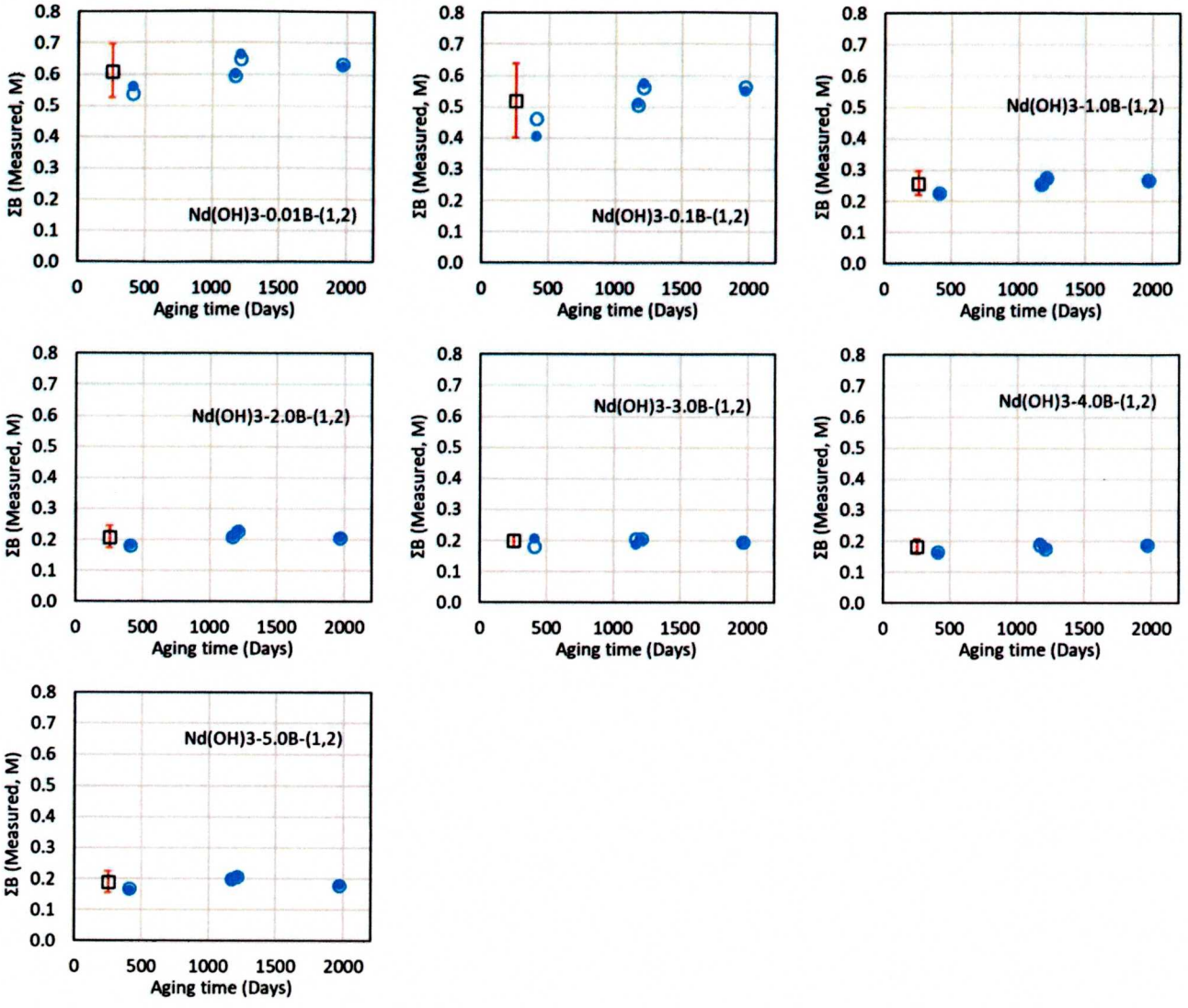

Table VIII.1-5. Statistics of ΣB measurements (M).

Reactor ID	Average	2SD	%2SD	Count
Nd(OH)3-0.01B-(1,2)	6.10E-01	8.67E-02	14%	8
Nd(OH)3-0.1B-(1,2)	5.19E-01	1.18E-01	23%	8
Nd(OH)3-1.0B-(1,2)	2.57E-01	3.91E-02	15%	8
Nd(OH)3-2.0B-(1,2)	2.09E-01	3.55E-02	17%	8
Nd(OH)3-3.0B-(1,2)	2.00E-01	1.93E-02	10%	8
Nd(OH)3-4.0B-(1,2)	1.82E-01	2.42E-02	13%	8
Nd(OH)3-5.0B-(1,2)	1.89E-01	3.46E-02	18%	8

Figure VIII.1-4. Change of ΣB as a function of NaCl loading. Dissolution of loaded $Na_2B_4O_7$ was not complete (see the text).

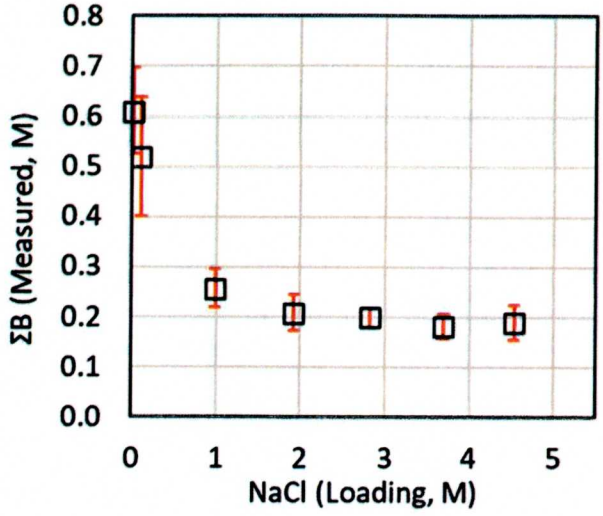

VIII.1.4.3. ΣNa

The measurements of ΣNa showed scatter (Table VIII.1-6; Figure VIII.1-5) within a maximum %2SD of 12% (Table VIII.1-7). Again, the consistent negative %Deviation of the measured ΣNa exceeding the %2SD indicates that the dissolution of the loaded $Na_2B_4O_7$ was not complete (Figure VIII.1-6).

Table VIII.1-6. Time-dependent measurements of ΣNa in M (DSP = Days Since Preparation, i.e., Aging time in days). Data from Table 3-20 of Kirkes and Hora (2020).

ΣNa, M	DSP			
Reactor ID	412	1176	1218	1972
Nd(OH)3-0.01B-1	2.94E-01	2.95E-01	2.99E-01	2.91E-01
Nd(OH)3-0.01B-2	2.88E-01	2.91E-01	2.97E-01	2.94E-01
Nd(OH)3-0.1B-1	2.89E-01	3.23E-01	3.41E-01	3.31E-01
Nd(OH)3-0.1B-2	3.39E-01	3.19E-01	3.31E-01	3.29E-01
Nd(OH)3-1.0B-1	1.04E+00	1.03E+00	1.01E+00	1.08E+00
Nd(OH)3-1.0B-2	1.09E+00	1.00E+00	1.03E+00	1.08E+00
Nd(OH)3-2.0B-1	1.82E+00	2.09E+00	2.14E+00	1.95E+00
Nd(OH)3-2.0B-2	1.96E+00	2.12E+00	2.12E+00	1.87E+00
Nd(OH)3-3.0B-1	3.19E+00	2.94E+00	2.92E+00	2.81E+00
Nd(OH)3-3.0B-2	3.17E+00	2.93E+00	2.93E+00	2.85E+00
Nd(OH)3-4.0B-1	3.79E+00	3.79E+00	3.85E+00	3.76E+00
Nd(OH)3-4.0B-2	3.86E+00	3.72E+00	3.76E+00	3.70E+00
Nd(OH)3-5.0B-1	4.22E+00	4.39E+00	4.35E+00	4.46E+00
Nd(OH)3-5.0B-2	4.61E+00	4.64E+00	4.65E+00	4.65E+00

Figure VIII.1-5. Time-dependent measurements of ΣNa.

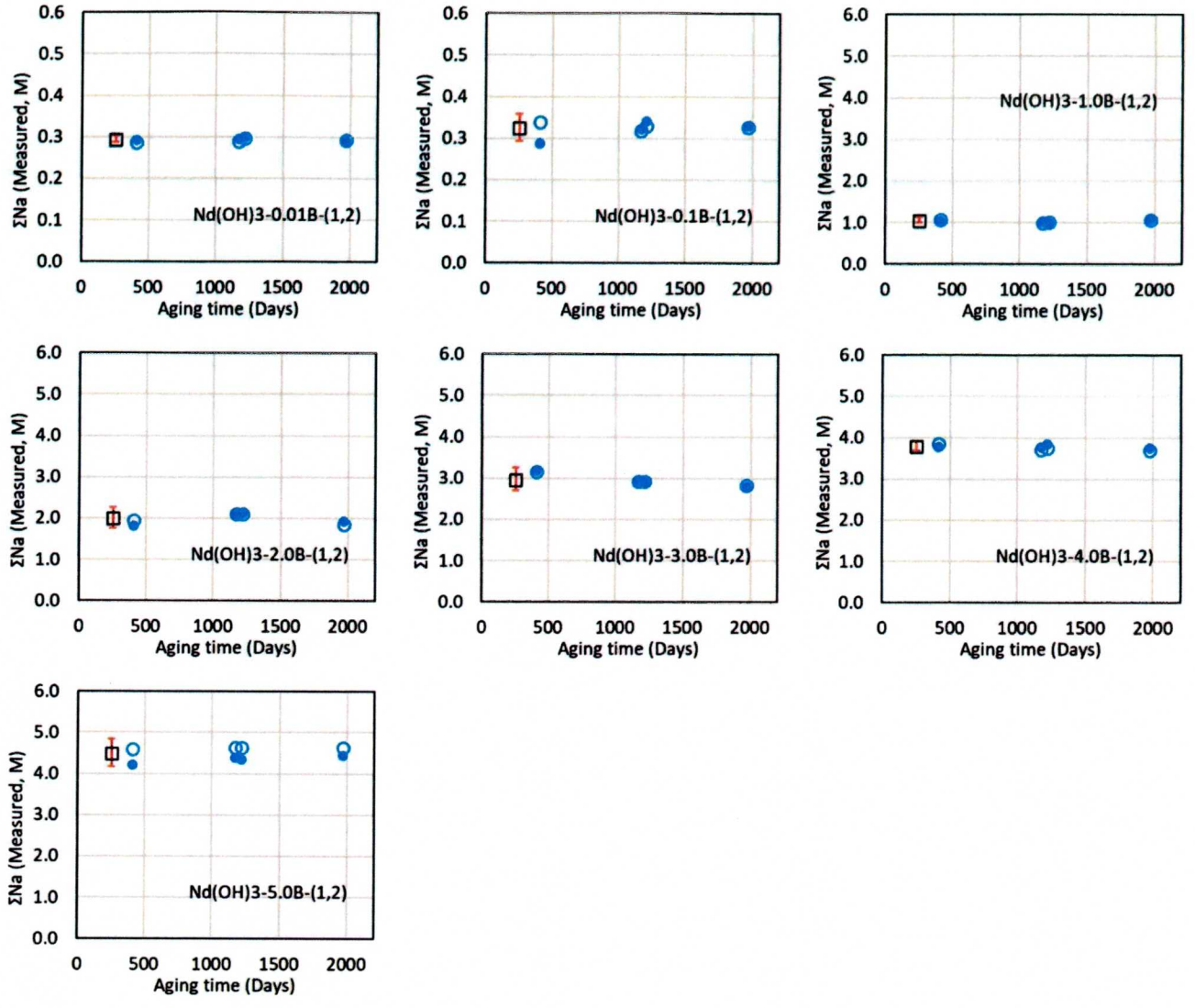

Table VIII.1-7. Statistics of measurements of ΣNa (M).

Reactor ID	Average	2SD	%2SD	%Deviation	Count
Nd(OH)3-0.01B-(1,2)	2.94E-01	7.09E-03	2%	-71%	8
Nd(OH)3-0.1B-(1,2)	3.25E-01	3.27E-02	10%	-70%	8
Nd(OH)3-1.0B-(1,2)	1.05E+00	6.85E-02	7%	-48%	8
Nd(OH)3-2.0B-(1,2)	2.01E+00	2.50E-01	12%	-32%	8
Nd(OH)3-3.0B-(1,2)	2.97E+00	2.78E-01	9%	-23%	8
Nd(OH)3-4.0B-(1,2)	3.78E+00	1.13E-01	3%	-20%	8
Nd(OH)3-5.0B-(1,2)	4.50E+00	3.31E-01	7%	-19%	8

Figure VIII.1-6. Accuracy and precision of ΣNa measurements as a function of ΣNa loading, where ΣNa loading = 2 × [$Na_2B_4O_7$] + [NaCl]. Dissolution of the loaded $Na_2B_4O_7$ was not complete (see the text to compare the recipe and observation).

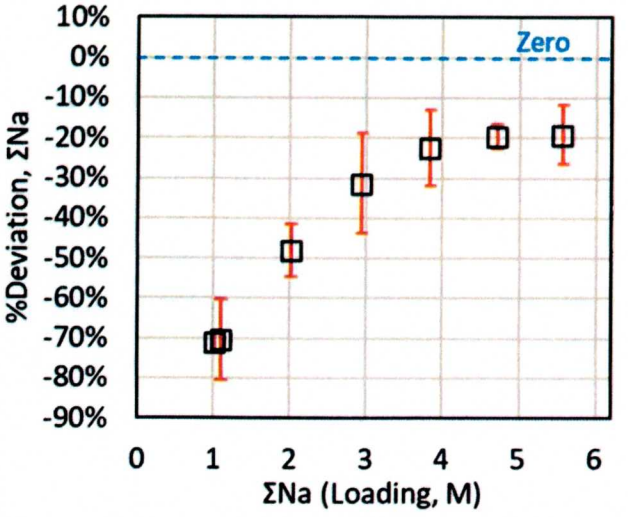

VIII.1.4.4. ΣCl

The time-dependent measurements of ΣCl showed scatter (Table VIII.1-8; Figure VIII.1-7). The scatter was less than the maximum %2SD of 19% (Table VIII.1-9). Accuracy and precision of Cl measurements are displayed in Figure VIII.1-8.

Table VIII.1-8. Time-dependent ΣCl in M (DSP = Days Since Preparation, i.e., Aging time in days). Data from Table 3-21 of Kirkes and Hora (2020).

ΣCl, M	DSP		
Set-up ID	412	1176	1218
Nd(OH)3-0.01B-1	1.02E-02	9.71E-03	9.98E-03
Nd(OH)3-0.01B-2	9.75E-03	9.61E-03	9.94E-03
Nd(OH)3-0.1B-1	9.88E-02	1.03E-01	1.05E-01
Nd(OH)3-0.1B-2	1.00E-01	1.00E-01	1.03E-01
Nd(OH)3-1.0B-1	9.89E-01	1.02E+00	1.07E+00
Nd(OH)3-1.0B-2	9.98E-01	1.06E+00	1.07E+00
Nd(OH)3-2.0B-1	2.02E+00	1.92E+00	2.08E+00
Nd(OH)3-2.0B-2	2.01E+00	2.05E+00	2.07E+00
Nd(OH)3-3.0B-1	3.69E+00	2.90E+00	2.97E+00
Nd(OH)3-3.0B-2	2.99E+00	2.95E+00	3.02E+00
Nd(OH)3-4.0B-1	3.88E+00	3.62E+00	3.75E+00
Nd(OH)3-4.0B-2	3.94E+00	3.80E+00	4.01E+00
Nd(OH)3-5.0B-1	4.71E+00	4.76E+00	4.85E+00
Nd(OH)3-5.0B-2	4.79E+00	4.91E+00	4.91E+00

Red fonts: In Table 3-21 of Kirkes and Hora (2020), they are listed as 9.89E+00 and 9.98E+00 because incorrect dilution factors were applied in the concentration conversion from instrument readings to concentrations in the reactors. The correction of the dilution factors were documented in Kirkes (2021). The corrections resulted in 10 times reduction of the concentrations reported in Table 3-21 of Kirkes and Hora (2020), which are the values in the red fonts of the Table above.

Figure VIII.1-7. Time-dependent ΣCl.

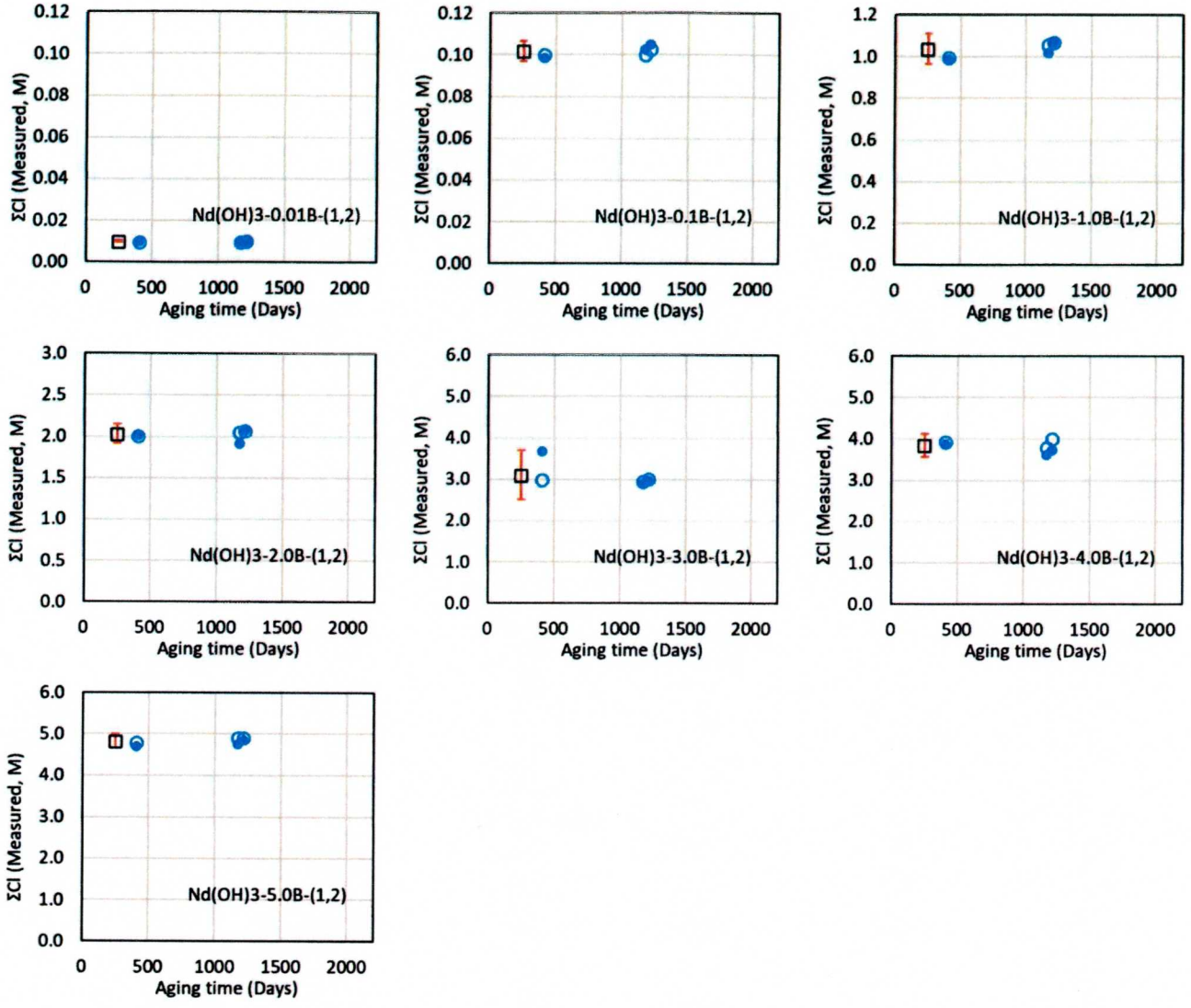

Table VIII.1-9. Statistics of measurements of ΣCl (M).

Reactor ID	Average	2SD	%2SD	%Deviation	Count
Nd(OH)3-0.01B-(1,2)	9.87E-03	4.32E-04	4%	-1%	6
Nd(OH)3-0.1B-(1,2)	1.02E-01	4.77E-03	5%	2%	6
Nd(OH)3-1.0B-(1,2)	1.03E+00	7.37E-02	7%	6%	6
Nd(OH)3-2.0B-(1,2)	2.03E+00	1.16E-01	6%	5%	6
Nd(OH)3-3.0B-(1,2)	3.09E+00	5.97E-01	19%	9%	6
Nd(OH)3-4.0B-(1,2)	3.83E+00	2.80E-01	7%	4%	6
Nd(OH)3-5.0B-(1,2)	4.82E+00	1.64E-01	3%	6%	6

Figure VIII.1-8. Accuracy and precision of ΣCl measurements as a function of NaCl loading.

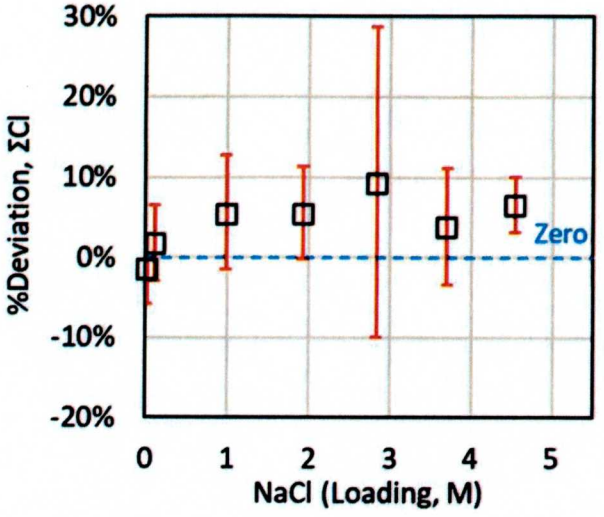

VIII.1.5. Data - Solids

Solids were collected at the end of experiments and examined by XRD (Figure VIII.1-9). Except for the first three, all scans indicated the co-existence of $Na_2B_4O_7.10H_2O(s)$ (borax) and $Nd(OH)_3(s)$.

Figure VIII.1-9. XRD scans of the solids collected at the end of experiments. Green dashed rectangle locates the positions of major peaks of borax.

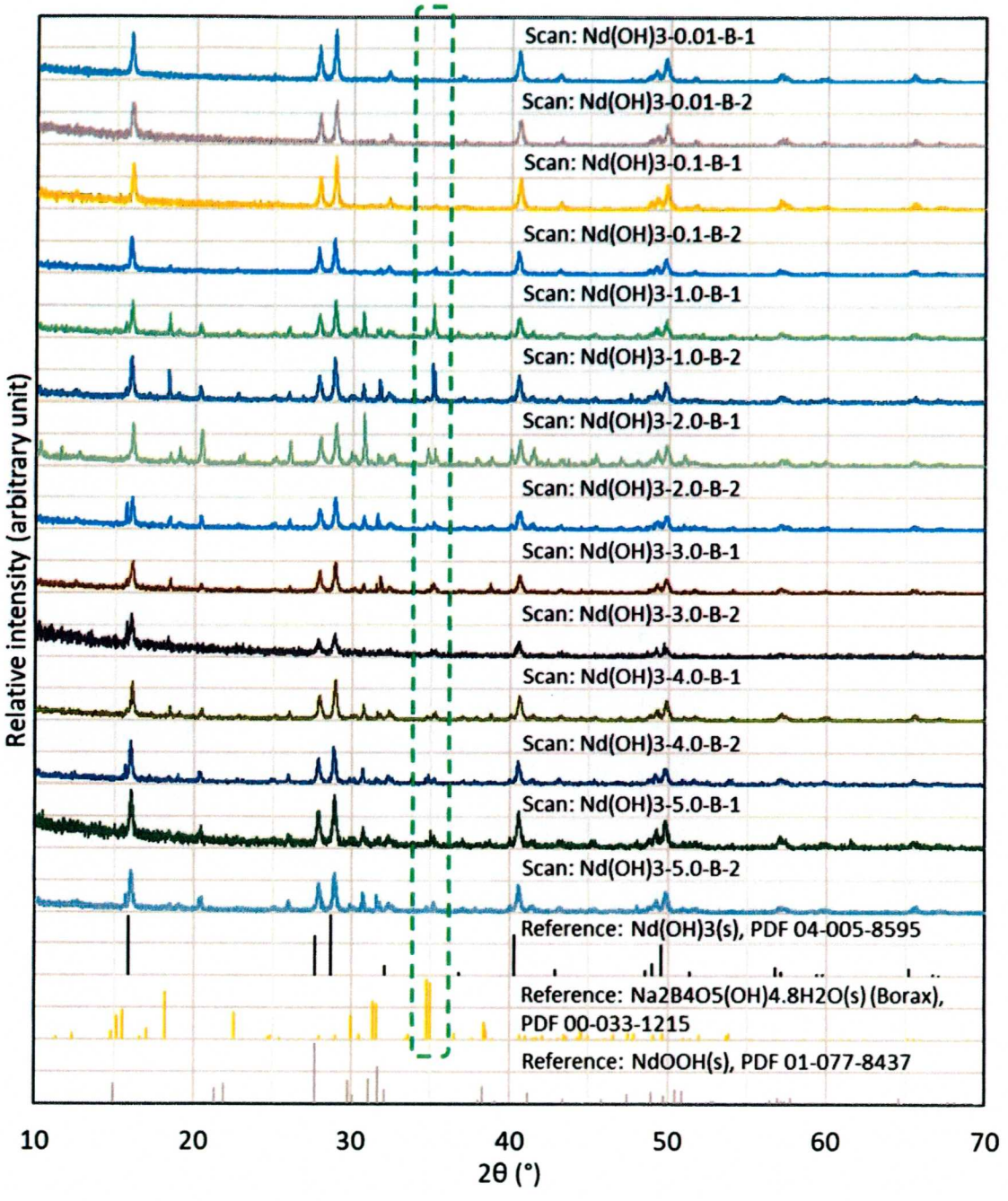

VIII.1.6. Observations

The measurements of ΣNa and ΣB indicated the incomplete dissolution of $Na_2B_4O_7$ in all experiments. 5.0 grams of $Na_2B_4O_7$ should remain in the solid based on the solution data. It is unclear why the borax peaks did not show up in the first three XRD scans displayed in Figure VIII.1-9.

VIII.1.7. Model Parameterization: Pitzer Approach

Based on the solution data, solubility equilibrium was assumed for borax. Thermodynamic quantities in data0.fm1 accurately predict the experimental results (Figure VIII.1-10). The influence of dissolved Nd on the speciation of B cannot be discussed because ΣNd << ΣB. The reverse could have been performed if the ΣNd measurements were of better precision.

Figure VIII.1-10. Model calculation vs. measurements.

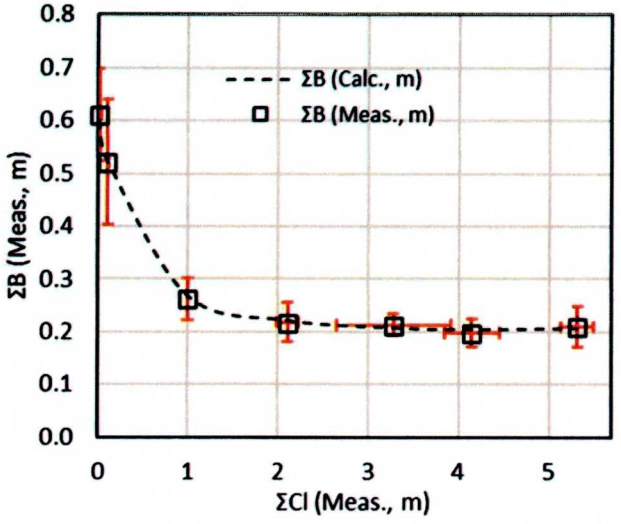

VIII.1.8. Summary

The current borate model in data0.fm1 adequately describes within the uncertainty the data in this section.

No update will be made to the borate model in data0.fm1.

IX. CONCLUSIONS

The following additions are to be made to data0.fm1.

IX.1. Iron (Fe)

Table IX.1-1. Reactions and 25 °C Log Ks for Fe that are added to data0.fm1.

Reaction	Log K (I = 0)	Reference
Aqueous Reaction		
$FeOH^+ + H^+ = Fe^{+2} + H_2O$	9.31	Shock et al. (1997)
$Fe(OH)_2(aq) + 2H^+ = Fe^{+2} + 2H_2O$	20.84	Lemire et al. (2013), Jang (2021b)
$Fe(OH)_3^- + 3H^+ = Fe^{+2} + 3H_2O$	31.00	Baes and Mesmer (1976)
$Fe(OH)_4^{-2} + 4H^+ = Fe^{+2} + 4H_2O$	46.00	Baes and Mesmer (1976)
$FeCO_3(aq) + H^+ = Fe^{+2} + HCO_3^-$	4.83	Bruno et al. (1992)
$Fe(CO_3)_2^{-2} + 2H^+ = Fe^{+2} + 2HCO_3^-$	13.89	Kim et al. (2017)

Reaction	Log K (I = 0)	Reference
$FeEDTA^{-2} = Fe^{+2} + EDTA^{-4}$	-16.1	Morel and Hering (1993)
$FeCitrate^{-} = Fe^{+2} + Citrate^{-3}$	-5.7	Morel and Hering (1993)
$FeOHCitrate^{-2} + H^{+} = Fe^{+2} + Citrate^{-3} + H_2O$	2.24	Section IV.5.8
Dissolution		
$Fe(OH)_2(s)$ (Ferrous Iron Hydroxide) + $2H^{+} = Fe^{+2} + 2H_2O$	12.89	Kim et al. (2017)
$Fe_2Cl(OH)_3(s)$ (Hibbingite) + $3H^{+} = 2Fe^{+2} + Cl^{-} + 3H_2O$	17.08	Kim et al. (2017)
$FeCO_3(s)$ (Siderite) + $H^{+} = Fe^{2+} + HCO_3^{-}$	-0.12	Kim et al. (2017), Stumm and Morgan (1996)
$Fe_2(OH)_2CO_3(s)$ (Chukanovite) + $3H^{+} = 2Fe^{2+} + HCO_3^{-} + 2H_2O$	12.32	Kim et al. (2017)

Table IX.1-2. 25 °C PIPs for Fe that are added to data0.fm1.

i	j	α_1/α_2[A]	$\beta^{(0)}$	$\beta^{(1)}$	$\beta^{(2)}$	C^{φ}	Reference
Fe^{+2}	Cl^{-}	2.0/12.0	0.37324	1.13499	0.0	-0.02152	Moog et al. (2004)
Na^{+}	$Fe(CO_3)_2^{-2}$	2.0/12.0	-0.230	6.26	0.0	0.0	Kim et al. (2017)
i	j	θ_{ij}	Reference	k	ψ_{ijk}	Reference	
Na^{+}	Fe^{+2}	0.10945	Moog et al. (2004)	Cl^{-}	-0.01605	Moog et al. (2004)	
Mg^{+2}	Fe^{+2}	0.14504	Moog et al. (2004)	Cl^{-}	-0.02985	Moog et al. (2004)	

IX.2. Lead (Pb)

Table IX.2-1. Reactions and 25 °C Log Ks for Pb that are added to data0.fm1. Log Ks in this table are extended to ionic strength of 6 m in Jang (2021. Revisit ...).

Reaction	Log K	Reference
Aqueous reactions		
$PbCl^{+} = Pb^{2+} + Cl^{-}$	-1.48±0.01	Millero and Byrne (1984) (6 m)
$PbCl_2(aq) = Pb^{2+} + 2Cl^{-}$	-2.03±0.01	Millero and Byrne (1984) (6 m)
$PbCl_3^{-} = Pb^{2+} + 3Cl^{-}$	-1.86±0.01	Millero and Byrne (1984) (6 m)
Dissolution		
$PbCl_2(s)$ (cotunnite) = $Pb^{2+} + 2Cl^{-}$	-4.83	Edwards et al. (1992)

Table IX.2-2. PIPs for Pb that are added to data0.fm1.

i	j	α_1/α_2[A]	$\beta^{(0)}$	$\beta^{(1)}$	$\beta^{(2)}$	C^{φ}	Source
H^{+}	$PbCl_3^{-}$	2.0/12.0	0.1077	0.0425	0.00	-0.0035	Jang (2021. Revisit ...) (6 m)
Na^{+}	$PbCl_3^{-}$	2.0/12.0	-0.10025	0.0	0.0	0.0	Section V.3.8[A]
Mg^{+2}	$PbCl_3^{-}$	2.0/12.0	0.23015	0.0	0.0	0.0	Section V.4.8[A]

[A] Verified in Domski (2021).

IX.3. Magnesium (Mg)

Table IX.3-1. Reactions and 25 °C Log Ks for Mg that are added to data0.fm1.

Reaction	Log K	Source
$Mg(Oxalate)_2^{-2} = Mg^{+2} + 2Oxalate^{-2}$	-4.94	Martell and Smith (1977)
$MgOxalate.2H_2O(s)$ (Glushinskite) = $Mg^{+2} + Oxalate^{-2} + 2H_2O$	-6.49	Section VI.1.8[A]

[A] Verified in Domski (2021).

No PIPs for Mg are added to data0.fm1.

IX.4. Neodymium (Nd)

Table IX.4-1. Reactions and 25 °C Log Ks for Nd that are added to data0.fm1.

Reaction	Log K	Source
$Nd(OH)_3(s) + 3H^+ = Nd^{+3} + 3H_2O$	16.9	Guillaumont et al. (2003)

Table IX.4-2. 25 °C PIPs for Nd that are added to data0.fm1.

i	*j*	θ_{ij}	Reference
$Nd(OH)_2^+$	Mg^{+2}	0.302	Section VII.1.8[A]

[A] Verified in Domski (2021).

IX.5. Borate (B)

No log Ks or PIPs for B are added to data0.fm1.

X. FUTURE WORK

The SNL WIPP Geochemistry Program is considering the assignment of uncertainties to the literature-retrieved and newly created thermodynamic quantities, based on the measurements presented in this report. The SNL WIPP Geochemistry Program is also considering issuance of follow-up memoranda for individual sections of this report, if such documents are requested in writing by DOE or WIPP regulators.

XI. REFERENCES

XI.1. A

Acros Organics, 2017. Certificate of Analysis for Lead Chloride, 99%, Catalogue number; 19331, Lot Number: A0387918, Quality Test/Release Date; 21 August 2017, Issued by C. Wygaerts (QA Manager) on 10 June 2021.

Altmaier, M., Metz, V., Neck, V., Muller, R., and Fanghanel, T., 2003. Solid-liquid equilibria of $Mg(OH)_2$(cr) and $Mg_2(OH)_3Cl{\cdot}4H_2O$(cr) in the system Mg-Na-H-OH-O-Cl-H_2O at 25 °C. *Geochimica et Cosmochimica Acta* **67**, 3595-3601.

XI.2. B

Baes, C. F., Jr. and Mesmer, R. E., 1976. *The Hydrolysis of Cations*. John Wiley & Sons, New York.

Borkowski, M., Moore, R. C., Bronikowski, M. G., Chen, J., Pokrovsky, O. S., Xia, Y., and Choppin, G. R., 2001. Thermodynamic modeling of actinide complexation with oxalate at high ionic strength. *Journal of Radioanalytical and Nuclear Chemistry* 248, 467-471.

Bruno, J., Wersin, P., and Stumm, W., 1992. On the influence of carbonate in mineral dissolution: II. The solubility of FeCO3 (s) at 25 °C and 1 atm total pressure. *Geochimica et Cosmochimica Acta* 56, 1149-1155.

XI.3. C

Choppin, G. R., Bond, A. H., Borkowski, M., Bronikowski, M. G., Chen, J. F., Lis, S., Mizera, J., Pokrovsky, O., Wall, N. A., Xia, Y.-X., and Moore, R. C., 2001. Waste Isolation Pilot Plant Actinide Source Term Test Program: Solubility Studies and Development of Modeling Parameters. *Sandia Report, SAND99-0943*. Sandia National Laboratories.

Clegg, S. L., and P. Brimblecombe, 1990. The solubility and activity coefficient of oxygen in salt solutions and brines. Geochimica et Cosmochimica Acta, 54(12), 3315-3328.

XI.4. D

Deacon, G. E. R., 1927. CCLXXII. - Studies of Equilibria in the Systems Sodium Chloride - Lead Chloride - Water, Lithium Chloride - Lead Chloride - Water. J. Chem. Soc., 1927, 2063-2065.

Domski, P. S., 2021. Memo on the estimation of the Log K values and Pitzer parameters for the Iron, Lead, and Neodymium Systems. Memo to SNL WIPP Records, Sandia National Laboratories, Carlsbad, New Mexico, U.S.A. ERMS pending as of 11/8/2021.

XI.5. E

Edwards, R., R. D. Gillard, P. A. Williams, and A. M. Pollard, 1992. Studies of secondary minerals formation in the PbO - H_2O - HCl system. Mineralogical Magazine, 56, 53-65.

XI.6. F

Fanghanel, Th., J. I. Kim, P. Paviet, R. Klenze, and W. Hauser, 1994. Thermodynamics of radioactive trace elements in concentrated electrolyte solutions: hydrolysis of Cm^{3+} in NaCl-solutions. Radiochimica Acta, 66/67, 81-87.

Fanghanel, T., Neck, V., and Kim, J. I., 1995. Thermodynamics of Neptunium(V) In Concentrated Salt-Solutions .2. Ion-Interaction (Pitzer) Parameters for Np(V) Hydrolysis Species and Carbonate Complexes. *Radiochimica Acta* 69, 169-176.

Fanghanel, Th., and Kim, J. I., 1998. Spectroscopic evaluation of thermodynamics of trivalent actinides in brines. *Journal of Alloys and Compounds,* v.271-273, 728-737.

Fanghanel, Th., Th. Konnecke, H. Weger, P. Paviet-Hartmann, V. Neck, and J. I. Kim, 1999. Thermodynamics of Cm(III) in concentrated salt solutions: Carbonate complexation in NaCl solution at 25 °C, Journal of Solution Chemistry, v.28, no.4, 447-462.

Felmy, A. R. and Weare, J. H., 1986. The prediction of borate mineral equilibria in natural waters: Application to Searles Lake, California. *Geochimica et Cosmochimica Acta* 50, 2771-2783.

Felmy, A. R., D. Rai, and R. W. Fulton. 1990. The solubility of $AmOHCO_3(c)$ and the aqueous thermodynamics of the system Na^+ - Am^{3+} - HCO_3^- - CO_3^{2-} - OH^- - H_2O. Radiochimica Acta, 50, 193-204.

Felmy, A. R., D. Rai, and M. J. Mason. 1991. The Solubility of Hydrous Thorium(IV) Oxide in Chloride Media: Development of an Aqueous Ion-Interaction Model. Radiochimica Acta, 55, 177-185.

Felmy, A. R., and D. Rai, 1992. An Aqueous Thermodynamic Model for a High Valence 4:2 Electrolyte Th^{4+} - SO_4^{2-} in the System Na^+ - K^+ - Li^+ - NH_4^+ - Th^{4+} - SO_4^{2-} - HSO_4^- - H_2O to High Concentration. Journal of Solution Chemistry, 21(5), 407-423.

Felmy, A. R., D. Rai, S. M. Sterner, M. J. Mason, N. J. Hess, and S. D. Conradson, 1997. Thermodynamic Models for Highly Charged Aqueous Species: Solubility of Th(IV) Hydrous Oxide in Concentrated $NaHCO_3$ and Na_2CO_3 Solutions. Journal of Solution Chemistry, 26(3), 233-248.

Felmy, A. R., and D. Rai, 1999. Application of Pitzer's Equations for Modeling the Aqueous Thermodynamics of Actinide Species in Natural Waters: A Review. Journal of Solution Chemistry, 28(5), 533-553.

XI.7. G

Giambalvo, E. R., 2002, Org. Recommended Parameter Values for Modeling Organic Ligands in WIPP Brines. *Memo to Laurence H. (Larry) Brush.*, July 25, 2002. ERMS 522981.

Giambalvo, E. R., 2002, Oxalate. Recommended u0/RT values for modeling the solubility of oxalate solids in WIPP brines. *Memo to Laurence H. Brush*, July 31, 2002. Sandia National Laboratories, Carlsbad, New Mexico, U.S.A. ERMS 523057.

Giambalvo, E. R., 2002, An(III). Recommended Parameter Values for Modeling An(III) Solubility in WIPP Brines. Memo to Laurence H. Brush, July 25, 2002. ERMS 522982.

Giambalvo, E. R., 2002, An(IV). Recommended Parameter Values for Modeling An(IV) Solubility in WIPP Brines. Memo to Laurence H. Brush, July 26, 2002. ERMS 522986.

Giambalvo, E. R., 2002, An(V). Recommended Parameter Values for Modeling An(V) Solubility in WIPP Brines. Memo to Laurence H. (Larry) Brush, July 26, 2002. ERMS 522990.

Giambalvo, E. R., 2003, FMT. Release of FMT database FMT_021120.CHEMDAT. Memo to Laurence H. (Larry) Brush, March 10, 2003. Sandia National Laboratories, Carlsbad, New Mexico, U.S.A. ERMS 526372.

Guillaumont, R., Fanghänel, T., Fuger, J., Grenthe, I., Neck, V., Palmer, D. A., and Rand, M. H., 2003. *Update on the chemical thermodynamics of uranium, neptunium, plutonium, americium and technetium*. OECD-NEA, Elsevier, Amsterdam.

XI.8. H

Harvie, C. E., Møller, N., and Weare, J. H., 1984. The prediction of mineral solubilities in natural waters: The Na-K-Mg-Ca-H-Cl-SO_4-OH-HCO_3-CO_3-CO_2-H_2O system to high ionic strengths at 25°C. *Geochimica et Cosmochimica Acta* 48, 723-751.

Herz, W., and M. Hellebrandt, 1923. Die Löslichkeit von Bleichlorid und Bleibromid in wäβrigen Lösungen von Alkali- und Erdalkalichloridsalzen (Translation on Web of Science on 20210923: The solubility of lead chloride and lead bromide in diluted solutions of alcali and alkaline earth chloride salts). Zeitschrift fur Anorganische und Allgemeine Chemie, 130(2/3), 188-198.

Hummel, W., G. Anderegg, L. Rao, I. Puigdomenech, O. Tochiyama, 2005. Chemical Thermodynamics of Compounds and Complexes of U, Np, Pu, Am, Tc, Se, Ni and Zr With Selected Organic Ligands, Volume 9, 1st Edition, Edited by F. J. Mompean, M. Illemassene, and J. Perrone, OECD Nuclear Energy Agency, Data Bank, Issy-les-Moulineaux, France.

XI.9. I

None

XI.10. J

Jang, J., 2020a. Factors for Conversion of Molarity to molality and molality to Molarity. Memo to SNL WIPP Records Center and SNL WIPP Geochemistry. October 16, 2020. Sandia National Laboratories, Carlsbad, New Mexico, U.S.A. ERMS 574276.

Jang, J., 2020b. Experimental Study of the Thermodynamic Equilibrium Constants for the Magnesium - Oxalate Systems using Pitzer Activity Model, Revision 0. Sandia National Laboratories, Carlsbad, New Mexico, U.S.A. ERMS 573285.

Jang, J., 2021a. Revisit to the Pitzer Geochemical Thermodynamic Model for the $PbCl_2$(s) - HCl - H_2O System. Memo to SNL WIPP Records Center and SNL WIPP Geochemistry, May 25, 2021. Sandia National Laboratories, Carlsbad, New Mexico, U.S.A. ERMS 575309.

Jang, J., 2021b. Corrected log K value for $Fe(OH)_2$ (aq) in the EQ3/6 Thermodynamic Database; Routine Calculation of log K for $Fe(OH)_2$(aq). Memo to SNL WIPP Records Center, July 27, 2021. Sandia National Laboratories, Carlsbad, New Mexico, U.S.A. ERMS 575665.

Jang, J., P. Hora, L. Kirkes, C. Miller, and L. Zhang, 2021. Analysis Report documenting the Assessment of the Solubility of Lead, EDTA and other Organic Ligands in non-Sulfide systems performed under TP 08-02 and under TP 20-01, Revision 0. GEOC-21-03. Sandia National Laboratories, Carlsbad, New Mexico, U.S.A. ERMS pending as of 11/8/2021.

XI.11. K

Kendall, J., and C. H. Sloan, 1925. The Solubility of Slightly Soluble Chlorides in Concentrated Chloride Solutions. J. Am. Chem. Soc., 47(9), 2306-2317.

Kim, S., C. Marrs, M. Nemer, and J.J. Jang, 2017. Solubility Model for Ferrous iron hydroxide, hibbingite, siderite, and chukanovite in high saline solutions of sodium chloride, sodium sulfate, and sodium carbonate, ACS Earth and Space Chemistry, vol. 1, 647-663.

Kirkes, L., and P. Hora, 2020. Third Milestone Report on Test Plan TP 12-02, "Experimental Investigation of Borate Interactions with Rare Earth Elements Under the WIPP Relevant Conditions

at Sandia National Laboratories Carlsbad Facility". GEOC-20-04. Sandia National Laboratories, Carlsbad, New Mexico, U.S.A. ERMS 574511.

Kirkes, L., 2021. Memo of Correction for Third Milestone Report on Test Plan TP 12-02, "Experimental Investigation of Borate Interactions with Rare Earth Elements Under the WIPP Relevant Conditions at Sandia National Laboratories Carlsbad Facility (ERMS 574511). ERMS 576206.

Konnecke, Th., Th. Fanghanel, and J. I. Kim, 1997. Thermodynamics of trivalent actinides in concentrated electrolyte solutions: Modelling the chloride complexation of Cm(III), Radiochimica Acta, 76, 131-135.

XI.12. L

Langmuir, D., 1965, Stability of carbonates in the system MgO - CO_2 - H_2O, Journal of Geology, v.73, 730-754.

Lemire, R. J., U. Berner, C. Musikas, D. A. Palmer, P. Taylor, and O. Tochiyama, 2013. *Chemical Thermodynamics of Iron, Part 1*. Chemical Thermodynamics, Volume 13a, OECD/NEA, Edited by J. Perrone.

XI.13. M

Martell, A. E. and Smith, R. M., 1977. *Critical Stability Constants. Volume 3: Other Organic Ligands.* Plenum Press, New York.

Mgaidi, A., W. Furst, and H. Renon, 1991. Representation of the Solubility of Lead Chloride in Various Chloride Solutions with Pitzer's Model. Metallurgical Transactions B, 22B, 491-498.

Millero, F. J. and Byrne, R. H., 1984. Use of Pitzer's equations to determine the media effect on the formation of lead chloro complexes. *Geochimica et Cosmochimica Acta* 48, 1145-1150.

Moog, H. C., Hagemann, S., and Rumyantsev, A. V., 2004. Isopiestic investigation of the systems $FeCl_2$-(Na, K, Mg, Ca)Cl_n-H_2O at 298.15 K. *ZEITSCHRIFT FUR PHYSIKALISCHE CHEMIE-INTERNATIONAL JOURNAL OF RESEARCH IN PHYSICAL CHEMISTRY & CHEMICAL PHYSICS,* 218, 1063-1087.

Moore, R. C., M. Borkowski, M. G. Bronikowski, J. Chen, O. S. Pokrovsky, Y. Xia, and G. R. Choppin, 1999. Thermodynamic modeling of actinide complexation with acetate and lactate at high ionic strength. Journal of Solution Chemistry, v.28, no.5, 521-531.

Morel, F. M. M., and J. G. Hering, 1993. Principles and Applications of Aqueous Chemistry. John Wiley & Sons, Inc.

XI.14. N

Neck, V., Fanghanel, T., Rudolph, G., and Kim, J. I., 1995. Thermodynamics of Neptunium(V) in Concentrated Salt Solutions: Chloride Complexation and Ion Interaction (Pitzer) Parameters for the NpO_2^+ Ion. *Radiochimca Acta,* 69, 39-47.

Neck, V., R. Muller, M. Bouby, M. Altmaier, J. Rothe, M. A. Denecke, and J. I. Kim, 2002. Solubility of amorphous Th(IV) hydroxide - application of LIBD to determine the solubility product and EXAFS for aqueous speciation. Radiochimica Acta, 90, 485-494.

Novak, C. F., 1995. Creation and Definition of the Database for FMT called "HMW_NP_AM.CHEMDAT," version date 94.01.17. Memo to Nancy J. Dhooge, 18 January 1995, Sandia National Laboratories, Albuquerque, New Mexico, U.S.A. WPO 20130.

Novak, C. F., 1996. Preliminary Inorganic Model for Thorium Solubility in WIPP Brines, in database file HMW_3TH5_960119.CHEMDAT. Memo to E. J. Nowak, 19 January 1996. Sandia National Laboratories, Albuquerque, New Mexico. WPO 30930.

Novak, C. F., Borkowski, M., and Choppin, G. R., 1996. Thermodynamic Modeling of Neptunium(V)-Acetate Complexation in Concentrated NaCl Media *Radiochimca Acta*. 74, 111-116.

Novak, C. F., I. Al Mahamid, K. A. Becraft, S. A. Carpenter, N. Hakem, and T. Prussin, 1997. Measurement and thermodynamic modeling of Np(V) solubility in aqueous K_2CO_3 solutions to high concentrations. Journal of Solution Chemistry, vol.26, no.7, 681-697.

Nowak, E. J., 2005. Recommended Change in the FMT Thermodynamic Data Base. Memo to Laurence H. (Larry) Brush, April 1, 2005. Sandia National Laboratories, Carlsbad, New Mexico, U.S.A. ERMS 539227.

XI.15. O

None

XI.16. P

Pitzer, K. S., 1991. Ion interaction approach: Theory and data correlation. In: Pitzer, K. S. (Ed.), *Activity Coefficients in Electrolyte Solutions, 2nd Edition*. CRC Press, Boca Raton, Florida.

Pitzer, K. S. and Silvester, L. F., 1976. Thermodynamics of electrolytes. VI. Weak electrolytes including H_3PO_4. *Journal of Solution Chemistry*, 5, 269-278.

Pokrovsky, O. S., Bronikowski, M. G., Moore, R. C., and Choppin, G. R., 1998. Interaction of Neptunyl(V) and Uranyl(VI) with EDTA in NaCl Media: Experimental Study and Pitzer Modeling. *Radiochimca Acta* 80, 23.

XI.17. Q

None

XI.18. R

Rai, D., A. R. Felmy, and R. W. Fulton, 1992a. Solubility and Ion Activity Product of AmPO4.xH2O(am). Radiochimica Acta, 56, 7-14.

Rai, D., A. R. Felmy, R. W. Fulton, and J. L. Ryan, 1992b. Aqueous Chemistry of Nd in Borosilicate-Glass/Water Systems. Radiochimica Acta, 58/59, 9-16.

Rai, D., A. R. Felmy, and R. W. Fulton, 1995a. Nd^{3+} and Am^{3+} ion interactions with sulfate ion and their influence on $NdPO_4(c)$ solubility. Journal of Solution Chemistry, 24(9), 879-895.

Rai, D., A. R. Felmy, S. M. Sterner, D. A. Moore, M. J. Mason, and C. F. Novak, 1997. The Solubility of Th(IV) and U(IV) Hydrous Oxides in Concentrated NaCl and $MgCl_2$ Solutions. Radiochimica Acta, 79, 239-247.

Robie, R. A., and B. S. Hemingway, 1973. The Enthalpies of Formation of Nesquehonite, $MgCO_3.3H_2O$ and Hydromagnesite, $5MgO.4CO_2.5H_2O$. Journal of Research of the U.S. Geological Survey, 1(5), 543-547.

Roy, R. N., Vogel, K. M., Good, C. E., Davis, W. B., Roy, L. N., Johnson, D. A., Felmy, A. R., and Pitzer, K. S., 1992. Activity coefficients in electrolyte mixtures: HCl + $ThCl_4$ + H_2O for 5-55 °C. *The Journal of Physical Chemistry,* 96, 11065-11072.

Ryan, J. L., and D. Rai, 1987. Thorium(IV) Hydrous Oxide Solubility. Inorg. Chem., 26, 4140-4142.

XI.19. S

Shock, E. L., Sassani, D. C., Willis, M., and Sverjensky, D. A., 1997. Inorganic species in geologic fluids: Correlations among standard molal thermodynamic properties of aqueous ions and hydroxide complexes. *Geochimica et Cosmochimica Acta* 61, 907-950.

Shock, E. L., and H. C. Helgeson, 1988. Calculation of the Thermodynamic and Transport Properties of Aqueous Species at High Pressures and Temperatures: Correlation Algorithms for Ionic Species and Equation of State Predictions to 5 kb and 1000°C." Geochimica Cosmochimica Acta, 52(8), 2009-2036.

Stumm, W. and Morgan, J. J., 1996. *Aquatic Chemistry.* John Wiley & Sons, New York. RN: 419.

XI.20. T

Tan, K. G., K. Bartels, and P. L. Bedard, 1987. Lead Chloride Solubility and Density Data in Binary Aqueous Solutions. Hydrometallurgy, 17, 335-356.

XI.21. U

None

XI.22. V

None

XI.23. W

Wagman, D. D.; Evans, W.H. ; Parker, V.B. ; Schumm, R.H. ; Halow, I. ; Bailey, S.M. ; Churney, K.L. ; Nuttall, R.L., 1982. The NBS Tables of Chemical Thermodynamic Properties: Selected Values for Inorganic and C_1 and C_2 Organic Substances in SI Units, Published by American Chemical Society and the American Institute of Physics for the National Bureau of Standards, Journal of Physical and Chemical Reference Data, Volume 11, Supplement No. 2, 392 p.)

Wolery, T., and R. L. Jarek, 2003. Software User's Manual, EQ3/6, Version 8.0, 01/01/2003. ERMS 548926.

Wolery, T. J. and C. Jove-colon. 2007. Qualification of Thermodynamic Data for Geochemical Modeling of Mineral–Water Interactions in Dilute Systems. ANL-WIS-GS-000003 REV 01. DTN: SN0612T0502404.014.

XI.24. X

Xiong, Y., 2004. A correction of the molecular weight of oxalate in FMT_021120.CHEMDAT, and Incorporation of calcium oxalate monohydrate (Whewellite) into CHEMDAT with its recommended dimensionless standard chemical potential value. Memo to Larry Brush, June 8, 2004, Sandia National Laboratories, Carlsbad, New Mexico, U.S.A. ERMS 535813.

Xiong, Y., 2005. Release of FMT_050405.CHEMDAT. Email to J. F. Kanney, J. J. Long, Copied to M. J. Chavez, L. H. Brush, 'Jim Nowak', E. J. Nowak, April 05, 2005, with an attachment "compare.txt". ERMS 539304.

Xiong, Y., H. Deng, M. Nemer, and S. Johnsen, 2010. Experimental determination of the solubility constant for magnesium chloride hydroxide hydrate ($Mg_3Cl(OH)_5 \cdot 4H_2O$, phase 5) at room temperature, and its importance to nuclear waste isolation in geological repositories in salt formations. *Geochimica et Cosmochimica Acta* 74(16), 4605-4611.

Xiong, Y., 2011. Release of EQ3/6 Database DATA0.FM1. Email to Jennifer Long, March 9, 2011. Sandia National Laboratories, Carlsbad, New Mexico. ERMS 555152.

XI.25. Y

None

XI.26. Z

None

(No broken link found by Jay Jang on 11/17/2021. Total line number = 1595 including this line)